DEFINING AND UNDERSTANDING THE CONVERSION, PROPAGATION AND TRAFFICKING OF PrP^{Sc} IN A PRION INFECTED CELLULAR SYSTEM

A thesis submitted in partial fulfillment for the degree of Doctor of Philosophy to the University college London

by

Samira Rabbanian BSc (Hons)
Institute of Neurology, University College London

Declaration

I, Samira Rabbanian, confirm that the work presented in this thesis is my original research work. Where contributions of others are involved, this has been clearly indicated in the thesis.

Acknowledgments

First and foremost, sincerest gratitude to my supervisor, Professor Sarah Tabrizi, for her teaching, support, advice and enthusiasm over the last three years. Thanks also to Professor Parmjit Jat, my secondary supervisor, and to Professor Giampietro Schiavo for his experimental advice. Dr Rob Goold deserves a special thank you for mentoring me throughout and for his hard work and dedication to the project, and for some of the data presented in this thesis. I would also like to acknowledge the members of stuff and students at the MRC Prion Unit/Department of Neurodegenerative Disease at the UCL Institute of Neurology for their intellectual and practical help. I would also like to acknowledge UCL for their Overseas Research Scholarship and the Brain Research Trust for funding me. I am also very grateful to Ray Young for his capable and calm assistance with the preparation of figures.

My special gratitude goes out to the amazing members, past and present, of 'Team Tabrizi': Dr Pelagia Deriziotis, Dr Rob Goold, Dr Ralph André, Chris McKinnon, Ulrike Träger, Julie Moonga, Anna Magnusson and Kate Perry, for their kindness, friendship, and intellectual and personal support. I would particularly like to thank Pela for her sisterly love and advice, and Ralph and Chris for their immense support during my writing-up period. I would also like to acknowledge my 'Prion Unit' friends, especially Jessica Lowe for being a great 'shopping buddy'!

Above all, I would like to thank my family, and in particular my parents and my brother, Amir, for being a statue of support not just through my PhD but through life in general. I would not have maintained my sanity through this period of my life without their constant love, support and encouragement. I am also indebted to James Bloom for his enormous patience, love, support and pragmatic advice.

For my parents

تقدیم به پدر و مادر عزیزم

Abstract

Prion diseases are fatal neurodegenerative disorders associated with conformational conversion of normal cellular prion protein (PrP^{C}) to an abnormal disease-associated conformer (PrP^{Sc}). The aim of this thesis was to investigate the earliest event in prion infection using a novel cell system. Specifically, it aimed to assess the timescale that PrP^{C} is converted to PrP^{Sc} following exposure to RML prions and identify the initial cellular site of PrP^{Sc} formation and propagation. The cell biology of the initial events of cellular prion infection are poorly understood since newly formed cellular PrP^{Sc} is immunologically indistinguishable from infectious prions in the inocula. As a solution to this problem, an epitope-tag was inserted into the sequence of endogenous PrP^{C} to delineate the formation of *de novo* PrP^{Sc}. A PrP-knock down neuroblastoma cell line was reconstituted with mouse 3F4-, FLAG- and MYC-tagged PrP^{C}. Following identification of cells expressing physiological levels of tagged PrP^{C}, prion-susceptibility was determined by exposure to disease-associated prions.

Cells expressing 3F4-tagged PrP, the MYC sequence at position 224 and the FLAG sequence at position 22 or 30 contained PrP resistant to formic acid and proteinase K digestion. A mouse bioassay demonstrated that the PrP-224AlaMYC cell line produce *bona-fide* infectious epitope-tagged PrP^{Sc} on exposure to RML prions. Investigation of *de novo* tagged PrP^{Sc} propagation in this novel cell system demonstrated that cellular prion infection is a dynamic process occurring within one minute of prion exposure and that the plasma membrane is the primary site of prion conversion. It was demonstrated that the late endosomes, lysosomes and endosomal recycling compartments do not appear to be key sites of PrP conversion and prion

propagation, whilst the plasma membrane and early endocytic compartments are involved in this key process.

The work in this thesis provides new insights into the cell biology of the initial stages of prion conversion and propagation and has implications for neurodegenerative diseases where prion-like mechanisms have been proposed.

Table of contents

Declaration **2**

Acknowledgments **3**

Abstract **5**

Table of contents **7**

Index of figures and tables **12**

Abbreviation list **17**

1 Introduction **20**

1.1 Animal prion diseases 20

1.1.1 Scrapie 20

1.1.2 Chronic wasting disease 21

1.1.3 Transmissble mink encephalopathy 22

1.1.4 Bovine spongiform encephalopathy 22

1.1.5 Other animal prion diseases 23

1.2 Human prion diseases 24

1.2.1 Sporadic prion disease 24

1.2.2 Inherited prion disease 25

1.2.3 Acquired prion disease 26

1.3 Neuropathology and diagnosis of human prion diseases 29

1.4 Protein-only hypothesis of prion transmission 32

1.5 Prion gene structure 34

1.6 Cell biology and life cycle of prion protein 35

1.6.1 PrP^{C} 35

1.6.2 PrP^{Sc} 46

1.7 Mechanisms of prion conversion 54

1.8 Prion strains and species barriers 55

1.9 Prion mediated neurotoxicity 57

1.9.1 PrP^{Sc} as the neurotoxic species 58

1.9.2 Gain and loss of PrP^{C} function 59

1.9.3 Aberrant PrP^{C} trafficking 61

1.9.4 Intermediate PrP species 63

1.10 Therapeutic approaches in prion diseases 65

1.11 Aims of the thesis 67

2 Materials and Methods 68

2.1 Cell culture 68

2.1.1 Cell lines 68

2.1.2 Cell culture methods 69

2.2 Molecular biology 71

2.2.1 Knock down of *Prnp* using RNA interference 71

2.2.2 Construction of mouse PrP-3F4, FLAG and MYC insertion mutants in pLNCX2 73

2.2.3 Tagged PrP expression 76

2.2.4 Isolation of mouse 3F4-tagged PrP expressing single cell clones 77

2.3 Protein chemistry and immunoblotting 79

2.3.1 Cell lysate preparation for inoculation of Tg20 mice 79

2.3.2 Protein assay 79
2.3.3 Extraction of protein from brain homogenates 80
2.3.4 Extraction of protein from cultured cells 81
2.3.5 Proteinase K digestion of cells for detection of PK resistant PrP^{Sc} 81
2.3.6 SDS-polyacrylamide gel electrophoresis (SDS-PAGE) of protein 81
2.3.7 Electroblotting of gels 82
2.3.8 Immunoblotting of gels 82
2.3.9 Determination of equal protein loading 83
2.3.10 Densitometry 84
2.4 Cell Biology 84
2.4.1 PrP^{Sc} trafficking impairment using pharmacological agents 84
2.4.2 Immunofluorescence methods 86
2.5 Assaying for PrP^{Sc} in cells (Scrapie Cell Assay) 89
2.6 Statistical analysis 91
3 Isolation of prion susceptible cell lines expressing tagged mouse PrP 93
3.1 Background 93
3.1.1 Aims 95
3.2 Methods 95
3.3 Results 96
3.3.1 Analysis of prion protein expression in knock down mouse PK1 cells 96
3.3.2 Generating a panel of nine differentially tagged mouse PrP^{C} molecules 100
3.3.3 Mouse 3F4-tagged PrP^{C} expression in PrP-KD PK1 cells 103

3.3.4 Conversion of MoPrP^{C}.3F4 into misfolded PrP 106

3.3.5 FLAG- and MYC-tagged mouse PrP^{C} expression in PrP-KD PK1 cells 114

3.3.6 Conversion of FLAG- and MYC-tagged mouse PrP^{C} into misfolded PrP in reconstituted P8(11)4.5 and PK1-10*Si8* cells 120

3.4 Discussion 130

3.5 Summary 135

4 Rapid *de novo* prion conversion revealed using a novel cell system 136

4.1 Background 136

4.1.1 Aims 137

4.2 Methods 137

4.3 Results 138

4.3.1 Characterisation of prion infected cells 138

4.3.2 Cellular prion infection is a rapid process 147

4.3.3 Two minutes exposure to RML prions is sufficient to cause stable prion propagation 154

4.3.4 Cellular PrP^{Sc} interaction is not sufficient to induce PrP^{Sc} propagation 156

4.4 Discussion 158

4.5 Summary 162

5 Cellular sites of *de novo* PrP^{Sc} formation and its intracellular trafficking 163

5.1 Background 163

5.1.1 Aims 165

5.2 Methods 166

5.3 Results 167

5.3.1 Conversion of PrP^{C} to PrP^{Sc} is a post-translational event 167

5.3.2 The role of plasma membrane and endocytic pathways in prion conversion and propagation 173

5.3.3 Prion conversion first occurs at the cell surface within one minute of prion exposure 189

5.4 Discussion 197

5.5 Summary 203

6 Conclusions and future plans 204

6.1 Thesis summary and conclusions 204

6.2 Suggestions for future work 205

6.2.1 Understanding the pathways by which PrP^{Sc} accesses the cytosol 205

6.2.2 A novel cell system to study the UPS activity 208

6.2.3 A novel cell system to study prion cytotoxicity 210

7 Appendices 213

Appendix I 213

Appendix II 213

Appendix III 214

Appendix IV 215

8 Reference list 218

Index of figures and tables

Figure 1-1 Schematic representation of the domain structure of murine PrP 38

Figure 1-2 Pathways of PrP^{C} internalisation 43

Figure 1-3 Proteinase K resistance of PrP 49

Figure 1-4 Role of PrP^{Sc} and mechanism of neurodegeneration 64

Figure 2-1 Isolation of RML prion susceptible single cell clones expressing 3F4-tagged PrP 78

Figure 3-1 Mouse PrP-KD PK1 cells do not express prions 99

Figure 3-2 Schematic representation of the domain structure of murine PrP 102

Figure 3-3 Transduced PK1-10*Si8* and P8(11)4.5 mixed clones express $moPrP^{C}$.3F4 104

Figure 3-4 Expression of $moPrP^{C}$.3F4 in transduced PK1-10*Si8* and P8(11)4.5 mixed clones 105

Figure 3-5 PK1-10*Si8*.3F4 and P8(11)4.5.3F4 mixed clones are not susceptible to RML prions 106

Figure 3-6 $moPrP^{C}$.3F4 expression in PK1-10*Si8*.3F4 and P8(11)4.5.3F4 single cell clones 108

Figure 3-7 Detection of $moPrP^{C}$.3F4 expression in PK1-10*Si8*.3F4 and P8(11)4.5.3F4 single cell clones by immunoblotting 109

Figure 3-8 Misfolded moPrP.3F4 propagation in seven RML prion-infected single cell clones 112

Figure 3-9 Seven moPrP.3F4 single cell clones infected with RML prions propagate misfolded PrP 113

Figure 3-10 Cloning strategy for inserting FLAG and MYC tag sequence in pLNCX2 115

Figure 3-11 Transduced P8(11)4.5 and PK-10*Si8* mixed clones express Mouse FLAG- and MYC-tagged PrP^{C} 118

Figure 3-12 Expression of FLAG- and MYC-tagged PrPC in reconstituted mixed clones 119

Figure 3-13 Misfolded PrP detection in P8(11)4.5.FLAG and PK-10Si8.MYC cells 123

Figure 3-14 PK-resistant detection in P8(11)4.5.FLAG and PK1-10Si8 cell lysates by immunoblotting 124

Figure 3-15 PrP-30GlyFLAG cells produce PK-resistant PrP following RML prion exposure 125

Figure 3-16 Tg20 mice inoculated intracerebrally with extracts of RML prion-infected PrP-224AlaMYC cells develop prion disease (Biochemical analysis)..... 128

Figure 3-17 Tg20 mice inoculated intracerebrally with extracts of RML prion-infected PrP-224AlaMYC cells develop prion disease (Histological analysis)..... 129

Figure 4-1 Comparison of the methods used to visualise PrP^{Sc} in RML prion-infected PrP-224AlaMYC cells..... 140

Figure 4-2 Comparison of the methods to visualise PrP^{Sc} in RML prion-infected PK1 cells 141

Figure 4-3 Characterisation of newly formed tagged PrP^{Sc} distribution in RML prion-infected cells..... 144

Figure 4-4 Intracellular localisation of tagged PrP^{Sc} in RML prion-infected cells 146

Figure 4-5 3F4- and MYC-tagged PrP^{Sc} propagation in RML prion-infected cells. 149

Figure 4-6 MYC-tagged PrP^{Sc} is synthesized rapidly following RML prion exposure 152

Figure 4-7 Formic acid- and PK- resistant tagged PrP^{Sc} is synthesized rapidly following RML prion exposure..... 153

Figure 4-8 Short RML prion exposure is sufficient to cause stable prion propagation..... 155

Figure 4-9 Cellular PrP^{Sc} interaction is not sufficient to induce PrP^{Sc} propagation 157

Figure 5-1 BFA disassemble the Golgi apparatus in PrP-224AlaMYC cells..... 170

Figure 5-2 PrP^{Sc} propagation in RML prion-infected PrP-224AlaMYC and iPK1 cells treated with BFA..... 171

Figure 5-3 Sub-cellular distribution of MYC-tagged PrPSc in RML prion-infected PrP-224AlaMYC cells treated with BFA..... 172

Figure 5-4 Inhibition of prion endocytosis reduces but does not eliminate PrP^{Sc} production and propagation..... 175

Figure 5-5 Sub-cellular distribution of MYC-tagged PrP^{Sc} in RML prion-infected PrP-224AlaMYC cells treated at 4°C 176

Figure 5-6 Cellular localisation of MYC-tagged PrP^{Sc} at 4°C in naive and prion-propagating PrP-224AlaMYC cells 177

Figure 5-7 Sub-cellular distribution of MYC-tagged PrP^{Sc} in naive PrP-224AlaMYC cells after treatment with nocodazole, bafilomycin or 20°C temperature shift 180

Figure 5-8 Sub-cellular distribution of MYC-tagged PrP^{Sc} in prion-propagating PrP-224AlaMYC cells after treatment with nocodazole, bafilomycin or 20°C temperature shift 181

Figure 5-9 Inhibition of PrP trafficking beyond the early endosomes does not affect PrP conversion and prion propagation 182

Figure 5-10 Cellular localisation of MYC-tagged PrP^{Sc} in naive and prion-propagating PrP-224AlaMYC cells treated with nocodazole 183

Figure 5-11 Inhibition of dynamin-dependent processes in RML prion-infected PrP-224AlaMYC and iPK1 cells does not affect PrP^{Sc} production and propagation..... 186

Figure 5-12 Sub-cellular distribution of MYC-tagged PrP^{Sc} in RML prion-infected PrP-224AlaMYC cells treated with dynasore 187

Figure 5-13 Cellular localisation of MYC-tagged PrP^{Sc} in naive and prion-propagating PrP-224AlaMYC cells treated with Dynasore 188

Figure 5-14 Prion conversion first occurs at the cell surface within one minute of prion exposure..... 191

Figure 5-15 De novo prion protein conversion, endocytosis and trafficking proceeds at similar rates or faster than transferrin trafficking..... 192

Figure 5-16 Conversion of PrPC to PrPSc occurs initially on the cell surface..... 194

Figure 5-17 Intact lipid raft integrity on the cell surface required for efficient prion conversion 196

Table 1-1 Neuropathological criteria for diagnosis of human prion diseases 31

Table 2-1 Location of siRNA target sequences in mouse *Prnp* mRNA..... 73

Table 2-2 Primary and secondary PCR reactions..... 74

Table 2-3 Pharmacological agents used to manipulate intracellular trafficking of PrP^{Sc} 85

Table 2-4 Antibody concentrations used for immunofluorescence analysis 87

Table 3-1 *In vivo* bioassay of the infectious and pathological properties of the novel tagged PrP molecules generated in PrP-224AlaMYC cells 127

Abbreviation list

°C - degrees Celsius

aa - amino acid(s)

AD - Alzheimer's disease

AEBSF - 4-(2-aminoethyl)benzenesulphonyl fluoride

AP - alkaline phosphatase

APP - amyloid precursor protein

ATCC - American Type Culture Collection

BBB - blood-brain-barrier

BCA - bicinchoninic acid

BFA - brefeldin A

BSA - bovine serum albumin

BSE - bovine spongiform encephalopathy

cDNA - complimentary DNA

Cdc-42 - cell division cycle 42

CHC - clathrin heavy chain

CJD - Creutzfeldt-Jakob disease

CLD - caveolae-like domain

cm - centimetre(s)

CNS - central nervous system

CO_2 - carbon dioxide

CWD - chronic wasting disease

Da - Dalton

DAPI - 4', 6-diamidino-2-phenylindole

DC - dendritic cell(s)

DMSO - dimethyl sulfoxide

DNA - deoxyribonucleic acid

dNTP - deoxynucleotide triphosphates

DRM - detergent-resistant microdomains

Drp1 - dystrophin-related protein 1

DY – drowsy

ECV - endosomal carrier vesicles

EEG – electrocephalographic

***e.g.* –** example

Eps15 - epidermal growth factor receptor substrate 15

ER - endoplasmic reticulum

ERAD - endoplasmic reticulum associated protein degradation

ERC - endosomal recycling compartment(s)

EU - European Union

EUE - exotic ungulate encephalopathy

FCS - foetal calf serum

FDC - follicular dendritic cell

FFI - fatal familial insomnia

FRT - Fischer rat thyroid

FSE - Feline spongiform encephalopathy

g - gram

***g* -** gravity (acceleration due to)

GAG – glycosaminoglycan(s)

GCSN - guanidinium thiocynate

GdnHCl - guanidinium hydrochloride

GFAP - glial fibrillary acidic protein

GPI - glycosyl phosphatidylinosiol

GSS - Gerstmann-Sträussler-Scheinker disease

hr - hour(s)

HD - hydrophobic domain

HPA - Health Protection Agency

Hsc70 - heat shock chaperone 70

HSPG - heparin sulphate proteoglycan

HY - hyper

***i.e.* -** that is

kDa – kiloDalton

KD - knock down

LDL - low density lipoprotein

LR - laminin receptor

LRP - laminin receptor precursor(s)

LRP1 - (LDL) receptor-related protein

M - molar

MBM - meat-and-bone-meal

MEM - minimum essential medium

mg - milligram(s)

min - minute(s)

ml – millilitre(s)

mM – millimolar

mm - millimetres

mRFP - monomeric red fluorescent proteins

mRNA - messenger ribonucleic acid

MV151 - TMR-Ahx3L3VS

MW - molecular weight

mW - megawatt

NPM- Nucleated polymerisation model

Ng - nanogram

nm - nanometre

NMR - nuclear magnetic resonance

NPM - nucleated polymerisation model

NSC - neuronal stem cells

ORF - open reading frame

PAGE - polyacrylamide gel electrophoresis

PBS - phospho-buffered saline

PBST - phosphate buffered saline with 0.5% Tween-20

PCR - polymerase chain reaction

PFA - paraformaldehyde

pH - hydrogen ion concentration

PIPLC - Phosphatidylinositol-specific phospholipase C

PK - proteinase K

PK1 cells - N2aPK-1 cells

PMCA - protein misfolding cyclic amplification

PMSF – phenylmethylsulphonyl fluorride

PNC - perinuclear compartment

pQC - ‘pre-emptive’ quality control

***PRNP* -** prion protein gene (human)

***Prnp*-** prion protein gene (mouse)

PrP - prion protein

PrP^{C}- normal isoform of the prion protein

PrP^{Sc} - disease-associated prion protein

PVDF - polyvinylidene difluoride

RANTES - regulated upon activation, normal T cell expressed, and secreted system

RML - Rocky Mountain laboratory

RNA - ribonucleic acid

RNAi - RNA interference

rpm - revolutions per minute

RT - room temperature

SAF - scrapie-associated fibrils

SCA - scrapie cell assay

ScN2a - scrapie-infected N2a

SDS - sodium dodecyl sulphate

ScHaB - scrapie-infected hamster brain

shRNA- short hairpin RNA

siRNA- small interfering RNA

TAM - template assisted model

TBST - tris-buffered saline Tween-20

TGN - trans-Golgi network

TME - transmissible mink encephalopathy

TNTs - tunnelling nanotubes

TSE - transmissible spongiform encephalopathies

TUNEL - terminal deoxynucleotidyl transferase (TdT)-mediated dUTP nick end labelling

U - units

U/ml - unit in millilitres

UPS - ubiquitin-proteasome system

UTR - un-translated region

UV - ultraviolet

V - voltage

v/v - volume in volume

w/v - weight in volume

µg - micrograms

µl - microlitters

µM - micromolar

1 Introduction

Prion diseases, or transmissible spongiform encephalopathies (TSE), are a family of fatal neurodegenerative disorders. These diseases affect both humans (*e.g.* Creutzfeldt-Jakob disease; CJD) and animals (*e.g.* bovine spongiform encephalopathy; BSE), and can be transmitted within or between animal species by inoculation or dietary exposure. They are associated with a conformational rearrangement of the normal cellular prion protein, PrP^{C} (C for cellular) to abnormal conformers, PrP^{Sc} (Sc for scrapie). PrP^{C} is soluble, monomeric and rich in α-helical structure, whereas disease-associated PrP^{Sc} is characterized by increased β-sheet structure, detergent insolubility and partial resistance to proteolysis. Neuro-pathologically, prion diseases produce a characteristic spongiform degeneration of the brain, with massive neuronal death, marked gliosis and the accumulation of amyloid plaques containing PrP^{Sc}. Currently, the cause of prion mediated neurodegeneration remains unknown and a major gap exists in understanding how the conversion of PrP^{C} to PrP^{Sc} leads to neuronal dysfunction and ultimately cellular death.

1.1 Animal prion diseases

This section summarises animal prion diseases including scrapie in sheep and goats, BSE in cattle and chronic wasting disease (CWD) in deer and elk.

1.1.1 Scrapie

Scrapie is a naturally occurring disease of sheep and goats that was first described in the 18^{th} century. Its name is derived from the predominant clinical symptom, whereby the animal has the tendency to rub against walls or fences to scrape off its wool. In 1936, scrapie was successfully transmitted to goats and two healthy

sheep by intraocular inoculation of brain or spinal cord tissue from an affected animal (Cuillé and Chelle, 1936). Thereby, the transmissible nature of the scrapie agent was firmly established. Further evidence came after scrapie was inadvertently transmitted to British sheep injected with a vaccine prepared from the brain, spinal cord, and spleen of affected sheep (Gordon, 1946). Since then, scrapie has been successfully transmitted between different species including laboratory mice (Chandler, 1961). To this date, the disease has never been shown to pose a threat to human health (Brown and Bradley, 1998). Despite all the studies into scrapie, remarkably little is known about its natural routes of transmission. Affected sheep and goats show the typical neuropathological symptoms for prion disease which are in general spongiosis, gliosis, and neural loss. Scrapie has been recognised in many countries, but its presence is imprecisely known in Europe, North America and Japan.

1.1.2 Chronic wasting disease

Chronic wasting disease (CWD) is a prion disease first recognised around 30 years ago affecting mule deer, white-tailed deer, and Rocky Mountain elk in a limited area of North America (Williams and Young, 1980; Spraker *et al*., 1997). The natural history of CWD is incompletely understood, but differs from scrapie and BSE by virtue of its occurrence in non-domestic and free-ranging species. As yet, there is no evidence for CWD transmission to humans (Miller and Williams, 2003; Mathiason *et al*., 2006). In CWD, disease-associated prion protein has an early widespread distribution in lymphoid tissues, with later involvement of central nervous system (CNS) and peripheral tissues (Browning *et al*., 2004). Symptoms include weight loss, behavioural changes and hypotonic muscles, and typically lead to death after 7-8 months (Williams and Young, 1980).

1.1.3 Transmissible mink encephalopathy

Transmissible mink encephalopathy (TME) affects ranched mink and was first seen in Wisconsin and Minnesota in 1947. Sporadic outbreaks have since appeared in several countries including Canada, Finland, Russia and former East Germany (Marsh, 1992). Mink appear to acquire TME through ingestion of scrapie and BSE contaminated meat (Marsh *et al*., 1991). Studies have shown that this disease can be experimentally transmitted to hamsters (Kimberlin and Marsh, 1975). A recent study in a transgenic mouse line suggests that the TME agent is not related to BSE agents, despite their apparent similarities (Baron *et al*., 2007). Initial symptoms include increased aggression and hyperaesthesia and usually progress to ataxia, tremors, and compulsive self-biting (Marsh *et al*., 1991). The time between initial symptoms and death vary from one week to several months (Marsh, 1992).

1.1.4 Bovine spongiform encephalopathy

BSE or ‘mad cow disease’ was recognised in Britain in 1986 by British veterinarians (Wells *et al*., 1987). In the UK, around 180,000 cattle have since developed clinical symptoms of the disease with the epidemic peak in 1992 (Beghi *et al*., 2004). Beside the UK, the disease has now been reported in most member states of the European Union, together with Switzerland, the United States, Canada and Japan (Ghani *et al*., 2002; Mallucci and Collinge, 2005). Affected cattle show typical prion disease neuropathology including diffuse cellular degeneration with spongiosis and astrocytic gliosis. The affected cattle die within six months of the initial signs of the disease.

It has been suggested that the BSE epidemic was caused by the use of contaminated meat-and-bone-meal (MBM) as a high protein supplement feed for

cattle. MBM contains brain material from sheep, cattle and chicken. One possible origin of BSE was feeding cattle with scrapie-containing MBM (Prusiner *et al*., 1991; Wilesmith and Wells, 1991) as BSE is neuropathologically similar to scrapie (Wilesmith and Wells, 1991; Wilesmith *et al.*, 1988; Smith and Bradley, 2003); It is, however, important to note that the BSE strain is molecularly and biologically different to the strain causing scrapie (Bruce *et al*., 1994). Another possibility is that BSE occurred sporadically in cattle and thus tissue from the affected animal was incorporated into MBM to seed the epidemic (Weissmann and Aguzzi, 1997). In 1988 feeding of MBM to sheep and cattle was banned and following the emergence of variant CJD in 1996 the ban on feeding mammalian proteins to any farmed animals was re-enforced. The feed ban was extended to the EU in 2001. The route of BSE transmission is thought to be oral and since BSE has a long incubation time (~ four years), new epidemic peaks cannot be fully excluded in affected countries.

1.1.5 Other animal prion diseases

In addition to TSEs described above, Feline spongiform encephalopathy (FSE) and Exotic ungulate encephalopathy (EUE) are other animal prion diseases reported first in the UK and then in other European countries. Both of these diseases are considered to be related to BSE and thought to be caused by feeding animals with BSE-contaminated MBM. EUE has been recognised in exotic hoofed animals and FSE has been described in captive cheetahs, pumas, ocelots, and tigers (Kirkwood and Cunningham, 1994). Affected animals show spongiform degeneration in the neuropil of the brain and spinal cord with the most severe lesions localised to the medial geniculate nucleus of the thalamus and the basal nuclei (Ryder *et al*., 2001).

1.2 Human prion diseases

Human prion diseases are rare and fatal disorders characterised by a wide range of clinical symptoms such as weight loss, insomnia, depression, memory problems, confusion, headache, and general pain sensation. Neurological features include cortical blindness, extrapyramidal signs, ataxia, and finally dementia. Human prion diseases have three distinct aetiologies (Prusiner, 1998a; Collinge, 2001): they might be acquired from exposure to prions; they may arise sporadically; or they can be inherited in an autosomal-dominant manner (Collinge, 2001; Kovacs *et al*., 2002b; Wadsworth *et al*., 2003; Mead, 2006b).

1.2.1 Sporadic prion disease

About 80 % of human prion disease cases occur sporadically as CJD (sporadic CJD). The disease occurs at a rate of 1-2 cases per million population per year across the world, with an equal incidence in men and women (Caramelli *et al*., 2006). The peak incidence is in the age group of 45-75 with median age at death of 68 years (Brown *et al*., 1987; Collins *et al*., 2006). Sporadic CJD progress rapidly and affected individuals show multifocal dementia, usually with myoclonus, leading to death within 6-12 month of disease onset (Gambetti *et al*., 2003). Definitive diagnosis of sporadic CJD is by brain biopsy or neuropathological analysis at post-mortem, both of which must demonstrate spongiform change, neuronal loss and astrocytosis (Bell *et al*., 1997). In sporadic CJD PrP amyloid plaques are not usually present, but PrP immunohistochemistry is nearly always positive (Budka *et al*., 1995). The cause of sporadic CJD is unknown, however, somatic mutation of the human PrP gene, *PRNP*, (Brown *et al*., 1987; Collinge, 1997; Wadsworth *et al*., 2006), or the spontaneous conversion of PrP^{C} into PrP^{Sc} as a rare stochastic event (Collinge, 1997) are current

hypotheses. Susceptibility to human prion diseases is affected by polymorphism at residue 129 of human PrP encoding either methionine (M) or valine (V) (Mead, 2006b). Approximately 38 % of Europeans are homozygous for the M allele, 51 % are heterozygous, and 11 % are homozygous for the V allele. Studies have suggested that homozygosity at *PRNP* codon 129 predisposes to the development of sporadic and acquired CJD (Collins *et al*., 2006; Collinge *et al*., 1991a; Palmer *et al*., 1991; Windl *et al*., 1996; Lee *et al*., 2001a; Mead *et al*., 2003). Further genetic studies have revealed that sporadic CJD is also associated with polymorphisms upstream of exon 1 of *PRNP* (Mead *et al*., 2001) and a 129 MV independent polymorphism in the 5' un-translated region (UTR) of *PRNP* locus (Vollmert *et al*., 2006).

1.2.2 Inherited prion disease

Around 15 % of human prion diseases are associated with automosal dominant pathogenic mutations in *PRNP* (Gambetti *et al*., 2003; Collinge, 1997; Collinge and Palmer, 1997; Kovacs *et al*., 2002a; Mead, 2006a). It is not known how pathogenic mutations in *PRNP* cause prion diseases. The mutations are thought to favour the spontaneous conversion of PrP^{C} to the PrP^{Sc} state in the absence of an exogenous infectious agent (Cohen *et al*., 1994). It has also been shown that experimental mutation of the prion gene can lead to spontaneous neurodegeneration without the formation of detectable protease resistant PrP (Muramoto *et al*., 1997; Hegde *et al*., 1998a). Traditionally, inherited prion diseases have been classified into three main sub-divisions of Gerstmann-Sträussler-Scheinker disease (GSS), familial CJD and fatal familial insomnia (FFI) according to their clinical symptoms. However, the existence of phenotypic overlap between individuals with different mutations and even in family members with the same *PRNP* mutation indicates that accurate classification of

inherited prion diseases should be based upon mutation alone (Collinge *et al*., 1992; Collinge and Prusiner, 1992). GSS presents the distinctive and defining neuropathological feature of widespread, multicentric amyloid plaques which are PrP positive. Mutation P102L of *PRNP* was the first to be reproducibly associated with GSS development (Hsiao *et al*., 1989); however, the disease is now linked to seven *PRNP* mutations. FFI is characterised by profound disruption of the normal sleep-wake cycle, prominent insomnia, sympathetic over-activity, diverse endocrine abnormalities and impaired attention. The disease is associated with a missense mutation at codon 178 of *PRNP*, substitution of asparagine for aspartic acid (D178N), and coexisting methionine at the polymorphic codon 129 of *PRNP* (Medori *et al*., 1992). Sporadic FFI with no causative mutation in *PRNP* has been reported (Montagna *et al*., 2003). Familial CJD segregates with D178N mutation when combined with valine at codon 129 (Zerr *et al*., 1998).

1.2.3 Acquired prion disease

Although human prion diseases are transmissible diseases, acquired forms are very rare and are associated with less than 5 % of human prion diseases.

Iatrogenic CJD

Iatrogenic CJD can arise after an individual is exposed to CJD-infected tissue, most commonly as a contaminant in medical procedures. For instances, cases of iatrogenic CJD, have been traced to corneal transplants, dura matter grafts, administration of growth hormone derived from cadaveric pituitary glands and the use of infected surgical instruments and electrocephalographic (EEG) electrodes (Brown *et al*., 1992; Brown *et al*., 2000). Patients with iatrogenic CJD display different symptoms on the route of exposure to human prions (Collinge and Palmer, 1997;

Brown *et al*., 2000; Belay, 1999). Where transmission is intracerebral, the symptoms are similar to sporadic CJD (Heath *et al*., 2006), whereas, peripherally acquired CJD resembles kuru due to the prominent early ataxia.

Variant CJD

Variant CJD was first reported in the United Kingdom in 1996 (Will *et al*., 1996) and has affected around 173 individuals in the UK to date (www.cjd.ed.ac.uk/figures.htm). Clinical, neuropathological, molecular and transmission characteristics of variant CJD all indicate that it is acquired by the consumption of beef from BSE-affected cattle (Bruce *et al*., 1997; Collinge, 1996; Will *et al*., 1996). Experimental evidence that variant CJD is caused by the same BSE prion strain detected in cattle has raised the possibility that a major epidemic of variant CJD will occur in the UK and other countries in which livestock were exposed to BSE prions (Cousens *et al*., 1997; Ghani *et al*., 1999; Collinge, 1999). Variant CJD affects primarily young adults and it is clinically characterised by a progressive neuropsychiatric disorder with ataxia, dementia, and involuntary movements. In contrast with sporadic CJD, patients with variant CJD are much younger (19-39 years old), have a longer duration of illness (7.5-22 months) and beyond the CNS, PrP^{Sc} can also be found in the spinal cord and immune cells in the periphery (Spencer *et al*., 2002).

To date, all definite variant CJD cases are homozygous for methionine at *PRNP* codon 129 (Hill *et al*., 1997; Hill *et al*., 1999). However, an unusual case published by Kaski *et al*. in 2009 reported a 30-year old man who was heterozygous at *PRNP* codon 129 (MV) and died of variant CJD (Kaski *et al*., 2009). Recent quantitative trait locus studies in mouse have shown that regions unrelated to *PRNP* play a role in the variable

incubation times in prion disease, including BSE (Stephenson *et al*., 2000; Lloyd *et al*., 2001; Lloyd *et al*., 2002). Further investigations have also identified two novel candidate loci, *RARB* and *STMN2*, as potential variant CJD risk factors (Mead *et al*., 2009). At present, there is concern that some individuals are carriers of the infection and thus pose a risk of horizontal spread. Variant CJD transmission by blood transfusion had already been documented (Llewelyn *et al*., 2004; Peden *et al*., 2004; Hewitt *et al*., 2006; Wroe *et al*., 2006). As a result, many countries have passed laws to diminish the use of blood from donors at risk of exposure to BSE or variant CJD. In February 2009, the ‘’Health Protection Agency’’ (HPA, London, UK) confirmed the first case of variant CJD transmission via blood in a patient with haemophilia.

Kuru

A well-known example of acquired human prion disease is kuru which was recognised as a major epidemic in the 1950s. The disease was transmitted by cannibalism among the Fore linguistic group of the Eastern Highlands of Papua New Guinea (Gajdusek, 1977; Mead *et al*., 2003). The epidemic of kuru is thought to have originated when brain tissue from an individual with sporadic CJD was consumed in a ritualistic mortuary feast. Besides dietary exposure as route of transmission, inoculation with brain or other tissue via cuts or sores could also have occurred (Prusiner *et al*., 1982). The central clinical feature of kuru is progressive cerebellar ataxia but, in contrast to CJD, dementia is often absent (Alpers, 1987). The incubation period for kuru can exceed 50 years (Collinge *et al*., 2006) and it has been shown that *PRNP* codon 129 genotype has a prominent effect on both incubation periods and susceptibility. Individuals with MM genotype have the shortest incubation period (Lee *et al*., 2001a), followed by VV homozygotes. Most elderly survivors of the kuru

epidemic, who were exposed to mortuary feasts, are MV heterozygotes (Collinge *et al*., 2006). The introduction of Christianity and subsequent prohibition of cannibalism resulted in virtual elimination of kuru, however some cases are still reported (Collinge, 2001).

1.3 Neuropathology and diagnosis of human prion diseases

Neuropathology in prion diseases has remained the most important tool in obtaining a definitive diagnosis, and neuropathological research has contributed considerably to our current pathogenetic understanding of prion diseases.

Gross inspection of prion infected brains does not reveal obvious abnormalities. However, some degree of brain atrophy is seen in occipital lobe, striatum, thalamus, and cerebellum based on preferential involvement of specific regions (Heidenhain *et al*., 1929; Brownell *et al*., 1965; Richardson and Masters, 1995). In contrast to other degenerative diseases, the hippocampus is usually well preserved in prion diseases even in cases of severe brain atrophy (Budka, 2003). Furthermore, prominent cerebellar atrophy and degeneration of spinal tracks is seen in individuals with GSS disease (Hainfellner *et al*., 1995).

Histopathological examination of brain tissue at post-mortem remains the best method of confirming prion disease diagnosis. Human prion diseases are characterised by a classical triad of spongiform change, neuronal loss, astro- and microglia-gliosis (Kubler *et al*., 2003). The spongiform change is the most specific feature of prion diseases and may be mild, moderate, or severe (Almer *et al*., 1999). Spongiosis is mostly seen in grey matter but cases involving white matter have also been described (Park *et al*., 1980). Spongiform change is observed as diffuse or focally clustered,

small, round vacuoles in the neurophil of the deep cortical layers, cerebella cortex or subcortical grey matter (Budka *et al*., 1997). Presence and distribution of spongiform change varies significantly between cases and disease subtypes. Spongiosis rarely presents in the brain stem and spinal cord, despite PrP^{Sc} accumulation at these sites (Almer *et al*., 1999). In sporadic CJD, the regional distribution of spongiform change was shown to depend upon codon 129 *PRNP* genotype PrP^{Sc} fragment sizes and glycotypes (Parchi *et al*., 1999; Hill *et al.*, 2003). However, some prion diseases such as FFI, have equivocal, little, or no spongiform changes (Almer *et al*., 1999). In these cases, immunohistochemistry for PrP and *PRNP* genotyping have a decisive diagnostic role (Hainfellner *et al*., 1996). In prion diseases as a whole, PrP^{Sc} accumulates in the CNS and has become an important diagnostic marker (Almer *et al*., 1999). Immunohistochemistry for PrP^{Sc} has emerged as an indispensable adjunct to the neuropathological confirmation of prion diseases, especially in cases with equivocal histopathological changes (Budka, 2003). Current neuropathological criteria for diagnosis of human prion diseases are listed in Table 1-1.

Table 1-1 Neuropathological criteria for diagnosis of human prion diseases[1]

Prion disease	Criteria
CJD Sporadic Iatrogenic Familial	Spongiform encephalopathy in cerebral +/or cerebellar cortex +/or subcortical grey matter; +/or encephalopathy with PrP immunoreactivity (plaque +/or diffuse synaptic +/or patchy/perivacuolar types)
vCJD	Spongiform encephalopathy with abundant PrP deposition, in particular multiple fibrillary PrP plaques surrounded by a halo of spongiform vacuoles ('florid' plaques, 'daisy-like' plaques) and other PrP plaques, and amorphous pericellular and perivascular PrP deposits especially prominent in the cerebellar molecular layer
GSS	Encephalo(myelo)pathy with multicentric PrP plaques
FFI	Thalamic degeneration, variably spongiform change in cerebrum
Kuru	Spongiform encephalopathy in the Fore population of Papua New Guinea

[1]From the World Health Organisation, http://www.WHO.int

1.4 Protein-only hypothesis of prion transmission

The transmissible nature of prion diseases was first demonstrated in 1937, when a population of Scottish sheep developed scrapie after inoculation against a common virus with a formalin extract of brain tissues unknowingly derived from an animal with scrapie. As aforementioned, scrapie was subsequently transmitted experimentally to sheep, goats and mice (Cuillé and Chelle, 1936; Cuillé and Chelle, 1939; Chandler, 1961). This was followed by the demonstration of transmission of human prion diseases such as kuru, CJD and GSS to monkeys (Gajdusek *et al*., 1966; Gibbs *et al*., 1968; Masters *et al*., 1981). The nature of the causative agent in prion diseases is the focus of much attention. Because of the unusually long incubation time of prion diseases, the agent was initially thought to be a slow virus (Cho, 1976). Further research, however, indicated that the agent differed substantially from viruses and other conventional agents. In 1967, Alper and colleagues reported that the disease agents were extremely resistant to treatments known to destroy nucleic acids, such as UV and ionising radiation (Alper *et al.,* 1967). In addition, the minimum molecular weight necessary for infectivity (~ 2 x 10^5 Da) was sufficiently small as to exclude viruses and any other known types of infectious agents (Alper *et al*., 1966). In 1967, Griffith introduced, for the first time, the possibility that the material responsible for disease transmission might be a protein that had the surprising ability to replicate in the body (Griffith, 1967). This 'protein-only' hypothesis of transmissible spongiform propagation was subsequently extended by Stanley Prusiner and colleagues, who chose the name 'prion' for this new proteinaceous infectious particle (Prusiner, 1982). According to the protein-only hypothesis the infectious agent in human and animal spongiform encephalopathies is composed exclusively of a single kind of protein

molecule, designated PrP^{Sc}, without any encoding nucleic acid (Cohen *et al*., 1994; Prusiner, 1998b; Collinge, 2001). PrP^{Sc} is, in fact, a conformationally altered form of normal host encoded membrane glycoprotein called PrP^{C} (Prusiner *et al*., 1991). These conformational changes are followed by alterations in other biochemical properties, such as protease resistance, solubility and ability to form large-order aggregates. PrP^{Sc} impresses its abnormal conformation on PrP^{C}, thereby generating additional molecules of PrP^{Sc} in an autocatalytic reaction. This self-propagating change in protein conformation therefore outlined a novel pathogenic mechanism specific for prion diseases.

A wealth of evidence has accumulated over the past decade supporting the protein-only hypothesis. As mentioned previousely, most familial cases of prion diseases are linked to mutation(s) in *PRNP* (Collinge, 2001; Prusiner, 1998b). These findings support the central role of PrP in disease pathogenesis; they also provide strong evidence in favour of the protein-only hypothesis by describing how a genetic disease could be propagated in an infectious way. Weissmann and colleagues showed that mice lacking the PrP gene were resistant to scrapie infection, neither developing clinical symptoms of scrapie nor allowing propagation of the disease (Bueler *et al*., 1993). They also demonstrated successful stable propagation of infectivity in neuroblastoma cells infected with brain homogenate containing PrP^{Sc} (Rubenstein *et al*., 1984; Race *et al*., 1987). A further milestone in the prion protein-only hypothesis was the discovery that pure PrP^{C}, and even recombinant PrP produced in E. coli can be converted into an abnormal conformer associated with disease. In their original system, Caughey and co-workers incubated radioactive PrP^{C} with unlabelled PrP^{Sc} in a cell-free system to show generation of radioactive PrP^{Sc}, as defined by its physical

properties (Kocisko *et al*., 1994). Interestingly, an increase in infectivity was not demonstrated in these experiments. A new *in vitro* conversion system called PMCA (protein misfolding cyclic amplification) has been shown to transform large quantities of PrP^{C} using a very low amount of PrP^{Sc} (Saborio *et al*., 2001). This system confirms the crucial feature of the protein-only hypothesis: prion replication is a cyclical process and prion propagation is maintained with newly produced PrP^{Sc} triggering further misfolding.

1.5 Prion gene structure

The PrP gene *(PRNP* in human, *Prnp* in mouse and PrP gene in other species) appears to be a single gene in the genomes of rodents, human and ruminants (Oesch *et al*., 1985; Westaway and Prusiner, 1986; Liao *et al*., 1986; Goldmann *et al*., 1990). It is located on the short arm of chromosome 20 in human and in the same region on the mouse chromosome two (Robakis *et al*., 1986; Sparkes *et al*., 1986). The PrP gene is highly conserved and so far it has been analysed in more than 70 species (Schätzl *et al*., 1995; Wopfner *et al*., 1999; Strumbo *et al*., 2001; Suzuki *et al*., 2002; Rivera-Milla *et al*., 2003). Beside mammals, the PrP gene is also found in birds (Harris *et al*., 1993b), marsupials (Windl *et al*., 1995), amphibians (Strumbo *et al*., 2001) and prion-related proteins have been identified in organisms such as Drosophila, the nematode Caenorhabditis elegans and even yeast (Westaway and Prusiner, 1986; Rivera-Milla *et al*., 2003; Premzl *et al*., 2003). The first description of an almost full-length PrP complimentary DNA (cDNA) in hamster (Oesch *et al*., 1985) was followed by descriptions of partial PrP gene sequences of other rodents, human, ruminants and a carnivore (Basler *et al*., 1986; Locht *et al*., 1986; Kretzschmar *et al*., 1986b; Liao *et*

al., 1986; Liao *et al*., 1987; Goldmann *et al*., 1990; Puckett *et al*., 1991; Goldmann *et al*., 1991; Kretzschmar *et al*., 1992).

The promoter region of the PrP gene has no TATA-Box but contains multiple copies of GC-rich repeats- a typical feature of house-keeping genes. These may acts as a binding for transcription factors SP-1 and AP-1 (McKnight and Tjian, 1986). All known PrP genes consist of one (*e.g.* in hamster, humans, wallaby) or two (*e.g.* in rat, mouse, bovine, sheep) short exons at the 5'- end and one bigger exon at 3'- end, the latter coding for the entire open reading frame (ORF) of the prion protein (Hsiao *et al*., 1989; Gabriel *et al*., 1992; Schätzl *et al*., 1995). The ORF exon of the PrP gene is about 85 % of the total messenger RNA (mRNA) length and since the entire protein-coding region is contained within one exon, the possibility of generating different proteins by alternative splicing of the mRNA is excluded (Basler *et al*., 1986; Westaway *et al*., 1994). PrP-mRNA is between 2.1 and 4 kb in length and codes for a protein of approximately 250 amino acids (aa) depending on species. In summary the PrP gene has a) a single exon for the entire PrP ORF and the entire 3' untranslated mRNA region b) one or two small exons coding for 5' leader sequence of PrP mRNA c) a promoter with regulatory elements and d) 1 or 2 introns separating the 5' exon(s) and promoter from the OFR exon.

1.6 Cell biology and life cycle of prion protein

1.6.1 PrP^C

Structure and biosynthesis

PrP^C is a normal cell surface glycosyl phosphatidylinosiol GPI-anchored protein which has a broad, diverse and developmentally regulated expression pattern.

This 30-35 kDa protein is expressed in skeletal muscle, kidney, heart, secondary lymphoid organs, and the CNS (Kretzschmar *et al*., 1986a; Moser *et al*., 1995). Within CNS, high PrP^{C} expression levels can be detected in synaptic membranes of neurons as well as astrocytes (Borchelt *et al*., 1994; Billette de Villemeur *et al*., 1995; Herms *et al*., 1999). In the periphery, PrP^{C} expression is detected on lymphocytes and at high levels on follicular dendritic cells (FDC) (Aguzzi and Polymenidou, 2004). PrP^{C} is encoded by the PrP gene (Section 1.5) and it consists of approximately 250 amino acids (Caughey *et al*., 1988; Diedrich *et al*., 1991).

This protein has an N-terminal signal peptide, a series of five proline and glycine-rich octapeptide repeats, a highly conserved hydrophobic domain (HD) in the centre, and a C-terminal hydrophobic region with a signal for addition of a GPI anchor (Figure 1-1) (Harris, 1999). Mutations in the N-terminal segment of PrP have been identified as the cause of some human prion diseases, raising the possibility that it may be an important factor in some PrP^{Sc} conformations and/or disease manifestation (Mead, 2006b; Mead *et al*., 2006; Hill *et al*., 2006). The octapeptide repeat region has been suggested to be important in association of PrP^{C} with copper and might be important in prion disease pathogenesis (Riek *et al*., 1998; Hosszu *et al*., 1999; Jackson *et al*., 2001). The internal HD (aa 112-135) of PrP was first described as a putative transmembrane domain (Lopez *et al*., 1990). Short peptides compromising amino acid residues 106-126 form fibrils *in vitro* (Tagliavini *et al*., 1993) and induce cell death in cultured cells (Brown *et al*., 1996; Forloni *et al*., 1993; Deli *et al*., 2000). Transgenic mice expressing PrP mutants lacking the HD (PrPΔHD) spontaneously develop a non-transmissible neurodegenerative disease (Baumann *et al*., 2007; Li *et al*., 2007b; Shmerling *et al*., 1998). Recently, it has been shown that the HD promotes

dimer formation of PrP, which is linked to a stress-protective activity (Rambold *et al*., 2008).

Structural studies of mature PrP^C have demonstrated that mouse, human, cattle and Syrian hamster share common PrP^C features including a long, flexible N-terminal tail (residues 23-128), three α-helices (residues 144-154, 175-193 and 200-219) and a two-stranded anti-parallel β-sheet (residues 128-131 and 161-164) that flanks the first α-helix. The carboxyl terminus of PrP^C is stabilised by a disulfide bond linking helices two and three (Riek *et al*., 1997) (Figure 1-1). Nuclear magnetic resonance (NMR) spectroscopy of mouse PrP has shown that the second β-sheet is connected to the third α-helix by a large loop which is very flexible in most species, with the exception of elk and deer (Gossert *et al*., 2005). This structural peculiarity might be related to susceptibility of elk and deer to develop CWD.

Like other membrane proteins, PrP^C is synthesised in the rough endoplasmic reticulum (ER) and travels to the membrane through the Golgi apparatus. During its biosynthesis, PrP^C undergoes several post-translational modifications, including cleavage of the amino (N)-terminal signal peptide, addition of N-linked oligosaccharide chains at two sites (asparagine residues 181 and 197), formation of a disulfide bond and attachment of a GPI anchor following cleavage of the C-terminal hydrophobic peptide, which facilitates its association with specific lipid membrane domains called ‘’rafts’’ (Harris, 2003; Campana *et al*., 2005). Studies on purified hamster PrP^C and PrP^{Sc} have demonstrated that there are at least fifty different sugar chains capable of attaching to the glycosylation sites, with differences between the two isoforms (Endo *et al*., 1989; Somerville and Ritchie, 1990; Rudd *et al*., 1999; Rudd *et al*., 2001). Prion protein is always isolated as a mixture of three forms; non-, mono-, or

di-glycosylated (Haraguchi *et al.*, 1989) and its final, processed form contain amino acids 23–231 from the original translation product of 254 amino acids.

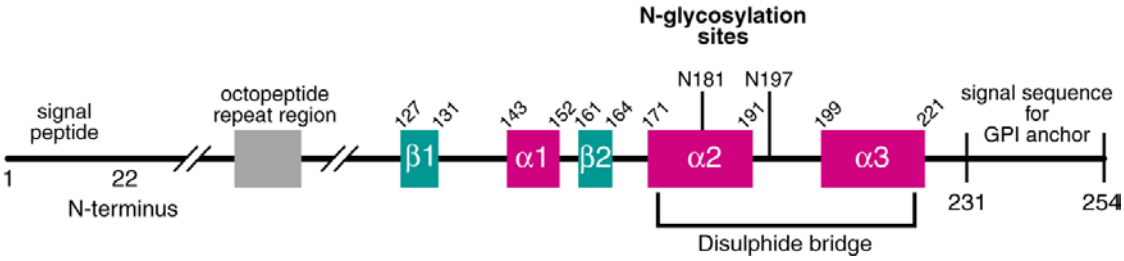

Figure 1-1 Schematic representation of the domain structure of murine PrP

The N- and C-terminal signal peptides are cleaved from the translation product and a GPI anchor is attached to the C-terminal end of the protein. The molecule can be N-glycosylated twice, and a disulphide bond is built. The final product consists of 209 aa.

Localisation and trafficking

To date, the precise cellular localisation of PrP^C in neurons remains elusive. Most studies have shown that PrP^C is predominantly present in detergent-resistant microdomains (DRM or lipid rafts) on the plasma membrane, in particular in the axon or synaptic membrane (Mironov *et al.*, 2003). Other putative sites of PrP^C localisation are: the ER (Sarnataro *et al*., 2004), the Golgi (Magalhaes *et al*., 2002), endolysosomes (Magalhaes *et al*., 2002), exsosomes (Fevrier *et al*., 2004), the plasma membrane (Sarnataro *et al*., 2002), clathrin coated pits (Sunyach *et al*., 2003), caveolae (Peters *et al*., 2003), lipid rafts (Vey *et al*., 1996; Kaneko *et al*., 1997a), and the cytosol (Mironov *et al*., 2003). Although PrP^C is known as a cell-surface GPI-anchored protein, it does not remain on the cell surface; it constitutively cycles between the plasma membrane and an endocytic compartment from which most of the PrP^C is recycled back to the cell surface (Shyng *et al*., 1993). More than 90 % of surface PrP^C is internalised within two minutes and returned to the cell surface within six minutes (Sunyach *et al*., 2003). During this process, PrP^C is cleaved near residue 110, probably in an acidic cellular compartment (Harris *et al*., 1993a). The biological role of PrP^C internalisation is unknown, but studies have demonstrated that internalisation is induced by copper and zinc ions and thus could have a physiological function in chelating extracellular copper ions or in modulating the signal activity of the protein (Pauly and Harris, 1998; Lee *et al*., 2001b; Watt and Hooper, 2003). Understanding the endocytic itinerary of PrP^C is fundamental, since data in the literature indicate that both general inhibition of endocytosis (Grigoriev *et al*., 1999; Godsave *et al*., 2008) and/or a direct modification of the internalization route of PrP^C, by replacing the GPI anchor with a transmembrane sequence containing a coated pits localization motif (Fournier *et*

al., 2000) affect both the infection and the conversion processes (Caughey *et al*., 1991; Borchelt *et al*., 1992; Beranger *et al*., 2002; Veith *et al*., 2008).

The mechanism of PrP^C uptake is currently debated and dynamin, clathrin-coated pits, rafts and caveolae appear to be involved (Figure 1-2). Immunogold localisation of PrP^C in clathrin coated pits and vesicles suggest that PrP^C internalises via clatrin-mediated endocytosis (Sunyach *et al*., 2003; Sarnataro *et al*., 2009). Magalhaes and co-workers also demonstrated that cells transfected with a dominant negative mutant of dynamin I (K44A), which blocks fission of invaginated coated pits from the plasma membrane, inhibited PrP^C endocytosis suggesting that PrP^C is internalised via a dynamin dependent pathway (Magalhaes *et al*., 2002). A basic amino acid motif in the N-terminal half of PrP^C polypeptide chain was shown to be essential for efficient clathrin-mediated endocytosis as deletion within this region diminishes internalisation of PrP^C (Sunyach *et al*., 2003). This finding led to the proposal that PrP^C binds through this N-terminal region to a 'PrP^C receptor', a transmembrane protein, that has a coated-pit localisation signal causing it to enter the clathrin-dependent internalisation pathway. Several candidate proteins have been proposed as PrP-interacting partners including 37-kDa laminin receptor precursor (Lee *et al*., 2003). It is believed that this receptor can only account for 25-50 % of all protein internalisation (Section 1.6.1, 'PrP^C partners in endocytosis') (Lee *et al*., 2003). Parkyn and colleagues also showed that low-density lipoprotein receptor-related protein 1 (LRP1), which binds to multiple ligands through basic motifs, associates with PrP^C during its endocytosis and is functionally required for this process (Parkyn *et al*., 2008).

In Chinese hamster ovary cells, which express caveolin-1, PrP^C is absent in clathrin-coated pits and vesicles, instead being localised in caveolae at the *trans*-Golgi network, the plasma membrane and in interconnecting chains of endocytic caveolae (Peters *et al*., 2003). To date, however, no caveolae have been identified in adult mammalian neuronal cells, suggesting this pathway is unlikely to be relevant to prion trafficking in neurons (Morris *et al*., 2006).

An alternative hypothesis regarding PrP^C internalisation involves lipid rafts, also called caveolae-like domains (CLDs) (Figure 1-2), which have similar lipid composition to caveolae but lack cavealin-1 (Orlandi *et al*., 1998; Sabharanjak *et al*., 2002; Deinhardt *et al*., 2006). Studies have suggested that PrP^C internalisation can be raft-dependent and/or raft-mediated depending on the cell type. Sarnataro and colleagues demonstrated that PrP^C is internalised in Fischer rat thyroid (FRT) cells via raft-mediated endocytosis. Cholesterol depletion and inactivation of cell division cycle 42 (Cdc-42) in FRT cells impaired uptake of PrP^C, suggesting a role for lipid rafts in PrP^C endocytosis. In the same cells, Inhibition of clathrin-dependent endocytosis by knock down of clathrin and by the expression of dominant negative epidermal growth factor receptor substrate 15 (Eps15) and Dynamin 2 mutants impaired PrP^C internalisation suggesting that a clathrin-dependent pathway was also participating in PrP^C endocytosis as well as lipid rafts (Sarnataro *et al*., 2009). Co-immunoprecipitation of PrP^C with clathrin and detergent-insoluble microdomains during internalization indicates that rafts and clathrin cooperate in the internalization of PrP^C (Sarnataro *et al*., 2009). Moreover, a raft-mediated mechanism for PrP^C internalization has been described in primary neurons and GT-1 cells (Schatzl *et al*., 1997; Galvan *et al*., 2005; Sarnataro *et al*., 2009). In contrast, Sunyach *et al*. and other

researchers have reported that PrP^C in N2a cells leaves lipid rafts to enter non-raft membrane from where it is internalized by the classical clathrin-mediated pathway (Sunyach *et al*., 2003; Morris *et al*., 2006). Recent work by Wadia and colleagues reported that recombinant PrP internalisation in N2a neuroblastoma cells is sensitive to cholesterol depleting agents and macropinocytosis inhibitors. This suggests that raft-dependent macropincytosis may also play a role in PrP uptake (Wadia *et al*., 2008).

In summary, the above studies support the hypothesis that PrP^C can be internalized by different mechanisms in different cell types, presumably reflecting differences in the expression of partner proteins that determine the trafficking of PrP^C that lacks a cytoplasmic domain into which endocytic trafficking motifs could be embedded. On N2a cells, PrP^C is endocytosed constitutively by means of coated pits (Shyng *et al*., 1994; sunyach *et al*., 2003); whereas cells that do not endogenously express PrP^C but transfected with a vector encoding PrP^C can require Cu^{2+} to initiate coated pit endocytosis (Taylor and Hooper, 2007) or else slowly internalise PrP^C by non-coated pit mechanisms (Peter *et al.*, 2003). The discovery of multiple endocytic pathways of PrP^C could be crucial in determining the ability of different strains to infect, replicate and induce cell death. Moreover, entry through distinct endocytic pathways in response to different stimuli could allow PrP^C to exert both the neuroprotective and neurodegenerative functions with which it has previously been associated.

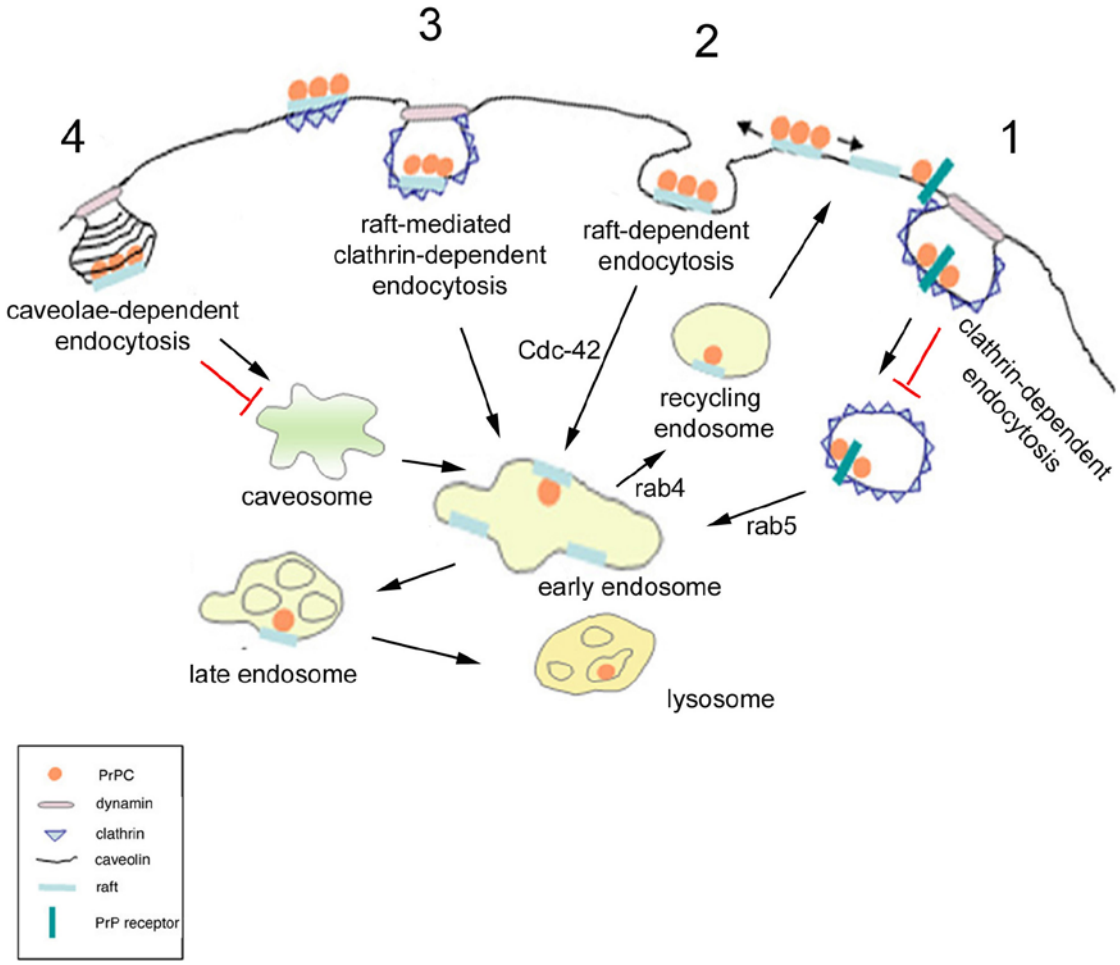

Figure 1-2 Pathways of PrP^C internalisation[2]

Internalization of PrP^C molecules can occur throughout many different pathways: the classical, clathrin-mediated pathway (1); the clathrin-independent raft-dependent pathway (2); the raft-mediated clathrin-dependent route (3) and caveolae (4). At the cell surface, PrP^C is localized in DRM. As PrP^C remains in these domains during its internalization a classical clathrin-dependent pathway (1) seems to be excluded. Conversely, PrP^C can undertake a rafts dependent pathway (2) and/or rafts might promote its recruitment to clathrin domains inducing its internalization (3). PrP^C resides in caveolae at the plasma membrane but is not internalized via the caveolae pathway (4).

[2]Reprinted from PLoS one, Vol 4, Sarnataro *et al.*, Lipid Rafts and Clathrin Cooperate in the Internalization of PrP^C in Epithelial FRT Cells, 2009, pp 5829-5844.

PrP^C partners in endocytosis

Different proteins have been proposed to bind to and act as endocytic partners of PrP^C. The basic residues (^{NH2}KKRPKP-) of the PrP^C N-terminal domain of PrP^C, which is necessary for coated pit endocytosis, have been identified as a major heparin sulphate/glycosoaminoglycan binding site (Sunyach *et al*., 2003; Pan *et al*., 2002; Warner *et al*., 2002). These residues also serve as binding motifs for extracellular cargos by binding to low density lipoprotein (LDL) receptor-related protein (LRP1). Recently, Parkyn *et al.* showed that LRP1 associates with endogenous PrP^C on the neuronal cell surface leading to PrP^C internalisation (Parkyn *et al*., 2008). In addition, LRP1 binds to PrP^C to facilitate its trafficking to the neuronal surface. Taylor and colleagues demonstrated that LRP1 is required for Cu^{2+}-dependent endocytosis of exogenous PrP^C in SH-SY5Y cells (Taylor *et al*., 2005). Cu^{2+} draws PrP^C from lipid rafts prior to its endocytosis (Taylor and Hooper, 2007). Non-integrin laminin receptor precursor (LRP; 37 kDa) and the mature laminin receptor (LR; 67 kDa) have also been reported to bind to recombinant PrP, suggesting a role as cell-surface receptors for PrP^C (Rieger *et al*., 1997; Gauczynski *et al*., 2001; Hundt *et al*., 2001), further research is required to assess whether these findings are also applicable to endogenously expressed PrP^C.

PrP^C function

The amino acid sequence of mammalian PrP^C is highly conserved between different species and suggests an important physiological role. Studies have demonstrated that both embryonic PrP^C-null and adult-onset PrP^C knock-out mice show no clear phenotypes (Bueler *et al*., 1992; Mallucci *et al.*, 2002). Importantly, PrP^C knock-out mice are completely resistant to prion disease following inoculation

and do not replicate prions (Bueler *et al*., 1993). However, embryonic PrP^{C}-null mice have been shown to develop abnormalities in synaptic physiology, circadian rhythm and sleep patterns (Collinge *et al*., 1994; Tobler *et al*., 1996). Furthermore, PrP^{C} knock-out mice display a reduction in the slow after-hyperpolarisations evoked by trains of action potentials (Tobler *et al*., 1996).

PrP^{C} has been implicated in a wide range of cellular functions: transport and metabolism of copper and/or zinc ions (Watt and Hooper, 2003; Brown, 2001), protection from oxidative stress (Brown, 2001), cellular signalling (Chiarini *et al*., 2002), membrane excitability (Mallucci *et al*., 2002), synaptic transmission (Collinge *et al*., 1994), neuritogenesis (Graner *et al*., 2000), self-renewal of hematopoietic stem cells (Zhang *et al*., 2006), differentiation of neuronal stem cells (Steele *et al*., 2006) and apoptosis (Solforosi *et al*., 2004). PrP^{C} can achieve these functions through its interaction with different partners, ligands and/or effectors, such as laminin, the chaperone BiP, glial fibrillary acidic protein (GFAP) and Bcl-2, at different locations in the cell (Lee *et al*., 2003; Campana *et al*., 2005). Recently, links between Alzeimer's disease (AD) and prion diseases have been proposed as PrP^{C} was shown to inhibit β-secretase cleavage of amyloid precursor protein (APP) and reduce Aβ formation (Parkin *et al*., 2007). As above mentioned, endogenous PrP^{C} is reported to associate with LRP1 on the cell surface and facilitate its internalisation (Parkyn *et al*., 2008). Furthermore, the same study showed that PrP^{C} binds to LRP1 in biosynthetic compartments to enable its trafficking to the neuronal surface. It remains unclear whether prion disease pathology arises from a loss of normal PrP^{C} function or a toxic gain of function by PrP^{Sc} (Campana *et al*., 2005), or more likely, a combination of both.

1.6.2 PrP^{Sc}

Structural and biochemical properties

It has been indicated that PrP^{C} and PrP^{Sc} are chemically identical; however, the biophysical features of PrP^{Sc} are significantly different from PrP^{C} in respect to solubility, structure and stability (Riesner, 2003). PrP^{C} has a high α-helix content (about 42 %) and relatively little β-sheet (about 3 %), whereas PrP^{Sc} is composed of around 30 % α-helices and 45 % β-sheet (Gasset *et al*., 1993; Pan *et al*., 1993; Pergami *et al*., 1996). Unlike PrP^{C}, PrP^{Sc} is detergent insoluble (Riesner, 2003) preventing detailed structural analysis by NMR or X-ray analysis. Electron microscopy and spectroscopic analysis of 2D crystalline-like arrays of PrP^{Sc} led to the development of an *in vitro* PrP^{Sc} model (Pan *et al*., 1993; Wille *et al*., 2002). In this model, the α-helical N-terminus of PrP^{Sc} is located on the inner part of the hexagonal unit, helices two and three face outwards and glycosyl-groups point towards the inter-hexagonal space. This structure does not offer a definitive description of PrP^{Sc}, but remains the best model described to date.

PrP^{C} is almost completely degraded with proteinase K (PK). In contrast, only the N-terminal domain of PrP^{Sc} (up to aa 23-90) is digested with PK (Prusiner *et al*., 1984; Oesch *et al*., 1985) leaving a well defined resistant core of apparent mass 27-30 kDa. This structure is termed $PrP^{27\text{-}30}$ and is known to be fully infectious (Turk *et al*., 1988) (Figure 1-3 A). Therefore, there is a clear biochemical distinction between the two isoforms of the prion protein (PrP^{C} and PrP^{Sc}). Western blot analysis of PrP following SDS-PAGE shows a characteristic three band pattern (*i.e*. without, with one and with two glycosyl groups). On PK digestion of uninfected samples, the triplet pattern disappears completely. In samples containing PrP^{Sc} bands remain at a similar

intensity but shift to lower molecular weights (Riesner, 2003) (Figure 1-3 B). The protease-resistant core of PrP^{Sc} re-arranges into amyloid rods, which stain with Congo red and show green-gold birefringence, typical of amyloids (Prusiner *et al*., 1983). As well as PK, PrP^{Sc} is also resistant to the protease thermolysin used for diagnosis of animal prion diseases (Owen *et al*., 2007). This thermostable protease cleaves at the hydrophobic residues Leu, Ile, Phe, Val, Ala and Met. These residues are absent in the protease accessible N-terminal region of PrP^{Sc} (Owen *et al*., 2007). Thus, PrP^{c} is fully digested with thermolysin, whilst full-length PrP^{Sc} remains resistant. This contrasts with PK digestion where an N-terminally truncated PrP^{Sc} species is produced, $PrP^{27–30}$. In general, routine tests presently available for BSE and scrapie are based on the PK resistance of $PrP^{27–30}$. Recently, however, thermolysin has been used in the diagnosis of prion diseases such as ovine scrapie, BSE and variant CJD and produced comparable sensitivity to assays using proteinase K digestion (Owen *et al*., 2007).

In addition to PK and thermolysin, cathepsin D is also reported to digest sequences in PrP. The protease targets the C-terminal end of PrP^{Sc}, liberating the GPI anchor, with no effect on amplification of PrP^{Sc} or prion infectivity (Lewis *et al*., 2006). Chesebro *et al*., generated a transgenic mouse line that expresses GPI-anchorless secreted PrP. When infected with the Rocky Mountain laboratory (RML) strain of mouse prions, the mice produce widespread deposits of PrP^{Sc} without evidence of a clinical syndrome (Chesebro *et al*., 2005), thereby suggesting that the GPI anchor is not a prerequisite for prion propagation. Unlike PrP^{C}, which can be readily cleaved from membranes by treatment with phosphatidylinositol-specific phospholipase C (PIPLC) (Stahl *et al*., 1987), PrP^{Sc} is resistant to such treatment (Caughey *et al*., 1990; Borchelt *et al*., 1993). This suggests that the conversion of PrP^{C}

to PrP^{Sc} involves a conformational change (Pan *et al*., 1993; Cohen *et al*., 1994) rather than a covalent modification (Stahl *et al*., 1993).

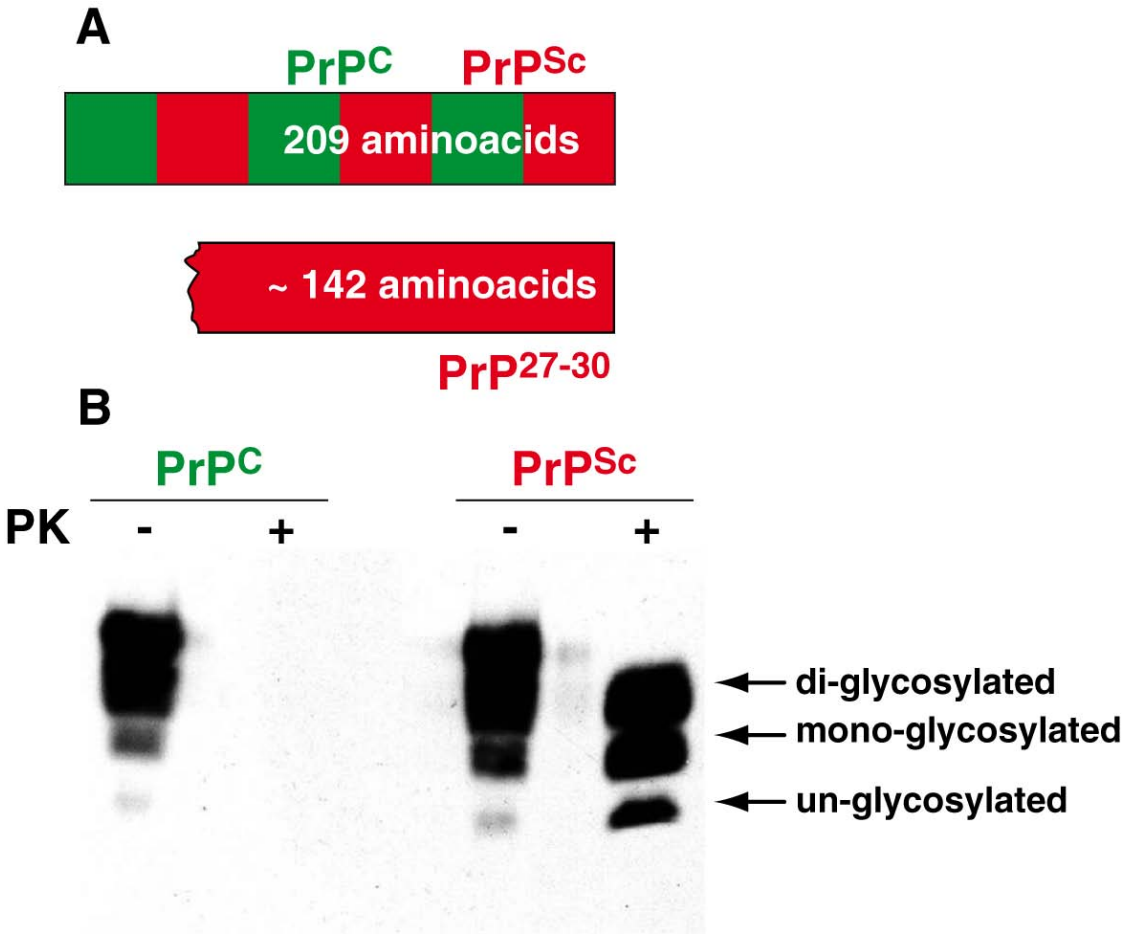

Figure 1-3 Proteinase K resistance of PrP[3]

(A) 'Full-length' and N-terminal truncated PrP are presented in this panel. Only the N-terminal domain of PrP^{Sc} is digested with proteinase K (PK), leaving resistant core of apparent mass 27-30 kDa. PrP^{27-30} is known to be fully infectious. **(B)** A denaturing polyacrylamide gel electrophoresis with antibody staining shows characteristic three band pattern of prion protein (di-glycosylated, mono-glycosylated and un-glycosylated). Note the triplet pattern disappears completely in non-infected sample (PrP^{C}) after PK digestion. However, in PK-digested samples containing PrP^{Sc} the triplet bands remain similar but shifts to lower molecular weights.

[3]Rienser D, Biochemistry and structure of PrP^{C} and PrP^{Sc}, Br Med Bull, 2003, 66: 21-33, by permission of Oxford University Press.

Cellular localisation of PrP^{Sc}

Investigation of the sub-cellular distribution of PrP^{Sc} remains challenging due to the lack of antibodies specific to PrP^{Sc}. Early studies reported that the majority of PrP^{Sc} is intracellular, mostly co-localised with Golgi markers and sequestered within lysosomes of scrapie-infected N2a (ScN2a) cells (Caughey *et al*., 1991; McKinley *et al*., 1991b; Borchelt *et al*., 1992). Vey *et al.*, demonstrated accumulation of PrP^{Sc} in CLDs derived from the plasma membrane in ScN2a cells (Vey *et al*., 1996). In prion-infected brains, PrP^{Sc} accumulates at the plasma membrane (Caughey and Raymond, 1991) and occasionally in structures which contain the cation-independent mannose 6-phosphate receptor, ubiquitin-protein conjugates, β-glucuronidase, and cathepsin B, termed late endosomal/lysosomal compartments (Arnold *et al*., 1995; Veith *et al*., 2008). More recent reports have described the accumulation of PrP^{Sc} in various cellular compartments: the perinuclear Golgi region of neurons in scrapie-infected transgenic mice (Barmada and Harris, 2005); the late endosomal compartments in infected GT1-7 and N2a cells (Pimpinelli *et al*., 2005) and the cell surface and early endocytic/ recycling vesicles in hippocampal neurons (Godsave *et al*., 2008). In SN56 cells and hamster cortical neurons, exogenous Alexa-labelled PrP^{Sc} internalised into vesicles which stain positive for late endosomal/lysosomal markers (Magalhaes *et al*., 2002). Mange *et al.* showed accumulation of PrP^{Sc} in the nuclei of prion-infected N2a cells (Mange *et al*., 2004) by demonstrating that nuclear PrP interacts with chromatin *in vivo*. Several *in vitro* studies have shown accumulation of PrP^{Sc}-like conformers (prion protein conformers that are not necessarily infective) in the ER (Lehmann and Harris, 1997; Ivanova *et al*., 2001), Golgi (Ivanova *et al*., 2001) and plasma membrane of infected cells (Ivanova *et al*., 2001). Under certain conditions, PrP^{Sc}-like conformers

have been reported to accumulate in the cytosol (Ma and Lindquist, 2002) and there is also evidence for cytosolic PrP^{Sc}-containing aggresomes in prion-infected cells following proteasome inhibition (Kristiansen *et al*., 2005). The tentative conclusion from these studies is that PrP^{Sc} is widely distributed within infected cells, although improved methods for in-situ detection of PrP^{Sc} are clearly needed to establish the relative proportion of the protein in these cellular sites.

PrP^{Sc} trafficking

In contrast to PrP^{C}, the trafficking of PrP^{Sc} is less well described. This is due to the fact that the site of conformational conversion of PrP^{C} to PrP^{Sc} has not been identified. Several studies have suggested that the PrP conversion could take place at the plasma membrane, where the first contact between endogenous PrP^{C} and exogenous PrP^{Sc} is likely to occur (Prado *et al*., 2004). Alternatively, the conversion may take place immediately after internalisation into the endolysosomal compartment (Borchelt *et al*., 1992).

Several studies indicate that PrP^{Sc} production is a post-translational event that occurs after PrP^{C} reaches the plasma membrane (Caughey and Raymond, 1991; Borchelt *et al*., 1992; Taraboulos *et al*., 1992). PrP^{Sc} formation can be prevented by exposure to monoclonal anti-PrP antibodies and PIPLC digestion which removes PrP^{C} from the cell surface (Enari *et al*., 2001). Taraboulos *et al.* found that treatment of ScN2a and scrapie-infected hamster brain (ScHaB) cells with brefeldin A (BFA) inhibits PrP^{Sc} synthesis by preventing PrP^{C} exit from the ER-Golgi (Taraboulos *et al*., 1992). Thus, transport of PrP^{C} to the plasma membrane is important in production of PrP^{Sc}.

In addition to the plasma membrane, the endocytic pathway has been implicated in the conversion of PrP^{C} to PrP^{Sc} (Borchelt *et al*., 1992; Taraboulos *et al*., 1992). In fact, blocking the endocytosis and internalisation of PrP^{C} by lowering the temperature is known to inhibit PrP^{Sc} formation (Borchelt *et al*., 1992). Biochemical analysis of PrP^{Sc} has revealed N-terminal truncation by endogenous proteases in lysosomes (Caughey *et al*., 1991; Borchelt *et al*., 1992). These results imply that the conversion of PrP^{C} to the protease-resistant state occurs in the plasma membrane or along an endocytic pathway, before PrP^{Sc} is exposed to proteases within endo-lysosomal compartments. Impairment of plasma membrane recycling through expression of dominant-negative mutant Rab4 (GDP-bound $Rab4^{S22N}$ mutant) in ScN2a cells results in an accumulation of PrP^{Sc}, suggesting that PrP^{Sc} formation occurs within an intracellular compartment (Beranger *et al*., 2002). A recent study by Marijanovic and colleagues suggested that prion conversion occurs in the endosomal recycling compartments (ERC), rather than early or late endosomes (Marijanovic *et al*., 2009). Another recent study by Wadia *et al.* showed that inhibition of macropinocytosis in N2a cells was sufficient to prevent conversion of PrP^{C} to PrP^{Sc} indicating that pathogenic amplification of PrP^{Sc} may occur in macropinosomes (Wadia *et al*., 2008).

Several lines of evidence suggest a role for rafts in the formation of PrP^{Sc} in scrapie infected cultured cells: a) both PrP^{C} and PrP^{Sc} are found in rafts (Taraboulos *et al*., 1995; Vey *et al*., 1996; Naslavsky *et al*., 1997; Baron *et al*., 2002; Botto *et al*., 2004); b) cholesterol depletion diminishes PrP^{C} degradation and PrP^{Sc} formation in ScN2a cells (Taraboulos *et al*., 1995); c) recombinant transmembrane forms of PrP^{C} which are not directed to rafts do not seed PrP^{Sc} formation in ScN2a cells (Taraboulos

et al., 1995; Kaneko *et al*., 1997b) and (d) treatment with pharmacological compounds disrupting rafts inhibits PrP^{Sc} synthesis (Taraboulos *et al*., 1990a; Marella *et al*., 2002). Thus, membrane lipid rafts are a clear candidate site for PrP^{Sc} conversion in cells.

Once PrP^{Sc} forms, it appears to accumulate on the cell surface, in intracellular vesicles such as lysosomes or autophagosomes, or in extracellular deposits (Jeffrey and Gonzalez, 2004). Internalised PrP^{Sc} can undergo retrograde transport to the Golgi apparatus and/or the ER, thereby disrupting the biogenesis of newly formed PrP^{C} and triggering the production of PrP^{Sc} from PrP^{C} precursor (Campana *et al*., 2005). Stimulating retrograde transport of PrP^{c} in the ER through over-expression of the constitutively active, small GTPase Rab6a leads to increased production of PrP^{Sc} in infected cells (Beranger *et al*., 2002). This suggests that the ER might have a significant role in the formation and production of PrP^{Sc}. Several studies have suggested that the presence of a mutation in the PrP gene favours spontaneous conversion of PrP^{C} to PrP^{Sc} in the ER, without contact with exogenous prions (Harris, 2003). Thus, it appears that the ER has two possible roles in the conversion of PrP^{C} to PrP^{Sc}. Firstly, in inherited prion diseases, the ER could be directly involved in mutant PrP^{C} conversion to PrP^{Sc} (Harris, 2003). Secondly, in infectious prion diseases, the ER could act as a site of amplification for PrP^{Sc} produced elsewhere in the cell (Campana *et al*., 2005).

Various mechanisms have been proposed to account for the spread of PrP^{Sc} infectivity between cells. PrP^{Sc} may transfer from one cell to another in exosomes secreted upon fusion of multivesicular endosomes with the plasma membrane. Studies have shown that exosomes bearing PrP^{Sc} are infectious (Fevrier *et al*., 2004). Alternatively, the spread of prions may be mediated by direct cell-surface contact

between PrP^{C} on uninfected neurons and PrP^{Sc} on infected neurons (Kanu *et al*., 2002). This hypothesis is supported by reports of infection by contact with contaminated stainless steel wires (Flechsig *et al*., 2001). Uninfected neurons can also incorporate PrP^{Sc} from the extracellular milieu using heparin sulphate proteoglycan (HSPG) and LRP/LR, distributing it along neural pathways and initiating propagation of new PrP^{Sc} (Morris *et al*., 2006). Recent evidence suggests that prions can be transferred from immune cells to neurons and between neurons via tunnelling nanotubes (TNTs) (Gousset *et al*., 2009). TNTs connect dendritic cells (DC) to primary hippocampal neurons and cells of CNS. These conduits permit the intracellular transfer of endogenous and exogenous PrP^{Sc} within neurons in the CNS and from the peripheral site of entry to the peripheral nervous system (Gousset *et al*., 2009).

1.7 Mechanisms of prion conversion

PrP^{C} is known to be essential for production and propagation of PrP^{Sc} since PrP knock-out mice can neither be infected nor transmit the disease (Bueler *et al*., 1993). Prion conversion from PrP^{C} to PrP^{Sc} is characterised by the formation of a large β-sheet structure from two shorter β-sheets and the first α-helix. The precise mechanisms underlying structural conversion remain unclear; however both the α-helices and intramolecular disulfide bond must be preserved for PrP^{Sc} infectivity (Hornemann *et al*., 1997; Prusiner, 1998b; Wille *et al*., 2002).

The current model of prion propagation proposes that PrP fluctuates between a native state, PrP^{C}, and a series of minor conformations, a subset of which can self-associate to form a stable supra-molecular structure, PrP^{Sc}, composed of misfolded PrP monomers. Studies using a recombinant protein mimetic of PrP^{Sc}, β-PrP, have shown that β-PrP aggregation occurs until it reaches a critical size at which a stable ‘seed’

structure is formed. Following this, the recruitment of unfolded PrP and/or β-PrP monomers can lead to an explosive, auto-catalytic formation of PrP^{Sc} (Brown et al., 1990; Jarrett and Lansbury, 1993; Caughey et al., 1995). Such a mechanism could explain all three aetiologies (sporadic, inherited and acquired) of human prion disease. Initiation of this pathogenic self-propagating conversion reaction, with accumulation of aggregated β-PrP, may be induced following exposure to a 'seed' of aggregated β-PrP following prion inoculation, as a rare stochastic conformational change, or as an inevitable result of expression of a pathogenic mutant PrP^{C} form, which is prone to form β-PrP (Collinge, 2005). Currently, it is unacquainted whether certain cofactors are needed for each or some steps in the PrP^{Sc} or amyloid formation, respectively.

1.8 Prion strains and species barriers

The protein-only hypothesis postulates that both pathogenic and infectious PrP^{Sc} consists only of protein and is derived from the normal prion protein isoform, PrP^{C} (Prusiner, 1982). There are several lines of evidence that support the protein-only hypothesis (Section 1.4). The existence of distinct strains or isolates in the absence of informational nucleic acid has proved challenging to accommodate within this model. Mammalian prion strains are classically defined by their different incubation times and neuropathological profiles in the CNS. Differences in glycosylation pattern and degrees of PK-resistant resolved by SDS-PAGE (Collinge *et al*., 1996; Safar *et al*., 1998) support the notion of different PrP^{Sc} strains (Telling *et al*., 1996b; Scott *et al*., 1997).

Prion strains can be serially propagated in inbred mice of the same genotype; therefore, they cannot be encoded by differences in PrP primary structure. Moreover, strains can be re-isolated in mice after passage in intermediate species with different

PrP primary structures (Bruce *et al*., 1994). Serial propagation of two distinct strains of TME prions (hyper (HY) and drowsy (DY)) in hamsters provided support for the idea that strain specificity is encoded by PrP structure alone. These strains showed different physicochemical properties of PrP^{Sc} (Bessen and Marsh, 1992; Bessen and Marsh, 1994). For example, HY and DY showed strain-specific migration patterns of PrP^{Sc} on polyacrylamide gels following limited proteolysis. Several human PrP^{Sc} types have also been identified and are associated with different CJD phenotypes (Collinge *et al*., 1996; Parchi *et al*., 1996). These types are distinguished diagnostically by the different fragment sizes of PK-treated samples on western blot. In summary, different prion strains seem to originate from different three-dimensional conformations of PrP^{Sc}, and different properties of the prion strains are likely to be encoded in different folds of PrP^{Sc}.

Infectious PrP^{Sc} has the capacity to infect across a range of species. This infectivity is restricted by a 'species barrier' (Pattison, 1965). When passaging prions from species A to species B, those that develop the disease have longer and more variable incubation periods than affected animals of the same species. Additionally, species B show an altered neuropathological distribution (Schatzl, 2003). During serial passages, the incubation period shortens in the foreign host and stable pathological properties are acquired (Kimberlin and Walker, 1979; Laurent, 1998). It has been hypothesised that the species barrier, and thereby transmission of prion diseases, is encoded by the PrP primary sequence (Scott *et al*., 1989; Scott *et al*., 1992; Scott *et al*., 1993; Telling *et al*., 1994; Priola *et al*., 2001). This hypothesis is supported by studies showing that transgenic mice expressing hamster PrP were, unlike wild type mice, highly susceptible to infection with Sc237 hamster prions (Prusiner *et al*., 1990).

Another line of evidence supporting the above hypothesis is that acquired or sporadic CJD mostly occurs in individuals homozygous at polymorphic residue 129 of PrP (Collinge *et al*., 1991b; Palmer *et al*., 1991; Collinge, 2001). Furthermore, in heterologous systems in which two different strains of prion protein are co-expressed, only the prion protein homologous to the pathogenic isoform is converted into the PK-resistant, pathogenic form. Studies with chimeric prion protein revealed that a defined sequence region (aa 112-187) is responsible for sequence specificity (Scott *et al*., 1992; Priola *et al*., 1995; Priola and Chesebro, 1995).

Human prion disease transmission studies have revealed an interesting connection between species barrier and prion strains. Sporadic CJD prions can be transmitted efficiently to transgenic mice expressing human PrP^C, but encounter a significant barrier on transmission to wild type mice (Collinge *et al*., 1995; Hill *et al*., 1997). Conversely, variant CJD prions transmit readily to wild type mice, whereas transmission to transgenic mice expressing human PrP^C is relatively inefficient (Hill *et al*., 1997). Therefore, since PrP molecules with identical amino acid sequences, but different strains have distinct patterns of transmissibility, the term 'transmission barrier' might be more appropriate than 'species barrier' (Collinge, 1999).

1.9 Prion mediated neurotoxicity

Despite extensive knowledge regarding the nature of the prion disease infectious agent, mechanisms of replication and associated neuropathology, the molecular pathways of neurotoxicity remains unclear. The ultimate cause of cell death mediated by prions appears to be caused via apoptosis; however the underlying mechanisms are still poorly understood. This section summarises current knowledge of prion mediated neurotoxicity.

1.9.1 PrP^{Sc} as the neurotoxic species

It has been proposed that prion mediated neurotoxicity may result from a toxic gain of function of PrP^{Sc}. Both full length PrP^{Sc} (Hetz *et al*., 2003) and shorter PrP peptides are toxic to primary neuronal cultures *in vitro* (Forloni *et al*., 1993), however their relevance to *in vivo* pathogenesis is under debate. For example, primary neuronal cultures underwent cell death when exposed to a low concentration of PrP106-126 (Forloni *et al*., 1993). Importantly, the PrP106-126 peptide has never been detected *in vivo*. Full length PrP^{Sc} has been shown to induce apoptosis *in vitro* in neuroblastoma cells with the induction of ER-stress and activation of caspase-12 (Hetz *et al*., 2003). In addition, there is evidence that exogenous PrP^{Sc} can induce the release of chemokines such as RANTES (regulated upon activation, normal T cell expressed, and secreted) that recruit microglia, which in turn could secrete neurotoxic factors (Marella *et al*., 2004). Kristiansen *et al*., demonstrated that PrP^{Sc} directly inhibits proteasome activity *in vitro* (Kristiansen *et al*., 2007). Furthermore, reduced proteasome activity was detected in prion infected cells and mice. These results suggest that PrP^{Sc} may access the cytosol of infected cells and inhibit the proteasome to cause neuronal death during disease pathogenesis through many different mechanisms, as the proteasome is involved in transcriptional regulation, cell cycle control, and control of apoptosis (Goldberg, 2003).

Whilst purified PrP^{Sc} is known to be neurotoxic at very low concentrations, several observations suggest this model is likely to be an oversimplification. For example, *Prnp* knockout mice do not show characteristic neurodegeneration, despite PrP^{Sc} deposition (Mallucci *et al*., 2003). Selective postnatal knockout of *Prnp* in neurons can stop or even reverse damage caused by pre-existing PrP^{Sc} and newly generated PrP^{Sc}

from adjacent non-neuronal cells (Mallucci *et al*., 2003). Another line of evidence against direct PrP^{Sc} toxicity comes from cases of CJD, where no direct correlation between PrP^{Sc} plaques and neuronal loss has been demonstrated (Parchi *et al*., 1996) Indeed, PrP^{Sc} is not detectable in some cases of fatal familial insomnia (Gambetti *et al*., 1995), in lethal scrapie-like diseases in mice over-expressing mutant PrP transgenes (Telling *et al*., 1996a) and wild type mice inoculated with BSE (Lasmézas *et al*., 1997; Manuelidis *et al*., 1997). Furthermore, prion-infected transgenic mice expressing PrP^{C} without a GPI anchor produce infectious prions, accumulate extracellular PrP amyloid plaques, but do not succumb to disease (Chesebro *et al*., 2005).

These observations have led to two theories of PrP^{Sc} toxicity, which are not mutually exclusive. Neurotoxicity of PrP^{Sc} may be linked to its propagation in neuronal cells and is therefore dependent on the expression of PrP^{C}. Alternatively; PrP^{Sc} may trigger a deadly signal through a PrP^{C} dependent signalling pathway (Section 1.9.2).

1.9.2 Gain and loss of PrP^{C} function

Although the physiological activity of PrP^{C} remains unknown (Section 1.6.1, 'PrP^{C} function'), it is possible that the corruption or subversion of the normal functions of PrP^{C} lead to the characteristic pathology seen in prion disease. Several experimental results support the idea that PrP^{C} functions as a cytoprotective molecule (Roucou and LeBlanc, 2005). For example, PrP^{C} over-expression has been shown to rescues cultured neurons, some mammalian cell lines, and yeast (Li and Harris, 2005) from several kinds of death-inducing stimuli. Endogenous PrP is known to protect cultured neurons against oxidative stress and brain tissue against ischemia or trauma *in vivo*

(Harris and True, 2006). In a recently published study, PrP was also found to be important for self-renewal of hematopoietic stem cells during serial transplantation, a phenomenon that may depend on an antiapoptotic activity of the protein (Zhang *et al*., 2006). Finally, co-expression of wild type PrP in Tg (PrPΔ32-134) mice, which express an N-terminally truncated form of PrP, completely abrogates their neurodegenerative phenotype (Behrens and Aguzzi, 2002). Moreover, N-terminally truncated PrP^{C} mutants have been shown to activate both Bax-dependent and independent neurotoxic pathways, suggesting that this region could be crucial for the putative neuroprotective function of PrP^{C} (Li *et al*., 2007a). Therefore, if the normal function of PrP^{C} is neuroprotection, then loss of this function by conversion to PrP^{Sc} might contribute to prion-induced neurodegeneration. The loss of function of PrP^{C} is unlikely to be the sole cause of pathology because neither embryonic nor adult knock-out of PrP^{C} results in neurodegeneration (Bueler *et al*., 1992; Manson *et al*., 1994; Mallucci *et al*., 2002).

Another possibility is that PrP^{C} may gain a toxic function due to either the presence of PrP^{Sc} or its interaction with it (Caughey and Baron, 2006). Several lines of evidence have shown that PrP^{C} acts as a signal transducer or mediator of neurotoxicity (Soto, 2008) (Figure 1-4 A). This concept has been supported by several experimental situations in which expression of membrane anchored PrP^{C} is essential for the development of neurodegeneration or toxicity in prion diseases (Solforosi *et al*., 2004). First, $Prnp^{0/0}$ neurons are resistant to the pathological effects of PrP^{Sc} supplied from grafted brain tissue (Brandner *et al*., 1996) or from nearby astrocytes (Mallucci *et al*., 2003). Second, scrapie-inoculated mice expressing a GPI anchor-negative version of PrP develop PrP develop minimal brain pathology and neurological dysfunction

despite the accumulation of substantial amounts of PrP^{Sc} amyloid (Chesebro *et al*., 2005). Third, PrP-null primary neurons in culture have been found to be resistant to apoptosis induced by exposure to the synthetic peptide PrP106-126, which has been used as a model for PrP^{Sc} (Brown *et al*., 1994). Finally, a recent study has shown that PrP^{C} exerts a protective activity against cellular stress, and that PrP^{Sc} abrogates this activity by activating stress-related signalling cascades (Rambold *et al*., 2008).

Taken together, the above evidence suggests a 'subversion-of-function' hypothesis to explain prion-induced pathology whereby interaction with PrP^{Sc} (or other pathogenic intermediates) alters normal, physiological activity of PrP^{C} leading to neurotoxicity (Figure 1-4 A).

1.9.3 Aberrant PrP^{C} trafficking

Several studies have shown that PrP can be neurotoxic when its import into the ER is partially or completely compromised (Hegde *et al*., 1998b; Hegde *et al*., 1999; Yedidia *et al*., 2001; Ma *et al*., 2002). Studies in cell-free translation/translocation systems have shown that PrP can be found in several topological forms (Hay *et al*., 1987). ^{Ctm}PrP is one minor isoform of PrP, which spans the membrane once (at a hydrophobic domain from residues 112-135) with the N-terminal domain exposed to the cytosol (Hegde *et al*., 1998b). Increased synthesis of ^{Ctm}PrP has shown to coincide with progressive neurodegeneration both in GSS patients with an A117V mutation and in transgenic mice carrying a triple mutation within the hydrophobic domain (Hsiao *et al*., 1991; Hegde *et al*., 1998b; Stewart *et al*., 2005). Indirect evidence in transgenic mice suggests that ^{Ctm}PrP levels might also be increased upon PrP^{Sc} accumulation (Hegde *et al*., 1999). Thus, ^{Ctm}PrP may be a critical intermediate in the pathway of

prion-mediated neurodegeneration, by means of escaping the ER quality control mechanisms (Hegde *et al*., 1998b; Hegde *et al*., 1999).

In separate studies, a transgenic mouse model revealed that preventing the import of PrP into the ER leads to the formation of a neurotoxic PrP species in the cytosol. Mice expressing a PrP mutant lacking the N-terminal ER targeting signal (cytoPrP) acquired severe ataxia due to rapid cerebellar granule neuron degeneration (Ma *et al*., 2002). A recent study supported the toxicity of cytoPrP and demonstrated that this activity is seen in different neuronal populations (Wang *et al*., 2009) and mammalian cell culture models (Ma *et al*., 2002; Rambold *et al*., 2008; Rane *et al*., 2004). The relevance of this observation to either familial or transmissible prion diseases remains unclear.

Several recent studies have linked cytoPrP production to prion disease pathogenesis. First, prion infection and PrP^{Sc} accumulation indirectly cause ER stress (Hetz and Soto, 2006; Rane *et al*., 2008). Second, during ER stress, translocation of PrP into the ER is reduced, leading to increased cytoPrP production (Kang *et al*., 2006; Coimbra *et al*., 2006). Third, reduced PrP translocation at levels comparable to that seen during ER stress was sufficient to cause mild age-dependent neurological dysfunction in transgenic mice despite essentially quantitative degradation of cytoPrP (Rane *et al*., 2008). Finally, proteasome activity may decline with age (Dahlmann, 2007) and upon PrP^{Sc} accumulation (Kristiansen *et al*., 2007). Thus, it is possible that through the combined effects of a weak PrP signal sequence, reduced PrP translocation during ER stress, and reduced proteasome activity due to PrP^{Sc} accumulation, sufficient amount of cytoPrP is generated during prion diseases to cause neurotoxicity (Rane *et al*., 2008; Chakrabarti and Hegde, 2009) (Figure 1-4 B).

1.9.4 Intermediate PrP species

Several lines of evidence have suggested that both PrP^{C} and PrP^{Sc} are required for toxicity. In addition to the models of neurotoxicity described above (Section 1.9.1, Section1.9.2 and Section 1.9.3) an alternative explanation is that an undetectable, cell-associated and transient oligomeric intermediate, which requires PrP^{C} expression for its continuous formation, might be responsible for neurotoxicity (Soto, 2008) (Figure 1-4 C). For example, Hill *et al.*, proposed the presence of a transient neurotoxic intermediate, PrP^{L} (L for lethal), which forms during the conversion of PrP^{C} to PrP^{Sc} (Hill *et al*., 2000; Hill and Collinge, 2003). It is important to note that the precise nature, or even existence, of such a species remains unclear.

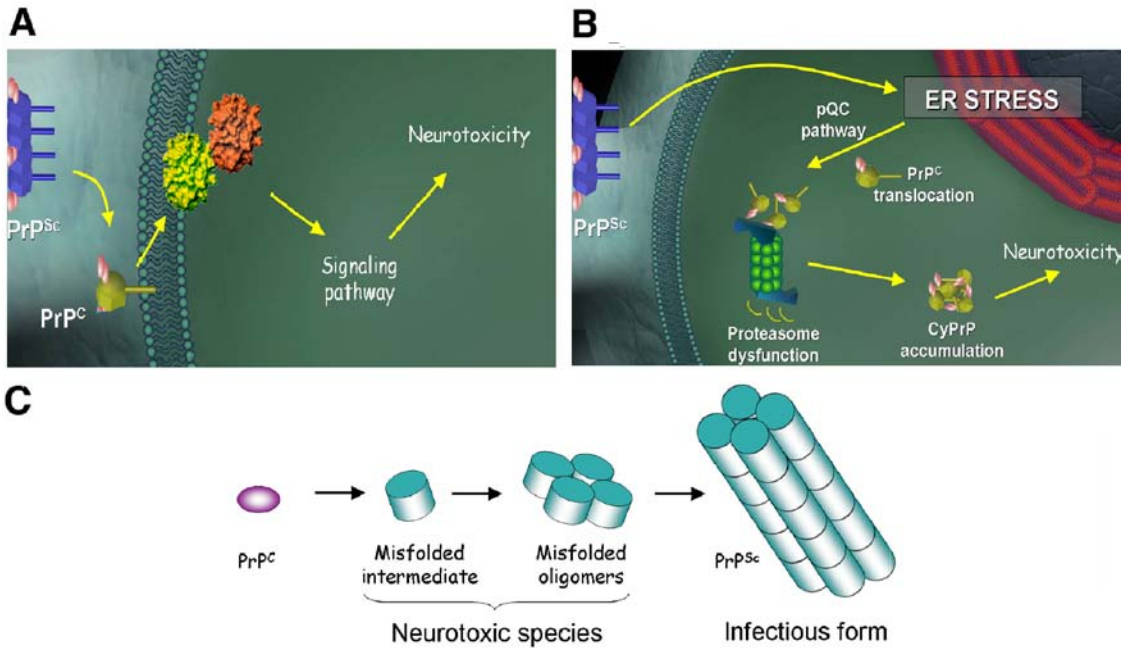

Figure 1-4 Role of PrP^{Sc} and mechanism of neurodegeneration[3]

Although PrP^{Sc} is certainly associated with the pathogenesis of TSEs, its role in neurodegeneration is controversial. Several observations suggest that PrP^{Sc} levels do not correlate with the extent of brain damage and that the natively folded PrP^{C} is required for neurodegeneration. Three non-mutually exclusive models can be proposed to explain the discrepancies and the implication of PrP^{C}. **(A)** PrP^{C} located in the cell surface may act as a receptor for PrP^{Sc}, triggering a signal transduction pathway leading to neurodegeneration. **(B)** As proposed by Rane and colleagues (Rane *et al*., 2008), induction of ER stress by PrP^{Sc} may lead to translocation of nascent PrP^{C} molecules to the cytosol for proteasomal degradation as a way to alleviate the damaged ER ('pre-emptive' quality control system (pQC) pathway). However, this mechanism of defence turns negative under chronic ER stress conditions, overwhelming the proteasome and leading to the cytosolic accumulation of potentially toxic PrP molecules. **(C)** The infectious and neurotoxic PrP species might not be the same. Indeed, it is possible that an undetectable misfolded intermediate might be responsible for neurotoxicity in a way similar to that proposed for other neurodegenerative diseases. The transient nature of these intermediates determines that its presence depends on the permanent synthesis of new PrP^{C}.

[3]Reprinted from Developmental Cell., Vol 15, Soto, C., Endoplasmic reticulum stress, PrP trafficking and Neurodegeneration, pp 339-341, ©2008, with permission from Elsevier.

1.10 Therapeutic approaches in prion diseases

Attempts to find a therapeutic for the treatment of prion disease patients has proved difficult due to long disease incubation times, a short symptomatic phase and the lack of a preclinical diagnostic.

In various model systems, thousands of compounds and substances with anti-prion activity have been identified (Gilch *et al*., 2008). For instance, sulphated glycans like pentosan polysulfate or dextrane sulphate 500 are known to interfere with binding of PrP to glycosaminoglycans (GAG) (Farquhar and Dickinson, 1986; Ladogana *et al*., 1992). Similarly, Congo Red (Caughey and Race, 1992; Ingrosso *et al*., 1995) induces reduction of cell surface PrP^{C} (Caspi *et al*., 1998), and suramin aggregates PrP^{C} and re-direct it to lysosomes (Gilch *et al*., 2001). Polyene antibiotics like amphotericin B which bind to cholesterol (Mangé *et al*., 2000) and tetracyclic compounds which may induce structural changes in proteins by direct interaction are other potent anti-prion compounds (Caughey *et al*., 1998). In addition, phosphorous containing dendrimers, known to induce proteolytic digestion of PrP^{Sc} by causing disaggregation at acidic pH (Solassol *et al*., 2004) and lysosomotropic agents like quinacrine (Doh-ura *et al*., 2000; Korth *et al*., 2001) have been identified as anti-prion compounds.

Small interfering RNAs (siRNA) targeting PrP mRNA abrogate PrP^{Sc} accumulation in cell culture (Daude *et al*., 2003) and successful knock down of PrP^{C} expression in livestock has been demonstrated (Golding *et al*., 2006). Expressing short hairpin RNA (shRNA) directed against PrP^{C} mRNA in neuronal cells prolongs incubation time in prion-infected chimeric mice (Pfeifer *et al*., 2006). Another approach to reduce levels of the infectious agent is to target the tertiary structure of

PrP^{Sc}. Structural transitions occurring in misfolded PrP^{Sc} have been reversed by beta-sheet breaker peptides (Soto *et al*., 2000). In addition, direct binding of RNA or peptide aptamers to PrP^{C} interferes with PrP^{Sc} biogenesis (Gilch *et al*., 2007).

In prion diseases, no obvious humoral immune response is stimulated due to autotolerance (Porter *et al*., 1973), however, various elements of the immune system can be manipulated. Efforts have focused on the therapeutic application of antibodies or of stimulation of antibody responses. Initial attempts to produce anti-prion antibodies included immunisation with purified proteins (Bendheim *et al*., 1984) or scrapie-associated fibrils (SAF) (Kascsak *et al*., 1987), with a greater response observed in prion knockout mice compared to wild type mice (Prusiner *et al*., 1993). These *in vivo* immunisation experiments suggest a possible use of anti-PrP antibodies as a therapy for prion diseases (Heppner *et al*., 2001; Sigurdsson *et al*., 2002; Gilch *et al*., 2003; Gilch and Schatzl, 2003). An alternative approach could be to target antibodies against the putative cellular prion receptor LRP since this has been shown to inhibit prion conversion in cell culture models (Zuber *et al*., 2008).

In summary, since prion diseases are fatal neurodegenerative disorders with no effective treatment, the search for efficient therapy and/or prophylaxis in prion disease will be critical. As TSE are diseases of the CNS, compounds selected for therapy must efficiently cross the blood-brain-barrier (BBB). Due to the short symptomatic phase of prion diseases, efforts have to be made to facilitate earlier diagnosis to allow therapeutic intervention before disease manifests.

1.11 Aims of the thesis

- To generate a unique cell system that can produce epitope-tagged PrP^{Sc} molecules in a neuroblastoma cell line where the endogenous PrP^{C} has been silenced
- To study the earliest events in prion infection of cells and subsequent PrP misfolding
- To assess the timescale that PrP^{C} is converted to PrP^{Sc} following exposure to mouse-adapted RML prions
- To identify the initial cellular site of PrP^{Sc} formation and propagation.
- To examine how trafficking impairment of PrP^{Sc} affects the PrP conversion and prion propagation.
- To map the intracellular trafficking pathways of PrP^{Sc}

2 Materials and Methods

All chemicals were purchased from Sigma-Aldrich Ltd and were used as received unless otherwise stated.

2.1 Cell culture

Work with mouse cell lines was carried out in a designated tissue culture facility using strict aseptic technique. All media and solutions were bought pre-sterilised and sterile plastic-ware was used. All procedures, including preparation of media, were performed in a tissue culture hood with a laminar flow unit. All solutions and media were pre-warmed to 37°C prior to use.

2.1.1 Cell lines

N2aPK-1 cell lines

N2aPK-1 cell line (PK1 cells) was a kind gift from Dr Peter Kloehn (MRC Prion Unit, UCL Institute of Neurology)**.** This cell line was driven from the mouse neuroblastoma cell line N2a (Klohn *et al*., 2003) purchased from the American Type Culture Collection (ATCC-CCL131). N2a cells were challenged with a 10^{-6} dilution of Mouse-adapted Rocky Mountain laboratory (RML) prions, to yield clone N2aPD88. Further sub-cloning of N2aPD8 yielded the more sensitive N2aPK-1 cell line (PK1 cells).

N2aPK-1 knock down cell lines

PrP-knock down cell lines (P8(11)4.5 and PK1-10*Si8*) were generated by Dr Liza Sutton and Professor Parmjit Jat in the MRC Prion Unit, UCL Institute of Neurology, using RNA interference (RNAi) technology (Section 2.2.1).

PhiNX-ecotropic packaging cell lines

PhiNX-eco cells were a kind gift from Professor Parmjit Jat (MRC Prion Unit, UCL Institute of Neurology). The cell line is a second generation retroviral producer line (MuLV-based) for the generation of helper-free ecotropic retroviruses. The line is based on the 293T cell line; a human embryonic kidney line transformed with adenovirus E1a, carrying a temperature sensitive T antigen co-selected with neomycin (Lamb *et al*., 1993). These were used for gene transfer into cells. PhiNX-eco cells produce virus particles that are able to infect mouse cells.

2.1.2 Cell culture methods

Cell growth condition

All chemicals were from Sigma unless otherwise stated. N2aPK-1 cells were grown in standard growth medium which consisted of Opti-MEM containing penicillin 50 U/ml (Invitrogen), streptomycin 50 µg/ml (Invitrogen), and 10 % v/v foetal calf serum (FCS, Invitrogen). For PK1-10*Si8* cells 4 µg/ml puromycin (Invitrogen) and for P8(11)4.5 cells 4 µg/ml puromycin as well as 50 µg/ml hygromycin (Invitrogen) were also added to the standard growth medium. 400 µg/ml Geneticin (G418, Invitrogen) was also added to the growth medium of cells reconstituted with tagged-PrP constructs.

Cell culture maintenance and harvesting

All cells were grown in 10 cm plastic culture dishes. Their medium was changed two to three times weekly. To subculture the cells, the existing medium were exchanged with pre-warmed medium and cells were suspended by trituration with a

Gilson pipette. Cells were seeded 1:3 to 1:8 in new culture plates and incubated at 37°C to grow in a humidified 5 % CO_2 incubator.

Cell freezing and defrosting

A confluent plate of cells were suspended in the existing media by trituration with a Gilson pipette and centrifuged at 200 x *g* for 5 minutes. The pellet was re-suspended in an appropriate volume of freezing media containing 30 % FCS and 8 % dimethyl sulfoxide (DMSO). 1 ml of cells were dispensed into sterile cryovials and put in isopropanol-regulated cryopreservation box at – 80°C overnight before transfer to vapour liquid nitrogen for long term storage.

Frozen cells were removed from liquid nitrogen and were thawed rapidly in a 37°C water bath. Cell suspension was transferred to 10 ml of appropriate pre-warmed media and was centrifuged at 200 x *g* for 5 minutes. Then, the supernatant was decanted and the cells re-suspended in 10 ml fresh standard growth medium overnight at 37°C. The day after, the media on the cells was replaced with fresh growth medium.

Nuclear fragmentation using DAPI for the detection of apoptosis

From time to time cells were checked for nuclear fragmentation to ensure cells were not infected with *Mycoplasma*; nuclear fragmentation is an early indicator of apoptosis (Simbulan-Rosenthal *et al*., 1999). This was done using 4', 6-diamidino-2-phenylindole (DAPI), a UV-excited, blue-emitting fluorochrome, (excitation 358 nm, emission 461 nm) which stains the nuclei of cells. Cells were plated on poly-L-lysine coated glass 13 mm coverslips. Coverslips were washed three times in PBS and fixed in fresh pre-warmed 4 % w/v paraformaldehyde (PFA), pH 7.4, for 20 minutes at room temperature (RT). After washing the coverslips three times in PBS, cells were

permeabilised with pre-cooled 100 % methanol for 15 minutes at - 20°C and then washed again three times in PBS. 1 µg/ml DAPI was added to each coverslip; coverslips were mounted on glass slides in 10 µl anti-fade (DAKO). Slides were left to dry and then placed at 4°C until analysis.

Prion infection of cell lines

Cells were infected with mouse adapted RML prions. Brains of scrapie-sick mice infected with RML prions was homogenized by passing eight times each through 21 and 25 gauge needles and adjusted to 10 % (w/v) with PBS. Brain homogenate was centrifuged for 5 minutes at 1,000 rpm at RT; supernatants were recovered and stored at – 80^{o}C. Cells were seeded into 6-well plates to yield 50 % confluence for 24 hours before exposure to 0.1 % RML-infected mouse brain homogenate. The homogenate was diluted in pre-warmed culture medium, mixed thoroughly by vortexing and added to cells for 72 hours unless otherwise stated. The inocula were then removed and the cells were either seeded on coverslips if it was necessary or were split 1:8 every 3 days. After three 1:8 splits, the infectivity of the cells (production of PrP^{Sc}) was screened by the scrapie cell assay (SCA) (Klohn *et al*., 2003) (Section 2.5). Cells were cultured in standard growth medium and maintained at 37^{o}C in 5 % CO_2.

2.2 Molecular biology

2.2.1 Knock down of *Prnp* using RNA interference

As mentioned in section 2.1.1, PrP-knock down PK1 cells were used for our experiments. The cells were produced by Professor Parmjit Jat and Dr Liza Sutton, at the MRC Prion Unit, UCL Institute of Neurology, using RNAi technology (unpublished data). Three 19-mer small interfering RNA (siRNA) duplexes were

designed to exactly target mouse *Prnp* mRNA and contained a 3´UU overhanging (to prevent nuclease digestion; Table 2-1). Sequence number 2 and 4 were designed by Professor Parmjit Jat using a set of empirical design rules. It includes targeting sequences 50-100 base pairs upstream of *Prnp*, starting with an AA dimer and using the next 19 nucleotides, avoiding stretches of more than four A and T (a termination signal for polymerase III) and ensuring the GC content was between 30 % and 50 %. Sequence number 8 was designed by Dharmacon Inc. (USA) using SMART Selection^{TM} technology, which employs an algorithm to select functional siRNAs (Reynolds *et al*., 2004). All three siRNAs targeted the 3´UTR of mouse *Prnp*.

SiRNA oligonucleotides were cloned into the pSUPER.retro.puro expression vector (OligoEngine Inc., USA). To allow for co-expression of two siRNA sequences in the same cell, siRNA 2 and 8 expression cassettes were cleaved from pSUPER.retro.puro vector and cloned into another retroviral vector: pMSCV, with a hygromycin B selectable marker (Clontech, USA). siRNA expression vectors were packaged in PhiNX-eco cells before transducing PK1 cells (unpublished data). Combination of construct 8 and 2 was used to generate P8(11)4.5 cell line and construct 8 alone was used to generate PK1-10*Si8* cell line.

Table 2-1 Location of siRNA target sequences in mouse *Prnp* mRNA

SiRNA number	Location in mouse prion protein mRNA	Base pair	Sequence
2	3´UTR	1072-1092	AATGTACAGTAGACCAGTTGC
4	3´UTR	2039-2059	AATCTGCATGTACTTCACGTT
8	3´UTR	1512-1530	TAGGAGATCTTGACTCTGA

2.2.2 Construction of mouse PrP-3F4, FLAG and MYC insertion mutants in pLNCX2

Mouse PrP expressing vectors

Mouse 3F4-tagged *Prnp* was generated by Dr Mark Kristiansen, MRC Prion Unit, UCL Institute of Neurology (unpublished data). Mouse FLAG- and MYC-tagged *Prnp* were generated by Dr Dave Emery, Henry Welcome Laboratories for Integrated Neuroscience (Appendix I and Appendix II). Mouse *Prnp* open reading frame was cloned as a EcoR I- Xho I restriction fragment into pBluescript SK(-) (Stratagene) to generate mouse FLAG- and MYC-tagged *Prnp*. They were then excised as a BamH I-Sa1 I fragment and transfected into Bg1 II-Sa1 I-digested retroviral vectors, pLNCX2 (Clontech, USA, Appendix III). To protect 3F4-, FLAG- and MYC-tagged PrP mRNAs from siRNAs directed at the 3´ untranslated region (3´-UTR) of PrP^C mRNA in PrP-KD cells (Section 2.2.1), only the mouse PrP^C open reading frame lacking 3´-UTR was inserted in pLNCX2 vectors.

Polymerase chain reaction (PCR)

Primary and secondary PCRs were carried out to generate mouse FLAG- and MYC- tagged PrP constructs, using the reactions showed in Table 2-2. For primary PCR, cycling conditions on the tetrad thermal cycler were polymerase activation step of 94°C for 5 minutes and then 30 cycles of DNA template denaturation at 94°C for 30 seconds, primer annealing at 57°C for 40 seconds, 72°C extension step for 1 minute, and a final extension step of 72°C for 7 minutes. For secondary PCR, cycling conditions on the tetrad thermal cycler were polymerase activation step of 94°C for 5 minutes, DNA template denaturation at 80°C for 10 minutes. After that, 1 µl (5 U) Herculase (stratagene) was added to the reaction prior and the extension step was carried out at 72°C for 10 minutes. Then, 2.5 µl of each flanking primer (Appendix IV) was added to the tube and then 30 cycles of DNA template denaturation at 94°C for 30 seconds, primer annealing at 57°C for 30 seconds, 72°C extension step for 1 minute, and a final extension step of 72°C for 7 minutes was carried out. PCR products were run on a 1.3 % agarose gel and were purified with a standard spin column purification kit following manufacturer's kit (Qiagen).

Table 2-2 Primary and secondary PCR reactions

Primary PCR reactions	Amount	Secondary PCR reactions	Amount
Template DNA (full length PrP template)	20 ng	N-C fragment of modified PrP (Appendix IV)	5 µl
5' flanking primer with C-N internal (Appendix IV)	1 µM	C-N fragment of modified PrP (Appendix IV)	5 µl
3' flanking primer with N-C internal (Appendix IV)	1 µM	10 times Herculase buffer	5 µl
Deoxyribonucleotide triphosphates (dNTP)	200 µM of each	Deoxyribonucleotide triphosphates (dNTP)	200 µM of each
Herculase buffer (Stratagene)	1 time	-	-
Herculase (Stratagene)	5 U	-	-

Cloning of mouse FLAG- and MYC- tagged *Prnp* into pBluescript SK(-)

Full length mouse FLAG- and MYC- tagged *Prnp* was digested with EcoR I and Xho I (10 U each) using Roche buffer H in a volume of 50 µl for 2 hours at 37°C. The digested products were gel purified as above and approximately 20 ng of pBluescript digested in a similar way was incorporated into ligation reactions with a molar (3 times) excess of fragment overnight at 17°C. Electrocompetent XL1-B E.coli was transformed and recombinant colonies were selected by Blue/White selection.

Sub-cloning of mouse FLAG- and MYC- tagged *Prnp* into pLNCX2

20 µl of pBluescript miniprep DNA for each FLAG and MYC clone was first digested with BamH I (10 U) with REACT 3 buffer (invitrogen, UK) in a final volume of 1 ml at 37°C for 2 hours. The DNA was ethanol precipitated; the pellet was washed with 70 % and 100 % ethanol and air-dried. It was then dissolved and digested with Sal I (10 U) in REACT 10 buffer (Invitrogen, UK)) in a final volume of 40 µl at 37°C for 2 hours and was run on a 1.3 % agarose gel and purified with a standard spin column purification kit following manufacturer's kit (Qiagen). Approximately 200 ng of each insert was ligated with approximately 10 ng of pLNCX2 vector prepared in the same way (replacing BamH I with Bgl II) in a total volume of 20 µl with 1 U ligase at 17°C overnight. These were then transformed into Electromax Stbl 4 E.coli (Invitrogen, UK).

Midipreps

100 ml cultures were grown overnight and DNA extracted using an Invitrogen kit. DNA was finally ethanol precipitated, air-dried and dissolved under tissue culture conditions.

2.2.3 Tagged PrP expression

Packaging of mouse 3F4-, FLAG-, and MYC-tagged PrP into retroviral producer cell line

Mouse 3F4-, FLAG-, and MYC-tagged PrP expression vectors, pLNCX2, was transiently transfected into the PhiNX-eco cell line to produce retroviral particles containing tagged mouse *Prnp* open reading frame (ORF). PhiNX-eco cells were used to produce supernatant to infect mouse lines. PhiNX cells were seeded at 1 x 10^6 cells per 10 cm dish 24 hours prior to transfection to achieve exponential growth phase. Transfection was performed with FuGene 6 (Roche) according to manufacturer's instructions; 10 µg plasmid DNA and 12 µl FuGene were used per transfection reaction. 10 ml retroviral tagged mouse PrP supernatant was harvested from each culture dish 48 hours and 72 hours after transfection and passed through a 0.45 µm filter to remove cells. Supernatant was used fresh or 5-10 ml aliquots made for storage at - 80°C.

Retroviral transduction of PK1 cell lines

Cells for retroviral transduction (P8(11)4.5 and PK1-10*Si8*) were seeded in 10 cm dishes to achieve exponential growth phase 24 hours later. 2 ml of viral supernatant were added dropwise to each dish supplemented with 8 ml of culture medium and 10 µl polybrene (Sigma, 8 µl/ml). Polybrene is a cationic polymer, which improved viral infection efficiency by facilitating membrane fusion. Cells were incubated overnight at 37^{o}C and the following morning, the existing media was replaced with fresh selection medium for RNAi knock down constructs (Section 2.2.1). In addition to tagged PrP construct vectors, cells were also transduced using pLNCX2 vector-only control supernatants. 72 hours after infection, transduced cells were split at a low density

(25,000 cells per 10 cm dish in quintuplicate). Cells successfully transduced with the PrP-tagged expression vector were selected with 400 µg/ml of G418. After the selection was completed, cells reconstituted with FLAG- and MYC-tagged PrP constructs were bulked up as mixed clones, however, single cell clones were isolated from the cells reconstituted with the 3F4-tagged PrP construct as described in section 2.2.4. PrP^C expression levels were assessed in the reconstituted cells by immunoblotting and immunofluorescence staining.

2.2.4 Isolation of mouse 3F4-tagged PrP expressing single cell clones

To produce single cell clones from the 3F4-tagged PrP transduced cells, the medium on top of the reconstituted cells was replaced with fresh medium in 10 cm dishes and single discrete colonies expressing sequence of interest were picked with a sterile 200 µl Gilson tip. Each clone was transferred to one well of a 96-well plate containing culture medium (50 µl per well). Clones were grown to confluence and passaged 1:8 to two replica 96-well plates. One plate of the pair was infected with mouse-adapted RML prions (Section 2.1.2, 'prion infection of cell lines'). The other plate was grown to confluence and frozen in 100 µl freezing medium (Section 2.1.2), wrapped in tissue and aluminium foil and stored at - 80^{o}C. If the infected plate revealed any RML prion-infected clones, its replica plate would be thawed and the RML prion-susceptible clones expanded and re-infected (Figure 2-1). Two hundred single cell clones were isolated from each 3F4-reconstituted cell line (P8(11)4.5 and PK1-10*Si8*) and their susceptibility to RML prion-infection was analysed by scapie cell assay (Section 2.6.1). Susceptible clones were expanded from the master plate for further analysis.

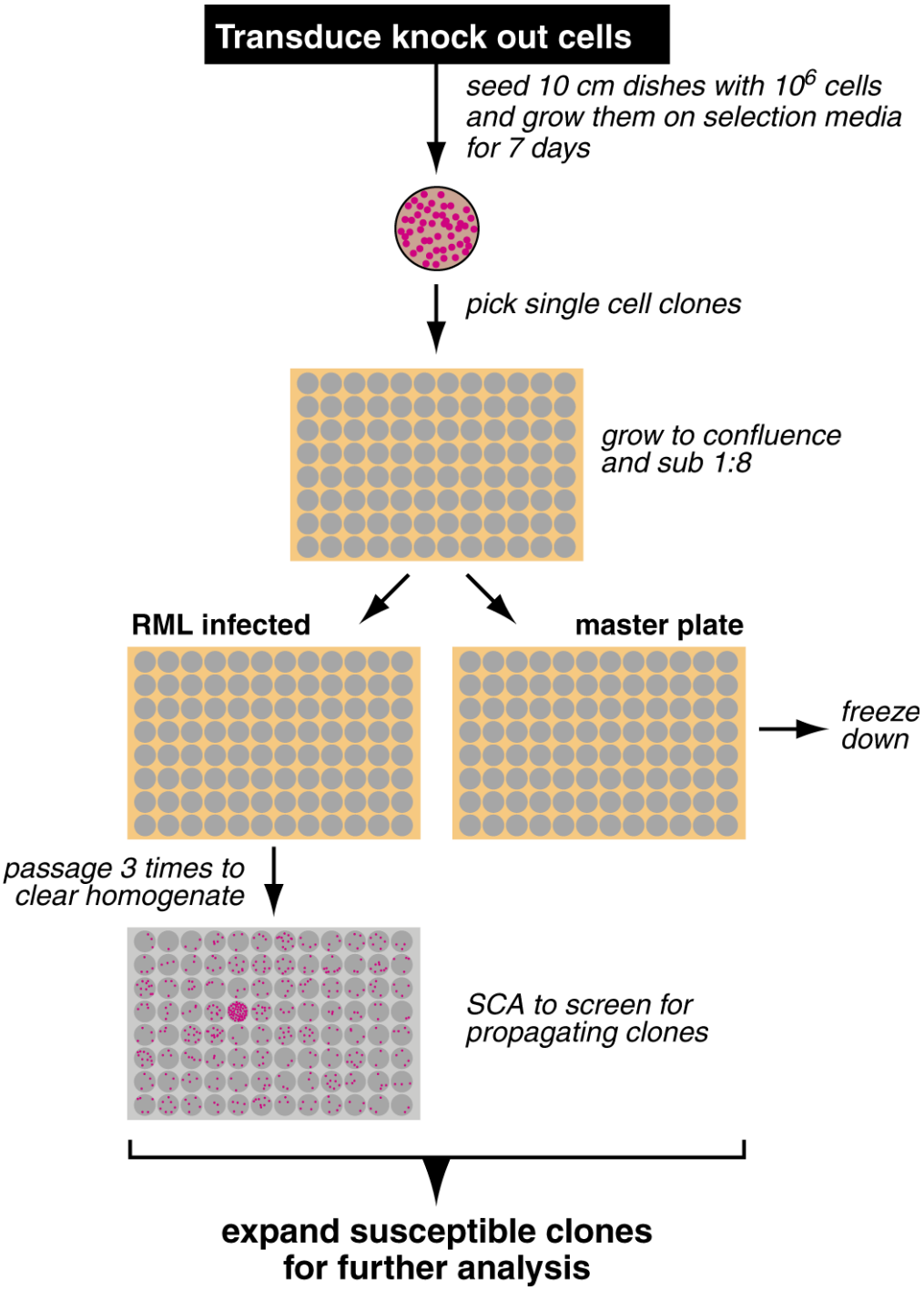

Figure 2-1 Isolation of RML prion susceptible single cell clones expressing 3F4-tagged PrP

Two hundred single cell clones were isolated from each 3F4-reconstituted cell line (P8(11)4.5 and PK1-10*Si8*) to assess their susceptibility to mouse-adapted RML prions following the method demonstrated in this figure.

2.3 Protein chemistry and immunoblotting

2.3.1 Cell lysate preparation for inoculation of Tg20 mice

Cell lysates were prepared from PK1, PrP-KD PK1 and PrP-224AlaMYC cell cultures exposed to RML prions for 72 hours then sub-passaged five times 1:8 as described in section 2.1.2 ('prion infection of cell lines'). Cells were harvested in sterile PBS, washed twice then re-suspended to 30 million cells/ml. Control PrP-224AlaMYC cells not exposed to RML prions were harvested the same way. Cell lysates were stored in sterile vessels at - 80°C until use. Animals were cared for per institutional and Home Office regulations. For each of the test conditions, groups of five Tg20 mice were inoculated intracerebrally with 30 µl of cell suspension. Animals were observed daily for clinical signs and culled on diagnosis of prion disease. Two animals not diagnosed with prion disease (control group) were culled in parallel with diseased animals, and the remaining animals were culled four to five weeks after the last diseased animal was diagnosed. Brains were excised and examined by immunoblotting (Section 2.3.3 and Section 2.3.6) and histopathology. Histopathological experiments were performed by Miss Caroline Powell, MRC Prion Unit, UCL Institute of Neurology and Miss Julie Moonga, Department of Neurodegenerative Disease, UCL Institute of Neurology.

2.3.2 Protein assay

The Pierce BCA^{TM} protein assay reagent was used to assess the protein concentration in cell lysates. This system combines the reduction of Cu^{2+} to Cu^{1+} by protein in an alkaline medium with the highly sensitive and selective colorimetric detection of the cuprous cation (Cu^{1+}) by bicinchoninic acid (BCA). The purple

reaction product of BCA and Cu^{1+} is water soluble and exhibits a strong absorbance at 562 nm. To conserve lysates, the microplate procedure was used. For each assay a fresh set of protein standards was prepared using dilutions of bovine serum albumin (BSA) in the same diluents as the unknown samples. The BSA standards were made to cover the range of protein concentrations expected for each type of sample, in the range 0, 25, 125, 250, 500, 750, 1000, 1500 and 2000 µg/ml. The assays were performed according to manufacturer's instructions. Each sample was pipette into a 96-well plate to which 200 µl working reagent (50 parts of BCA reagent A and 1 part of BCA reagent B) was added. This was done in duplicate for standards and triplicate for unknown samples. The plate was covered and incubated at 37^{o}C for 30 minutes. The plate was cooled to RT before reading at 562 nm on a Tecan plate reader (Sunrise). A standard curve was prepared and unknown protein concentrations calculated using a statistical analysis program (GraphPad Instant Version 3.02, GraphPad Software).

2.3.3 Extraction of protein from brain homogenates

100 µl of 10 % w/v mouse brain homogenate was treated with benzonase for 20 minutes on ice (50 U/ml; Merck) to hydrolyse the nucleotides in the solution. After that an aliquot was taken off for protein assay to ensure equal loading. According to the protein assay results, brain homogenate samples were diluted to 1 mg/ml in PBS and 0.01 % v/v Tween-20 on ice. The samples were digested with proteinase K (PK; Roche; 5 µg/ml) if it was necessary for 45 minutes at 37°C. The PK digestion was ended by adding 1 mM PMSF to each sample and then 900 µl of pre-cold 100 % methanol was added to both PK and non-PK treated samples and they were stored in -20°C for at least 15 minutes. Samples were then centrifuged at 16,000 x *g* for 15

minute to pellet the debris. The supernatant was discarded and the pellet was air-dried. 100 µl of 2 X reducing sample buffer (125 mM Tris, pH 6.8, 20 % glycerol, 0.05 % bromophenol blue, 4 % SDS) was added to each sample and then they were stored at -80°C.

2.3.4 Extraction of protein from cultured cells

Cells were harvested on ice and spun twice at 4°C (1000 x *g*, 5 minutes) in ice-cold PBS to eliminate any media. The resulting pellet was then re-suspended in minimal volume of ice-cold PBS on ice. Cells were lysed 3 times by freeze-thawing in liquid nitrogen. Lysates were benzonase-treated for 15 minutes on ice (50 U/ml; Merck). Ice-cold PBS was added to acceptable viscosity and an aliquot was taken off for protein assay to ensure equal loading. The remaining supernatant was frozen at –80°C.

2.3.5 Proteinase K digestion of cells for detection of PK resistant PrP^{Sc}

To digest the cells with proteinase K, upon thawing cells were treated by adding PK (Roche) to a final concentration of 50 µg/ml for 30 minutes at 37°C. Samples were then centrifuged at 16,000 x *g* for 1 minute to pellet cellular debris; digestion was ended in samples by adding 8 mM AEBSF (Merck) in an equal volume of 2 X reducing sample buffer.

2.3.6 SDS-polyacrylamide gel electrophoresis (SDS-PAGE) of protein

Reducing sample buffer was added to 1 X concentration and samples were boiled at 100°C for 10 minutes. Samples were then spun at 16,000 x *g* for 1 minute,

briefly vortexed and finally spun at 16,000 x *g* for 1 minute before loading onto 16 % Tris-Glycine mini gels (Novex, Invitrogen). Gels were electrophoresed vertically in Tris/Glycine SDS running buffer (National Diagnostics) in a X-Cell *SureLock*™ Mini-Cell system (Invitrogen) for 80 minutes at 200 V (or until the dye front run off at the end of the gel). Pre-stained Seeblue® Protein Standard (Novex, Invitrogen) was used as a molecular weight marker.

2.3.7 Electroblotting of gels

Protein was transferred onto PVDF membranes (Millipore). PVDF membrane was pre-cut at the same size as the gels and pre-soaked in 100 % methanol for 2 minutes to ensure even hydration prior to transfer into blotting buffer (National Diagnostics). Protein was transferred from the gel to the membrane in Novex X-Cell II™ Blot modules (Invitrogen) at either 35 V for 90 minutes or 14 V overnight.

2.3.8 Immunoblotting of gels

After electroblotting, membranes were transferred to square tissue culture petri dishes and washed in PBS containing 0.05 % v/v Tween-20 (1 X PBST). Blots were then blocked for 1 hour at RT with gentle agitation using either 5 % w/v BSA or 5 % w/v non-fat milk powder. Blocking solution was made in 1 X PBST. Membranes were washed briefly with 1 X PBST before overnight incubation with the appropriate primary antibody at RT with gentle agitation. To detect prion protein, mouse monoclonal ICSM35 anti-PrP antibody (D-GEN; 0.25 µg/ml) was used. After incubation with the primary antibody, the membranes were then washed in 1 X PBST for a minimum of 45 minutes changing buffer 5 times. Secondary detection was performed by incubating with the appropriate secondary antibody (diluted in 1 X

PBST) for 45 minutes at RT. Alkaline phosphatase goat anti-mouse IgG (fab-specific) was diluted 1:10,000 and used as a secondary antibody to detect prion protein. Detection of bound antibody was performed with SuperSignal West Pico Chemiluminescent substrate (Pierce) or by CDPStar (Tropix) according to manufacturer's instructions. Excess reagents were poured off and the membranes were placed between acetate films and transferred to a photographic cassette. Biomax MR Films (Kodak from Anachem) were developed using Kodak developer and fixer by hand or by using a Xograph imaging machine (Xograph Imaging Systems). Developed films were scanned using an Epson scanner for electronic format and densitometry of digital images was achieved by using a Kodak Image Station 440 CF.

2.3.9 Determination of equal protein loading

The *Re-Blot Plus* Western Blot Strong Antibody Stripping Solution (Chemicon) consists of specially formulated solutions that quickly and effectively remove antibodies from Western blots without significantly having an effect on the immobilized proteins. Blots were washed in 1 X PBST buffer for 10 minutes before being incubated for 15 minutes with 1 X Re-Blot Plus (in water) Strong Antibody Stripping solution. Following this, blots were briefly washed with 1 X PBST and subsequently blocked with 5 % milk powder in 1 X PBST for 1 hour. Mouse monoclonal anti-β-actin antibody (1:10,000) was added for an overnight incubation to probe for the control loading protein.

2.3.10 Densitometry

Densitometry on immunoblots was performed using the Kodak™ Digital Science Image station 440CF (IS440CF) system and analysed using the Kodak™ ID Image Analysis Software (PerkinElmer Life Sciences).

2.4 Cell Biology

2.4.1 PrP^{Sc} trafficking impairment using pharmacological agents

Cells were grown on poly-L-lysine coated coverslips to about 70 % confluence. The medium was aspirated from cells and was replaced with different pharmacological agents (Table 2-3) diluted in pre-warmed media. The plate was rocked gently and incubated at 37°C for 4 hours unless otherwise stated (see Section 5.3 for details of each treatment). 5 µg/ml Texas-red labelled transferrin (Invitrogen) was added to cells for the last 10 minutes of the incubation period to assess the efficacy of manipulations on the cellular endocytosis unless otherwise specified. After that, the cells were washed with PBS three times and were fixed to be observed. Control experiments replicating the conditions for each treatment but lacking the active reagents were carried out to check that conditions outside of our treatments did not affect RML prion infection. No significant differences were observed. All the inhibitors were obtained from Sigma-Aldrich Ltd, except U18666A that was purchased from Merck-Chemicals Ltd.

Table 2-3 Pharmacological agents used to manipulate intracellular trafficking of PrP^{Sc}

Reagents	Final concentration
U18666A	3 μg/ml
Dynasore monohydrated	80 μM
Bafilomycin	200 nM
Brefeldin A	5 μg/ml
Nocodazole	20 μM
Filipin	1 μg/ml

2.4.2 Immunofluorescence methods

Preparation of coverslips

For immunofluorescence experiments, autoclaved 22 or 13 mm glass coverslips (VWR) were coated with 1 mg/ml poly-L-lysine for 10 minutes at RT. Coverslips were subsequently washed three times with sterile double-distilled water and air dried. Poly-L-lysine enhances electrostatic interaction between negatively-charged ions of the cell membrane and positively-charged surface ions of attachment factors on the culture surface. When adsorbed to the culture surface it enhances the number of positively-charged sites available for cell binding.

Immunofluorescence analysis protocol

Cells were grown on poly-L-lysine coated coverslips until to 70 % confluence. They were washed three times with PBS and were fixed with 4 % w/v pre-warmed PFA, pH 7.4, for 20 minutes at RT. 4 % pre-warmed PFA, pH 7.4, was used to fix the coverslips unless otherwise specified. After fixation, coverslips were washed three times with PBS, and then were permeablised in 100 % methanol at - 20°C for 15 minutes. After washing cells 3 times with PBS, cells were then incubated with 10 % normal goat diluted in PBS for 30 minutes at 37°C in a humid chamber. Primary antibodies (Table 2-4) were diluted to appropriate concentrations in 1 % normal goat serum in PBS and applied to coverslips at 37°C for 1 hour. After washing, suitable AlexaFluor488 and 543 labelled secondary antibodies diluted in 1 % normal goat serum was applied to cells at 37°C for 45 minutes. Coverslips were then washed several times in PBS and mounted in anti-fade medium (DAKO) containing 1 ug/ml DAPI.

Table 2-4 Antibody concentrations used for immunofluorescence analysis

Antibody	Detected protein	Source	Stock concentration (mg/ml)	Dilution	Isotype
Anti-3F4	3F4-tagged PrP (prion protein)	Signet	2	1:500	Mouse IgG2a
Anti-PrP (ICSM18)	PrP (prion protein)	D-GEN	3	1:300	Mouse IgG1
Anti-FLAG (M2)	FLAG -tagged PrP (prion protein)	Sigma	N/A	1:200	Mouse IgG1
Anti-MYC (9B11)	MYC -tagged PrP (prion protein)	Cell Signalling	N/A	1:1000	Mouse IgG2a
Anti-GM130	Golgi matrix protein of 130 KDa	BD Bioscience	0.25	1:50	Mouse IgG1
Anti-EEA-1	Early endosome antigen 1	Sigma	1	1:50	Rabbit IgG
Anti-Tfr	Transferrin receptors	Invitrogen	0.5	1:100	Mouse IgG1
Anti-TGN38	Trans-Golgi networks	AbD SeroTec	N/A	1:50	Rabbit IgG
Anti-LAMP-1	Lysosome associated membrane protein type 1	Santa Cruz	0.2	1:500	Rat IgG2a
Anti-20S	Proteasome 20S core subunits	Enzo Life Sciences	N/A	1:200	Rabbit IgG

Removal of PrP^{c} immunoreactivity using formic acid

98 % formic acid was used to remove PrP^{C} and reveal PrP^{Sc} (Kristiansen *et al*., 2005). Coverslips seeded with cells were incubated for 20 minutes in 4 % pre-warmed PFA, pH 7.4, at RT and then transferred to 98 % formic acid at RT for 5 minutes. Cells were washed 3 times in PBS, and then were permeablised with methanol at - 20°C for 15 minutes. Complete removal of PrP^{C} was checked by incubating non-infected cells alongside RML prion-infected cells. It was seen that 5 minutes formic acid is efficient enough to denature most of PrP^{C}.

Removal of PrP^{c} immunoreactivity using Guanidine hydrochloride

Guanidine hydrochloride (GdnHCl) is a chaotropic agent used as a denaturant to disrupt the structure of proteins, unfold them and turn them into their original polypeptide chains. GdnHCl is widely used in prion field to denature PrP^{C} and expose PrP^{Sc}. 4 % pre-warmed PFA, pH 7.4, was added to the cells for 20 minutes at RT. Coverslips were washed three times with PBS, and then were permeablised in 100 % methanol at - 20°C for 15 minutes. After washing cells 3 times with PBS, cells were

then treated with 6 M GdnHCl for 10 minutes at room temperature and washed 3 times with PBS and were stained as explained above. Complete removal of PrP^C was checked by incubating non-infected cells alongside RML prion-infected cells.

Removal of PrP^c immunoreactivity using PK

Cells were grown on poly-L-lysine coated coverslips to about 70 % confluence. Cells were washed three times with PBS and were fixed and permeablised with 8 % formaldehyde/ 0.1 % glutaraldehyde and 0.1 % digitonin for 1 hour at RT. Coverslips were washed three times with PBS, and then were treated with PK (20 µg/ml, Roche) for 15 minutes at 37°C and washed once with PBS. Digestion was stopped with 2 mM phenylmethylsulphonyl fluorride (PMSF) for 15 minutes at RT. The coverslips were washed with PBS three times and then were stained as explained above. Complete removal of PrP^C was checked by incubating non-infected cells alongside RML prion-infected cells.

Dual-labelling immunofluorescence

For dual labelling experiments, the two sets of antibodies were added sequentially, *i.e.* primary antibody was applied followed by the appropriate fluorochrome-conjugated secondary antibody. After washing, the second primary antibody was added followed by the appropriate flurochrome-conjugated secondary antibody. Then the protocol was followed as explained above (Section 2.4.2, 'immunofluorescence analysis protocol'). All the necessary controls, including secondary antibodies only, were performed to examine for any potential cross-reactivity.

Image acquisition

Confocal microscope (Zeiss microscope LSM510 META) was used to take fluorescence images equipped with 'plan-Apochromat' 63 x/1.40 Oil DIC objectives at RT and is controlled by Zeiss LSM software. Fluorescence was recorded at 488 nm using 30 mW Ar-laser for excitation or at 543 nm using 1 Mw HeNE-laser for excitation. Zeiss Immersol^{TM} 518 F was used as imaging medium. Images taken for countings were obtained using an Axioplan 2 MOT microscope (Zeiss) with filters for FITC, Rhodamine and DAPI and Plan Neofluar 10x/0.30 Ph1 objective at RT. An AxioCam MRm (Zeiss) camera was used and was controlled using the Axiovision Control software (Zeiss). Orthogonal projections were generated from z-stacks using Zeiss LSM software.

Quantification of RML prion infected cells

Control non-infected cells were processed for each experiment and LSM settings were chosen to give minimal background staining. The same settings were used to examine all RML prion-infected cells in that experiment. To determine RML prion infection, at least 300 cells from eight randomly chosen fields (unless otherwise specified) were counted for each condition, and the proportion of cells showing PrP^{Sc} immunostaining after PrP^{C} removal was calculated.

2.5 Assaying for PrP^{Sc} in cells (Scrapie Cell Assay)

The scrapie cell assay (SCA) is an ELISA-based assay that was developed in the MRC Prion Unit as a quantitative, highly sensitive in vitro assay for mouse-adapted RML prions (Klohn *et al*., 2003) that can detect single PrP^{Sc} positive cells. The assay was used to detect infectivity in cells following infection with mouse-

adapted RML prions. All steps were carried out at RT unless otherwise stated and the assay was undertaken in class I microbiological safety cabinet in containment level III laboratory. Solutions were aspirated by a vacuum pump into a trap containing sodium hypochlorite (20 % final concentration) for decontamination. Guanidinium thiocynate (GCSN)-containing solutions were decontaminated with 2 M sodium hydroxide because GCSN-containing solutions react with sodium hypochlorite to produce chlorine gas.

Elispot plates (Enzyme-Linked Immunospot Multiscreen Immobilon-P 96-well Filtration Plates, Millipore) were activated by wetting the 0.45 µl PVDF membrane of each well with 70 % ethanol, aspirating and washing once with PBS. 25,000 cells were transferred to the membrane of an Elispot plate. SCA controls were always seeded onto the same plate: non-infected or PrP-KD PK1 cells as negative controls and chronically RML prion-infected PK1 cells (iPK1) as positive controls (25,000 cells per well). Cells were seeded onto the membrane by applying a vacuum and drying them onto the membrane in a 50^{o}C oven in biocontainment boxes. PK concentration to digest PrP^{C} was determined for each cell line. 50 µl of PK (0.5 µg/ml, Roche) diluted in lysis buffer was added to each well for 30 minutes at 37^{o}C before it was aspirated. The plate was washed twice with PBS, exposed to 160 µl per well of 1 mM PMSF for 10 minutes to inhibit the action of the PK, washed once with PBS before incubation with 120 µl of 3 M GCSN in 10 mM Tris-HCL (pH 8.0) for 10 minutes to expose the PrP^{Sc} epitopes. GCSN was discarded into 2 M NaOH and the wells washed five times with PBS.

For immunoprobing of PrP^{Sc}, 120 µl per well superblock buffer (Pierce) was added to plates for 1 hour and aspirated. 60 µl per well anti-PrP ICSM18 monoclonal

antibody was added at 0.6 µg/ml in 1 X TBST with 1 % non-fat milk powder (Marvel, Premier Brands, UK) and incubated for 1 hour at RT. The primary antibody was discarded into 2 M NaOH and the wells were washed seven times with 1 X TBST. 60 µl per well of alkaline phosphatase (AP)-conjugated secondary antibodies diluted in TBST/1 % non-fat milk powder was added and plates were incubated for 1 hour. Anti-IgG1 antibody was used as a secondary antibody for anti-PrP ICSM18 antibody. Appropriate dilution was established for each new vial of secondary antibody by titration.

54 µl per well AP-conjugated substrate (prepared as recommended by Bio-Rad) was added until there was a clear colour change in the positive controls (approximately 15 minutes). The AP-substrate was discarded and the plates were washed twice with de-ionised water before being dried under airflow. Plates were stored in the dark at -20^{o}C until analysed. PrP^{Sc}-positive cells were counted using the Zeiss KS Elispot system and each well was assigned a SCA value. Stemi 2000-C stereo microscope equipped with a KL 1500 LCD scanner, Hitachi HV-C20A colour camera and WELLSCAN software from Imaging Associates (Bicester, UK) was used for analysis. Detection settings were optimised to give a maximal signal to noise ratio (PrP^{Sc}-positive sample counts). Parameters were adjusted by using the training feature of the software program according to the manufacturer's instructions. RML prion-infected wells were defined as those for which SCA value (counts per well) was significantly greater than background.

2.6 Statistical analysis

Data were expressed as mean plus standard error of the mean (SEM) unless otherwise stated. Data were compared by 2-tailed *t*-tests and considered significantly

different when $P < 0.05$. Degree of significance was expressed as follows: * $P < 0.05$; ** $P < 0.01$; *** $P < 0.001$, unless otherwise specified.

3 Isolation of prion susceptible cell lines expressing tagged mouse PrP

3.1 Background

According to the widely accepted 'protein-only' hypothesis, PrP^{Sc} is the principal component that is responsible for disease transmission (Bolton *et al*., 1982; Prusiner, 1982). Specifically, PrP^{Sc} impresses its abnormal conformation on PrP^{C}, thereby generating additional molecules of PrP^{Sc} in an autocatalytic reaction (Prusiner, 1998a; Weissmann, 1994; Caughey and Chesebro, 1997). A widely accepted model of prion formation and replication proposes that direct interaction of endogenous PrP^{C} with the pathogenic PrP^{Sc} template is required to drive conversion to the infectious PrP conformers (Weissmann, 1994; Caughey and Chesebro, 1997). However, there is little consensus on the molecular details of the process by which PrP^{C} is converted into PrP^{Sc}. Likewise, the chain of events emanating from prion infections and leading to neurodegenerative changes and clinical signs are unknown.

Studies in prion infected animals and tissue culture cells indicate that sequence compatibility between PrP^{C} and PrP^{Sc} molecules is necessary for efficient PrP^{Sc} formation (Prusiner *et al*., 1990; Priola *et al*., 1994; Scott *et al*., 1992; Come and Lansbury, 1994; Goldfarb *et al*., 1993). The structure of PrP^{C} has been extensively studied in neuroblastoma cells persistently infected with prions and in transgenic mice expressing mutant PrP in order to understand the regions of PrP^{C} that are indispensable for PrP^{Sc} formation and prion propagation. Several lines of evidence have shown that the extreme N-terminal region of PrP^{C} (from aa 23 to aa 32) modulates prion propagation (Fischer *et al*., 1996; Flechsig *et al*., 2000; Supattapone *et al*., 1999).

However, studies have also demonstrated that the region between aa 32 and 90 is not essential for production of PrP^{Sc} and propagation of prions (Flechsig *et al*., 2000; Legname *et al*., 2005; Muramoto *et al*., 1996; Zulianello *et al*., 2000). The residues 114 to 121 comprise the most amyloidogenic region of PrP and they are essential for conversion of PrP^{C} into PrP^{Sc} (Hölscher *et al*., 1998; Norstrom and Mastrianni, 2005). A deletion mutant of PrP^{C} lacking residues 23 to 88 and 141 to 176 can convert into PrP^{Sc} and support prion propagation in transgenic mice, suggesting that the residues 141 to 176 are not essential for prion propagation (Muramoto *et al*., 1996; Supattapone *et al*., 1999). Moreover, the cysteine residue at 178 that forms an intramolecular disulfide bond with another cysteine residue at 213 is essential for PrP^{Sc} formation (Muramoto *et al*., 1996). Additionally, amino acid substitutions at 167 and 218 prevent PrP^{Sc} formation and show dominant-negative effect on prion propagation (Kaneko *et al*., 1997b; Perrier *et al*., 2002). Taken together, these studies indicate that the primary structure of PrP^{C} is essential in the conversion process and small amino acid changes may interrupt the formation and propagation of PrP^{Sc}.

The cell biology of the disease process, both in terms of the toxic mechanism associated with PrP^{Sc} formation, and on the details of the misfolding of PrP into its abnormal conformation are poorly understood. This is due to the difficulties involved in discriminating the exogenous and endogenous PrP in transgenic mouse models and cell culture systems, as well as in cell free conversion experiments. In addition, there are no antibodies specific to PrP^{Sc}. Therefore, different epitope tags, for which high-affinity antibodies are available, have been rationally designed into the PrP molecule as an instrument to study prion infection. However, the generation of true infectious prions containing an epitope tag has not yet been convincing in cells and animals. This

is probably because the sequence sensitivity of the conversion process prevents the misfolding of most tagged PrP^{C} molecules (Moore *et al*., 2005). The sequence sensitivity is such that the prion seed (exogenous PrP^{Sc}) and PrP^{C} substrate (endogenous cellular PrP^{C}) must have homologous primary structures for efficient conversion to take place, particularly in certain key regions of the PrP molecule (Caughey, 2001; Priola *et al*., 1994). Hence, previous attempts to produce PrP constructs with GFP reporter inserts or epitope tags have not generated PrP chimerae capable of prion conversion (Barmada and Harris, 2005; Rutishauser *et al*., 2009). Several recent studies have used epitope-tagged PrP such as MYC-, FLAG- and 3F4-tagged PrP molecules to study prion susceptibility and propagation *in vivo*, purify PrP, identify proteins interacting with PrP or examine PrP^{Sc} uptake in mouse neuronal and fibroblast cells (Vorberg *et al*., 2004b; Rutishauser et al., 2009; Greil *et al*., 2008; Magalhaes *et al*., 2005; Raeber *et al*., 1992). However, no one has yet described using tagged PrP to examine the initial events of infection.

3.1.1 Aims

The aim of this study was to generate a cell line that can produce epitope-tagged PrP^{Sc} molecules in a PrP-knock down (KD) neuroblastoma cell line. This would allow for the use of anti-tag antibodies to specifically detect the production of cellular *de novo* PrP^{Sc} (without detecting PrP^{Sc} in the inocula), allowing the earliest events in prion infection to be analysed.

3.2 Methods

Immunoblotting was used for detection of PrP expression (Section 2.3) in collaboration with Dr Rob Goold (Department of Neurodegenerative Disease, UCL

Institute of Neurology). Immunofluorescence analysis was undertaken for detection of PrP^{C} and misfolded PrP expression (Section 2.4.2). Mouse 3F4-tagged *Prnp* was generated by Dr Mark Kristiansen (MRC Prion Unit, UCL Institute of Neurology). Mouse FLAG- and MYC-tagged *Prnp* were generated by Dr Dave Emery (Henry Welcome Laboratories for Integrated Neuroscience) (Section 2.2.2). The scapie cell assay (SCA) was used to isolate RML prion-susceptible cell lines expressing tagged-PrP (Section 2.5). Biochemical and histological analysis was done to assess the infectivity of misfolded MYC-tagged PrP on the brains of Tg20 mice inoculated with RML prion-infected lysates of cells expressing MYC-tagged PrP (Section 2.3.1 and Section 2.3.3). Histology experiments were performed by Miss Caroline Powell (MRC Prion Unit, UCL Institute of Neurology) and Miss Julie Moonga (Department of Neurodegenerative Disease, UCL Institute of Neurology).

3.3 Results

3.3.1 Analysis of prion protein expression in knock down mouse PK1 cells

The mouse neuroblastoma PK1 cell line (Section 2.1.1), which is highly-susceptible to mouse-adapted prions (Klohn *et al*., 2003), was used throughout the experiments in this chapter. In order to generate a cell system to study prion infection in cells expressing tagged PrP without interference from the host wild-type PrP^{C}, PK1 cells were depleted of endogenous PrP using gene silencing. The inhibition of PrP^{Sc} formation by non-homologous PrP^{C} molecules has been observed in transgenic mouse models, cell cultures and cell-free conversion assays and considerable data suggest this is due to 'dominant negative' inhibition of non-homologous prion propagation by endogenous mouse PrP^{C} (Prusiner *et al.*, 1990; Bueler *et al*., 1993; Priola *et al*., 1994;

Telling *et al*., 1994; Telling *et al*., 1995; Collinge *et al*., 1995; Horiuchi *et al*., 2000; Perrier *et al*., 2002). The basis for this inhibitory phenomenon of PrP^{Sc} formation is thought to be that non-homologous PrP^{C} molecules readily interact with PrP^{Sc} but cannot be converted (Horiuchi *et al*., 2000). Therefore, in this study, to eliminate the inhibition of tagged-PrP^{Sc} formation and propagation by endogenous mouse PrP^{C} in PK1 cells, the mouse *Prnp* gene was specifically silenced. RNAi, using the pSUPERretro system, was exploited to stably knock down the host mouse *Prnp* in PK1 cells (courtesy of Professor Parmjit Jat, MRC Prion Unit, UCL Institute of Neurology, unpublished data, Section 2.2.1). Stable cell lines were isolated and analysed for PrP expression and prion susceptibility. Immunofluorescence analysis (Figure 3-1 A) and immunoblotting (Figure 3-3) on PrP-KD PK1 cells (P8(11)4.5 and PK1-10*Si8*) demonstrated effective *Prnp* silencing with PrP levels reduced by approximately 90-95 % in the cell lines selected for further study. The scrapie cell assay was used to test the susceptibility of these PrP-KD cells to prion infection (Section 2.5). This assay measures the number of cells containing detectable levels of PK-resistant PrP (PrP^{Sc}) following 72 hours exposure to RML prions and three cell passages. It can be used as a measure of the level of prion infection in a given cell culture (Klohn *et al*., 2003). The SCA showed that the cells were unable to propagate prions, as expected (Figure 3-1 B).

Dr Liza Sutton (MRC Prion Unit, UCL Institute of Neurology) reconstituted PrP-KD PK1 cells with mouse PrP^{C} to determine if siRNA expression affected the innate susceptibility of PK1 cells to RML prions. It was observed that mouse PrP^{C} expression can be reconstituted in the PrP-KD cell lines to levels equivalent or greater than wild type cells. Moreover, it was demonstrated that reconstitution of mouse PrP^{C}

in PrP-KD PK1 cells restored susceptibility to RML prions (Dr Liza Sutton, unpublished data).

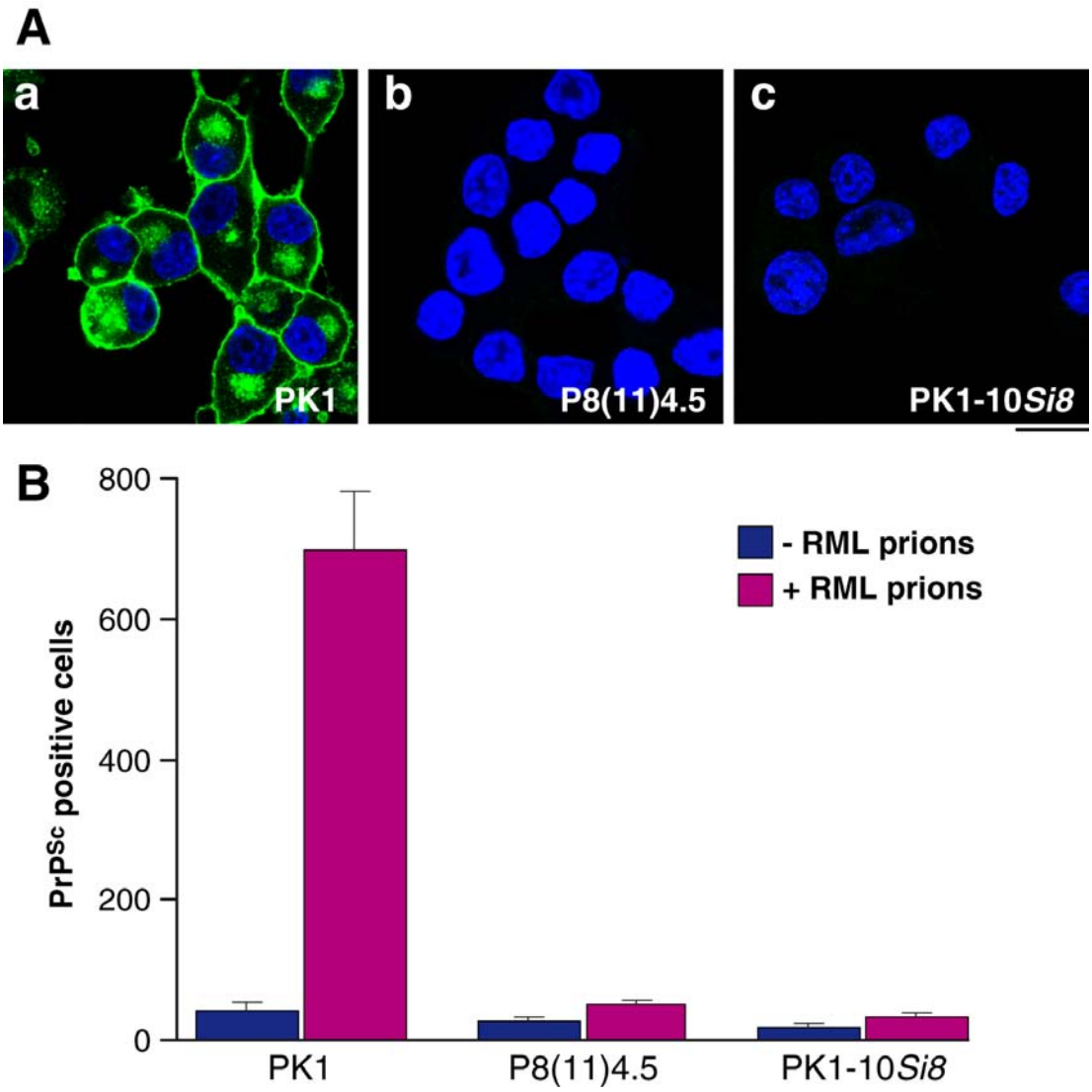

Figure 3-1 Mouse PrP-KD PK1 cells do not express prions

(A) Confocal images of PK1 cells, PrP-KD P8(11)4.5 and PK1-10*Si8* cells stained with anti-PrP antibody (green; ICSM18). Note PrP^{C} is expressed in PK1 cells, but not in PrP-KD P8(11)4.5 and PK1-10*Si8* cells. Nuclei were stained with DAPI (blue). Scale bar = 15 µm. **(B)** PK1, PrP-KD P8(11)4.5 and PK-10*Si8* cells were exposed to 0.1 % RML prion-infected mouse brain homogenate for 72 hours and then passaged at 1:8 splits three times to clear the prion inocula. Cells were analysed for their prion-susceptibility by the SCA using ICSM18 anti-PrP antibody. No detectable PK-resistant PrP (PrP^{Sc}) was seen in PrP-KD cells. The mean + SEM of six wells are shown.

3.3.2 Generating a panel of nine differentially tagged mouse PrP^C molecules

To generate a tagged mouse PrP^C construct able to support efficient prion protein conversion and replication a panel of novel PrP^C molecules was designed with 3F4, FLAG or MYC tags inserted at various points within the PrP sequence (Figure 3-2). In the 3F4 construct, the mouse *Prnp* was modified to express Methionine 108 and 111 ($PrP^{L108M/V111M}$). This allows it to be specifically recognised by the 3F4 antibody, which although able to bind to hamster and human PrP^C, is not able to bind to the mouse homolog. Inserting the 3F4 epitope does not impair the folding of PrP^C as it undergoes conversion to PrP^{Sc} following RML infection in both neuronal cells (Atarashi *et al*., 2006) and mice (Telling *et al*., 1995).

As well as the 3F4 construct, PrP constructs tagged with the FLAG peptide sequence, Asp-Tyr-Lys-Asp-Asp-Asp-Asp-Lys, and MYC peptide sequences, Glu-Gln-Lys-Leu-Ile-Ser-Glu-Glu-Asp-Leu, were also produced (Figure 3-2). They were used largely because the 3F4 construct cannot be used for detailed ultra-structural studies without antigen retrieval since the epitope is buried into the native protein (Peretz *et al*., 1997; Safar *et al*., 1998; Safar *et al*., 2005; Yuan *et al*., 2005). The MYC tag was chosen as they are small and are unlikely to affect the tagged prion's biochemical properties. The MYC tag has also been used widely to detect cellular localisation of tagged-proteins by immunofluorescence analysis and there are excellent antibodies against the MYC epitope. The FLAG tag was chosen as it is relatively hydrophilic as compared to other common protein tags, and therefore the least likely to become buried within the core of the folded protein. Furthermore, this approach has been validated by Telling and colleagues using FLAG-tagged PrP at positions 22 and

88 of mouse PrP^{C}, demonstrating conversion of PrP^{Sc} in transgenic mice following prion infection (Telling *et al*., 1997). Both MYC and FLAG tags were placed in the unstructured regions of the PrP (Figure 3-2). These sites are thought not to impinge on any regions suggested to be of importance in the binding of PrP^{C} to PrP^{Sc} and therefore they are less likely to interfere with PrP^{Sc} formation (Horiuchi and Caughey, 1999; Caughey, 2001).

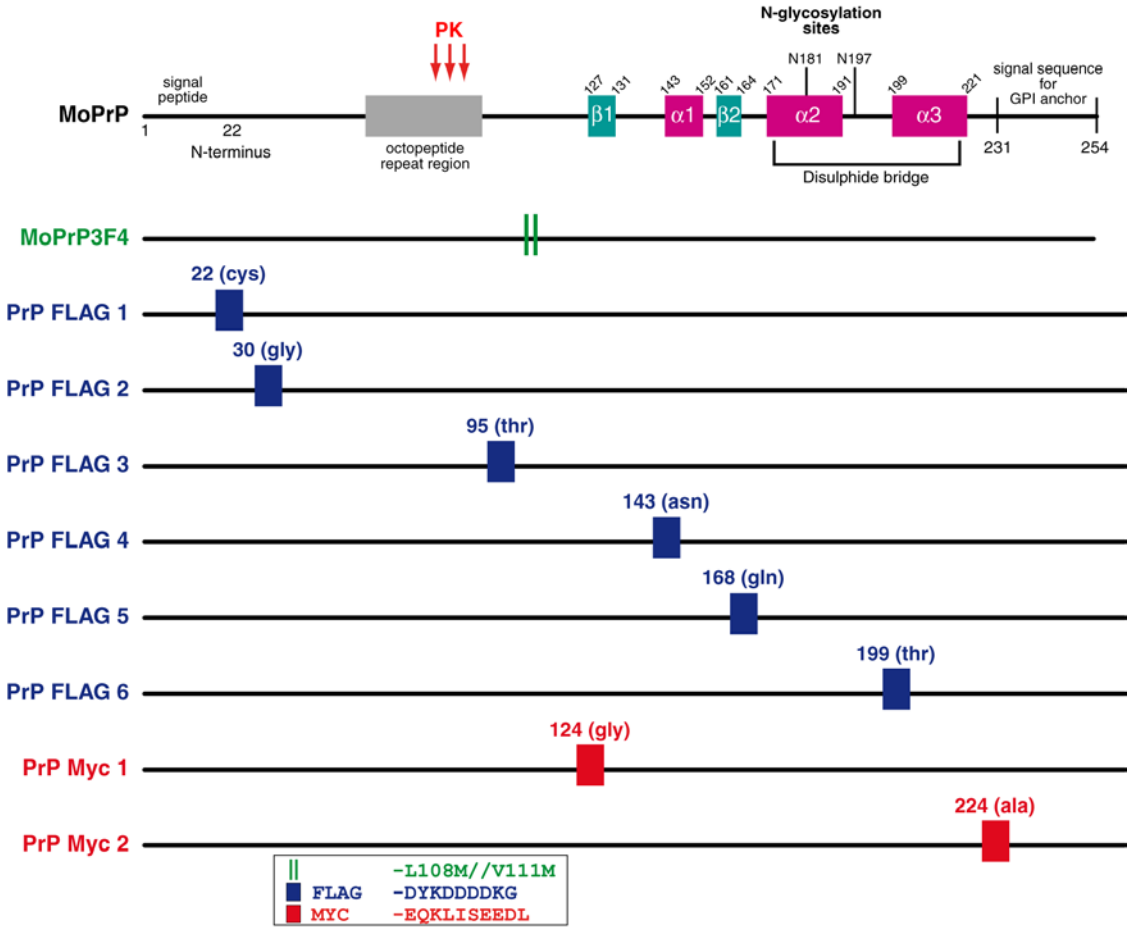

Figure 3-2 Schematic representation of the domain structure of murine PrP

Substitution of leucine 108 and valine 111 to methionine generates the 3F4 epitope in the mouse PrP molecule. FLAG and MYC epitope tags have been positioned in unstructured regions of PrP not thought to be involved in the conformational rearrangement of PrP.

3.3.3 Mouse 3F4-tagged PrP^C expression in PrP-KD PK1 cells

Mouse 3F4-tagged *Prnp* was cloned into the retroviral expression vector, pLNCX2, and packaged into the PhiNX-eco retroviral producer cell line (Section 2.2.3). Ecotropic virus was harvested and used for retroviral transduction of two PrP-KD PK1 cell lines (P8(11)4.5 and PK1-10*Si8*) with the mouse 3F4-tagged PrP^C construct (moPrP^C.3F4). Successfully transduced cells were isolated by appropriate antibiotics as described in section 2.2.3 and mixed clones stably expressing mouse 3F4-tagged PrP^C were established. Immunoblotting of lysates from transduced cells, using anti-PrP ICSM35 and the 3F4 antibody, confirmed reconstitution of PrP-KD cells with 3F4-tagged PrP^C (Figure 3-3, middle blot, lanes 2 and 3). Furthermore, immunofluorescence analysis in the transduced cells demonstrated the expression of moPrP^C.3F4 (Figure 3-4, panels b and d), confirming the immunoblotting results. Non-transduced cells did not express any detectable PrP^C and were used as negative controls (Figure 3-3, lanes 4 and 5, Figure 3-4, panels a and c). The 3F4 antibody could not be used to detect prion protein without antigen retrieval, since the 3F4 epitope is buried in the native protein (Peretz *et al*., 1997; Safar *et al*., 1998; Safar *et al*., 2005). Therefore, well characterised ICSM18 anti-PrP antibody was used in immunofluorescence analysis to detect 3F4-tagged PrP^C expression in transduced cells.

Taken together, these results indicate that the transduction of the moPrP^C.3F4 construct was successful, but the level of tagged-PrP^C expression varies across the cell population (Figure 3-4, panels b and d).

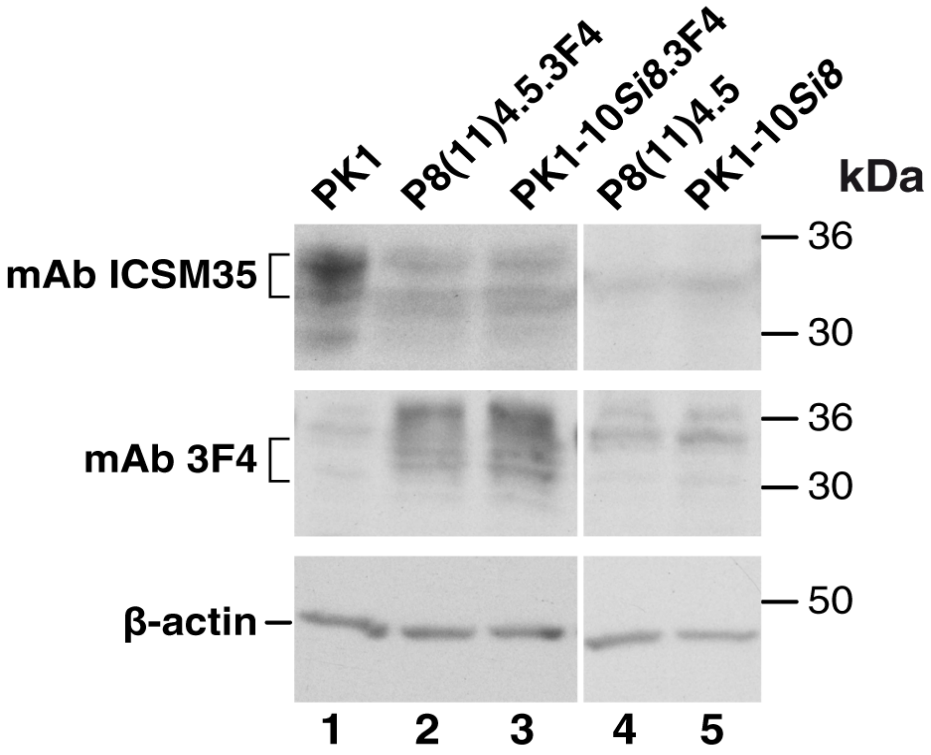

Figure 3-3 Transduced PK1-10*Si8* and P8(11)4.5 mixed clones express moPrP^{C}.3F4

Lysates from PK1, PK1-10*Si8* and P8(11)4.5, as well as from PK1-10*Si8*.3F4 and P8(11)4.5.3F4 mixed clones were analysed by SDS-PAGE electrophoresis and immunoblotted with anti-PrP ICSM35 (top blot) and the 3F4 (middle blot) antibodies. MoPrP^{C}.3F4 was detected in the 3F4 transduced cells (PK1-10*Si8*.3F4 and P8(11)4.5.3F4, lanes 2 and 3), however no 3F4 tagged-PrP^{C} was noticed in PK1, PK1-10*Si8* and P8(11)4.5 cells when the 3F4 antibody was used (bottom blot, lanes 1, 4 and 5). Imunoblotting of β-actin confirmed equal protein loading (bottom blot). Quantitative densitometry of similar blots showed PrP expression was reduced by 90-95 % in PrP-KD cells.

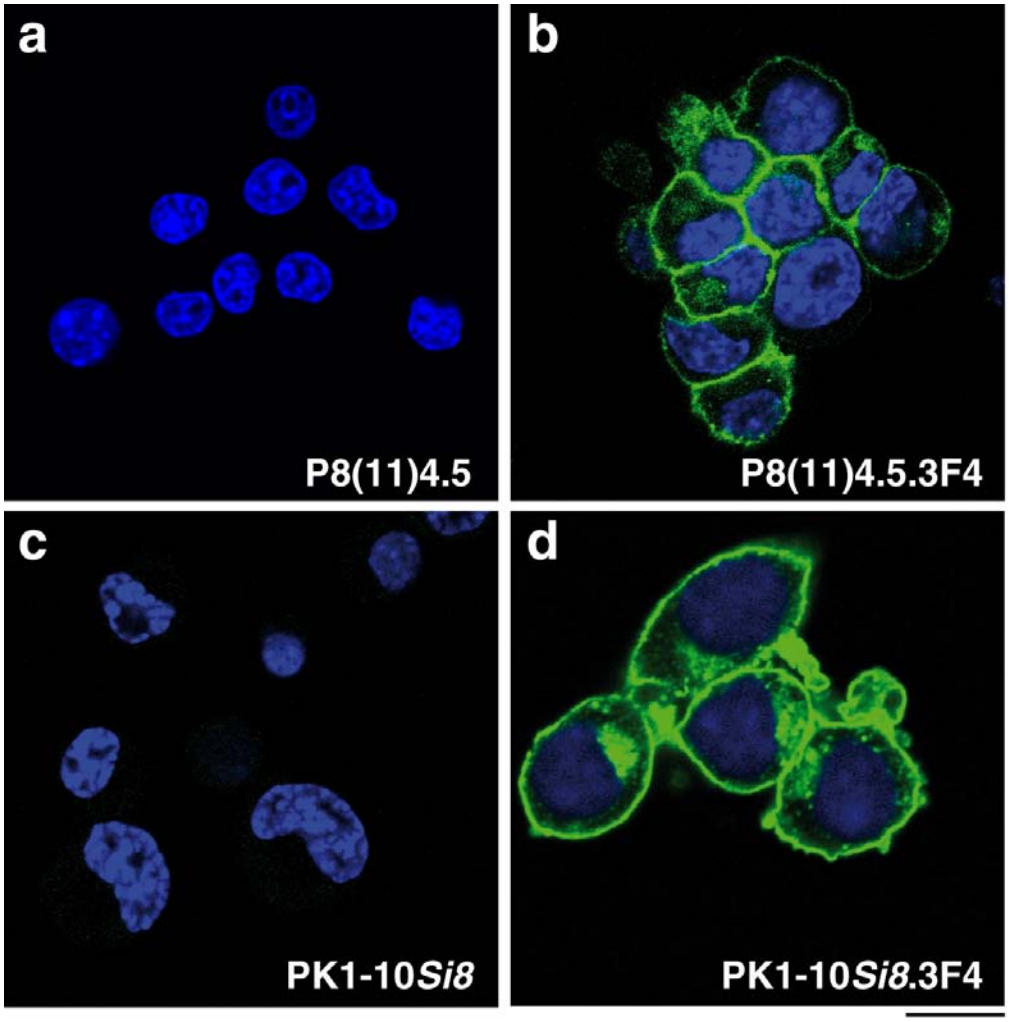

Figure 3-4 Expression of moPrP^{C}.3F4 in transduced PK1-10*Si8* and P8(11)4.5 mixed clones

MoPrP^{C}.3F4 (green; ICSM18) is expressed in the P8(11).4.5.3F4 and PK1-10*Si8*.3F4 cells, as showing by confocal images. Note the predominant membrane expression of MoPrP^{C}.3F4 in the transduced cells. P8(11)4.5 and PK1-10*Si8* cells were used as negative controls. Nuclei were stained with DAPI (blue). Scale bar = 15µm.

3.3.4 Conversion of MoPrP^{C}.3F4 into misfolded PrP

In order to determine whether PrP-KD PK1 cells reconstituted with moPrP^{C}.3F4 were susceptible to RML prions, P8(11)4.5.3F4 and PK1-10*Si8*.3F4 mixed clones were infected with 0.1 % RML prion-infected mouse brain homogenate. Prion infection was assessed by the SCA, however, no detectable levels of the disease-related isoform were found (Figure 3-5).

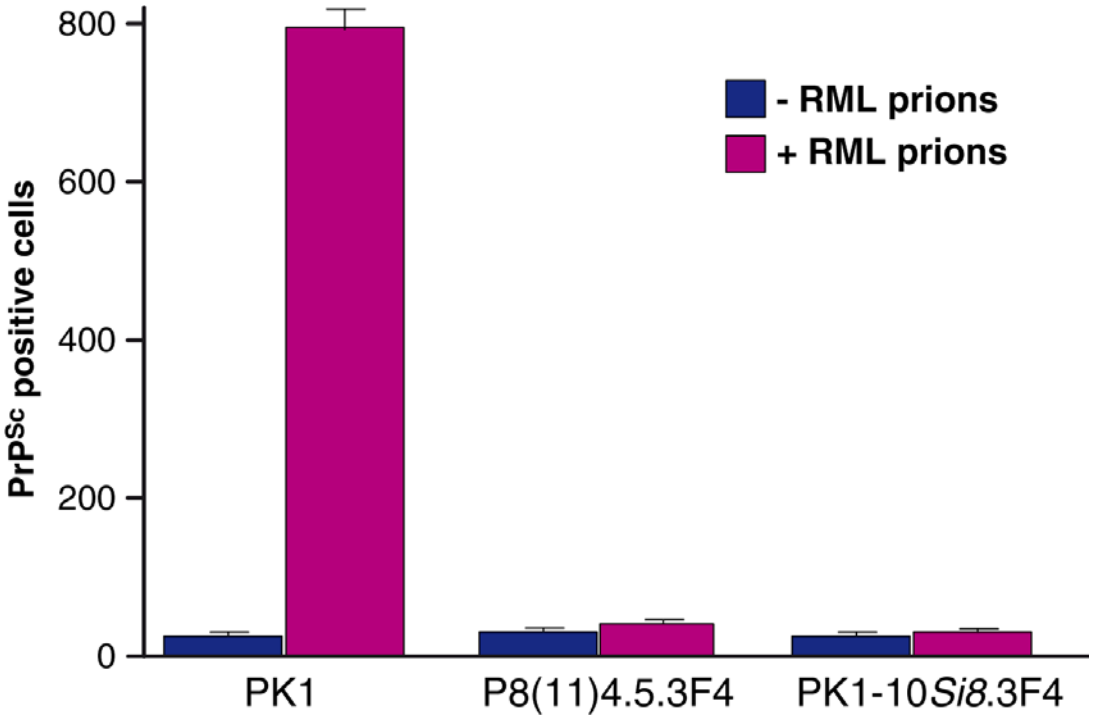

Figure 3-5 PK1-10*Si8*.3F4 and P8(11)4.5.3F4 mixed clones are not susceptible to RML prions

Non-infected and RML prion infected PK1-10*Si8*.3F4 and P8(11)4.5.3F4 were analysed for their susceptibility to RML prions by the SCA. No measurable level of RML prion infection was detected in the MoPrP^{C}.3F4 expressing mixed clones using ICSM18 anti-PrP antibody. Non-infected, and RML prion infected PK1 cells were used as positive controls. The mean + SEM of six wells are shown.

Isolation of moPrP^{C}.3F4 prion-susceptible single cell clones

To find the rare clones susceptible to RML prions, a clonal selection strategy was developed (Section 2.2.4). Two hundred single cell clones were picked of each of the moPrP^{C}.3F4 transduced P8(11)4.5 and PK1-10*Si8* cell lines and grown in culture. Clones were then infected with 0.1 % RML prion-infected mouse brain homogenate and each clone was screened for RML prion-infectivity by scrapie cell assay (Section 2.5) at every passage up to passage six. The twenty four most susceptible clones from each of the cell lines (P8(11)4.5.3F4 and PK1-10*Si8*.3F4) were selected for expansion. They were then assayed by the SCA and immunofluorescence analysis. These forty eight highly-susceptible single cell clones were analysed further to isolate the seven most susceptible ones. Non-infected master clones of seven selected cell clones were expanded and studied further.

Immunofluorescence analysis was done on the selected cell clones to confirm that they express moPrP^{C}.3F4, using an anti-PrP antibody, ICSM18, (Figure 3-6). MoPrP^{C}.3F4 was detected in each of the isolated prion-susceptible clones, predominantly on the plasma membrane (Figure 3-6). Immunoblotting of lysates of the susceptible clones, using anti-PrP ICSM35 and the 3F4 antibodies, confirmed expression of moPrP^{C}.3F4 (Figure 3-7, lanes 3-5 and lanes 7-10), but the expression levels varied across the different clones. PK1 cells were used to show the physiological expression of wild type PrP^{C} (positive control). PK1-10*Si8* and P8(11)4.5 cells were used as negative controls since they do not express significant levels of PrP^{C} (Figure 3-6 and Figure 3-7).

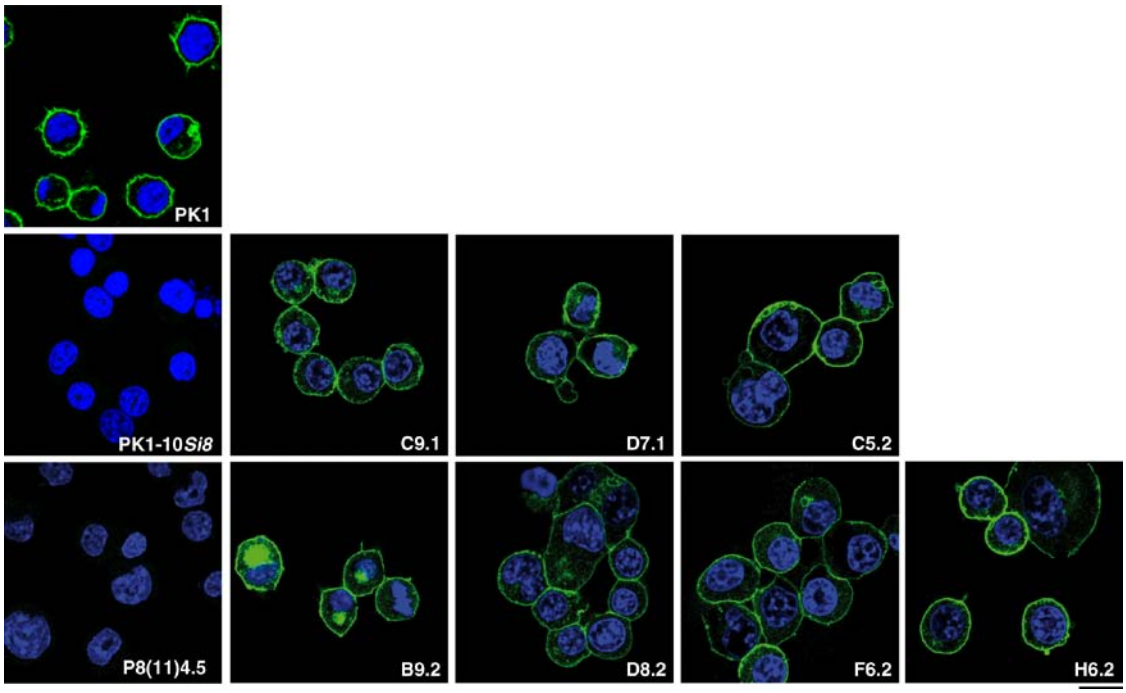

Figure 3-6 moPrP^{C}.3F4 expression in PK1-10*Si8*.3F4 and P8(11)4.5.3F4 single cell clones

Immunofluorecence staining showed moPrP^{C}.3F4 expression (green) in seven susceptible single cell clones, using an anti-PrP antibody (ICSM18). Nuclei were stained with DAPI (blue). Note the predominant expression of 3F4-tagged mouse PrP^{C} on the plasma membrane. PK1 and parental PrP-KD cells were used as positive and negative controls, respectively. Scale bar = 15 µm

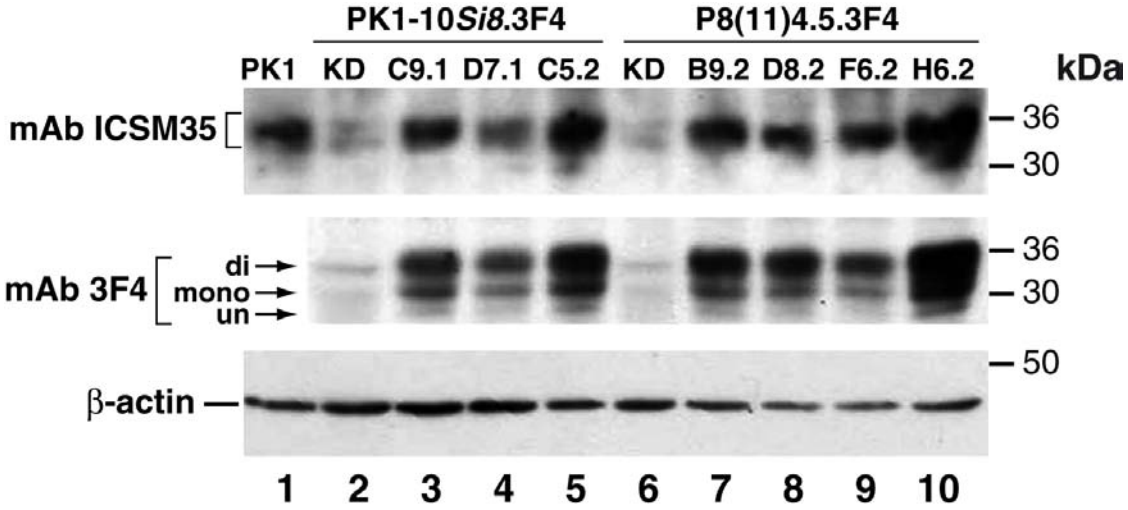

Figure 3-7 Detection of moPrP^{C}.3F4 expression in PK1-10*Si8*.3F4 and P8(11)4.5.3F4 single cell clones by immunoblotting

Lysates of single cell clones from PK1-10*Si8*.3F4 (C9.1, D7.1, C5.2) and P8(11)4.5.3F4 (B9.2, D8.2, F6.2, H6.2) cells were analysed by SDS-PAGE electrophoresis for the expression of 3F4-tagged mouse PrP^{C}. Mouse monoclonal anti-PrP antibody (ICSM35; top blot) and mouse monoclonal 3F4 antibody (middle blot) were used for immunoblotting. PrP^{C} runs between 30-50 kDa in its three glycosylation states (di-glycosylated, mono-glycosylated, and un-glycosylated), as seen in PK1 cells and moPrP^{C}.3F4 reconstituted single cell clones but not in PrP-KD cell lines. MoPrP3F4 expression is shown in the single cell clones from the reconstituted cells. PK1 lysates are included to indicate physiological expression of PrP^{C}. Lysates from PrP-KD cells, which do not express substantial levels of PrP^{C}, are included as negative controls. Levels of an endogenous mouse protein, β-actin, were assessed by immunoblotting to confirm equal protein loading (bottom blot).

Misfolded moPrP.3F4 propagation in prion-susceptible single cell clones

The seven susceptible single cell clones were analysed in more details. Clones were exposed to 0.1 % RML prion-infected mouse brain homogenate, following which they were screened for their susceptibility to prion infectivity by the SCA and immunofluorescence analysis (Figure 3-8, Figure 3-9 A and B). The SCA analysis of the susceptible single cell clones showed that of the RML prion-infected PK1-10*Si8*.3F4 cells, D7.1 single cell clone contained the highest amount of misfolded moPrP.3F4. The RML prion-infected P8(11)4.5.3F4 single cell clones had similar spot numbers, but it was found that P8(11)4.5.3F4;H6.2 single cell clone displayed a consistent level of infectivity in repeated experiments as compared to the other P8(11)4.5.3F4 clones (Figure 3-8).

The susceptibility of selected single cell clones to RML prions were also assessed with Immuno-fluorescence analysis, using a mouse monoclonal 3F4 antibody following five minutes formic acid treatment. Due to the lack of antibodies specific for PrP^{Sc}, it is necessary to treat cells post-infection to remove detectable PrP^{C}, leaving PrP^{Sc} available for immunodetection. Five minutes treatment of RML prion-infected cells with 98 % formic acid has been shown to hydrolyse PrP^{C} and reveal PrP^{Sc} (Kristiansen *et al*., 2005). Formic acid was also used to expose the 3F4 epitope. To determine the percentage of cells producing misfolded moPrP.3F4, pictures of the stained cells were taken using a fluorescent microscope and the number of 3F4 positive cells was counted (Figure 3-9 A). The results for the PK1-10*Si8*.3F4 cells corroborated the SCA results, but, counts for P8(11)4.5.3F4 single cell clones showed that P8(11)4.5.3F4;B9.2 clone had the highest percentage of 3F4 positive cells. Therefore, experiments were

continued using the P8(11)4.5.3F4;H6.2 clone as it showed more consistent infectivity by both immunofluorescence and the SCA analysis. The P8(11)4.5.3F4;H6.2 clone was also the only single cell clone that significantly over-expressed moPrP.3F4 as compared to wild type PK-1 cells (Figure 3-7, lane 10). Therefore, P8(11)4.5.3F4;H6.2 as well as PK1-10*Si8*.3F4;D7.1 clones (henceforth termed H6.2 and D7.1 cells, respectively) were expanded for use in experiments. Confocal images of RML prion-infected D7.1 and H6.2 cells showed the presence of intracellular and plasma membrane formic acid-resistant moPrP.3F4 in the cells (Figure 3-9 B).

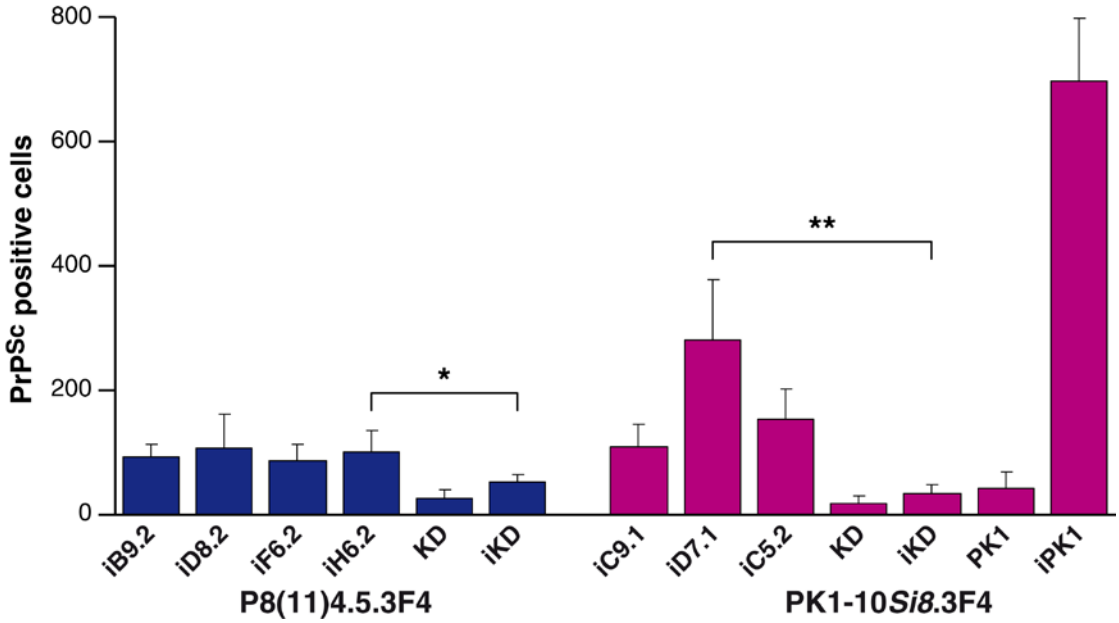

Figure 3-8 Misfolded moPrP.3F4 propagation in seven RML prion-infected single cell clones

P8(11)4.5.3F4 and PK-10*Si8*.3F4 single cell clones, parental PrP-KD lines and PK1 cells were exposed to 0.1 % RML prion-infected mouse brain homogenate for 72 hours and then passaged at 1:8 splits three times to clear the prion inocula. Cells were analysed for their prion-susceptibility by the SCA (ICSM18). i = RML prion-infected. The mean + SEM of six wells are shown. * $P < 0.05$, ** $P < 0.01$.

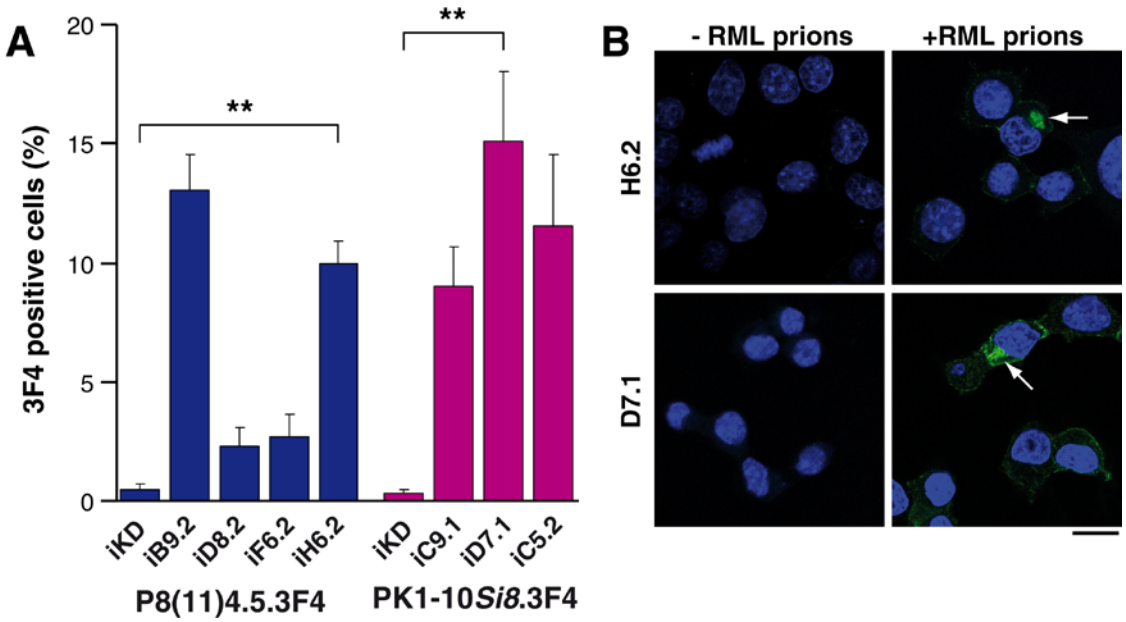

Figure 3-9 Seven moPrP.3F4 single cell clones infected with RML prions propagate misfolded PrP

(A) Non-infected and RML prion-infected cells were treated with formic acid for five minutes prior to staining with the 3F4 antibody. The percentage of cells positive for 3F4 staining was counted. PrP-KD cells, which do not express PrP^{C}, were used as negative controls. i = RML prion-infected. The mean + SEM of 20 fields of view are shown. ** $P < 0.01$. **(B)** Confocal images of the non-infected (- RML prions) and RML prion-infected (+ RML prions) H6.2 and D7.1 clones stained with mouse monoclonal 3F4 antibody (green) following five minutes formic acid treatment. Residual 3F4 staining (white arrows) indicates that some of the cells contain formic acid-resistant PrP, which corresponds to misfolded PrP. Nuclei were stained with DAPI (blue). Scale bar = 15 µm.

3.3.5 FLAG- and MYC-tagged mouse PrP^C expression in PrP-KD PK1 cells

Mouse FLAG- and MYC-tagged *Prnp* (Appendix I and Appendix II) were generated by Dr Dave Emery (Henry Wellcome Laboratories for Integrated Neuroscience) and were cloned into the retroviral expression vector, pLNCX2, (Appendix III) using the following cloning strategy (Figure 3-10).

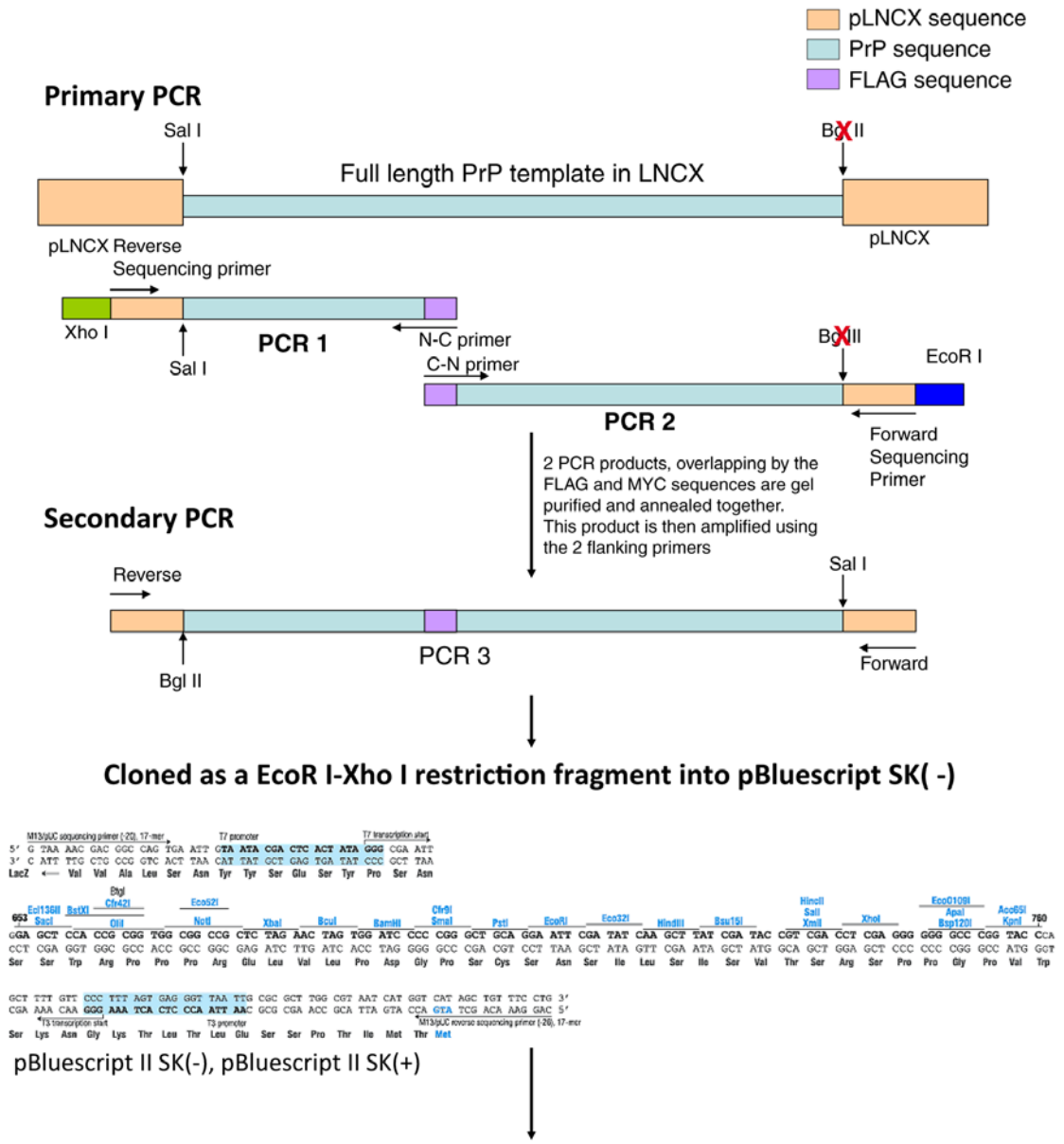

Figure 3-10 Cloning strategy for inserting FLAG and MYC tag sequence in pLNCX2

The PCR scheme has been adapted from that previously seen with the incorporation of an EcoR I site into the 5' sequencing (flanking PCR) primer and an Xho I site into the 3' primer. *This cloning strategy was developed by Dr Dave Emery (Henry Wellcome Laboratories for Integrated Neuroscience).*

pLNCX2 vectors expressing FLAG- and MYC- tagged PrP were packaged into the PhiNX-eco retroviral producer cell line and ecotropic viruses were harvested and used for retroviral transduction of PrP-KD PK1 cells as described in section 2.2.3. P8(11)4.5 cells were transduced with six different mouse FLAG-tagged PrP constructs and PK-10*Si8* cells were transduced with two different mouse MYC-tagged PrP constructs. Successfully transduced cells were isolated by appropriate antibiotic selections (Section 2.2.3) and mixed clones stably expressing tagged mouse PrP^C were generated. Cells were screened for FLAG- and MYC-tagged PrP^C expression by immunoblotting and immunofluorescence analysis (Figure 3-11 A, B and Figure 3-12).

Immunoblotting of stable transformants of P8(11)4.5 and PK-10*Si8* cell lysates transfected with FLAG- and MYC-tagged mouse PrP^C constructs, respectively, using anti-PrP ICSM35 and anti-tag antibodies showed that the inclusion of the FLAG and MYC epitope in mouse *Prnp* does not prevent normal biosynthesis of PrP^C (Figure 3-11 A, lanes 3-8, B, lanes 3 and 4). SDS-PAGE analyses showed a slightly decreased mobility of PrP-95ThrFLAG, PrP-143ThrFLAG, PrP-168ThrFLAG and PrP-124GlyMYC construct when compared to N-terminal FLAG-tagged PrP (PrP-22CysFLAG and PrP-30GlyFLAG), C-terminal MYC-tagged PrP (PrP-224AlaMYC) and wild type PrP (Figure 3-11 A, B). This was assumed to be due to conformational affects that result in a reduced migration. Detection of PrP^C expression in PrP-95ThrFLAG cells (Figure 3-11 A, top blot, lane 5) using anti-PrP ICSM35 antibody was failed by immunoblotting, since the 95ThrFLAG tag had been inserted into the same position as the epitope detected by the anti-PrP ICSM35 antibody (amino acid residues 93-105 on the N-terminal region of *Prnp*). Figure 3-11 A and B show that in comparison to non-transfected PK1 cells (top blots, lane 1), all the cells transduced

with FLAG- and MYC-tagged PrP^C are expressing PrP^C to different levels. In particular PrP-30GlyFLAG cells are heavily over-expressing FLAG-tagged PrP^C (Figure 3-11 A, lane 4). Furthermore, the molecular weight of PrP^C in the transfected cells appears slightly different from the endogenous PrP^C produced in PK1 cells due to the insertion of the FLAG and MYC tag into *Prnp*.

Immunofluorescence analysis of P8(11)4.5.FLAG and PK-10*Si8*.MYC cells demonstrated that the cellular distribution of FLAG- and MYC-tagged PrP^C were similar to that of wild type PrP^C in PK1 cells, predominantly on the plasma membrane, (Figure 3-12). Therefore, the presence of FLAG and MYC tag in *Prnp* does not seem to affect the normal physiological distribution of PrP^C. PrP^C expression could not be detected in cells expressing PrP-143Asn FLAG, as the tag has been inserted in the epitope recognised by the ICSM18 anti-PrP antibody (amino acid residues 142–153).

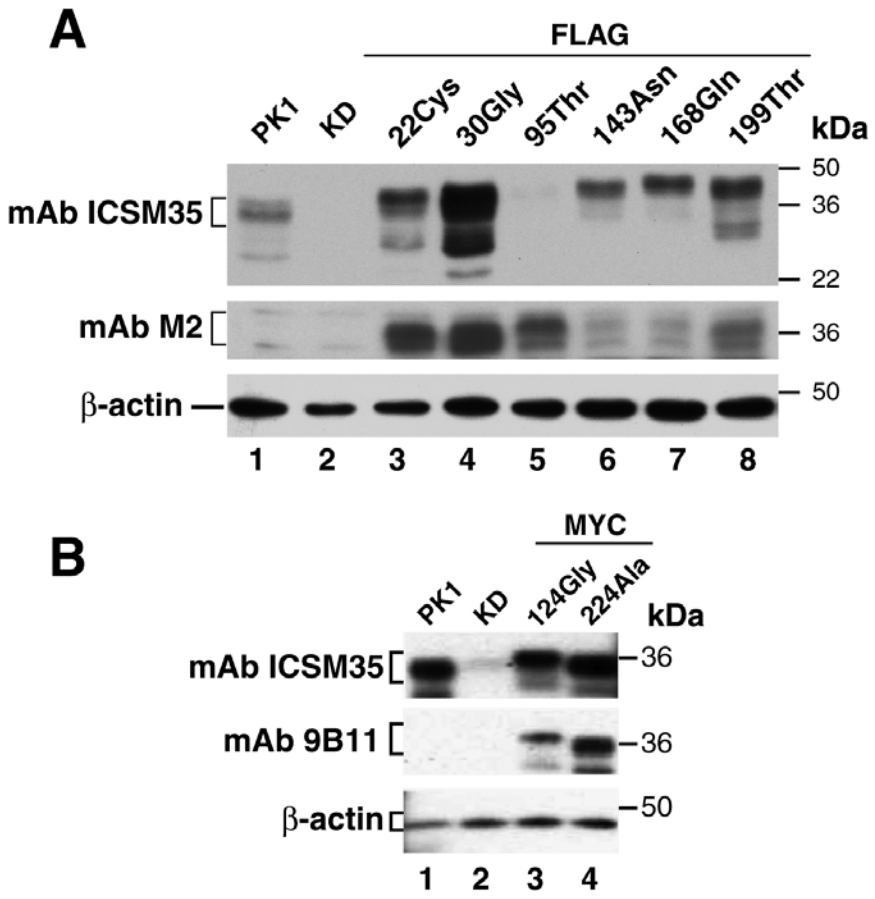

Figure 3-11 Transduced P8(11)4.5 and PK-10*Si8* mixed clones express Mouse FLAG- and MYC-tagged PrP^{C}

Lysates of the P8(11)4.5 and PK-10*Si8* cell lines reconstituted with FLAG- and MYC-tagged PrP constructs were analysed by SDS-PAGE electrophoresis using mouse monoclonal anti-PrP antibody (ICSM35; top blot; A and B) and mouse monoclonal anti-FLAG (M2) and anti-MYC (9B11) antibody (middle blot; A and B). PK1 lysate is included to indicate physiological expression of PrP^{C} (lane 1; A and B) and parental PrP-KD cell lines, P8(11)4.5 (lane 2; A) and PK-10*Si8* (lane 2; B), were used as negative controls. Immunoblotting of β-actin, confirmed equal protein loading (A and B). **(A)** Expression of FLAG-tagged PrP^{C} in the reconstituted cells was shown (lanes 3 to 8). Cells reconstituted with FLAG tag inserted in different position of *Prnp* express PrP^{C} in different levels. PrP-30GlyFLAG cells are heavily over-expressing FLAG-tagged PrP^{C} (lane 4). No PrP^{C} expression was detected in PrP-95ThrFLAG cells (lane 5) since the 95ThrFLAG tag has been inserted in the ICMS35 epitope (aa 96 and 109). **(B)** Immunoblotting analysis of MYC-tag reconstituted cells showed that MYC epitope in mouse *Prnp* does not prevent normal biosynthesis of PrP^{C} (lanes 3 and 4).

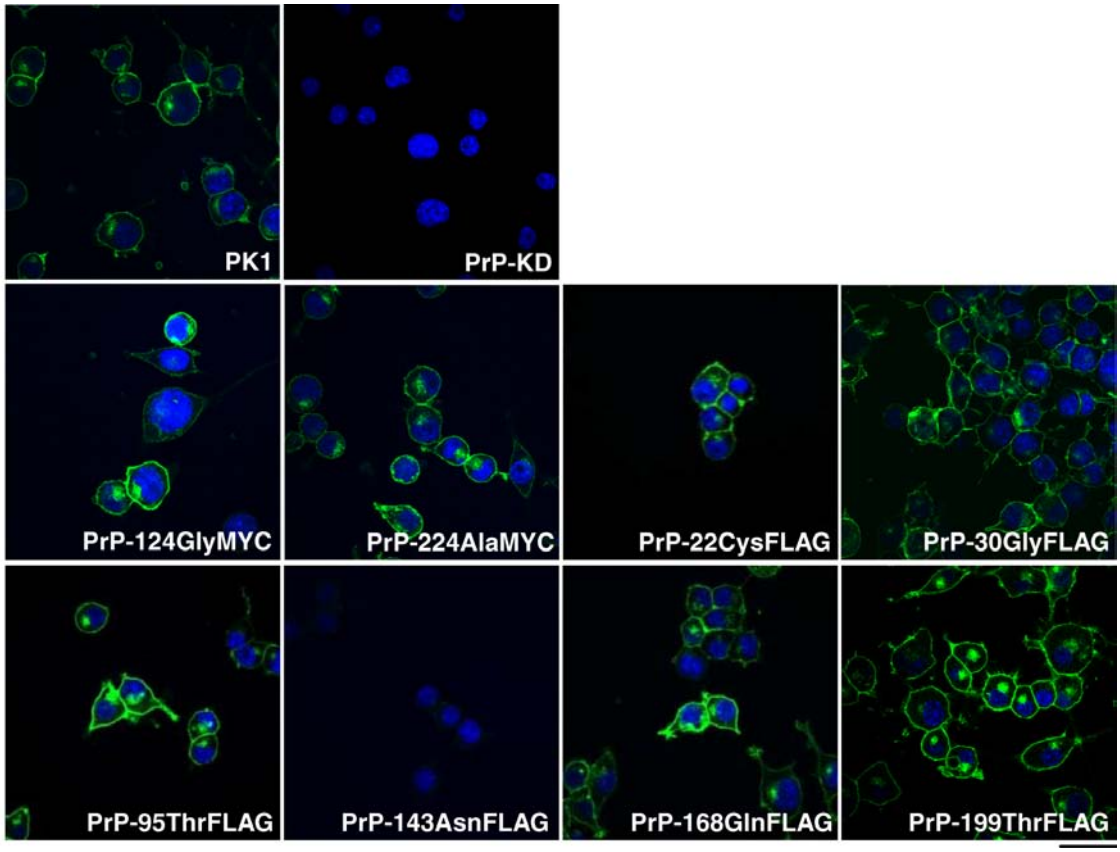

Figure 3-12 Expression of FLAG- and MYC-tagged PrP^C in reconstituted mixed clones

Immunofluorescence staining was performed on reconstituted mixed clones expressing FLAG- and MYC-tagged PrP^C using an anti-PrP antibody (Green; ICSM18). PrP^C was dominantly expressed on the plasma membrane of the cells. Note that PrP^C expression levels vary depends on where the FLAG and MYC tags are inserted. Nuclei were stained with DAPI (blue). PK1 and PrP-KD cells were used as positive and negative controls, respectivel. Scale bar = 30 µm.

3.3.6 Conversion of FLAG- and MYC-tagged mouse PrP^C into misfolded PrP in reconstituted P8(11)4.5 and PK1-10*Si8* cells

To check whether FLAG- and MYC-tagged PrP expressing cells were susceptible to prion infection, mixed clones were exposed to 0.1 % RML prion-infected mouse brain homogenate and their infectivity levels were analysed (Figure 3-13 and Figure 3-14). The SCA analysis demonstrated that PrP constructs with FLAG-tag inserted near the N-terminus of the protein (22CysFLAG, and particularly 30GlyFLAG) reconstituted prion propagation very efficiently and contained high levels of PK-resistant PrP (Figure 3-13 A). Cells expressing molecules with tags inserted centrally within the PrP sequence did not support prion propagation (Figure 3-13 A and B). However, cells expressing MYC-tagged PrP with the tag inserted near the C-terminus (224AlaMYC) were found to propagate prions robustly and reproducibly (Figure 3-13 B).

This finding was corroborated by immunoblotting on the PK-digested cell lysates of RML prion-infected P8(11)4.5-FLAG and PK1-10*Si8*-MYC cells (Figure 3-14 A and B). RML prion-infected PrP-22CysFLAG contained PK-resistant prion protein, a characteristic feature of PrP^{Sc}, to a similar level as wild type PK1 cells (Figure 3-14 A, lane 3). RML prion-infected PrP-224AlaMYC cell extracts contained low levels of PK-resistant PrP consistent with the SCA data (Figure 3-14 B, lanes 8, 9 and 12). Finally, RML prion-infected PrP-30GlyFLAG cells heavily over-expressed PK-resistant PrP (Figure 3-14 A, lane 4). No significant levels of PK-resistant PrP were found in cells expressing the other FLAG (Figure 3-14 A, lanes 5-8) and MYC (data not shown) constructs. RML prion-infected PK1 cells were used as positive

controls to show the PK-resistant band in prion-infected cells and RML prion-infected PrP-KD PK1 cells were used as negative controls (Figure 3-14 A, lanes 1 and 2, B, lanes 1-5). Single cell cloning of FLAG- and MYC-tagged reconstituted PK1 cells was deemed unnecessary since the mixed clones were able to propagate misfolded tagged PrP.

As aforementioned, PrP-30GlyFLAG cells were heavily over-expressing FLAG-tagged PrP^{C}. Therefore to confirm that the PK-resistant PrP seen in the immunoblotting and the SCA analysis is true misfolded PK-resistant PrP molecules and not partially digested PrP^{C} molecules, immunoblotting was performed on the lysates of non-infected and RML prion-infected PrP-30GlyFLAG cells (Figure 3-15). Expression of PrP in non-infected and RML prion-infected PrP-30GlyFLAG cells was shown respectively in figure 3-15, lane 1 and 2. Treatment of non-infected PrP-30GlyFLAG cells with PK for 30 minutes at 37°C was sufficient to digest PrP^{C} completely as no bands were seen on the blot (Figure 3-15, lane 3). Therefore, this demonstrates that the PK-resistant PrP of prion-infected PrP-30GlyFLAG cells seen on the SCA and immunoblots are not due to the partial digestion of PrP^{C}. In addition, lower molecular bands were seen in the non-PK digested, RML prion-infected PrP-30GlyFLAG cell lysates similar to the expected PrP^{Sc} signal in their PK-digested counterparts. This result follows the finding from Caughey and his colleagues that misfolded PrP are partially proteolysed within neuroblastoma cells (Caughey *et al*., 1991).

Taken together, N-terminally FLAG- and C-terminally MYC-tagged PK1 cells were able to propagate misfolded FLAG- and MYC-tagged PrP after exposure to RML prions and among those N-terminally FLAG-tagged cells, PrP-30GlyFLAG cells were

highly propagating the misfolded PrP. However, it became apparent during the course of my study that the N-terminal FLAG tag was readily cleaved during cellular processing such that a proportion of the tagged PrP^{Sc} in the cells was not detected by the anti-FLAG antibodies, making them unsuitable for this study. Therefore PrP-224AlaMYC cells were expanded for further analysis and use in future experiments.

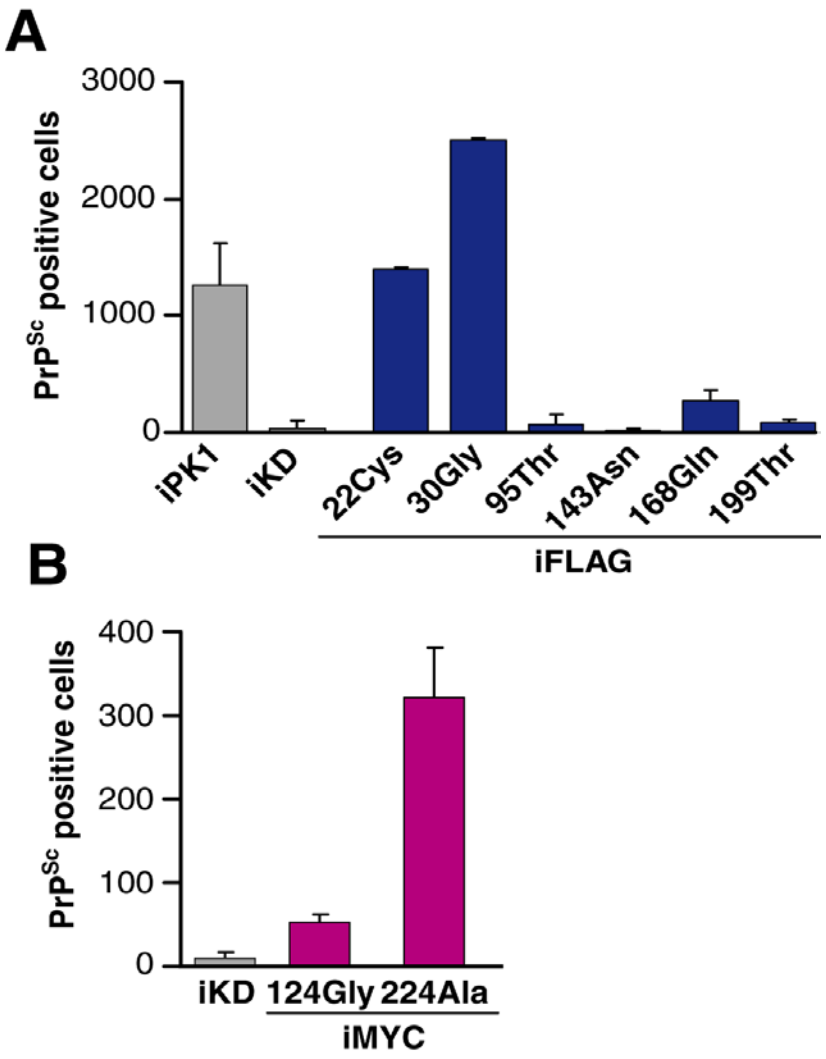

Figure 3-13 Misfolded PrP detection in P8(11)4.5.FLAG and PK-10*Si8*.MYC cells

Susceptibility of RML prion-infected FLAG- and MYC-tagged PrP reconstituted cells to prion infection was analysed by the SCA at passage four using a mouse monoclonal anti-PrP antibody (ICSM18). **(A)** The SCA showed presence of PK-resistant PrP in P8(11)4.5 cells expressing 22CysFLAG and 30GlyFLAG constructs. RML prion-infected PK1 and parental PrP-KD cells were used as positive and negative controls, respectively. i = RML prion-infected. The mean + SEM of six wells are shown. **(B)** The SCA data showed the relative prion susceptibility of cell lines expressing MYC-tagged PrP constructs compared with PrP-KD cells. PrP molecules with the MYC tag inserted near the C-terminus at Ala224 support prion propagation. RML prion-infected PrP-124GlyMYC cells and PrP-KD cells do not contain PK-resistant PrP. i = RML prion-infected. The mean + SEM of six wells are shown.

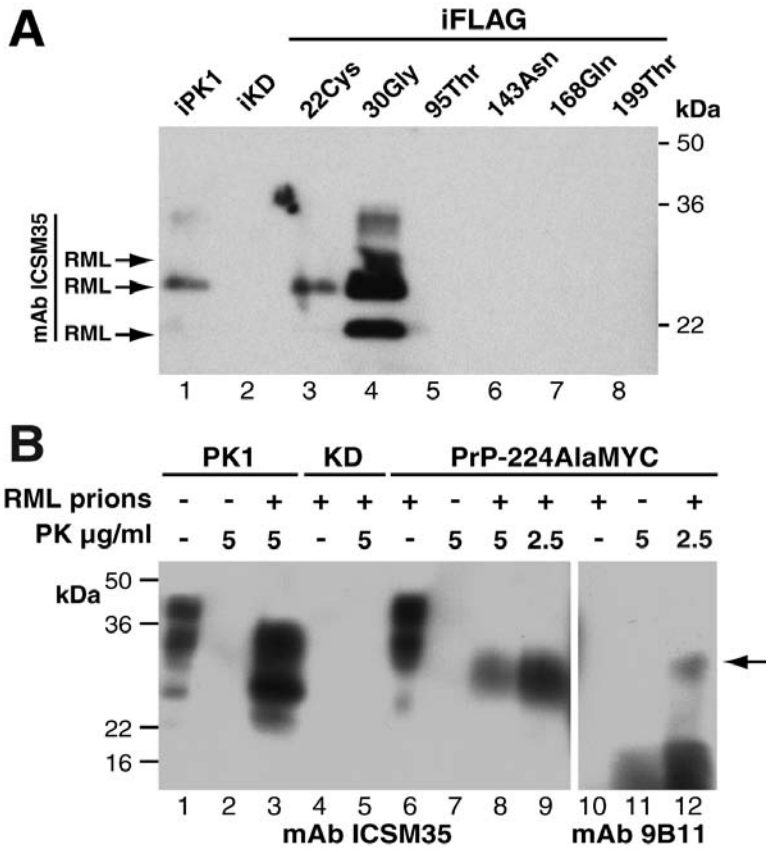

Figure 3-14 PK-resistant detection in P8(11)4.5.FLAG and PK1-10*Si8* cell lysates by immunoblotting

(A) Western blot analysis of RML prion-infected P8(11)4.5-FLAG cells, demonstrated similar results as the SCA. Lysates were Immunoblotted with a mouse monoclonal anti-PrP antibody (ICSM35). RML prion-infected PK1 cells were included as a positive control (lane 1) and parental PrP-KD cell line, P8(11)4.5, was used as a negative control for PK-resistant PrP expression (lane 2). i = RML prion-infected **(B)** Western blots developed with anti-PrP and anti-MYC antibodies showing levels of PK-resistant PrP in control and RML prion-infected PK1, PrP-KD and PrP-224AlaMYC cell extracts. The cell extracts were harvested after passage five and analysed undigested or subjected to PK digestion by the indicated concentrations of PK prior to SDS-PAGE. RML Prion-infected PK1 cells contain PK-resistant fragments characteristic of PrP^{Sc} (lane 3) whereas non-infected cells do not (lane 2). PrP-KD cells exposed to prions do not contain PK-resistant PrP demonstrating that no residual inocula derived PrP^{Sc} remains in the cells (lane 5). Consistent with the SCA data RML prion-infected PrP-224AlaMYC cell extracts contained low levels of PK-resistant PrP such that the most abundant PK-resistant fragment in RML prion-infected cells was detected (lane 8). No PK resistant fragments were detected in non-infected cells treated in the same way (lane 7). Reducing the PK concentration increased the levels of MYC-tagged PK-resistant PrP (lane 9) and allowed detection with anti-MYC antibodies (lane 12).

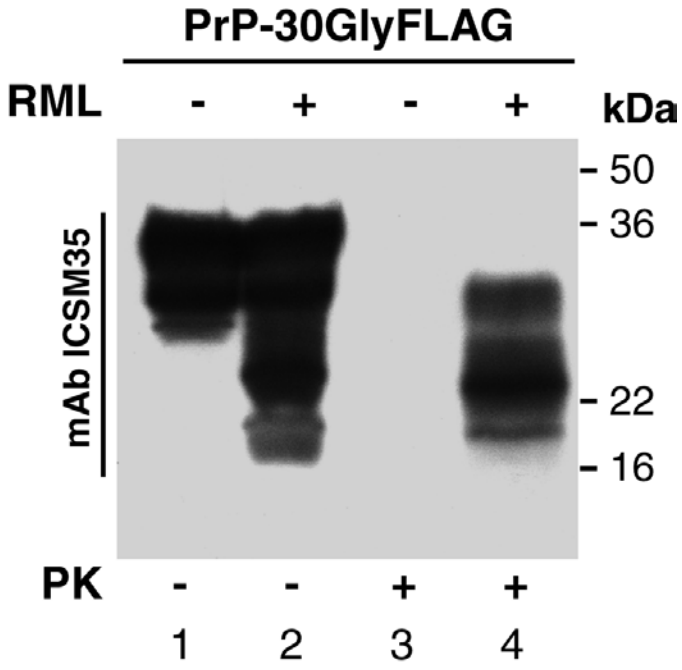

Figure 3-15 PrP-30GlyFLAG cells produce PK-resistant PrP following RML prion exposure

Lysates from non-infected and RML prion-infected PrP-30GlyFLAG cells were analysed by SDS-PAGE electrophoresis and were immunoblotted with a mouse monoclonal anti-PrP antibody (ICSM35). Expression of PK-resistant PrP was detected in RML prion-infected PrP-30GlyFLAG cells (lanes 2 and 4). PrP^{C} runs between 30-50 kDa in its three glycosylation states (di-glycosylated, mono-glycosylated, and un-glycosylated). Following PK treatment, which distinguishes between the PrP^{C} and PrP^{Sc}, PrP bands shift to lower molecular weight in RML prion-infected PrP-30GlyFLAG cells (lane 4). Note PK digested PrP^{C} completely in PrP-30GlyFLAG cells (lane 3).

PrP-224AlaMYC molecules generate true infectious prions

As novel PrP molecules, the infectious and pathological properties of misfolded PrP-224AlaMYC protein generated by prion exposure are untested. Therefore, to confirm that the infected PrP-224AlaMYC cells were generating *bona-fide* prions, Tg20 mice, a transgenic mouse line that over-expresses PrP, were inoculated intracerebrally with extracts from RML-prion infected and non-infected PrP-224AlaMYC cells. PK1 and PrP-KD cells infected in parallel with these cultures were used as positive and negative controls, respectively. As expected, inoculation of mice with RML prion-infected PK1 cell extracts resulted in prion disease in the mice (Table 3-1, Figure 3-16 and Fiure 3-17). In contrast, inoculation of extracts from RML prion treated PrP-KD cells, which do not propagate prions, did not result in prion diseases (Table 3-1, Figure 3-16 and Fiure 3-17), confirming that the cells at this stage (Passage five after RML prion exposure) do not contain residual inocula-derived RML prions. Inoculation of mice with RML prion-infected PrP-224AlaMYC cell extracts resulted in early clinical signs of scrapie, whereas, non-infected cell extracts from PrP-224AlaMYC cultures not exposed to prions did not (Table 3-1).

Mice inoculated with RML prion-infected PrP-224AlaMYC and PK1 cells were diagnosed with prion disease at an average of 67 days post-inoculation showing that the amount of PrP^{Sc} and presence of the tagged sequence in the misfolded PrP is not affecting the incubation time (Table 3-1). Biochemical analysis of the brains of the scrapie-affected mice showed that they contained PK-resistant PrP with a band pattern similar to that seen with RML prions (Figure 3-16, lanes 2 and 8). Histological analysis revealed classical prion neuropathology with PrP^{Sc} deposition, neuronal loss, spongiosis and gliosis (Figure 3-17). Control animals culled in parallel with scrapie-

affected mice did not contain PrP^{Sc} or show any pathologic features (Figure 3-17). These experiments demonstrated that cells expressing PrP-224AlaMYC propagate true infectious tagged prions following RML prion exposure and cause diseases identical from that caused by RML prions expressed in wild type PK1 cells.

Table 3-1 *In vivo* bioassay of the infectious and pathological properties of the novel tagged PrP molecules generated in PrP-224AlaMYC cells

RML prion-infected PrP-224AlaMYC cells were screened for their infectivity by the SCA at passage five before they were injected intracerebrally into Tg20 mice (the mean from six replicates is shown). Non-infected PrP-224AlaMYC cells and RML prion-infected PK-10Si8 PrP-KD cells were used as negative controls. RML prion-infected PK1 cells were used as positive controls. Pathological and biochemical analysis showed that inoculation of mice with RML prion-infected PrP-224AlaMYC cell extracts result in prion disease, however, mice inoculated with RML prion-infected PK-10*Si8* PrP-KD cells and non-infected PrP-224AlaMYC cells were not diagnosed with prion disease. Pathological and biochemical analysis were performed on the indicated number of animals from each group. Note the disease incubation time was similar in mice inoculated with RML prion-infected PrP-224AlaMYC cells and RML prion-infected PK1 cells. The mean ± SD of four independent experiments are shown.

Inocula		SCA	Incubation time (mean ± SD days)	Analysis	
				Pathological	Biochemical
PrP-224AlaMYC cells	+RML	321	67 ± 1.03	4/4	2/2
	Control	24	-	0/2	0/4
PK1 cells	+RML	1628	66 ± 1.38	5/5	2/2
PK1-10*Si8* PrP-KD cells	+RML	15	-	0/2	0/4

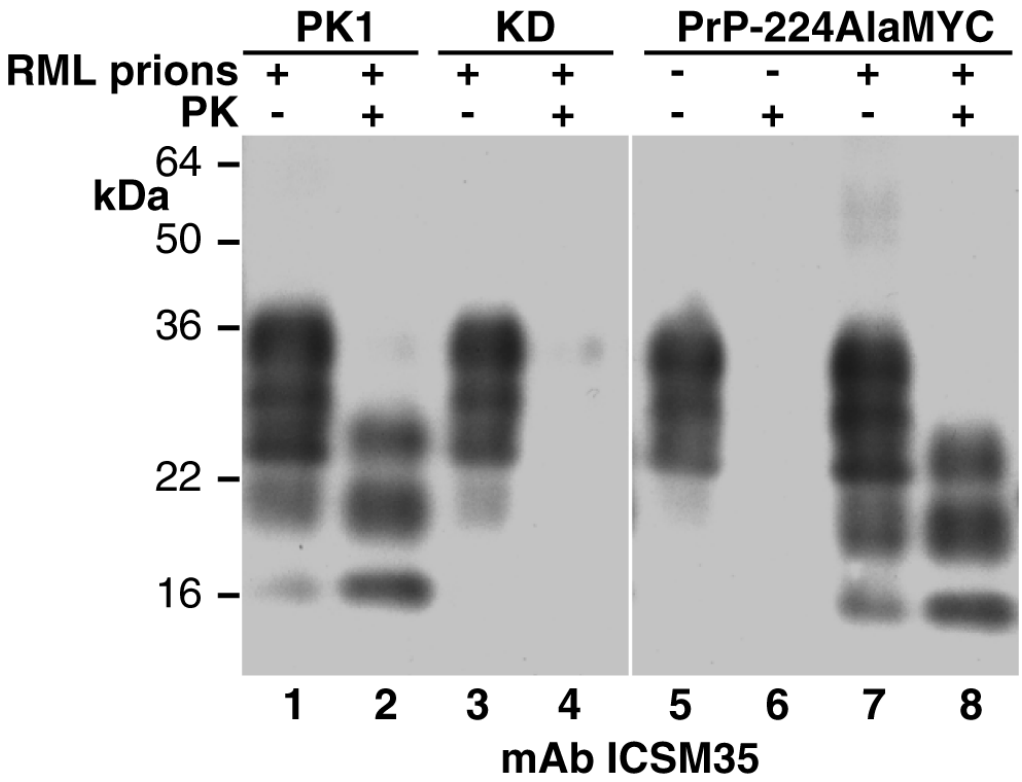

Figure 3-16 Tg20 mice inoculated intracerebrally with extracts of RML prion-infected PrP-224AlaMYC cells develop prion disease (Biochemical analysis)

(A) Western blots developed with anti-PrP ICSM35 antibody showed that Tg20 mice inoculated with extracts of RML prion-infected PK1 and PrP-224AlaMYC cells generate PK-resistant PrP (PrP^{Sc}) with a triplet band pattern similar to RML prions (lanes 2 and 8), a diagnostic biochemical feature of prion disease. Inoculations with control cell extract (non-infected PrP-224AlaMYC cells) or extracts from PrP-KD cells exposed to RML prions do not produce PK-resistant PrP (lanes 4 and 6).

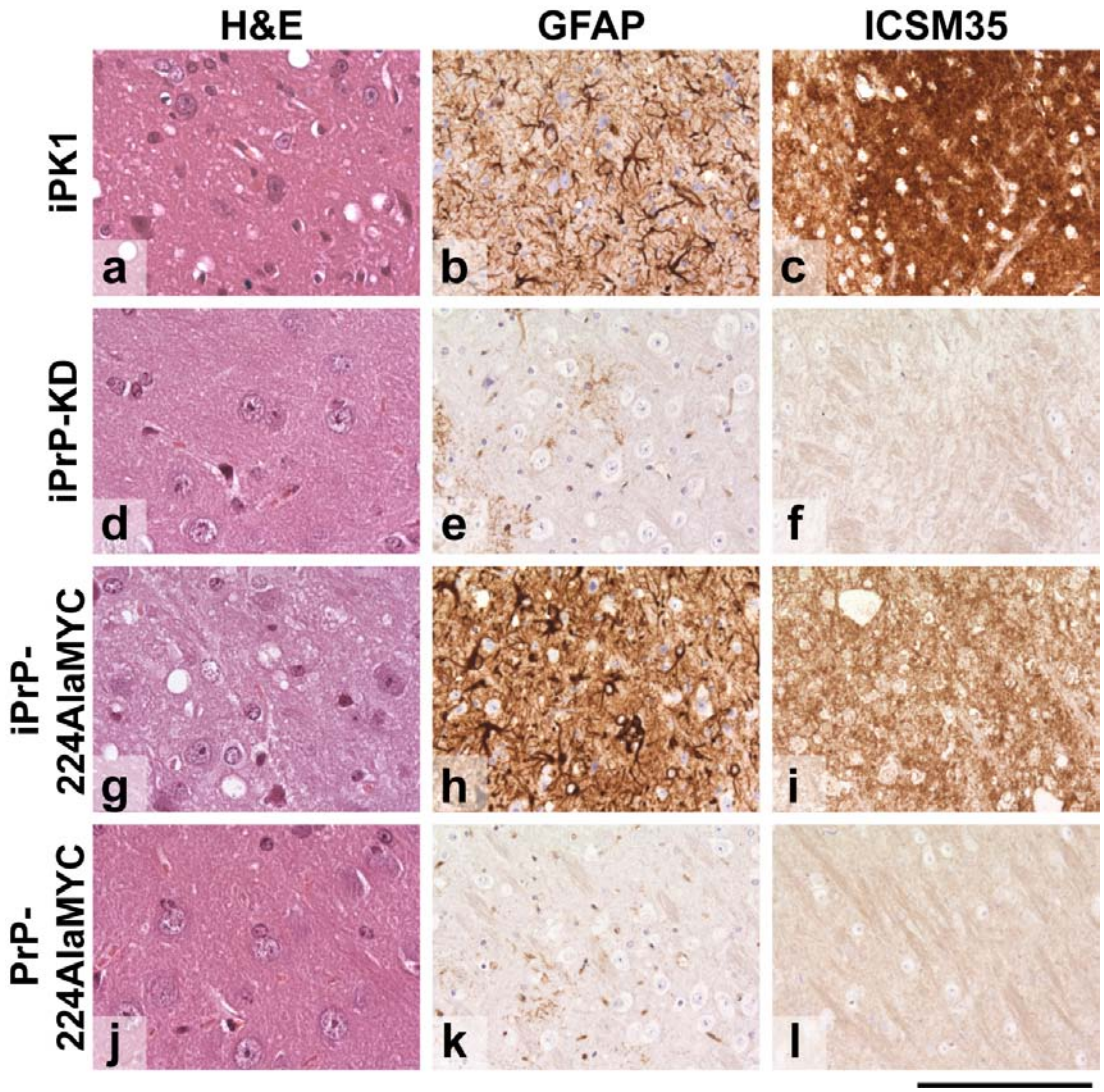

Figure 3-17 Tg20 mice inoculated intracerebrally with extracts of RML prion-infected PrP-224AlaMYC cells develop prion disease (Histological analysis)

Histological analysis of Tg20 mice brains inoculated intracerebrally with extracts of RML prion-infected PK1 cells (panels a–c) and PrP-224AlaMYC cells (panels g–i) revealed classical prion neuropathology with PrP^{Sc} deposition (ICSM35 immunostaining), neuronal loss and spongiosis (hematoxylin and eosin (H&E) staining) and gliosis (GFAP immunostaining). Brains from animals inoculated with extracts of RML prion-infected PrP-KD cells (panels d–f) or control non-infected PrP-224AlaMYC cells (panels j–l) did not contain PrP^{Sc} or show other diagnostic features. i = RML prion-infected. Scale bar = 80 μm on the H&E stained sections (panels a, d, g, j) and 160 μm for all other panels. *Histology experiments were performed by Miss Caroline Powell (MRC Prion Unit, UCL Institute of Neurology) and Miss Julie Moonga (Department of Neurodegenerative Disease, UCL Institute of Neurology).*

3.4 Discussion

At present, little is known about the site of conversion of PrP^{C} to PrP^{Sc}, and the details of cellular PrP^{Sc} trafficking. This is particularly true of the initial stages of infection when prions are first applied to previously non-infected cells. This is mostly due to the difficulties involved in differentiating de novo produced PrP^{Sc} from endogenous cellular PrP^{c} and the PrP forms present in the inocula. Studies have shown that proteasome inhibition in prion-infected cell lines and mouse brain leads to the formation of PrP^{Sc}-containing aggresomes, which in turn activate caspase 3 and 8 and subsequently leads to cell death (Kristiansen *et al.*, 2005; Dron *et al*., 2009). It has also been reported that disease-associated PrP specifically inhibits the proteolytic β subunits of the 26S proteasome in prion-infected cells and mice (Kristiansen *et al*., 2007), indicating that misfolded PrP must have access to the cytosol. The site of conversion of PrP^{C} to PrP^{Sc} has been suggested to be at the plasma membrane (Caughey and Raymond, 1991), or at the endolysosomal system (Campana *et al*., 2005; Arnold *et al*., 1995). Hence, the development of experimental tools to study the early events of prion infection and investigate how PrP^{Sc} traffic around the cell and access the cytosol to interact with the UPS is important.

To this end, PrP-KD PK1 cells were reconstituted with several differently tagged mouse PrP constructs, which were subsequently infected with RML mouse-adapted prions to ascertain if the tagged PrP can be converted into PrP^{Sc}. The use of tagged PrP^{Sc} allows for differentiation between newly formed PrP^{Sc} (*de novo* production) and PrP^{Sc} already in the prion-containing inocula. This will also allow the study of the early temporal and spatial events in prion infection as well as PrP^{Sc} trafficking around the cell. Various forms of tagged PrP have been used in prion

research, including mouse PrP mutated to contain the commonly used 3F4 epitope and GFP, MYC and FLAG fusion proteins, however, most of them do not convert into PrP^{Sc} or have been expressed in a cell background where endogenous PrP is present (Rutishauser *et al*., 2009; Vorberg *et al*., 2004b; Greil *et al*., 2008; Magalhaes *et al*., 2005; Raeber *et al*., 1992). Hence, generating an epitope-tagged PrP^{C} chimera that supports prion conversion and generates an infectious tagged PrP^{Sc} is challenging. A C-terminal GFP tagged PrP^{C} construct produced by Barmada and Harris failed to form PrP^{Sc} (Barmada and Harris, 2005), and even the insertion of a small ten amino acid MYC tag at position 230Ser of murine PrP abrogated prion conversion when expressed in a PrP^{C} knockout mouse background (Rutishauser *et al*., 2009).

Furthermore, the inhibition of PrP^{Sc} formation by non-homologous PrP^{C} molecules has been observed in transgenic mouse models and cell cultures where endogenous PrP is expressed. Human PrP transgenic mice with endogenous mouse *Prnp* expression are as resistant as wild type mice to sporadic CJD prions and require the ablation of *Prnp* to acquire susceptibility (Telling *et al*., 1994; Telling *et al.*, 1995). Similarly, mice expressing both the hamster PrP transgene and endogenous mouse *Prnp* exhibit longer disease incubation period for hamster scrapie compared to those in which mouse *Prnp* has been ablated (Bueler *et al*., 1993; Race *et al*., 2000). This inhibitory phenomenon of PrP^{Sc} formation is thought to be that non-homologous PrP^{C} molecules readily interact with PrP^{Sc} but cannot be converted due to 'dominant negative' inhibition by endogenous PrP (Prusiner *et al.*, 1990; Priola *et al*., 1994; Collinge *et al*., 1995; Horiuchi *et al*., 2000; Perrier *et al*., 2002). Therefore, in the unique cell system presented in this chapter, tagged PrP is expressed in a PrP-KD

neuroblastoma cell line essentially devoid of endogenous PrP, at least in terms of prion propagation.

In this study, the ability of 3F4-, MYC- and FLAG-tagged PrP^{C} to convert into PrP^{Sc} in prion-infected PK1 cells was measured. PrP-KD PK1 cells reconstituted with FLAG-, MYC- and 3F4-tagged PrP constructs expressed PrP^{C} at near physiological levels seen in wild type PK1 cells and showed a normal sub-cellular PrP^{C} distribution. Therefore, insertion of the tags into the *Prnp* does not seem to impair the expression or processing of mouse PrP^{C}.

The data presented here illustrates that replacement of leucine (L) 108 and valine (V) 111 with methionine (M) in the mouse PrP sequence to generate 3F4 epitope or insertion of the MYC sequence at amino acid position 224 of the *Prnp* do not impair the PrP conversion. However, the PrP^{C} conversion efficiency was reduced in cells expressing 3F4-tagged PrP compare to wild type PrP^{C}; these results are in agreement with previous studies (Priola *et al*., 1994; Safar *et al*., 1998; Safar *et al*., 2005; Rutishauser *et al*., 2009; Geissen *et al*., 2009). The reduced ability of 3F4-tagged PrP^{C} to convert to PrP^{Sc} might be due to a disruption of the process by which PrP^{C} is converted into PrP^{Sc}. For instance, interactions between dissimilar PrP^{Sc} and PrP^{C} molecules might reduce the aggregation and accumulation of PrP^{Sc} by interfering with the interactions between different PrP monomers (Bolton and Bendheim, 1988; Hope *et al*., 1986).

It was also demonstrated that prion-infected PrP-KD PK1 cells expressing 22CysFLAG and 30GlyFLAG produce PK- and formic acid-resistant PrP, whereas no misfolded PrP was detected in cells transduced with the FLAG-tag at positions Thr95, Asn143, Gln168 and Thr199, despite careful consideration of their positioning outside

of the known structured regions of the PrP molecule (Caughey, 2001; Telling *et al*., 1997). Therefore, it seems that the N-terminus of PrP^{C} is not critical for the conversion process (Flechsig *et al*., 2000; Legname *et al*., 2005; Muramoto *et al*., 1996; Zulianello *et al*., 2000), whereas any changes in the central region of PrP will prevent PrP^{C} conversion to PrP^{Sc} (Caughey, 2001; Priola *et al*., 1994). Hence, impairment of prion propagation by inserting the FLAG- and MYC-tag centrally within the PrP sequence highlights the significance of the hydrophobic region of PrP^{C} for prion conversion, where only minor substitutions or insertions of a few amino acids can prevent the accumulation of PrP^{Sc}. This finding is consistent with previous reports on the importance of sequence conservation in this region for efficient conversion (Hölscher *et al*., 1998; Zulianello *et al*., 2000).

Results shown here suggest that placement of a FLAG tag at amino acid positions 22 and 30 of the PrP sequence does not interfere with PrP^{Sc} formation; however such constructs cannot be used to study trafficking of newly synthesised PK-resistant FLAG-tagged PrP^{Sc} as the FLAG tags are in the PK-sensitive region of PrP^{C} (amino acid residues 22-88). Previous studies have shown that the protease-resistant core of PrP^{Sc} extends from amino acid residues 89-230 (Telling *et al*., 1997). Therefore, PK treatment of the FLAG-tagged PrP results in the loss of the FLAG epitope when inserted at residues 22 and 30 making them unsuitable for this study. An alternative method could be to detect PrP^{Sc} in RML prion-infected cells expressing N-terminal FLAG-tagged PrP using the protease thermolysin (Owen *et al*., 2007; Wadsworth *et al*., 2008). This thermostable protease cleaves at the hydrophobic residues Leu, Ile, Phe, Val, Ala, and Met that are absent from the protease accessible N-terminal region of PrP^{Sc}. Therefore, although thermolysin readily digests PrP^{C} into

small protein fragments, full-length PrP^{Sc} are resistant to such proteolysis. In addition, these results showed that the misfolded PrP species (PK-resistant PrP molecules) have lower molecular masses than the normal, protease-sensitive PrP species and are not affected by moderate PK treatment. Further studies have shown that that the PrP^{Sc} N-terminus is readily cleaved by the proteases in neuroblastoma cells (Caughey *et al*., 1991; Borchelt *et al*., 1992). Hence, albeit thermolysin can be used to expose full length PrP^{Sc}, the N-terminal site of the protein cannot be protected from the cellular proteases. Therefore, using any N-terminal tag to study trafficking of tagged PrP^{Sc} will be challenging.

Furthermore, the mouse bioassay studies on the novel PrP molecules (PrP-224AlaMYC) showed that presence of MYC-tag at amino acid position 224 of PrP^{Sc} does not diminish PrP^{Sc} infectivity and Tg20 mice inoculated with cell extracts of the prion infected PrP-224AlaMYC developed prion diseases. These results also showed that there is no correlation between the amount of cell-derived PrP^{Sc} that is inoculated into the animals and the disease incubation time as all the animals injected with RML prion-infected PK1 and PrP-224AlaMYC cell extracts, which each line produces different amount of cell-derived PrP^{Sc}, developed neurodegeneration in the similar time. This mouse bioassay clearly demonstrates that a high titre of infectivity is present in both RML prion-infected PrP-224AlaMYC and PK1 cell lines. However, to measure the difference in infectivity levels between the samples, the infectivity titre needs to be calculated.

Collectively, the data presented here supported the view that changes in the N-terminal and extreme C-terminal segment of PrP protein do not interrupt the prion

conversion efficiency. While any changes in the central region of PrP^{C} impinge prion propagation confirming the importance of this region in prion protein conversion.

3.5 Summary

Work in this chapter describes the successful transduction of PrP-KD PK1 cells with different 3F4-, FLAG- and MYC-tagged PrP constructs and the isolation of cell lines that were able to propagate misfolded PrP. Importantly, these cell lines were shown to express PrP^{C} at near physiological levels and demonstrated a normal sub-cellular PrP^{C} distribution. The N-terminal region of PrP^{C} was demonstrated to not be indispensable for PrP^{Sc} formation and prion propagation, whereas the highly conserved hydrophobic segment and the C-terminal hydrophobic region of PrP^{C} are important for conversion of PrP^{C} to PrP^{Sc}. It was demonstrated that H6.2 and D7.1 cells (expressing moPrP.3F4), PrP-224AlaMYC, PrP-22CysFLAG and PrP-30GlyFLAG cells are susceptible to RML prions. PrP-30GlyFLAG cells were shown to produce N-terminal FLAG-tagged misfolded PrP to levels greater than wild type PK1 cells. Furthermore, it was demonstrated that MYC-tagged PrP^{Sc} are true infectious particles and inoculation of them into Tg20 mice cause prion disease.

4 Rapid *de novo* prion conversion revealed using a novel cell system

4.1 Background

Chronically prion-infected cells synthesise PrP^{Sc} over multiple serial passages following exposure to prion-infected brain homogenates, and these cell lysates can cause prion diseases when inoculated into experimental animals (Doh-ura *et al*., 2000; Gilch *et al*., 2001; Aucouturier *et al*., 2001). Indeed both neuronal and non-neuronal cells can become persistently infected following exposure to specific prion strains (Race *et al*., 1987; Butler *et al*., 1988; Baron *et al*., 2006). Much of what is currently understood, therefore, about the process of cellular infection and subsequent PrP^{Sc} formation has resulted from studies using such chronically infected cellular models. Therefore, little is known about the immediate events of infection following initial exposure of susceptible cells to prions, and fundamental questions such as the timescale of the infection process or where PrP conversion initially occurs have not yet been unequivocally established. Attempts to study these early events of prion infection are difficult for several reasons: i) only relatively few cell culture systems have been described that are susceptible to prion infection; ii) newly-formed, host synthesised PrP^{Sc} is immunologically indistinguishable from both the PrP^{C} expressed by the recipient cell and various PrP^{Sc} species present in the prion-infected brain homogenate inoculum; and, iii) the amount of PrP^{Sc} produced in susceptible cell lines is often relatively low (Vorberg *et al*., 2004b).

However, several recent *in vitro* studies have studied the earlier stages of prion infection, showing that mouse neuroblastoma cells as well as fibroblast cells produce

de novo PrP^{Sc} after only four hours of scrapie exposure (Vorberg *et al*., 2004a) and that 72 hours exposure to prion-infected material is necessary for PrP^{Sc} production in neuroblastoma N2a cells (Klohn *et al*., 2003). *In vivo* studies conducted by Flechsig and colleagues have shown that prion-infected stainless steel wires need only be inserted in recipient brains for 30 minutes to induce infection (Flechsig *et al*., 2001). Still most of these earlier studies remained limited by the difficulty of specifically distinguishing PrP^{Sc} in the inoculums from newly synthesised PrP^{Sc} in the cell, which may help to explain the apparently conflicting results. To our knowledge, however, no one has yet utilised a cellular model in which epitope-tagged PrP^{Sc} molecules are produced following inoculation, allowing investigation of the earliest timescales of PrP conversion and prion propagation.

4.1.1 Aims

The aim of this part of my thesis work was to study the earliest events in prion infection of cells and subsequent PrP misfolding and to assess the timescale that PrP^{C} is converted to PrP^{Sc} following exposure to exogenous RML prions.

4.2 Methods

Formic acid extraction, PK digestion and GdnHCl denaturation followed by immunofluorescence staining were used to hydrolyse PrP^{C} and expose PrP^{Sc} for subsequent detection in RML prion-infected cells (Section 2.4.2). RML prion infected cells were quantified as described in chapter two (Section 2.4.2, 'Quantification of RML prion infected cells'). Data in figure 4-3, figure 4-6 and figure 4-9 were generated in collaboration with Dr Rob Goold (Department of Neurodegenerative Disease, UCL Institute of Neurology).

4.3 Results

4.3.1 Characterisation of prion infected cells

Removal of PrP^C and exposure of PrP^{Sc} in RML prion-infected cells

In order to study the biology of prion infection in cells it is essential to differentiate *de novo* synthesised PrP^{Sc} from the host PrP^C. As there are no available antibodies that are specific for PrP^{Sc}, it is necessary to treat cells post-infection to remove detectable PrP^C, leaving PrP^{Sc} available for immunodetection. As mentioned in Section 3.2.4, formic acid extraction is one technique used routinely in our lab to hydrolyse PrP^C and reveal PrP^{Sc} (Kristiansen *et al*., 2005). However, there are two other established methods for achieving this that utilise the biochemical differences between PrP^C and PrP^{Sc}. These are proteinase K (PK) digestion and guanidinium hydrochloride (GdnHCl) denaturation (Taraboulos *et al*., 1995; Veith *et al*., 2008). To compare each method in detail, PrP-224AlaMYC cells were treated with formic acid, PK or GdnHCl and subsequently stained with anti-MYC antibodies (Figure 4-1 A and B). RML prion-infected PrP-224AlaMYC cells contained a moderate level of resistant MYC-tagged PrP^{Sc} when treated with formic acid or PK (~ 15 % and 22 %, respectively) (Figure 4-1 A and B, + RML prions), whereas only low levels of background immunostaining (~ 3 %) were detected in non-infected cells, indicating PrP^C had been effectively removed by these treatments (Figure 4-1 A and B, - RML prions). The low background level of staining remaining in the non-infected cells was mostly attributable to clumps of cells to which access of the formic acid or PK was restricted. Confocal imaging of these RML prion-infected PrP-224AlaMYC cells showed that both PK- and formic acid-resistant PrP^{Sc} were distributed at the plasma

membrane and in the perinuclear compartment (PNC) (Figure 4-1 A, arrows), consistent with previous observations of the sub-cellular distribution of PrP^{Sc} (Section 1.6.2). As compared to formic acid and PK treatment, however, GdnHCl denaturation was less effective at removing PrP^{C} staining, as higher levels of background immunostaining were detected in non-infected PrP-224AlaMYC cells (~ 11 %) (Figure 4-1 A and B, - RML prions). Results obtained from PK, formic acid and GdnHCl treated PK1 cells were consistent with those from PrP-224AlaMYC cells. Non-tagged PrP^{Sc}, visualised in formic acid and PK treated RML prion-infected PK1 cells and immunostained with the ICSM18 anti-PrP antibody, had a very similar sub-cellular distribution (Figure 4-2 A and B, + RML prions). This indicates that the MYC-tagged PrP^{Sc} displays a physiologically relevant cellular localisation.

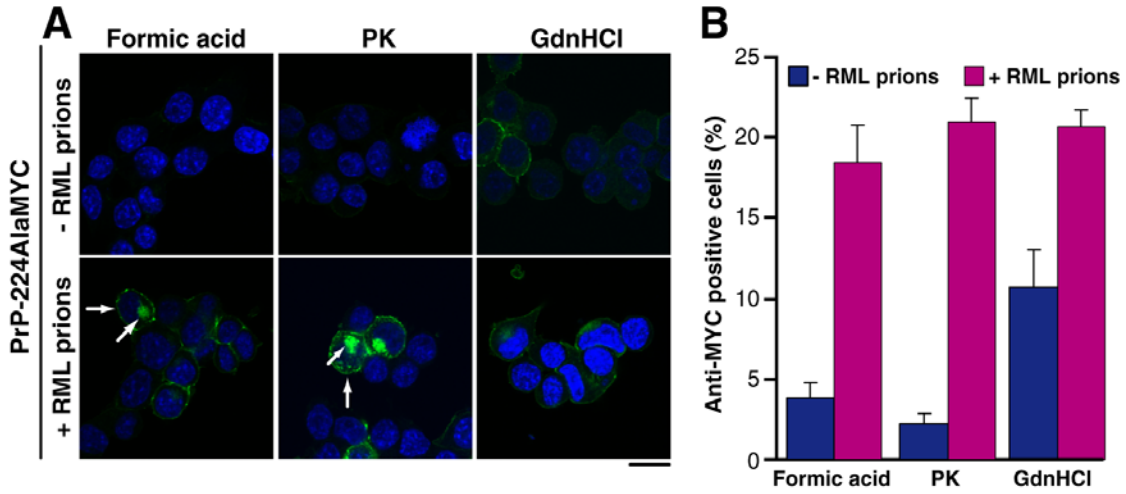

Figure 4-1 Comparison of the methods used to visualise PrP^{Sc} in RML prion-infected PrP-224AlaMYC cells

(A) Non-infected PrP-224AlaMYC (top panel) or chronically RML prion-infected PrP-224AlaMYC (passage five following RML prion exposure - bottom panel) were fixed and treated with formic acid, PK or GdnHCl prior to staining with anti-MYC antibodies (green). Non-infected PrP-224AlaMYC cells showed no green staining after formic acid and PK treatment indicating that the PrP^{C} had been removed. However, some residual staining was observed in non-infected cells after GdnHCl treatment. A proportion of RML prion-infected cells contained formic acid- and PK-resistant PrP (PrP^{Sc}) with a characteristic plasma membrane/perinuclear compartment distribution (arrow). Nuclei were stained with DAPI (blue). Scale bar = 15 µm. **(B)** Quantification of randomly chosen cell fields after the indicated treatments. Approximately 20 % of PrP-224AlaMYC cells in cultures exposed to RML prions contained formic acid- and PK-resistant PrP (PrP^{Sc}). The background staining observed in the non-infected PrP-224AlaMYC cells after formic acid and PK treatment is mostly attributable to clumped cells where access to the PrP^{c} is restricted. GdnHCl treatment was less effective at removing PrP^{C} staining. The mean + SEM of 20 fields of view are shown.

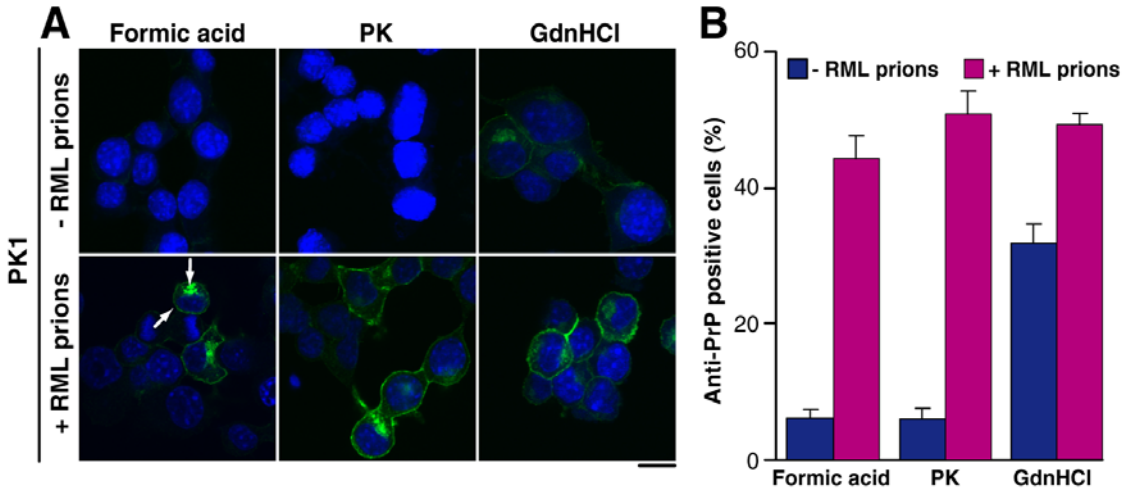

Figure 4-2 Comparison of the methods to visualise PrP^{Sc} in RML prion-infected PK1 cells

(A) Non-infected PK1 cells (top panel) or iPK1 cells (from chronically RML prion infected cultures, bottom panel) were fixed and treated with 98 % formic acid, PK or GdnHCl prior to staining with ICSM18 anti-PrP antibody (green). Merged confocal images are shown. Uninfected cells showed no staining after formic acid and PK treatment indicating that the PrP^{C} has been removed. Some residual staining was observed after GdnHCl treatment. RML prion-infected cells contained formic acid and PK resistant PrP (PrP^{Sc}) with a characteristic plasma membrane/perinuclear compartment distribution. Nuclei were stained with DAPI (blue). Scale bar = 15 µm **(B)** Quantification of randomly chosen cell fields after the indicated treatments. Approximately half of the iPK1 cells contained PrP^{Sc}. The low level of background staining observed in the PK1 cells after formic acid and PK treatment was mostly attributable to clumped cells where access to the PrP^{C} is restricted. GdnHCl treatment was less effective at removing PrP^{C} staining. The mean + SEM of 20 fields of view are shown.

The effective removal of PrP^{C} in non-infected cells, and the appearance of formic acid- and PK- resistant PrP^{Sc} in infected cells, indicates that both formic acid extraction and PK digestion are effective at revealing PrP^{Sc} in RML prion-infected cells. Therefore, the distribution of formic acid-resistant tagged PrP^{Sc} was analysed in detail in 3F4-, FLAG- and MYC-tagged PrP expressing cells by dual staining of formic acid treated cells with anti-tag and anti-PrP antibodies (Figure 4-3). Cellular localisation of formic acid-resistant PrP^{Sc} in PK1-10*Si8*.3F4;D7.1 cells (expressing 3F4-tagged PrP) (Section 3.3.4) and PrP-224AlaMYC cells (expressing MYC-tagged PrP) was similar to that described above, with strong staining at the plasma membrane and PNC. Importantly, anti-3F4 and anti-MYC tag antibodies colocalised perfectly with the ICSM18 anti-PrP antibody (Figure 4-3 D, E, I and J) and non-infected cells showed only very low background levels of immunostaining (Figure 4-3 A and F). In contrast, the FLAG-tag antibody used to immunostain RML prion-infected PrP-30GlyFLAG cells (expressing FLAG-tagged PrP) did not overlap exactly with the staining from the anti-PrP antibody (Figure 4-3 N and O), and it appeared to cross-react with other naturally occurring FLAG-like epitopes within the cells. Furthermore, unlike 3F4- and MYC-tagged PrP expressing cells, non-infected PrP-30GlyFLAG cells also showed very high levels of background immunostaining (Figure 4-3 K). This is possibly attributable to the very high expression of FLAG-tagged PrP in these cells (Figure 3-11 A, lane 4), making the formic acid extraction process less efficient. Moreover, since the N-terminus of PrP^{Sc} is truncated by endogenous proteases in lysosomes (Caughey *et al*., 1991); (Borchelt *et al*., 1992), it is also likely that a proportion of the N-terminal FLAG-tagged PrP^{Sc} in PrP-30GlyFLAG cells could not

be detected (Section 3.3.6). Therefore, PrP-30GlyFLAG cells were not used for any further studies.

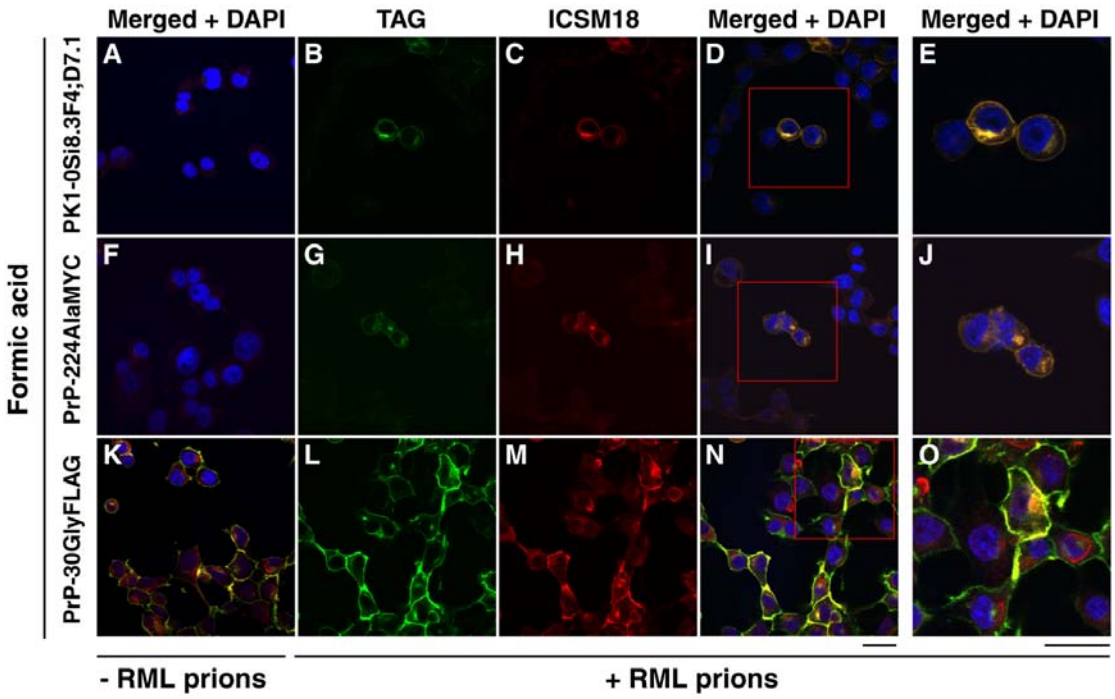

Figure 4-3 Characterisation of newly formed tagged PrP^{Sc} distribution in RML prion-infected cells

Chronically RML prion-infected PK1-10Si8.3F4;D7.1, PrP-224AlaMYC and PrP-30GlyFLAG cells were fixed and treated with 98 % formic acid prior to staining with anti-tag (green) and ICSM18 anti-PrP (red) antibodies. Single channels and merged confocal images are shown as indicated. The anti-3F4 and anti-MYC staining overlapped exactly with the PrP antibody staining (panels D and I). However, the anti-FLAG antibody did not colocalise perfectly with the ICSM18 anti-PrP antibody (panels N). Panels E, J and O are enlarged images of the regions indicated by red squares in panels D, I and N. Note formic acid extraction was less efficient in removing PrP^{C} in non-infected PrP-30GlyFLAG cells (panel k). Nuclei were stained with DAPI (blue). Scale bar = 30 µm.

Colocalisation of tagged-PrP^{Sc} with intracellular organelles

To better understand the molecular events involved in PrP conversion and prion propagation, and how PrP^{Sc} might transport to the cytosol, it is important to know which sub-cellular compartments are implicated in the trafficking of PrP^{Sc}. Formic acid extracted PrP-224AlaMYC cells were dual-stained with an anti-MYC antibody and antibodies directed against various intracellular compartments, including early endosomes, recycling endosomes, lysosomes, the Golgi stack, the trans-Golgi network and the proteasome (Figure 4-4 A). Formic acid-resistant MYC-tagged PrP^{Sc} was partially colocalised with each of compartments above consistent with previous reports (Caughey *et al*., 1991; McKinley *et al*., 1991b; Borchelt *et al*., 1992; Kristiansen *et al*., 2005; Marijanovic *et al*., 2009). Dual staining experiments were also done on prion susceptible 3F4-tagged PrP expressing cells (PK1-10*Si8*.3F4;D7.1) (Section 3.3.4) and identical results to PrP-224AlaMYC cells were obtained (Figure 4-4 B).

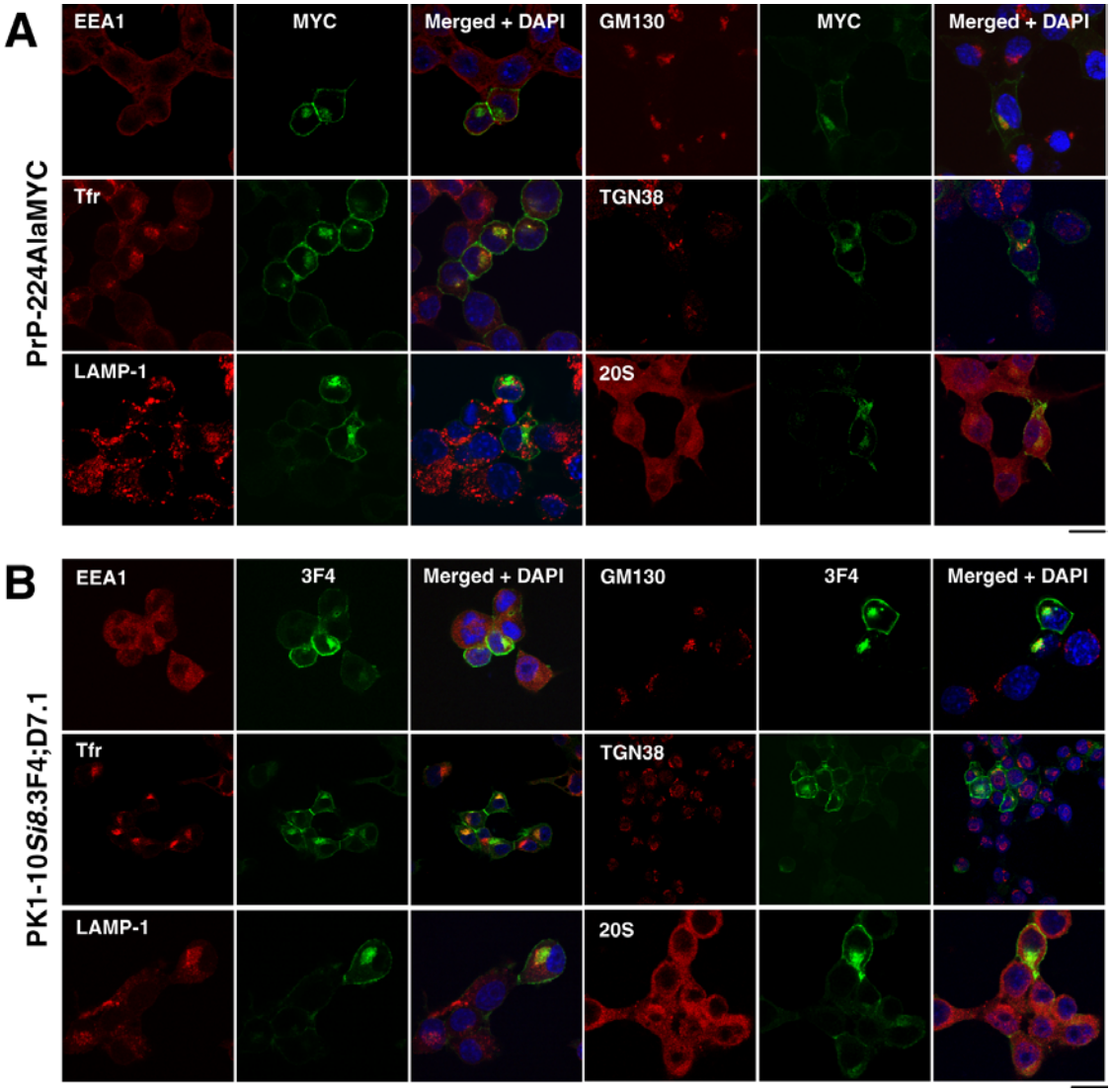

Figure 4-4 Intracellular localisation of tagged PrP^{Sc} in RML prion-infected cells

Chronically RML prion-infected PrP-224AlaMYC **(A)** and PK1-10*Si8*.3F4;D7.1 **(B)** cells were fixed and treated with 98 % formic acid for 5 minutes. Cells were stained with the anti-MYC and anti-3F4 antibodies (green) together with marker antibodies for various cell compartments (red). Partial colocalisation of MYC- and 3F4-tagged PrP^{Sc} with early endosomes (EEA-1), recycling endosomes (TfR), lysosomes (LAMP-1), the Golgi (GM130), the trans-Golgi network (TGN38) and proteasomes (20S) was observed. Nuclei were stained with DAPI (blue). Scale bar = 15 µm except PK1-10*Si8*.3F4;D7.1 stained with Tfr and TGN38 has the scale bar of 30 µm.

4.3.2 Cellular prion infection is a rapid process

In order to further understand the details of PrP misfolding into its abnormal conformation; it is necessary to understand when the initial conversion of PrP^{C} to PrP^{Sc} occurs in cells. The novel cell system expressing tagged PrP molecules in a prion susceptible environment, combined with effective PrP^{C} removal by formic acid extraction allows *de novo* produced PrP^{Sc} to be clearly distinguishable from the PrP^{Sc} within the inoculum. This makes it possible to do a detailed temporal and spatial study of the earliest stages of prion infection for the first time.

My initial experiments were focused on the time-course of RML prion infection. Previous work in the field suggests that 72 hours exposure to prion infected material is necessary to fully infect susceptible cells (Klohn *et al*., 2003). Hence, prion susceptible 3F4-tagged PrP expressing single cell clones PK1-10*Si8*.3F4;D7.1 (D7.1) and P8(11)4.5.3F4;H6.2 (H6.2) (Section 3.3.4) as well as PrP-224AlaMYC cells were first infected with 0.1 % RML prion-infected mouse brain homogenate for three days, and they were fixed either immediately or passaged in fresh media for up to 20 days prior to fixation. Non-infected D7.1, H6.2 and PrP-224AlaMYC were also fixed as negative controls. Following formic acid extraction and anti-tag antibody staining, immunofluorescent images were taken at each time-point (3 days, 4 days, 5 days, 6 days and 14 days) and the number of 3F4- or MYC-tagged positive cells was counted. As mentioned previously, formic acid extraction does not necessarily hydrolyse all of the PrP^{C} and some residual PrP^{C} staining is almost always seen in formic acid extracted non-infected cells. Therefore, to ensure that the residual PrP^{C} is not detected instead of PrP^{Sc}, the number of 3F4 and MYC positive cells in non-infected cultures with remaining PrP^{C} were counted and subtracted from the number of positive cells in

those cultures infected with RML prions (Figure 4-5). Such quantification demonstrated that both RML prion-infected D7.1 and PrP-224AlaMYC cells have their highest percentage of cells producing RML prion-infected tagged PrP^{Sc} (~ 15 % and 28 %, respectively) after six days post-infection (Figure 4-5, red and blue) and stable prion propagation in a proportion of the cells was observed up to 20 days post infection (5^{th} passage, data shown up to 14 days post-infection in Figure 4-5). In contrast, H6.2 cell cultures had their maximum numbers of RML prion-infected cells (~ 18 %) after four days post-infection, but the cells had lost their infectivity by 14 days post-infection (Figure 4-5, green). Moreover, a significant proportion of D7.1, H6.2 and PrP-224AlaMYC cells already contained tagged PrP^{Sc} after three days RML prion exposure (Figure 4-5). This led, therefore, to examination in more detail of the first 72 hours of RML prion exposure. Since the prion infectivity of H6.2 cells was transient and D7.1 cells had lower levels of PrP^{Sc} expression, further experiments were performed on PrP-224AlaMYC cells reproducibly infected with RML prions.

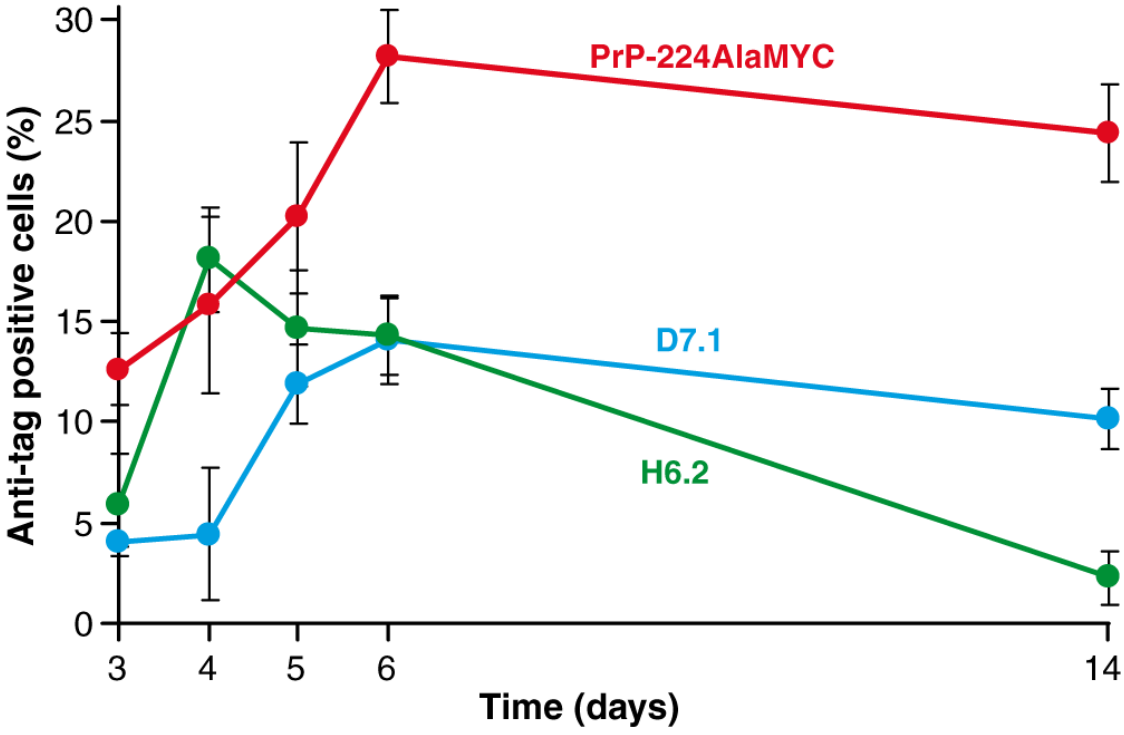

Figure 4-5 3F4- and MYC-tagged PrP^{Sc} propagation in RML prion-infected cells

D7.1, H6.2 and PrP-224AlaMYC cells were exposed to RML prions for 72 hours then fixed immediately or washed and cultured in fresh media (without RML prions) for the indicated times prior to fixation and formic acid extraction. Non-infected D7.1, H6.2 and PrP-224AlaMYC were also fixed, formic acid extracted and immunostained at each time point as negative controls. Total numbers of non-infected cells staining positive using anti-3F4 or anti-MYC antibodies were counted and subtracted from the number of 3F4- and MYC-positive cells in RML prion-infected H6.2, D7.1 and PrP-224AlaMYC cells. D7.1, H6.2 and PrP-224AlaMYC cells contained formic acid-resistant PrP (PrP^{Sc}) after 72 hours RML prion exposure. At 14 days post-infection H6.2 cells lost their infectivity, whereas D7.1 and PrP-224AlaMYC cells remained infected. The mean ± SEM of four independent experiments are shown.

Figure 4-6 A shows the proportion of infected cells over the first 72 hours of exposure of PrP-224AlaMYC cells to RML prions, revealing that they produce PrP^{Sc} very early in the time-course. Prior to RML prion exposure (0 hour), very few formic acid-resistant cells were detected, but subsequent RML prion exposure caused the rapid build up of formic acid-resistant PrP^{Sc}. MYC-tagged PrP^{Sc} positive cells were clearly detectable after two hours, and the maximum number of PrP^{Sc} positive cells was observed between three and four hours (~ 21 %). The number of RML prion-infected cells then declined slightly to under 15 % at 72 hours (Figure 4-6 A). This was consistent with the number of RML prion-infected cells observed after three days post infection in the initial experiments (Figure 4-5). No MYC-tagged PrP^{Sc} was detected in RML prion-infected PrP-KD cells confirming that the anti-MYC antibody is specific in detecting only MYC-tagged PrP^{Sc} (Figure 4-6 A). These observations suggest that cellular prion infection is a dynamic process and occurs far more quickly than previously thought. Therefore, the first few minutes of prion exposure (0- 32 minutes) was examined in further detail. PrP-224AlaMYC cells were exposed to 0.1 % RML prions for short periods prior to rapid washing and fixation. A significant proportion of the cells showed clearly detectable levels of formic acid-resistant MYC-tagged PrP^{Sc} after as little as one minute exposure to RML prions (Figure 4-6 B), the shortest time period technically and reproducibly possible within the limits of the experimental system. Of note also was that the number of infected cells rose steeply in the first two minutes following exposure to RML prions indicating that this is when most cells first begin to synthesise *de novo* PrP^{Sc}. Figure 4-7 shows the confocal images of PrP-224AlaMYC cells from 0 to 72 hours post-RML prion exposure. Formic acid-resistant MYC-tagged PrP^{Sc} were clearly detectable at the plasma membrane and in the PNC of

prion-exposed cells exposed to RML for less than 72 hours, consistent with them being stably infected cultures. Similar experiments using PK digestion confirmed the generation of protease resistant MYC-tagged PrP^{Sc} after very short periods of prion exposure (Figure 4-7, bottom panel). These studies were replicated by two independent investigators and analysed blinded by a third.

Taken together, these time-course studies demonstrate that prion infection is a rapid process and cells exposed to RML prions start to produce newly formed PrP^{Sc} as early as one minute after infection. Seventy two hours exposure to RML prions is not, therefore, an absolute requirement for the infection of susceptible cell lines, with much shorter periods of time proving sufficient.

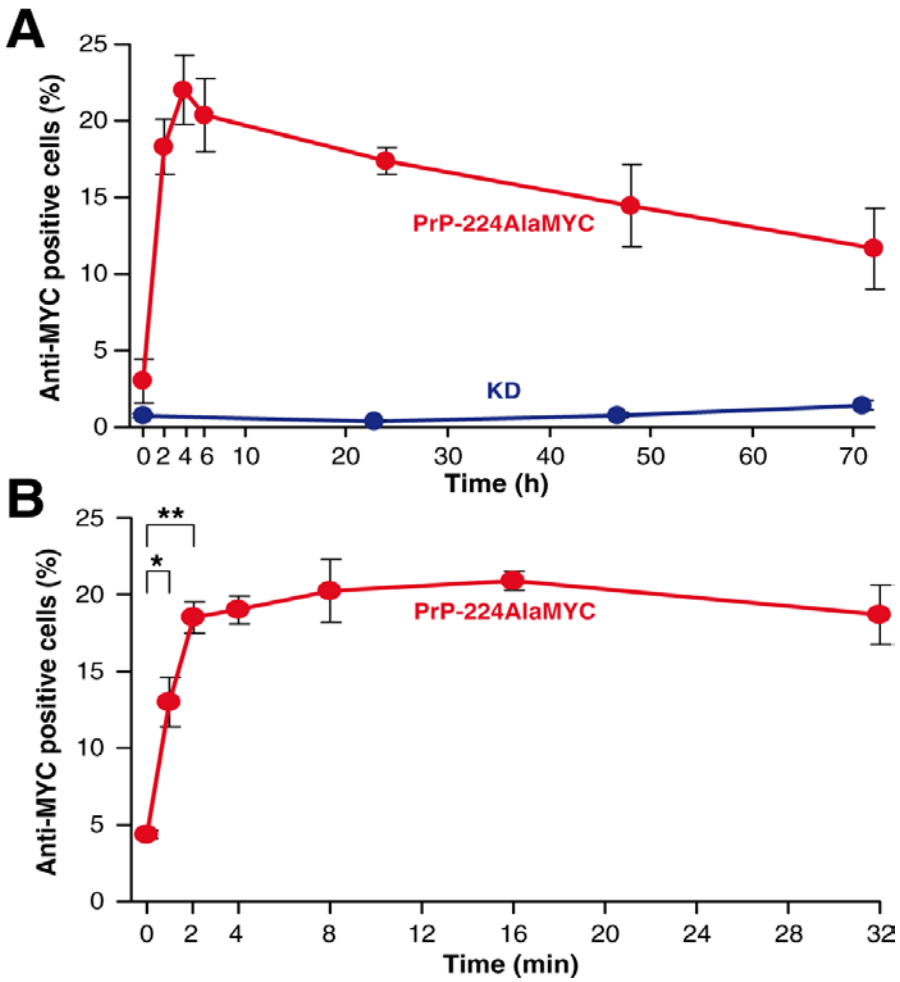

Figure 4-6 MYC-tagged PrP^{Sc} is synthesized rapidly following RML prion exposure

(A) PrP-224AlaMYC cells were exposed to RML prions for 0 – 72 hours then fixed and formic acid extracted. The proportion of anti-MYC positive (RML prion-infected) cells fixed at the indicated times was quantified (red). As a control PrP-KD cells were exposed to RML prions and processed in parallel (blue). Note that PrP-224AlaMYC cells contain formic acid-resistant PrP (PrP^{Sc}) as early as two hours RML prion exposure whereas PrP-KD cells do not stain significantly. The mean ± SEM of eight independent experiments are shown. **(B)** PrP-224AlaMYC cells were exposed to RML prions for 0 – 32 minutes prior to fixation and formic acid extraction. The proportion of anti-MYC positive (RML prion infected) cells fixed at the indicated times was quantified. The number of infected cells rises steeply in the first two minutes after RML prion addition indicating that this is when most cells first begin to synthesize *de novo* PrP^{Sc}. The 4, 8 and 32 minute time points are the mean ± SEM of four independent experiments, whereas the 0, 1 and 2 minute time points are the mean ± SEM of 8 independent experiments. * $P < 0.05$, ** $P < 0.01$.

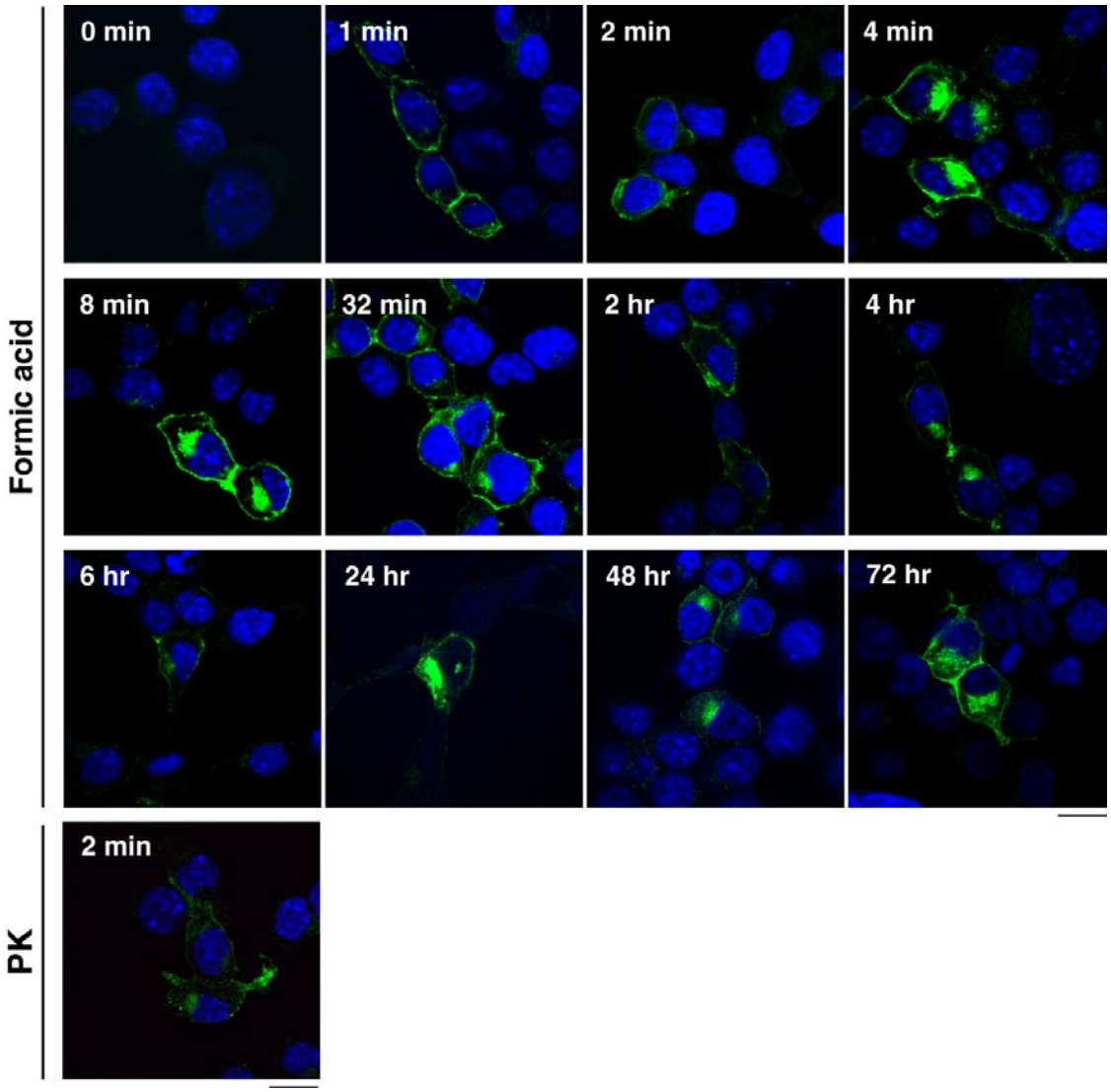

Figure 4-7 Formic acid- and PK- resistant tagged PrP^{Sc} is synthesized rapidly following RML prion exposure

Confocal images of RML prion-infected PrP-224AlaMYC cells fixed and formic acid extracted and PK digested prior to staining with anti-MYC antibodies (green). Formic acid-resistant MYC tagged PrP positive cells were found as early as one minute post-RML prion exposure. PK digested PrP-224AlaMYC cells exposed to RML prions for two minutes contained PK-resistant PrP^{Sc} (bottom panel). Nuclei were stained with DAPI (blue). Scale bars = 15 µm.

4.3.3 Two minutes exposure to RML prions is sufficient to cause stable prion propagation

To determine whether acute exposure to RML prions is sufficient to cause long term PrP^{Sc} propagation, PrP-224AlaMYC cells were exposed to 0.1 % RML prion-infected mouse brain homogenates for two minutes, after which the cells were immediately fixed or washed thoroughly with fresh media and cultured for a further 48 hours in the absence of the RML inocula. This demonstrated that approximately 22 % of the cells contained MYC-tagged PrP^{Sc} after two minutes RML prion exposure (Figure 4-8, 2 min). This level was maintained for 48 hours in the absence of RML prions (Figure 4-8, 2 min + 48 hr), showing that two minutes of prion exposure was sufficient to generate cells that stably propagate PrP^{Sc}.

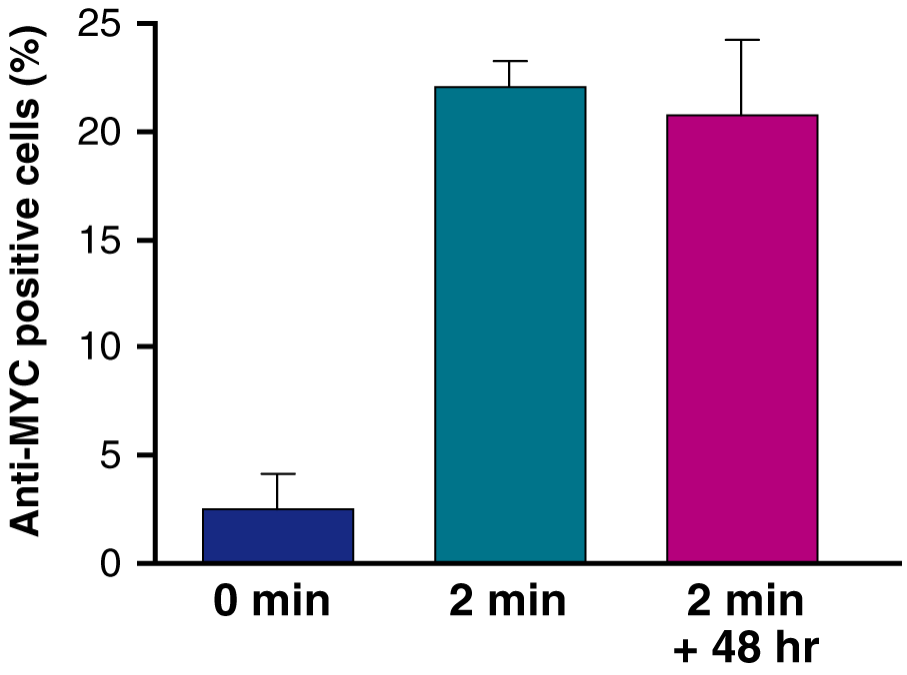

Figure 4-8 Short RML prion exposure is sufficient to cause stable prion propagation

PrP-224AlaMYC cells were exposed to RML prions for 2 minutes and fixed immediately or washed and cultured in fresh media (without RML prions) for 48 hours prior to fixation and formic acid extraction. The proportion of anti-MYC positive (RML prion-infected) cells fixed at the indicated times was quantified. Non-infected PrP-224AlaMYC cells (0 minute) were also fixed, formic acid extracted and immunostained in parallel to RML prion-infected PrP-224AlaMYC cells as negative controls. Note cells exposed to RML prions for only 2 minutes maintained their infectivity for at least 48 hours. The mean + SEM of three independent experiments are shown.

4.3.4 Cellular PrP^{Sc} interaction is not sufficient to induce PrP^{Sc} propagation

In analysing the presence of PrP^{Sc} in prion-infected cells, co-staining using anti-PrP and anti-MYC antibodies clearly showed that some cells stained positive at the plasma membrane for PrP^{Sc}, but not, for example, the MYC tag (Figure 4-9, arrows). This demonstrates that the PrP^{Sc}-staining in some cells can only be derived from the inoculum, as the absence of positive co-staining for the MYC tag after formic acid extraction indicates that it has not been synthesised by the cell. Therefore, these data demonstrate that the binding of RML prions alone to the plasma membrane of the cells and/or the internalisation of exogenous PrP^{Sc} is not necessarily sufficient to catalyse the conversion of endogenous PrP^{C} to PrP^{Sc}, suggesting that other unknown factors are also required. They also suggest that the formic acid- and PK-resistant PrP (PrP^{Sc}) seen in cells shortly after exposure to RML prions is not merely due to detecting tagged-PrP^{C} protected from formic acid treatment or PK digestion by a tight association with PrP^{Sc} from the inoculum. If tagged-PrP^{C} and exogenous PrP^{Sc} were associating in this manner, it would be expected that all cells showing formic acid- or PK-resistant PrP would co-stain for both PrP and the MYC tag. That this is not the case indicates that those cells (~ 20 %) that do demonstrate co-localised PrP and MYC must be doing so as a result of producing *de novo* PrP^{Sc}.

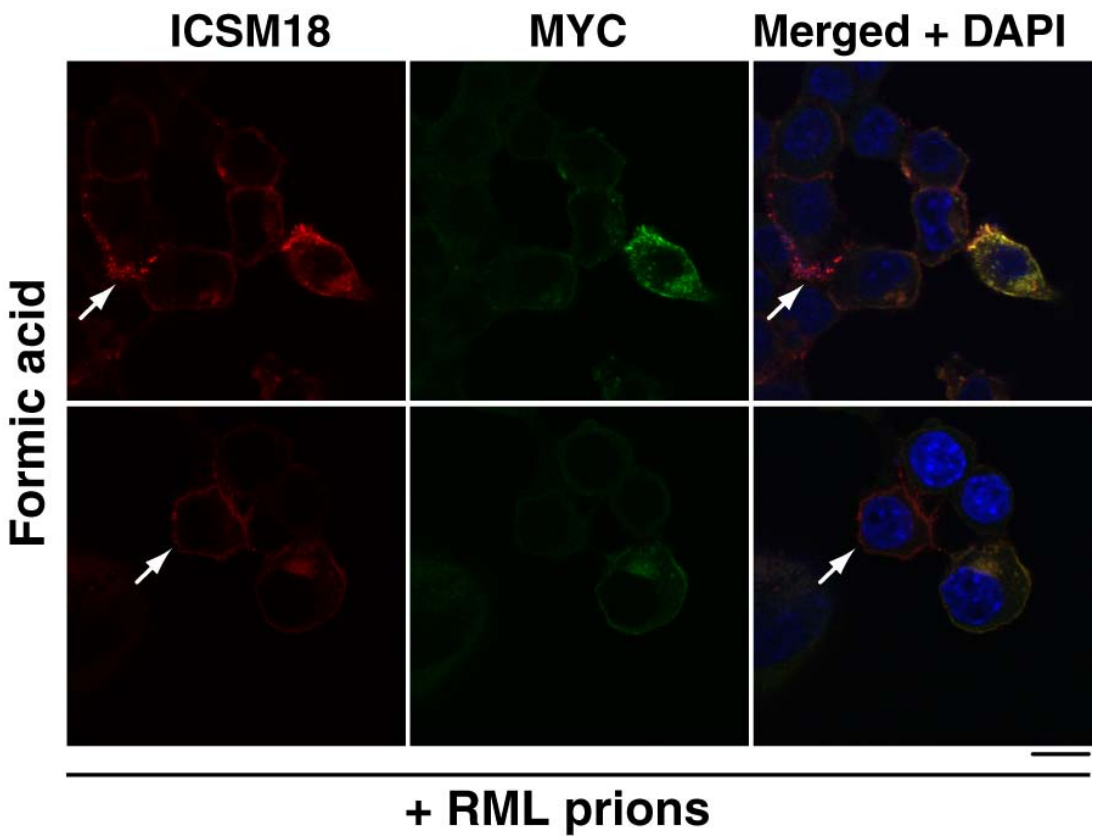

Figure 4-9 Cellular PrP^{Sc} interaction is not sufficient to induce PrP^{Sc} propagation

PrP-224AlaMYC cells exposed to RML prions for six hours were fixed and treated with 98 % formic acid prior to staining with ICSM18 anti-PrP (red) and anti-MYC (green) antibodies. Single channels and merged confocal images are shown as indicated. Note that some of the cells do not have newly synthesised PrP^{Sc}, albeit the RML prions are associated with their plasma membrane and/ or is internalised in those cells (arrows). Nuclei were stained with DAPI (blue). Scale bar = 15 µm.

4.4 Discussion

Temporal analysis of the events immediately following cellular exposure to prion infected material has previously proven difficult, as newly formed PrP^{Sc} is immunologically indistinguishable from both the PrP^{C} expressed by the recipient cells and PrP^{Sc} species in the brain homogenate inocula. The unique cell system generated here in which MYC epitope tagged-PrP^{Sc} is produced, combined with effective protocols to remove PrP^{C}, allowed examination of PrP misfolding when prions initially contact and infect susceptible cells; this is the first time such an analysis has been possible.

In view of the close similarity between the structures of PrP^{C} and PrP^{Sc}, and the lack of antibodies specific for PrP^{Sc}, pre-treatments have been devised for immunostaining of PrP^{Sc} (Diedrich *et al*., 1991; Bell and Ironside, 1993). These are intended to exploit differing protease and detergent sensitivities, thereby destroying PrP^{C} whilst retaining or enhancing the antigenicity of the pathogenetic isoforms. To immunostain disease-associated PrP^{Sc}, a variety of pre-treatments have been previously employed including incubation in formic acid (Kitamoto and Tateishi, 1988; Lantos *et al*., 1992; Kristiansen *et al*., 2005), guanidine thiocyanate (Bell and Ironside, 1993; Ironside *et al*., 1993; Veith *et al*., 2008), and proteinase K (Taraboulos *et al*., 1990b; Fevrier *et al*., 2004; Veith *et al*., 2008). These studies have generally shown positive staining for PrP^{Sc} at the plasma membrane and in the perinuclear compartments (Caughey and Raymond, 1991; Arnold *et al*., 1995). In contrast, PrP^{C} is fully hydrolysed by these treatments (Kristiansen *et al*., 2005; Veith *et al*., 2008). In agreement with these findings, results presented in this chapter revealed that formic acid and PK treatment were very efficient in removing PrP^{C} and exposing PrP^{Sc} in

RML prion-infected PrP-224AlaMYC and PK1 cells. Previous studies have shown that the immunoreactivity of PrP^{C} is lost when the normal isomer of PrP is exposed to 6 M GdnHCl (Thackray *et al*., 2007). This reflects the loss of surface exposed PrP epitopes within PrP^{C} as a consequence of chaotropic agent-induced denaturation. In contrast, the immunoreactivity of disease-associated PrP is increased upon exposure to 6 M GdnHCl, which reflects the exposure of previously buried epitopes within PrP^{Sc} that are no longer accessible in denatured PrP^{C} (Hilmert and Diringer, 1984; McKinley *et al*., 1991a). However, the data presented here shows that although GdnHCl was effective in denaturing of PrP^{C}, it was not as efficient as formic acid and PK treatment in exposing PrP^{Sc}.

Studies on persistently prion-infected cells reported the accumulation of PrP^{Sc} at the cells surface (Vey *et al*., 1996), and in association with the Golgi (Barmada and Harris, 2005), early endosomes (Godsave *et al*., 2008), late endosomes, lysosomal compartments (Arnold *et al*., 1995; Veith *et al*., 2008) and recycling vesicles (Godsave *et al*., 2008). Characterisation of susceptible cell lines producing tagged-PrP^{Sc} showed that formic acid-resistant 3F4- and MYC- tagged PrP^{Sc} has an identical cellular distribution to that reported previously for PrP^{Sc} that is not tagged. These data, therefore, confirm that the presence of the 3F4 and MYC tag does not affect the sub-cellular localisation of PrP^{Sc} and further supported the use of formic acid treatment to reveal PrP^{Sc} in cultured cells.

Earlier reports on the cell biology of prion infection indicate that cells take up inocula-derived PrP^{Sc} slowly (*i.e.* over days) and, several days of exposure to prions are necessary for susceptible cell lines to become infected (Magalhaes *et al*., 2005; Bergstrom *et al*., 2006). Conversely, however, data presented here shows that the

infection of cells is far quicker than previously supposed. This finding is supported by a previous study in which prions were immobilised on stainless steel metal rods that were then used to infect mice, showing that 30 minutes exposure or less was sufficient to generate prion infection *in vivo* (Flechsig *et al.*, 2001). Another study has demonstrated the rapid endocytosis of semi-purified prions within minutes of application, suggesting that prion cell interactions may be very rapid (Jen *et al.*, 2010). However, neither of these studies analysed *de novo* cellular prion conversion itself. The results presented here clearly show an accumulation of *de novo* cellular PrP^{Sc} as early as one minute exposure to RML prions. This is similar to an earlier study showing that PrP^{Sc} can be formed almost immediately following exposure to infectious scrapie inoculums; however, in this case, acute exposure to scrapie agents resulted for the most part in the transient formation of PrP^{Sc} (Vorberg *et al.*, 2004b). In contrast, here it is demonstrated that only two minutes exposure to RML prion brain homogenate is sufficient to generate cells that continue to produce PrP^{Sc} in the absence of further prion exposure and the similarity in the appearance of PrP^{Sc} in these cells to persistently infected cells suggest that stable prion infection can become established over a very short time period.

Interestingly, the data presented here show that association of RML-derived PrP^{Sc} to the plasma membrane of the cells and/or its internalisation, does not always necessarily lead to prion conversion. This confirms that the MYC-tagged PrP^{Sc} detected in cells shortly after RML exposure is true *de novo* PrP^{Sc}, rather than the MYC-tagged PrP^{C} tightly bound to inocula-derived PrP^{Sc}. These findings are also supported by data presented in the previous chapter (Chapter 3), whereby it was demonstrated that insertion of FLAG or MYC tags into the hydrophobic segment or at

the C-terminal hydrophobic region of *Prnp* (Section 3.3.6) prevent PrP^{C} conversion to PrP^{Sc}. This suggests that if the tagged-PrP^{Sc} detected in the susceptible cell lines was due to the binding between the tagged-PrP^{C} and PrP^{Sc} in the inoculum, tagged PrP^{Sc} would be also detected in cells with the tag inserted in any regions of their *Prnp*.

Several reasons can be attributed to a lack of PrP conversion in some cells that are associated and in contact with inocula-derived PrP^{Sc} molecules. The first possibility is that some cells are inherently slower in their conversion of PrP^{C} to PrP^{Sc} and that the individual cells that were analysed may have gone on to demonstrate *de novo* PrP^{Sc} at some point after their fixation. Another possibility is that the reconstitution of PrP-KD cells with tagged PrP^{C} does not have full penetrance. Therefore, there could always be some cells in the culture that do not express the PrP^{C} that is essential for conversion (Bueler *et al*., 1993) to PrP^{Sc}. Hence, an association of prions with these cells would not result in the production of PrP^{Sc} without any PrP^{C} to nucleate the conversion process. And finally, it is also possible these cells lacked prion susceptibility factors, as yet unknown, other than RML and PrP^{C} expression that are required for the prion conversion process to take place.

In conclusion, the unique cell system utilised here allowed the study of the earliest events in cellular prion conversion. The data presented in this chapter showed that cellular prion infection is a dynamic process that occurs within one minute of prion exposure. These results have important implications for understanding of the conversion and spread of prions *in vivo*. Once a sufficient of seed of infectious prions has been established in the brain, it is possible that prion cellular spread is likely to proceed far more rapidly than previously thought. These data cast new light on why prion infection can be very aggressive *in vivo* and affect the whole neuronal axis in a

few weeks. They suggest also that prion disease therapeutics aimed at preventing the conversion process itself by stabilising PrP^{C} are likely to be more effective than strategies aimed at cleaning infectious prions once the disease is established.

4.5 Summary

The work in this chapter revealed that formic acid extraction and PK digestion are better than GdnHCl for hydrolysing PrP^{C} and exposing PrP^{Sc} in RML prion infected PrP-224AlaMYC and PK1 cells. It was shown that formic acid-resistant tagged PrP^{Sc} accumulated mostly at the cell surface and perinuclear region of RML prion infected cells. Most importantly, study of the early events of prion infection showed that conversion of PrP^{C} to PrP^{Sc} is very dynamic and it occurs as early as one minute exposure to RML scrapie prions. The data also demonstrated that two minutes of prion exposure is sufficient to generate cells that continue to stably propagate PrP^{Sc} in the absence of RML and finally it was demonstrated that association of RML prions with cells does not always lead to prion infection.

5 Cellular sites of *de novo* PrP^{Sc} formation and its intracellular trafficking

5.1 Background

Conversion of PrP^{C} to PrP^{Sc} is the central event in the pathogenesis of transmissible prion diseases. In the established model of prion formation and propagation, direct interaction of endogenous PrP^{C} with the pathogenic PrP^{Sc} template is required to drive conversion to the infectious PrP conformers (Weissmann, 1994; Caughey and Chesebro, 1997). Despite decades of research, however, there is little consensus as to the precise mechanism(s) of prion conversion, the location in the cell where this process occurs and the means of toxicity associated with the formation of PrP^{Sc}.

A number of studies have already attempted to identify the intracellular site of prion conversion, mostly by analysing the sub-cellular localisation of PrP^{C} and PrP^{Sc} in primary neurons (Shyng *et al*., 1993; Sunyach *et al*., 2003; Galvan *et al*., 2005), the brains of infected animals (Jeffrey *et al*., 1994; Grigoriev *et al*., 1999; Fournier *et al*., 2000; Barmada and Harris, 2005; Godsave *et al*., 2008) and in infected cell lines (Borchelt *et al*., 1992; Beranger *et al*., 2002) using different techniques. However, these results remain controversial and the evidence for the involvement of any specific cellular compartment is not unequivocal.

Characterising the precise cellular localisation of PrP^{C} and PrP^{Sc} is essential to yield insights as to the site of prion conversion and the mechanisms that underlie prion formation. PrP^{C} is a cell surface GPI-anchored protein which is synthesised in the

rough ER and travels to the membrane through the Golgi apparatus. PrP^{C} has been shown to localise to different compartments depending on the cell type (Section 1.6.1), but it is generally found at the cell surface membrane associated with cholesterol-rich microdomains called lipid rafts (Turk *et al*., 1988; Caughey and Raymond, 1991; Vey *et al*., 1996), in the Golgi apparatus (Caughey *et al*., 1991; McKinley *et al*., 1991b; Borchelt *et al*., 1992), in early endosomes (Godsave *et al*., 2008), and in the endosomal recycling compartments (ERC) (Marijanovic *et al*., 2009). In primary neurons and N2a neuroblastoma cells, PrP^{C} is internalised and then recycled back to the cell surface, with some being sent for degradation in lysosomes (Shyng *et al*., 1993; Sunyach *et al*., 2003).

In contrast to PrP^{C}, the sub-cellular localisation of PrP^{Sc} is less well described. This is mainly due to the lack of antibodies that are specific to PrP^{Sc}. However, studies to date suggest a wide cellular distribution, in particular at the cell plasma membrane, in the Golgi and the endolysosomal compartment (McKinley *et al*., 1991b; Caughey and Raymond, 1991; Jeffrey *et al*., 1992; Arnold *et al*., 1995) (Section 1.6.2).

Several studies indicate that PrP^{Sc} formation itself occurs either at the plasma membrane, where the initial contact between endogenous PrP^{C} and exogenous PrP^{Sc} is likely to occur, or immediately after its internalisation in the endolysosomal compartments (Campana *et al*., 2005). Blocking PrP^{C} endocytosis has been revealed to inhibit PrP conversion (Borchelt *et al*., 1992). Conversely, expression of dominant-negative mutants of Rab 4, which inhibits recycling to the plasma membrane, results in an accumulation of PrP^{Sc} (Beranger *et al*., 2002). This suggests that PrP^{Sc} formation does not require recycling of PrP^{C} to the cell surface and occurs at the initial contact between PrP^{C} and PrP^{Sc} at the cell surface or within an intracellular compartment.

Indeed, a variety of evidence suggests that plasma membrane lipid rafts are the site of conversion, as both PrP^{Sc} and PrP^{C} can be found in these rafts (Taraboulos *et al*., 1995; Vey *et al*., 1996; Naslavsky *et al*., 1997; Baron *et al*., 2002; Botto *et al*., 2004), however, Marijanovic *et al*. showed evidence that the ERC are the likely site of prion conversion (Marijanovic *et al.*, 2009) (Section 1.6.2).

Proteins can enter the cell through several different routes (Mayor and Pagano, 2007). However, regardless of the means of internalisation, endocytosed proteins are first delivered to early endosomes. At this level, proteins to be recycled are returned to the cell surface either by a fast-recycling pathway, directly from early endosomes, or they are transported first to the ERC and then to the cell surface. In contrast, cargo destined for degradation is sorted to multi-vesicular late endosomes and finally to lysosomes, where degradation occurs (Gruenberg and Maxfield, 1995; Maxfield and McGraw, 2004). Using anti-MYC antibodies in the PrP-224AlaMYC cells in conjunction with methods presented in chapter four to remove PrP^{C}, and to specifically detect newly formed PrP^{Sc} (*i.e.* pre-treatment with formic acid or proteinase K) the intracellular trafficking of *de novo* PrP^{Sc} can be tracked to answer some of the questions described above.

5.1.1 Aims

The aims of the current study were to identify the initial cellular site of PrP^{Sc} production and examine how trafficking impairment of PrP^{Sc} affects the PrP conversion and prion propagation.

5.2 Methods

Treatment of PrP-224AlaMYC and iPK1 cells with pharmacological agents were undertaken as described in section 2.4.5 and section 5.3. Formic acid extraction followed by immunofluorescence staining was used to hydrolyse PrP^{C} and expose PrP^{Sc} for subsequent detection in RML prion-infected cells (Section 2.4.2). RML prion infected cells were quantified as described in chapter two (Section 2.4.2, 'Quantification of RML prion infected cells') unless otherwise specified. Confocal images and Orthogonal projections were generated as described in chapter two (Section 2.4.2, 'Image acquisition'). For cell phenotypic analyses, z stacks encompassing the entire cell were obtained and cells were grouped into one of three or one of seven categories based on the localisation of MYC-tagged PrP^{Sc}; three categories are exclusively plasma membrane, plasma membrane/diffuse intracellular and plasma membrane/prinuclear. Seven categories are plasma membrane/prinuclear, perinuclear, diffuse perinuclear, plasma membrane/diffuse perinuclear, peripheral, plasma membrane/peripheral, exclusively plasma membrane. In each experiment, at least 50 cells were analysed for each condition. Immunoblotting was performed by Dr Rob Goold (Department of Neurodegenerative Disease, UCL Institute of Neurology) for detection of PrP^{Sc} expression in chronically infected PK1 cells (iPK1) treated with different pharmacological agents or incubated at different temperatures (Section 2.3.5 - 2.3.8). Quantitative densitometry of iPK1 blots were performed as described in section 2.3.10. Data presented in this chapter for naive cells were generated in collaboration with Dr Rob Goold (Department of Neurodegenerative Disease, UCL Institute of Neurology).

5.3 Results

Sub-cellular trafficking of PrP is likely to play an important role in the mechanism that catalyses PrP misfolding, leading to the formation of PrP^{Sc}. The unique cell system described previously (Chapters 3 and Chapter 4), in which MYC-tagged PrP^{C} is able to convert to misfolded MYC-tagged PrP^{Sc}, allows the study of PrP^{Sc} trafficking, and analysis of the sites of PrP^{C} conversion to PrP^{Sc} when the cells are exposed to infectious prions. To study the site of prion conversion, naive PrP-224AlaMYC cells (*i.e.* cells not previously exposed to RML prions) were treated with different pharmacological agents (Section 2.4.1) or incubated at different temperatures for 30 minutes, and then were exposed to RML prions for a further four hours still in the presence of the agent or remaining at the set temperature. These pharmacological treatments or temperature shifts were also used on stable RML prion-propagating PrP-224AlaMYC cells (*i.e.* cells that had been propagating PrP^{Sc} for four days). Texas-red labelled transferrin, widely used to characterise trafficking through endocytosis compartments, was added to both naive and prion-propagating cells towards the end of each incubation period to assess the efficacy of manipulations on the cellular endocytosis (Section 2.4.1).

5.3.1 Conversion of PrP^{C} to PrP^{Sc} is a post-translational event

To delineate the cellular pathways utilised during the biosynthesis of protease-resistant PrP^{Sc}, naive and prion-propagating PrP-224AlaMYC cells were treated with brefeldin A (BFA). BFA inhibits transport of proteins from the ER to the Golgi, and induces retrograde protein transport from the Golgi apparatus to the ER (Misumi *et al.*, 1986; Doms *et al.*, 1989; Lippincott-Schwartz *et al.*, 1989; Taraboulos *et al.*, 1994).

This leads to an accumulation of proteins inside the ER. PrP-224AlaMYC cells treated with BFA were stained with a Golgi marker to validate the effects of BFA on the treated cells showing that the Golgi apparatus is disassembled in cells treated with BFA (Figure 5-1, bottom panel, red, white arrow). Moreover, numbers of RML prion-infected cells were counted, demonstrating that BFA reduced the proportion of cells producing *de novo* PrP^{Sc} (as shown using naive cells), as well as the number of cells propagating PrP^{Sc} (as shown using prion-propagating cells) by about 80 % (Figure 5-2 A and B). This suggests that PrP^{C} transport to the plasma membrane is essential for PrP conversion and prion propagation. Figure 5-3 shows the confocal images of both naive and prion-propagating PrP-224AlaMYC cells treated with BFA and, as the vehicle used, dimethyl sulfoxide (DMSO, control condition). Close examination of control DMSO-treated cells infected with RML prions revealed that PrP^{Sc} had a sub-cellular distribution that was essentially the same as non-DMSO treated PrP-224AlaMYC and wild type PK1 cells (Section 4.3.1); *i.e.* strong staining at the plasma membrane and the PNC. However, the sub-cellular distribution of PrP^{Sc} changed dramatically in BFA-treated RML prion-infected PrP-224AlaMYC cells, in which diffuse PrP^{Sc} staining was noted at the plasma membrane and inside the cells (plasma membrane/diffuse perinuclear staining) (Figure 5-3 A and B, bottom panels, green). These confocal images of BFA-treated cells also showed that BFA does not inhibit the internalisation of transferrin, as Texas-red labelled transferrin was internalised into the cells and localised with the PNC.

In addition to naive and prion-propagating PrP-224AlaMYC cells, chronically infected PK1 cells (iPK1) (*i.e.* cells producing PrP^{Sc} for at least 25 days) were also treated with BFA and the levels of PrP^{Sc} in the cells were measured directly using

quantitative immunoblotting. The amount of PrP^{Sc} was significantly reduced in BFA-treated iPK1 cells, consistent with the findings obtained for naive and prion-propagating PrP-224AlaMYC cells (Figure 5-2 C).

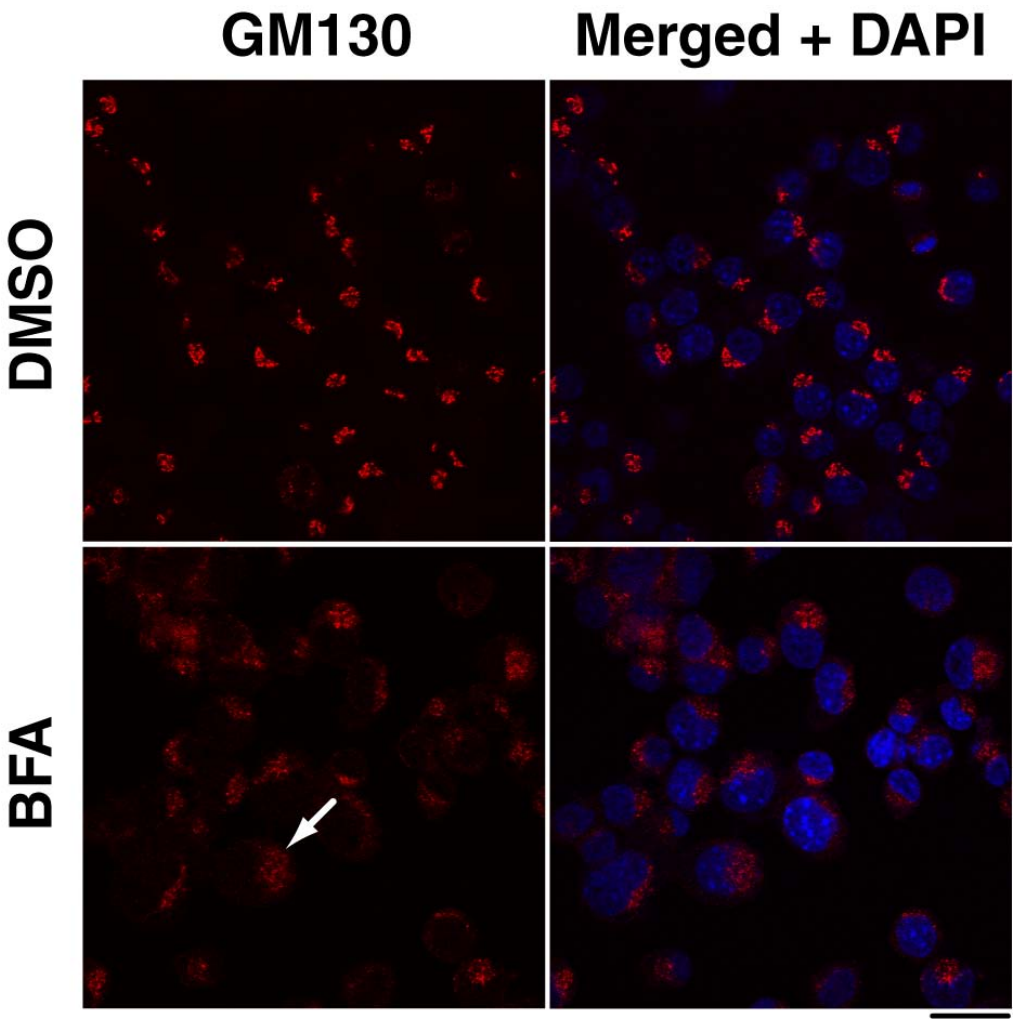

Figure 5-1 BFA disassemble the Golgi apparatus in PrP-224AlaMYC cells

PrP-224AlaMYC cells were treated with BFA and DMSO (control condition) prior to staining with GM130 (Golgi marker, red). The Golgi sacks were clearly dispersed in PrP-224AlaMYC cells treated with BFA (bottom panel, red, white arrow). Nuclei were stained with DAPI (blue). Scale bar = 30 µm.

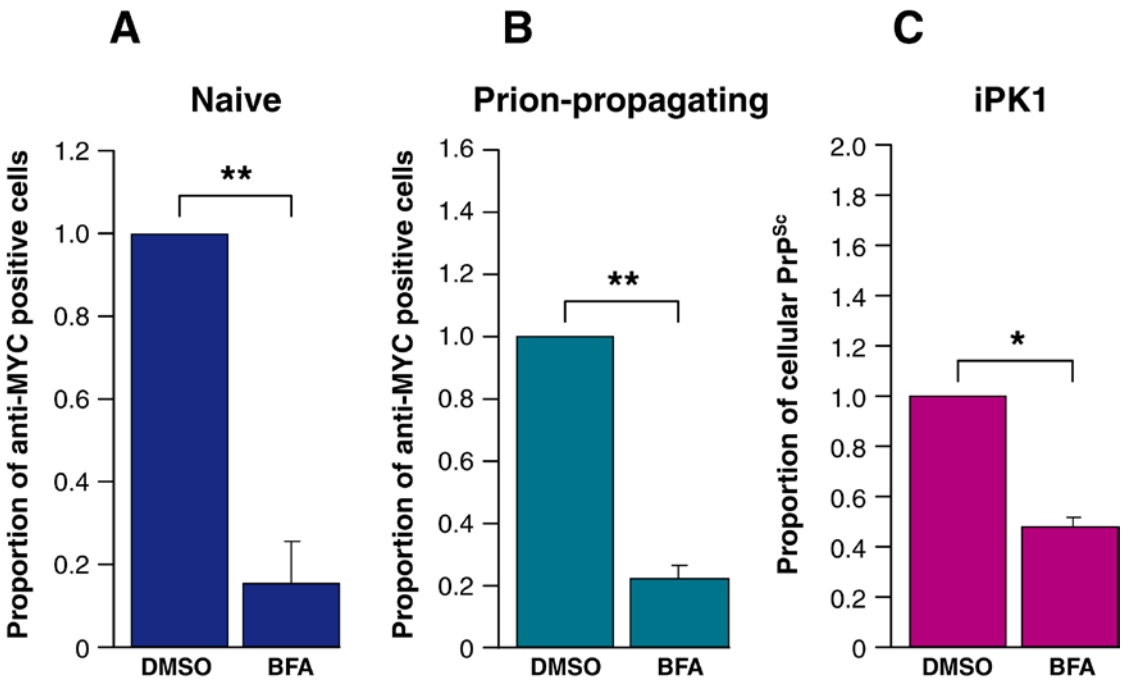

Figure 5-2 PrP^{Sc} propagation in RML prion-infected PrP-224AlaMYC and iPK1 cells treated with BFA

(A) Naive PrP-224AlaMYC cells were pre-treated with BFA or DMSO for 30 minutes, and then they were exposed to 0.1 % RML prions for a further four hours. **(B)** Prion-propagating PrP-224AlaMYC cells were exposed to BFA or DMSO for four hours prior to formic acid extraction and immunostaining with anti-MYC antibodies. The numbers of anti-MYC positive cells were counted in both BFA- and DMSO- treated cells. The results were normalised to the control condition (DMSO) and is shown as a proportion of the control. Note that in both naive and prion-propagating cells BFA reduces the number of RML prion-infected cells by about 80 %. **(C)** Lysates from chronically infected PK1 cells (iPK1 cells) (*i.e.* cells producing PrP^{Sc} for at least 25 days) treated with BFA or DMSO were analysed by SDS-PAGE electerophoresis and immunoblotted with an anti-PrP antibody (ICSM35). The band intensity for PrP^{Sc} was measured in iPK1 cells treated with BFA or DMSO and is shown as proportion of cellular PrP^{Sc}. Quantitative densitometry of blots showed PrP^{Sc} expression was reduced by about 60 % in BFA-treated cells. Mean + SEM of four independent experiments are shown. * $P < 0.05$, ** $P < 0.01$.

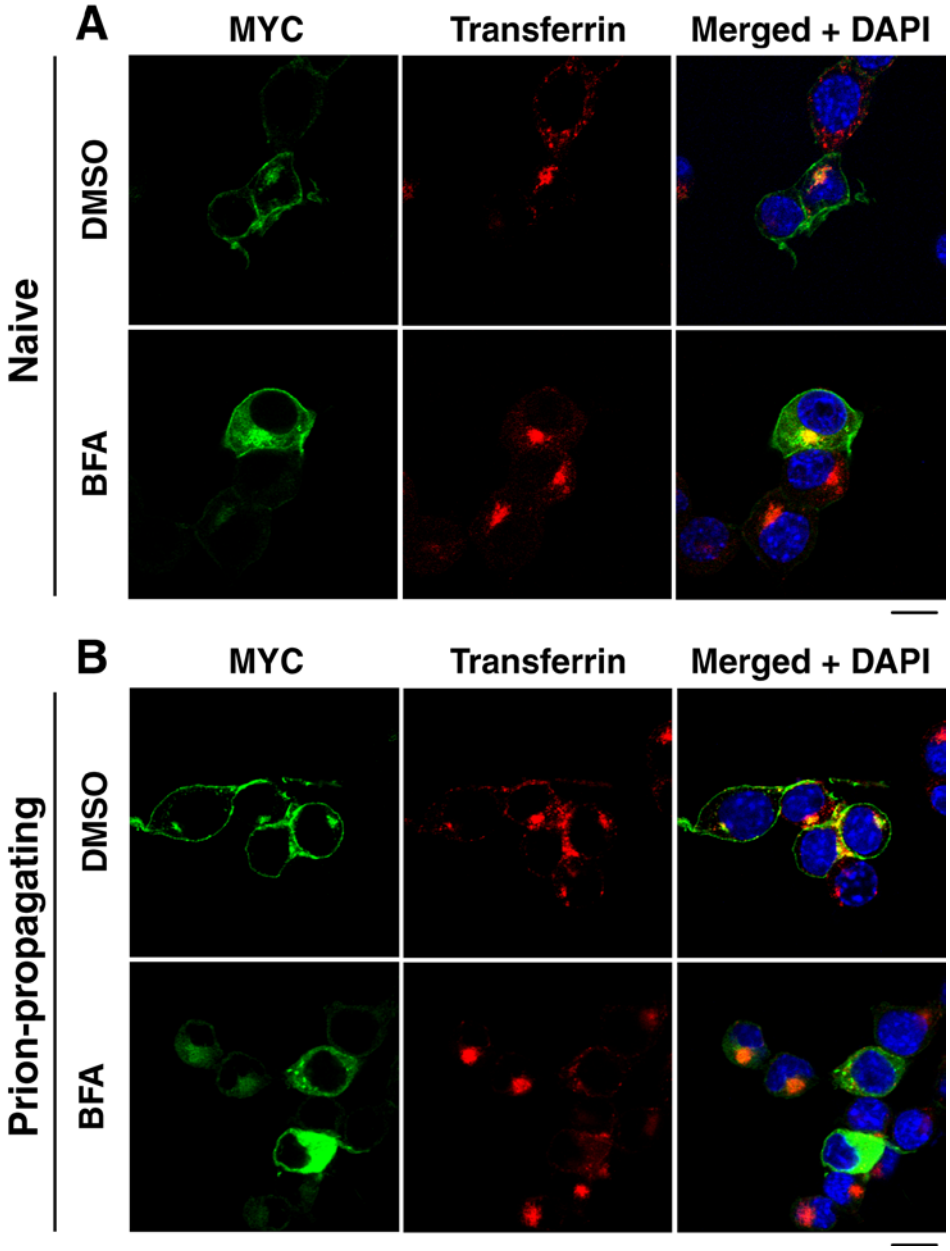

Figure 5-3 Sub-cellular distribution of MYC-tagged PrP^{Sc} in RML prion-infected PrP-224AlaMYC cells treated with BFA

(A) Naive and **(B)** prion-propagating PrP-224AlaMYC cells were exposed to BFA or DMSO and Texas red-labelled transferrin (red). Cells were fixed and formic acid extracted prior to immunostaing with anti-MYC antibodies (green). Single channels and merged confocal images are shown, as indicated. Note that neither BFA nor DMSO has affected the internalisation of transferrin (red, A and B). Cells treated with DMSO showed the typical plasma membrane and PNC PrP^{Sc} distribution (green, A and B top panels). However, cells treated with BFA had membrane diffuse perinuclear staining (green, A and B bottom panels). Nuclei were stained with DAPI (blue). Scale bar = 15 µm.

5.3.2 The role of plasma membrane and endocytic pathways in prion conversion and propagation

To examine the role of plasma membrane and endosomal compartments in prion conversion, naive and prion-propagating PrP-224AlaMYC cells were incubated at 4°C / 20°C or treated with nocodazole or bafilomycin. To identify the pathways involved in prion conversion, it was necessary to determine the extent to which each treatment affected endocytic pathways in pharmacologically manipulated PrP-224AlaMYC cells. To this end, the trafficking of Texas-red labelled transferrin was analysed (Section 5.3). Immunostaining of cells infected with RML prions following formic acid extraction under control conditions (*i.e.* addition of DMSO vehicle) had normal sub-cellular PrP^{Sc} localisation. Prominent plasma membrane and PNC staining of PrP^{Sc} was observed in nearly all of the DMSO-treated cells. Texas-red labelled transferrin was localised with the PNC, marking early/late and recycling endosomes. Consistent with earlier observations, a partial colocalisation of PrP^{Sc} with Texas-red labelled transferrin was observed (Figure 5-5 A and B, top panels, Figure 5-7 and Figure 5-8 top panels, Figure 5-12 A and B, top panels).

Endocytosis is not essential for prion conversion and propagation

Studies have shown that cellular endocytosis is blocked at 4°C in mammalian cells (Goldenthal *et al.*, 1984). To examine, therefore, the role of endocytosis in PrP conversion and prion propagation, naive and prion-propagating PrP-224AlaMYC cells were both incubated at 4°C (Section 5.3). Inhibition of endocytosis by incubating the cells at 4°C was shown to reduce the number of RML prion-infected cells significantly, but did not completely eradicate RML prion infection (Figure 5-4 A and B). No Texas-red labelled transferrin was internalised into the cells incubated at 4°C,

demonstrating that endocytosis was severely restricted (Figure 5-5 A and B, bottom panels, red). To observe the cellular localisation of PrP^{Sc}, RML prion-infected cells treated under different conditions, were categorised into seven phenotypes of PrP^{Sc} distribution (Figure 5-6 A and B) and the percentage of the cells showing each phenotype in different treatment conditions were quantified. In cells incubated at 37°C (control condition), PrP^{Sc} was mostly localised at the plasma membrane and PNC (Figure 5-5 A and B, top panels, green, Figure 5-6 A and B), whereas a significant number of RML prion-infected cells (about 50 %) incubated at 4°C showed PrP^{Sc} staining only at the plasma membrane (Figure 5-5 A and B, bottom panels, green, Figure 5-6 A and B). This suggests that the plasma membrane may play an important role in the conversion of PrP^{C} to PrP^{Sc}, and endocytosis may not be necessary for PrP conversion and prion propagation. Incubation of iPK1 cells at 4°C also reduced the level of PrP^{Sc} significantly (Figure 5-4 C), suggesting that the mechanisms that results in initial PrP conversion and prion propagation are similar.

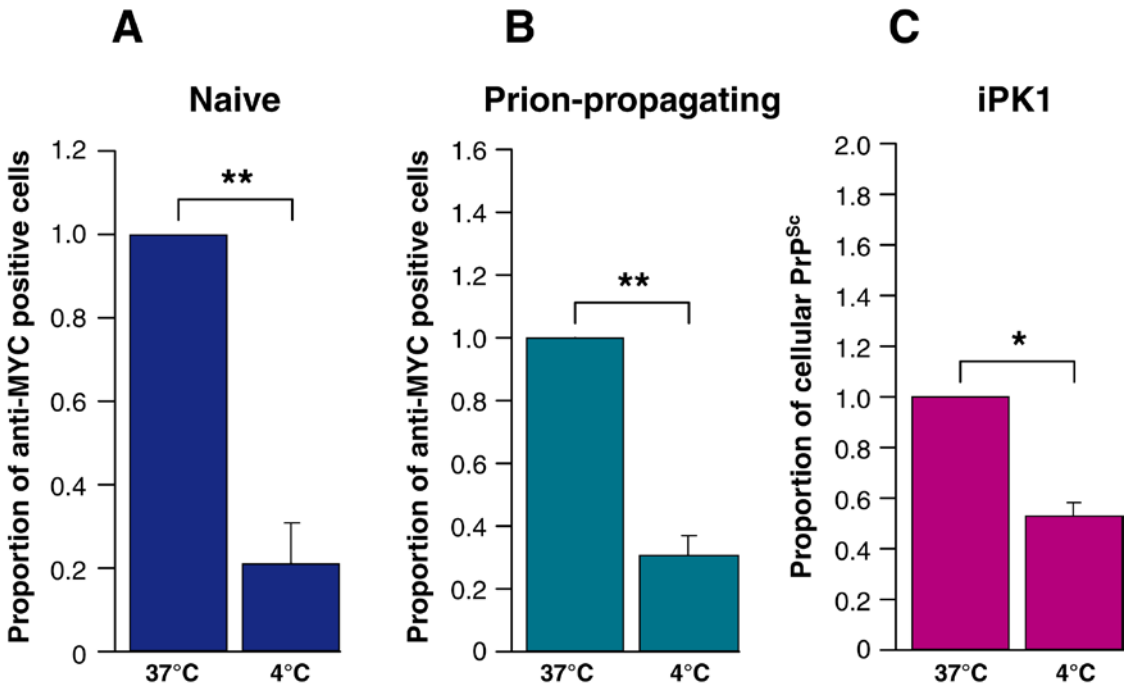

Figure 5-4 Inhibition of prion endocytosis reduces but does not eliminate PrP^{Sc} production and propagation

(A) Naive and **(B)** prion-propagating PrP-224AlaMYC cells incubated at 4°C or control temperature (37°C) were fixed, formic acid extracted and immunostained with anti-MYC antibodies. The numbers of anti-MYC positive cells were counted in both DMSO and 4°C treated cells. The results were normalised to the control condition (37°C) and is shown as proportion of the control. Incubation of naive and prion-propagating cells at 4°C radically decreased the number of RML prion- infected cells but it did not completely eliminate PrP conversion and prion propagation. **(C)** Lysates from iPK1 cells incubated at 4°C or control temperature (37°C) were analysed by SDS-PAGE electerophoresis and immunoblotted with anti-PrP antibody (ICSM35). The amount of PrP^{Sc} in iPK1 cells after each treatment was measured using quantitative densitometry. The levels of PrP^{Sc} expression was reduced by about 60 % at 4°C. Mean + SEM of four independent experiments are shown. * $P < 0.05$, ** $P < 0.01$.

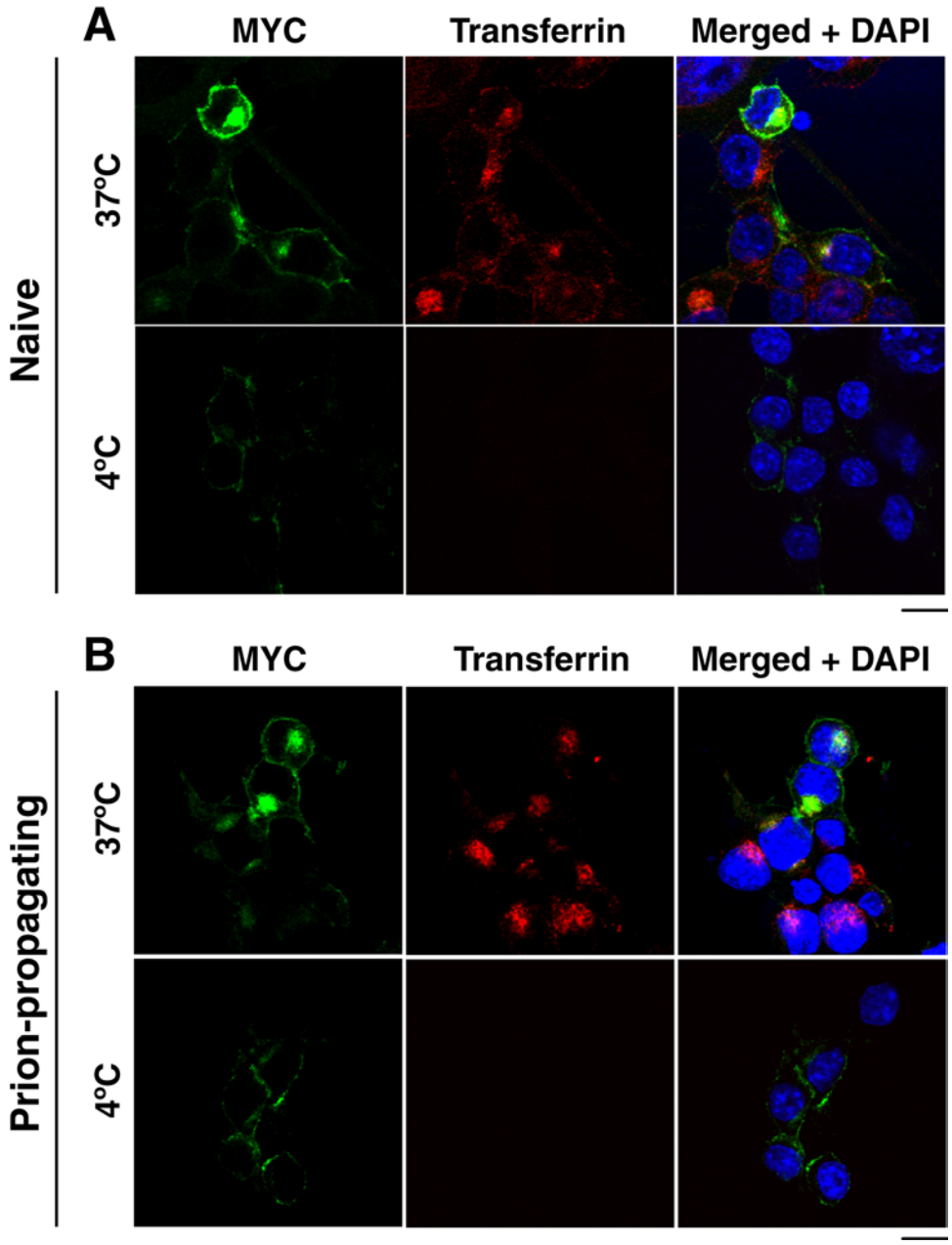

Figure 5-5 Sub-cellular distribution of MYC-tagged PrP^{Sc} in RML prion-infected PrP-224AlaMYC cells treated at 4°C

Confocal images of **(A)** naive and **(B)** prion-propagating PrP-224AlaMYC cells incubated at 4°C or control temperature (37°C) and exposed to Texas red-labelled transferrin (red). Cells were fixed and formic acid extracted prior to immunostaing with anti-MYC antibodies (green). Single channels and merged confocal images are shown as indicated. Note that incubation at 4°C has severely inhibited the internalisation of transferrin (red, A and B). Cells incubated at 4°C mostly had PrP^{Sc} localised on their cell surface (green, A and B top panels). Nuclei were stained with DAPI (blue). Scale bar = 15 µm.

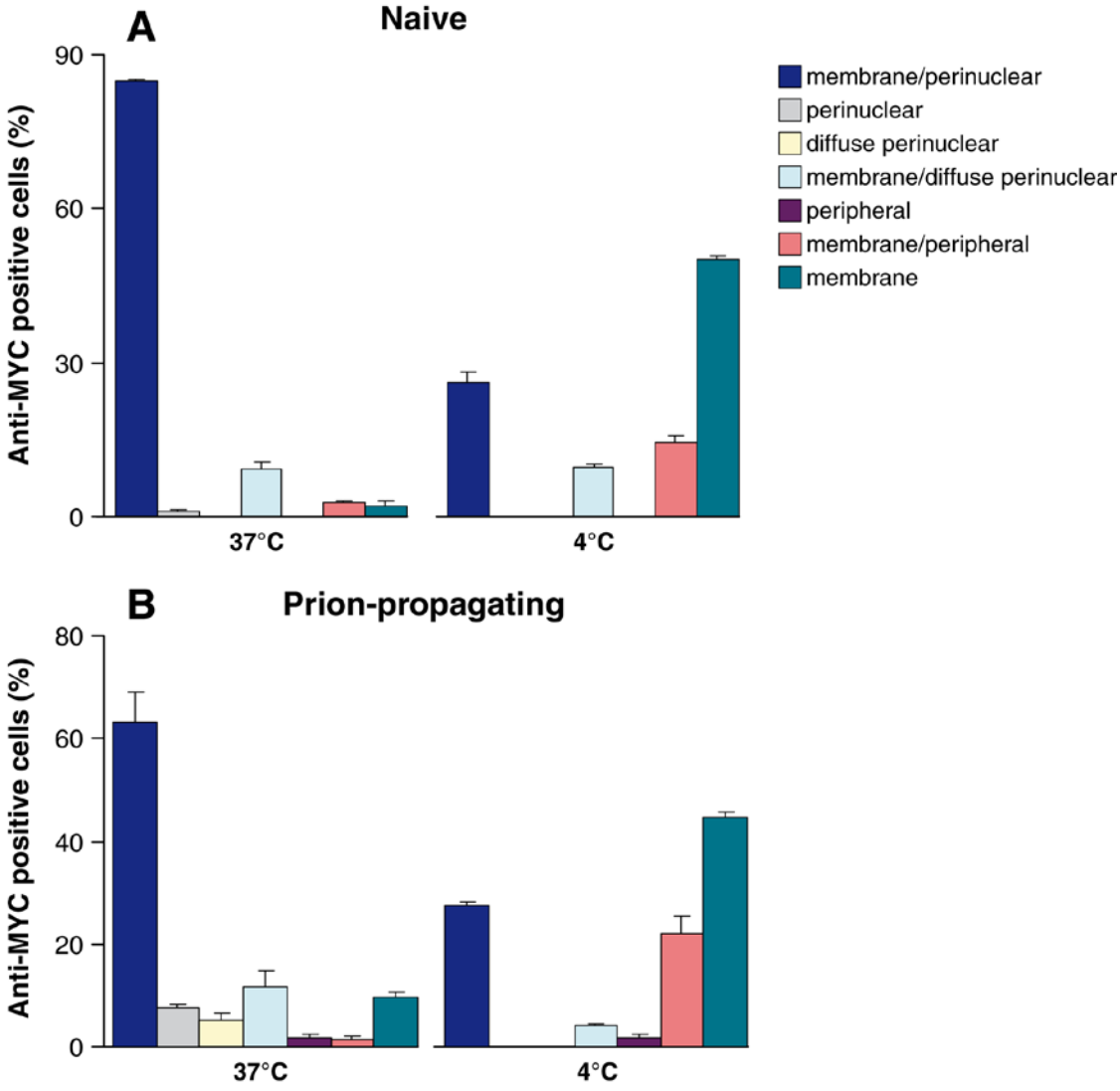

Figure 5-6 Cellular localisation of MYC-tagged PrP^{Sc} at 4°C in naive and prion-propagating PrP-224AlaMYC cells

The cell phenotypes of **(A)** naive and **(B)** prion-propagating PrP-224AlaMYC cells were observed and quantified after incubation at 4°C. In compare to cells treated at 37°C, higher percentages of both naive and prion-propagating cells have the plasma membrane staining at 4°C. Mean + SEM of four independent experiments are shown.

Trafficking events downstream of early endocytosis do not appear to be involved in PrP conversion and prion propagation

Nocodazole is an anti-neoplastic agent that interferes with polymerisation of microtubules and results in the loss of microtubule dependent processes in the cell (Bayer *et al.*, 1998). One consequence of treating cells with nocodazole is an accumulation of endocytosed material in endosomal carrier vesicles (ECV), a compartment intermediate between early and late endosomes (Gruenberg *et al*., 1989). This causes inhibition of cellular trafficking immediately following endocytosis, as progression to downstream compartments including late endosomes, lysosomes and endosomal recycling compartments is prevented. In naive and prion-propagating PrP-224AlaMYC cells, this resulted in the accumulation of small endocytic vesicles labelled with Texas-red labelled transferrin at the cell periphery, with little or no staining apparent at the PNC (Figure 5-7 and Figure 5-8, second panels, red). Nocodazole did not have a significant effect on the number of RML prion-infected cells (Figure 5-9 A and B). However, treatment of naive and prion-propagating PrP-224AlaMYC cells with nocodazole had a noticeable effect on the sub-cellular distribution of PrP^{Sc}. Nearly all of the RML prion-infected cells showed a strong plasma membrane and peripheral PrP^{Sc} distribution (Figure 5-7 and Figure 5-8, second panels, green, Figure 5-10 A and B), whilst PrP^{Sc} was mostly found at the typical plasma membrane and PNC appearance in DMSO-treated cells (Figure 5-7 and Figure 5-8, top panels, green, Figure 5-10 A and B). In cells treated with nocodazole, intracellular staining of PrP^{Sc} was restricted to small puncta that showed only a low level of colocalisation with labelled transferrin (Figure 5-7 and Figure 5-8, second panels).

To confirm the results obtained from treating cells with nocodazole, naive and prion-propagating PrP-224AlaMYC cells were also treated with bafilomycin or incubated at 20°C. Bafilomycin arrests the transport of endocytosed materials in early endosomes and, therefore, inhibits cellular trafficking from early to late compartments (Bayer *et al.*, 1998). A shift in temperature to 20°C has been shown to slow trafficking progression to lysosomes and the ERC in many cell types (Blighta and Morgana, 1987). Neither treatment with bafilomycin treatment nor a 20°C temperature shift affected Texas-red labelled transferrin transport into the PrP-224AlaMYC cells (Figure 5-7 and Figure 5-8, third and fourth panels, red), and consistent with the effect of nocodazole shown above, they did not reduce the number of RML prion-infected PrP-224AlaMYC cells (Figure 5-9 A and B). Taken together, these findings suggest that PrP conversion and prion propagation take place at the plasma membrane and/or early in the endocytic pathway and late endosomes/lysosomes are not involved in the PrP^{Sc} formation and propagation. Further validation was obtained by manipulating iPK1 cells in the same way. The levels of PrP^{Sc} found in iPK1 cells treated with nocodazole, bafilomycin or incubated at 20°C correlated well with the proportion of RML prion-infected cells in manipulated PrP-224AlaMYC cells (Figure 5-9 C).

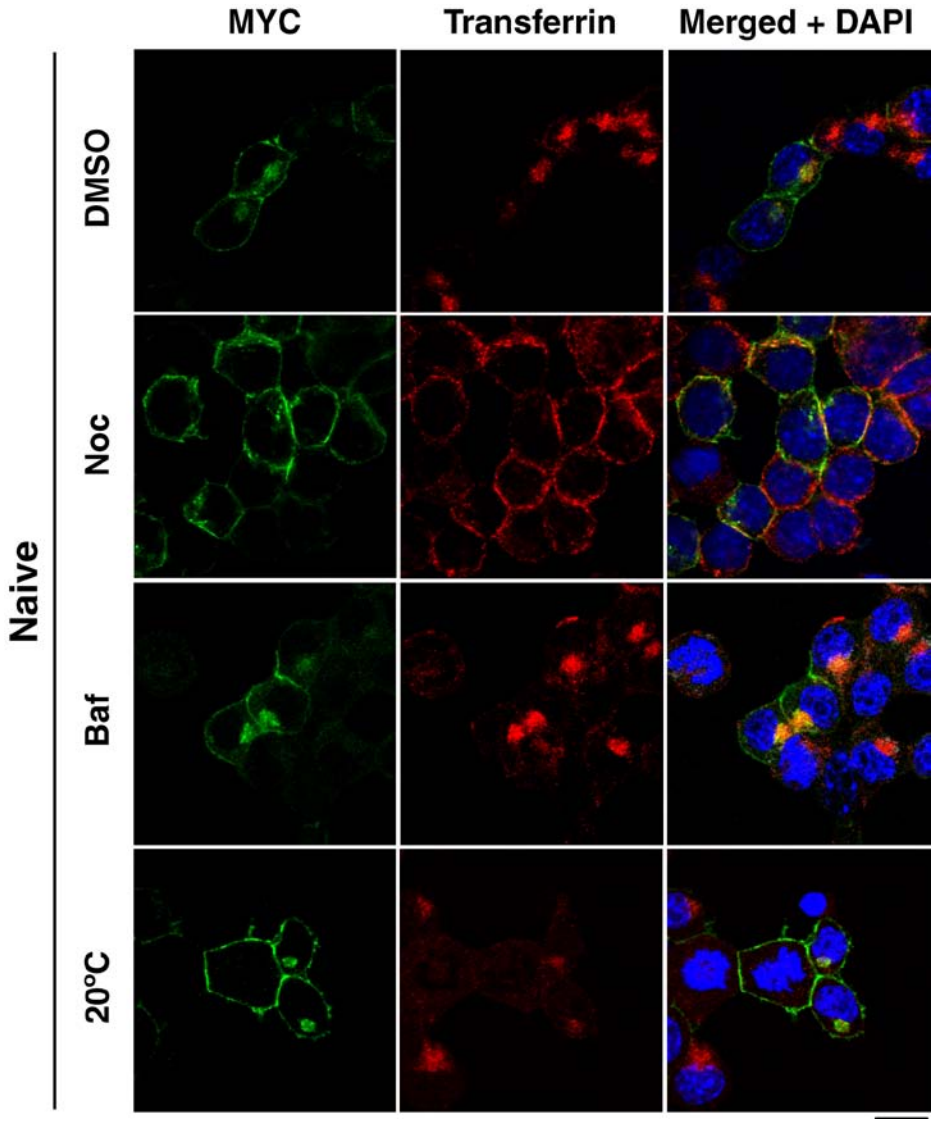

Figure 5-7 Sub-cellular distribution of MYC-tagged PrP^{Sc} in naive PrP-224AlaMYC cells after treatment with nocodazole, bafilomycin or 20°C temperature shift

Naive PrP-224AlaMYC cells were incubated at 20°C or exposed to DMSO, nocodazole or bafilomycin and Texas red-labelled transferrin (red) then fixed and formic acid extracted prior to immunostaing with anti-MYC antibodies (green). Single channel and merged confocal images are shown as indicated. RML prion-infected PrP-224AlaMYC cells treated with nocodazole showed strong plasma membrane and peripheral PrP^{Sc} distribution. However, RML prion-infected cells incubated at 20°C, or treated with DMSO or bafilomycin mostly had PrPSc localised at their plasma membrane and PNC. Note that in cells treated with nocodazole, Texas-red labelled transferrin has accumulated in the small endocytic vesicles at the cell periphery, with little or no staining apparent at the PNC and only a low level of colocalisation with PrP^{Sc}. Nuclei were stained with DAPI (blue). Scale bar = 15 µm.

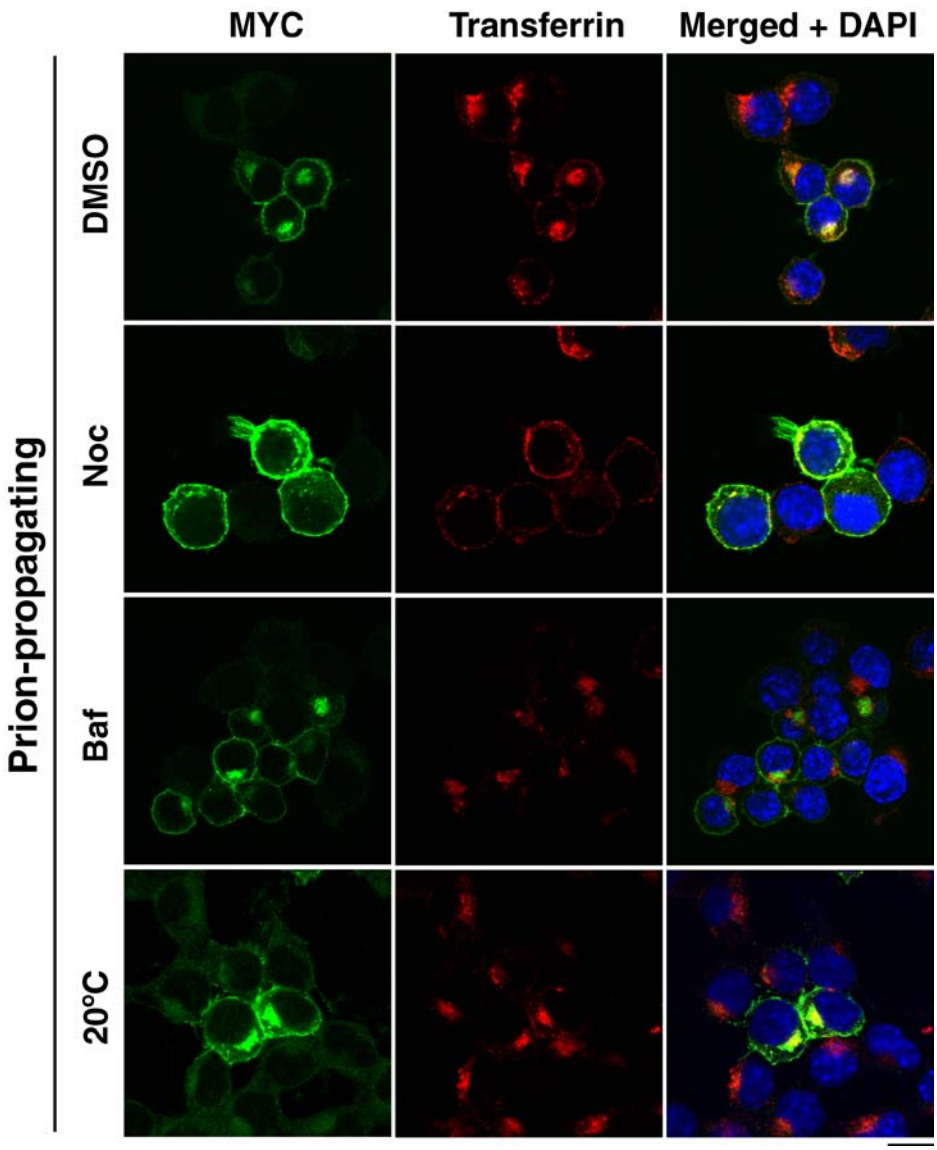

Figure 5-8 Sub-cellular distribution of MYC-tagged PrP^{Sc} in prion-propagating PrP-224AlaMYC cells after treatment with nocodazole, bafilomycin or 20°C temperature shift

Confocal images of prion-propagating PrP-224AlaMYC cells treated with nocodazole or bafilomycin or incubated at 20°C, and exposed to Texas red-labelled transferrin (red). Cells were fixed and formic acid extracted prior to immunostaing with anti-MYC antibodies (green). Single channels and merged confocal images are shown as indicated. Nocodazole has blocked trafficking of transferrin to the PNC; however, the trafficking of transferrin is not impaired by bafilomycin treatment or a 20°C temperature shift (red). Note that cells treated with nocodazole mostly had PrP^{Sc} localised on the plasma membrane and cell periphery (green). Nuclei were stained with DAPI (blue). Scale bar = 15 µm.

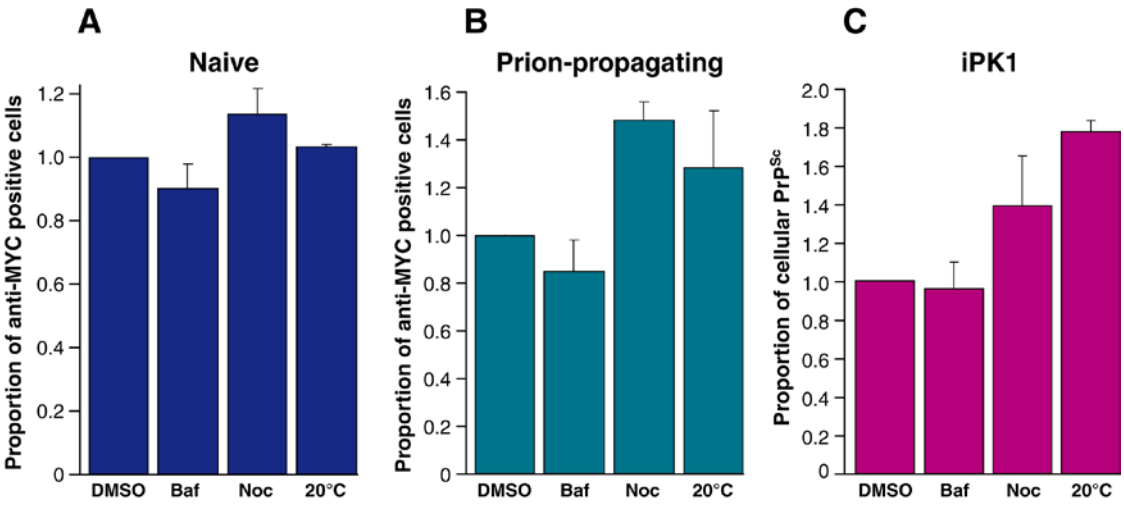

Figure 5-9 Inhibition of PrP trafficking beyond the early endosomes does not affect PrP conversion and prion propagation

(A) Naive and **(B)** prion-propagating PrP-224AlaMYC cells exposed to nocodazole or bafilomycin, or incubated at 20°C were fixed, formic acid extracted and immunostained with anti-MYC antibodies. Cells treated with DMSO were used as the control condition. The numbers of anti-MYC positive cells were counted, the results were normalised to DMSO-treated cells and are shown as proportion of the control. Note that the number of RML prion-infected cells was slightly increased after nocodazole treatment and 20°C temperature shift, whereas bafilomycin did not affect the proportion of PrP^{Sc} positive cells. **(C)** Lysates from iPK1 cells treated as above were analysed by SDS-PAGE electerophoresis and immunoblotted with an anti-PrP antibody (ICSM35). The amount of PrP^{Sc} in iPK1 cells after each treatment was measured using quantitative densitometry. The levels of PrP^{Sc} expression did not change significantly in manipulated iPK1 cells. Mean + SEM of four independent experiments are shown.

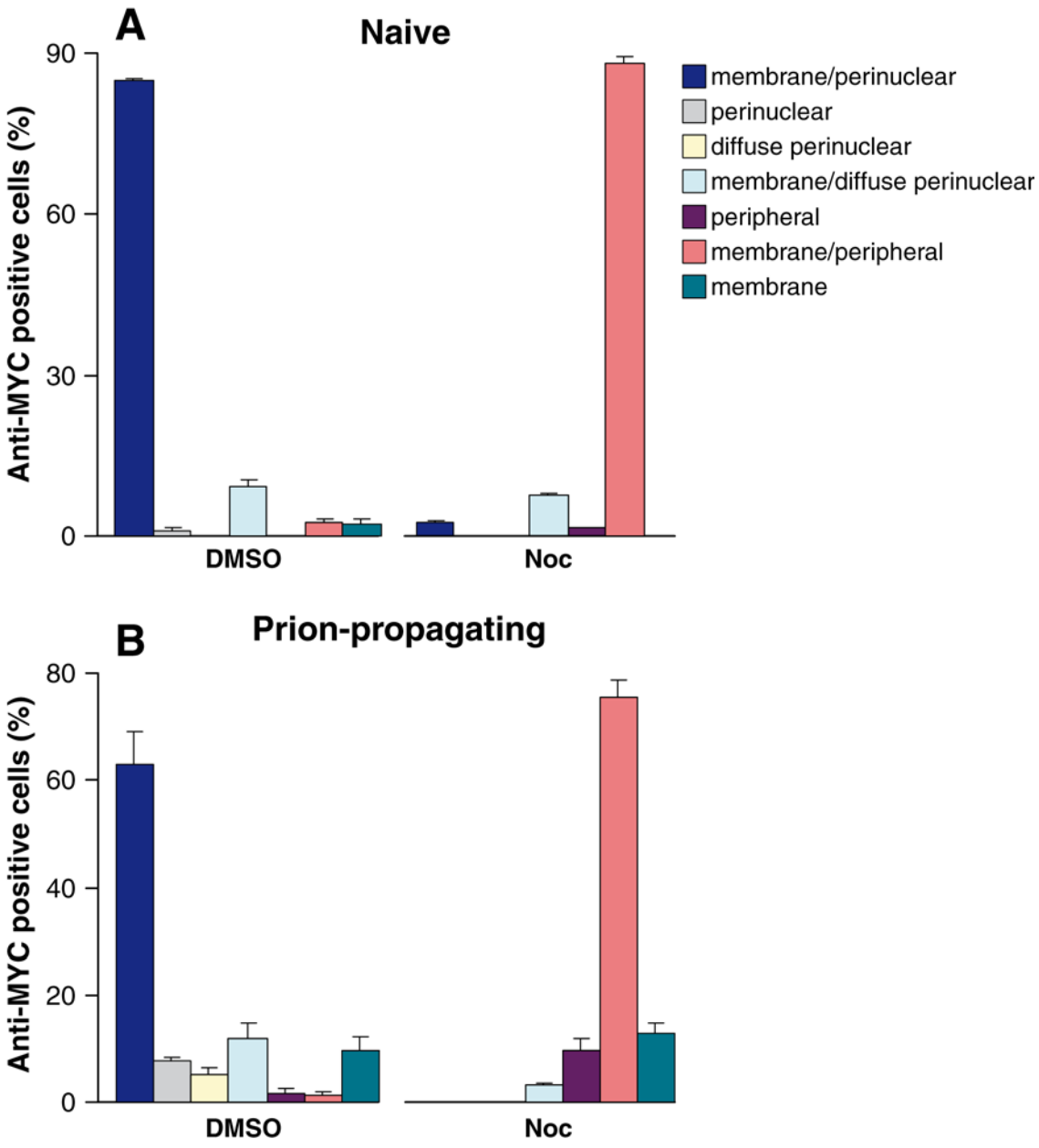

Figure 5-10 Cellular localisation of MYC-tagged PrP^{Sc} in naive and prion-propagating PrP-224AlaMYC cells treated with nocodazole

Cellular phenotypes of **(A)** naive and **(B)** prion-propagating PrP-224AlaMYC cells were observed and quantified after indicated treatments. Note that the cellular localisation of PrP^{Sc} has shifted from membrane/perinuclear to membrane/peripheral after nocodazole treatment. Cells treated with DMSO were used for the control condition. Mean + SEM of four independent experiments are shown.

PrP endocytosis is not dependent on dynamin

Several lines of evidence have suggested that PrP^{C} is internalised via a dynamin dependent pathway (Magalhaes *et al*., 2002; Sunyach *et al*., 2003; Sarnataro *et al*., 2009). To examine the mechanisms by which PrP^{Sc} is endocytosed, and observe how impairment of dynamin-dependent endocytosis affects PrP conversion and cellular trafficking of PrP^{Sc}, naive and prion-propagating PrP-224AlaMYC cells were treated with dynasore. Dynasore is a small molecule GTPase inhibitor that targets dynamin-1, dynamin-2 and dystrophin-related protein 1 (Drp1, the mitochondrial dynamin) (Macia *et al.*, 2006). Therefore, Dynasore is meant to block any dynamin-dependent processes in the cell such as clathrin-coated vesicle formation in endocytosis, ligand uptake through caveolae and the pathway from recycling endosomes to the plasma membrane (Abazeed *et al*., 2005; Cao *et al*., 2005; Damke *et al*., 1994; Hill *et al*., 2001; Van Dam and Stoorvogel, 2002; Nabi and Le, 2003). Treatment of PrP-224AlaMYC cells with dynasore did not change the number of RML prion-infected cells (Figure 5-11 A and B), but had a partial effect on the distribution of PrP^{Sc}, with most of the cells showing a localisation with the PNC but lacking the typical plasma membrane staining (Figure 5-12 A and B, bottom panels, green - arrows, Figure 5-13 A and B). Significantly, very little Texas-red labelled transferrin was internalised into the dynasore treated cells (Figure 5-12 A and B, bottom panels, red), indicating that dynamin, which is essential for clathrin-mediated endocytosis of transferin, was effectively inhibited. The lack of PrP^{Sc} on the plasma membrane and its presence at the PNC in the absence of transferrrin suggest that endocytosis of PrP^{Sc} does not require dynamin, whereas its recycling to the cell surface does. As shown in several studies, formation of the ERC and their transport to the cell surface require

dynamin (Van Dam and Stoorvogel, 2002; Pagano *et al*., 2004). The effect of dynasore was also tested in chronically infected PK1 cells. The proportion of cells that were infected with RML prions in iPK1 cells was similar to those seen in naive and prion-propagating cells (Figure 5-11 C). In a recent study by Marijanovic *et al.*, the ERC was suggested to be the likely site of prion conversion. Their results showed that the recycling of PrP through the ERC is required for PrP^{Sc} production (Marijanovic *et al*., 2009). Figure 5-11 C shows that blocking the formation of the ECR does not affect the number of cells producing PrP^{Sc}. Hence, in contrast to the finding presented by Marijanovic *et al.*, the results presented here showed that the ERC and/or return of PrP^{Sc} to the cell surface are not required for PrP conversion and prion propagation. Moreover, these observations demonstrate that internalisation of PrP^{Sc} is independent of both caveolae- and clathrin-mediated endocytosis.

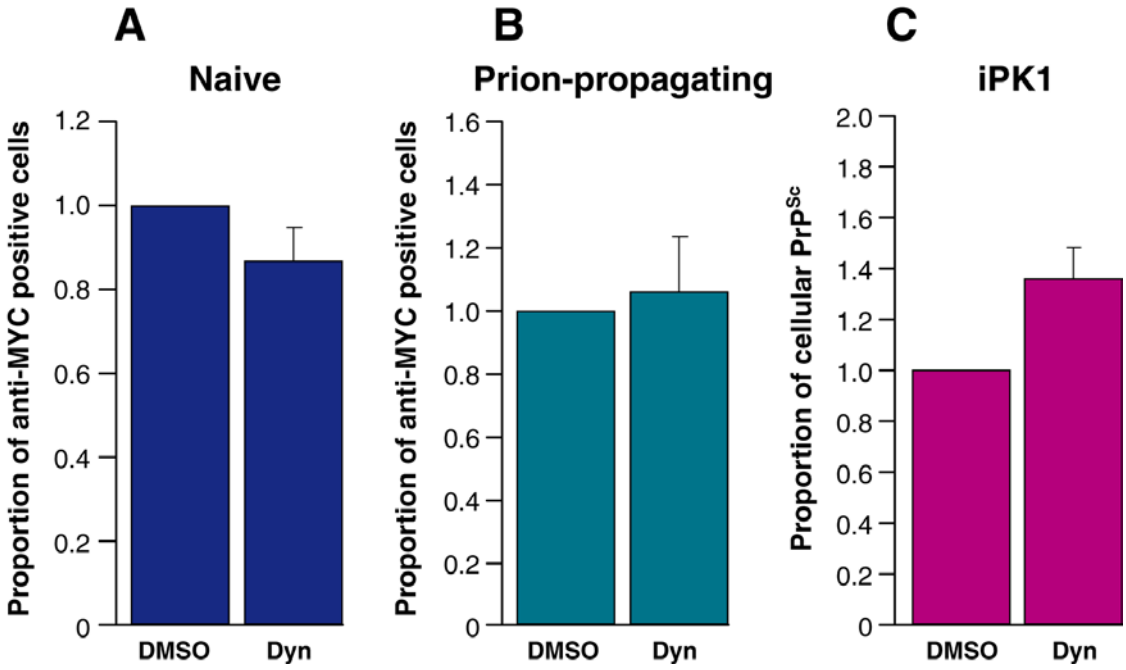

Figure 5-11 Inhibition of dynamin-dependent processes in RML prion-infected PrP-224AlaMYC and iPK1 cells does not affect PrP^{Sc} production and propagation

(A) Naive and **(B)** prion-propagating PrP-224AlaMYC cells were treated with dynasore and DMSO, and then fixed, formic acid extracted and immunostained with anti-MYC antibodies. The numbers of anti-MYC positive cells were counted in both DMSO- and dynasore-treated cells. The results were normalised to the control condition (DMSO) and are shown as a proportion of the control. Inhibition of dynamin-dependent processes in naive and prion-propagating cells using dynasore did not affect the number of RML prion- infected cells **(C)** Lysates from iPK1 cells treated with dynasore and DMSO were analysed by SDS-PAGE electrophoresis and immunoblotted with an anti-PrP antibody (ICSM35). The amount of PrP^{Sc} in iPK1 cells after each treatment was measured using quantitative densitometry. Note that the levels of PrP^{Sc} expression did not change after the indicated treatments. Mean + SEM of four independent experiments are shown.

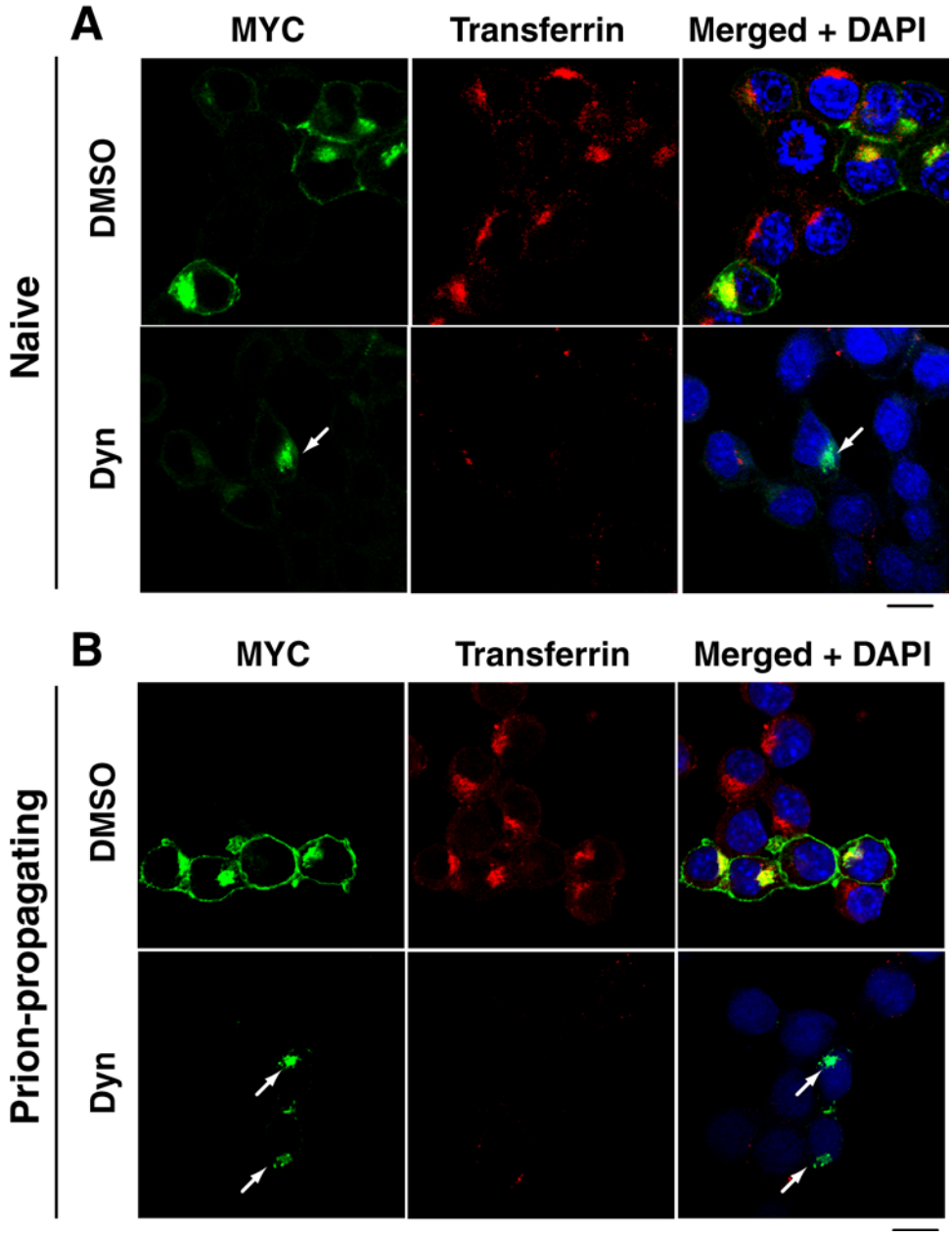

Figure 5-12 Sub-cellular distribution of MYC-tagged PrP^{Sc} in RML prion-infected PrP-224AlaMYC cells treated with dynasore

Confocal images of **(A)** naive and **(B)** prion-propagating PrP-224AlaMYC cells exposed to dynasore and Texas red-labelled transferrin (red). DMSO treatment was used as the control condition. Cells were fixed and formic acid extracted prior to immunostaing with anti-MYC antibodies (green). Single channels and merged confocal images are shown as indicated. It was noticed that dynasore treatment at 4°C had severely inhibited the internalisation of transferrin (red, A and B). Dynasore- treated cells mostly had PrP^{Sc} localised in their PNC with no PrP^{Sc} on their plasma membrane (green, A and B bottom panels, arrows). Nuclei were stained with DAPI (blue). Scale bar = 15 µm.

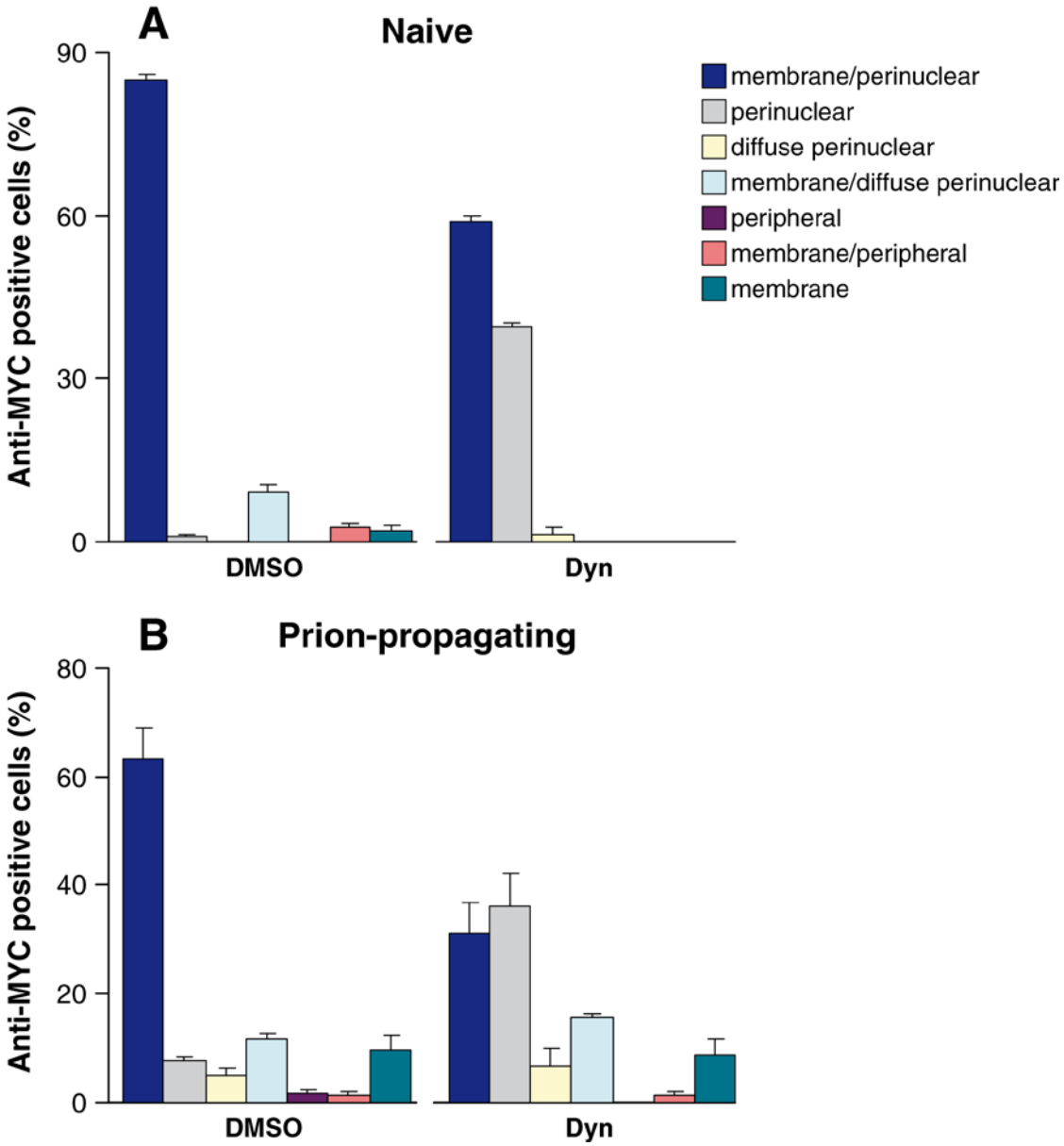

Figure 5-13 Cellular localisation of MYC-tagged PrP^{Sc} in naive and prion-propagating PrP-224AlaMYC cells treated with Dynasore

Cellular phenotypes of **(A)** naive and **(B)** prion-propagating PrP-224AlaMYC cells were observed and quantified after indicated treatments. Note that the number of cells with PrP^{Sc} localised in the PNC significantly increased as compared to DMSO-treated cells. Mean + SEM of four independent experiments are shown.

5.3.3 Prion conversion first occurs at the cell surface within one minute of prion exposure

Impairing protein trafficking in PrP-224AlaMYC cells suggested that conversion of PrP^{C} to PrP^{Sc} occurs on the plasma membrane and/or early in the endocytic pathway. Moreover, the data presented in the previous chapter revealed that PrP-224AlaMYC cells produce PrP^{Sc} as little as one minute exposure to RML prions (Section 4.3.2). It was also demonstrated that the number of RML prion-infected cells rose steeply in the first two minutes following RML prion exposure indicating that this is the period when most cells first begin to synthesise *de novo* PrP^{Sc} (Figure 4.6 B). These findings allowed the cellular site of initial prion conversion to be studied.

Examination of cells fixed after one minute of prion exposure revealed that the MYC-tagged PrP^{Sc} signal was only present at the plasma membrane (Figure 4.7, 1 min). Orthogonal projections of serial confocal sections also clearly showed that PrP^{Sc} was localised only at the cell surface (Figure 5-14 A, 1 min, white arrows). This cellular distribution was strikingly different from the more typical plasma membrane and intracellular localisation observed in cells that had been exposed to prions for longer times (Figure 5-14 A, 180 min, arrows). Categorising the cells into three phenotypes of different PrP^{Sc} distributions (plasma membrane, plasma membrane /diffuse intracellular and plasma membrane/perinuclear) and examining each phenotype at different times following RML prion exposure revealed a rapid transition from the plasma membrane distribution seen at the earliest time-point to the typical plasma membrane/PNC distribution observed later (Figure 5-14 B). Indeed, cells showing exclusively plasma membrane MYC-tagged PrP^{Sc} staining disappeared after

two minutes exposure to RML prions, consistent with rapid PrP^{Sc} formation, endocytosis and trafficking.

To confirm this result, the endocytosis of Texas-red labelled transferrin was directly compared with the formation and trafficking of MYC-tagged PrP^{Sc}. Transferrin endocytosis and trafficking occurred rapidly, reaching a steady-state distribution at the PNC between 8 and 16 minutes (Ghosh, 1994) (Figure 5-15, red, yellow arrows). In the same cells, PrP^{Sc} attained a steady-state distribution in nearly all cells by four minutes exposure to prions (Figure 5-14 B, Figure 5-15, green, white arrows). Therefore, *de novo* prion protein conversion, endocytosis and trafficking proceeds at similar rates or faster than transferrin trafficking.

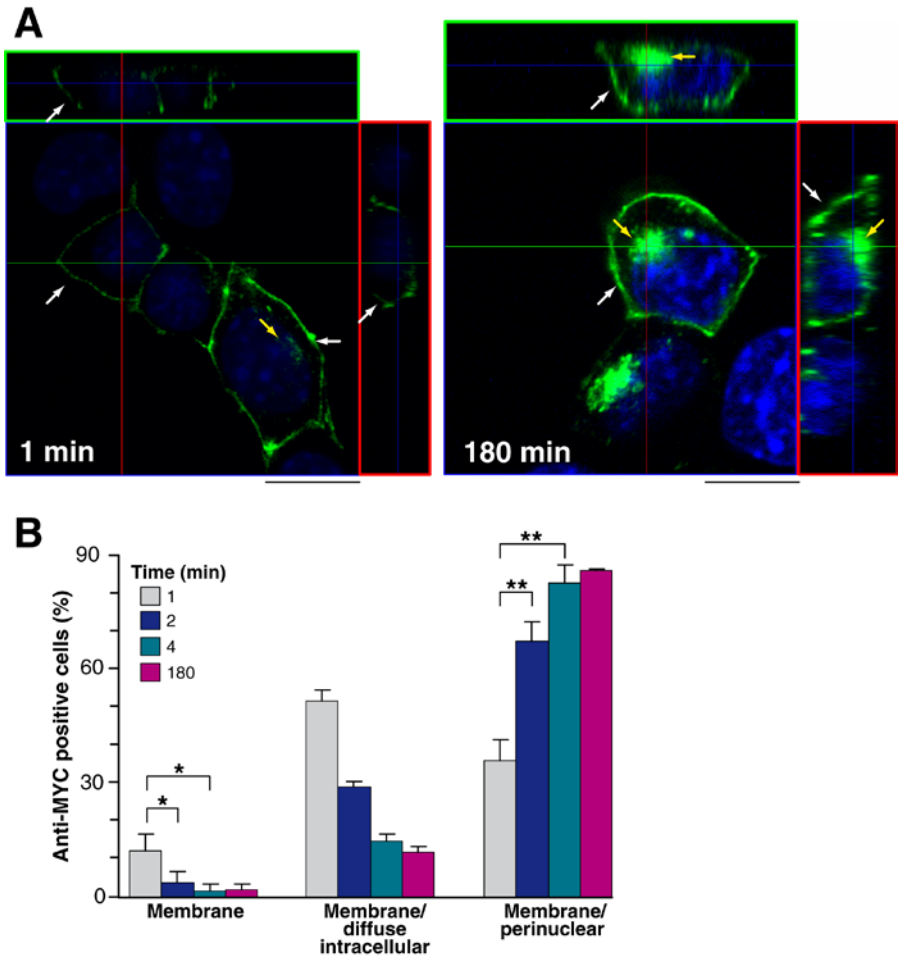

Figure 5-14 Prion conversion first occurs at the cell surface within one minute of prion exposure

(A) PrP224-AlaMYC cells were exposed to RML prions for the indicated times then fixed and formic acid extracted prior to staining with anti-MYC antibodies (green). Orthogonal projections (red and green squares) of serial confocal sections are shown alongside one z-section taken from the middle of the cell (as indicated by the guide lines). A cell fixed after 1 min exposure to RML prions shows PrP^{Sc} immunostaining only at the cell surface (1 min, white arrow). An adjacent cell in the field that has high levels of plasma membrane PrP^{Sc} also shows low intracellular levels of PrP^{Sc} (1 min, yellow arrow). Cells exposed to prions for 180 minutes show the typical equilibrium distribution of PrP^{Sc}, with strong immunostaining at the plasma membrane (white arrows – 180 min) and in the PNC (yellow arrow -180 min). Nuclei were stained with DAPI (blue). Scale bar = 10 µm. **(B)** Quantification of cell phenotypes observed at different time points following prion exposure. Transition from the plasma membrane or diffuse intracellular PrP^{Sc} distribution to the steady-state distribution is rapid and reflects the steep rise in the proportion of infected cells. Mean + SEM of four independent experiments are shown. * $P < 0.05$, ** $P < 0.01$.

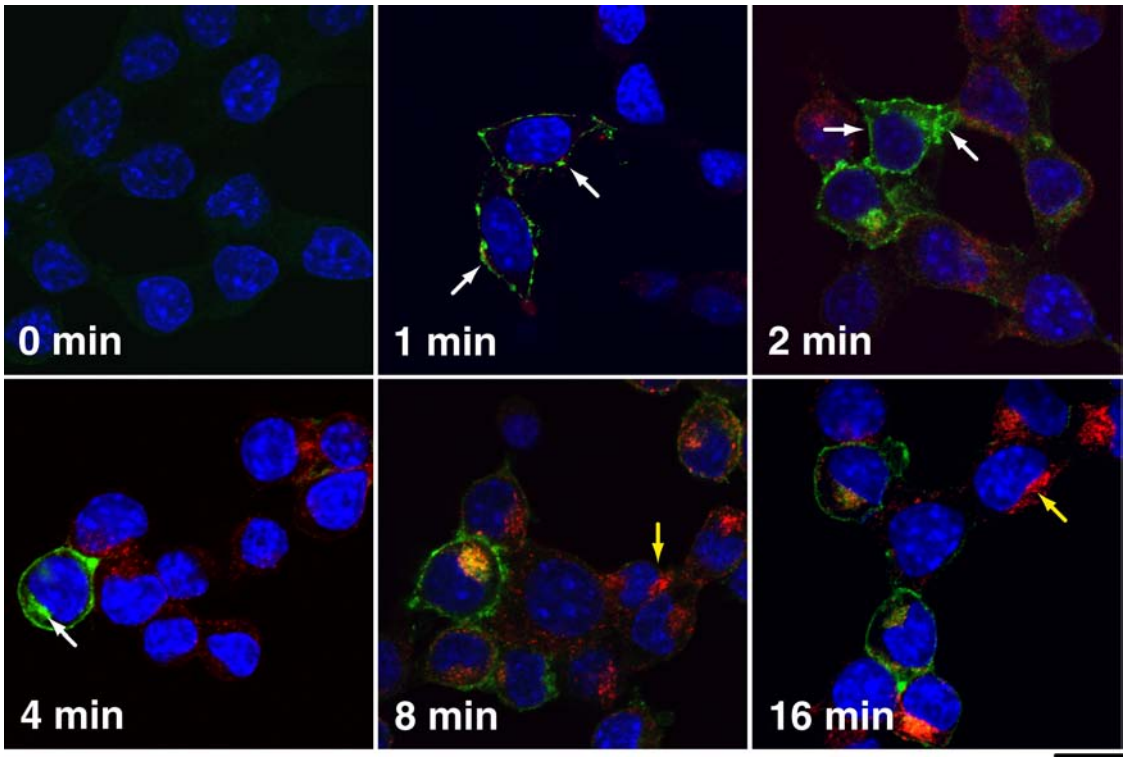

Figure 5-15 *De novo* prion protein conversion, endocytosis and trafficking proceeds at similar rates or faster than transferrin trafficking

PrP-224AlaMYC cells were exposed to RML prions and Texas red-labelled transferrin (red) for the indicated times then fixed and formic acid extracted. Merged confocal images of cells stained with anti-MYC antibodies (green). Initially PrP^{Sc} shows a plasma membrane distribution (1 min, arrow) and/or diffuse intracellular distribution (2 min, arrow) then rapidly attains its steady-state distribution concentrated at the plasma membrane and PNC (4 min, white arrow indicates strong PNC stain). Transferrin could be observed in small puncta at the cell periphery, reaching its equilibrium distribution in recycling endosomes at the PNC (yellow arrows) between 8 and 16 minutes. Nuclei were stained with DAPI (blue). Scale bar = 15 µm.

Lack of intracellular MYC-tagged PrP^{Sc} and its presence at the cell surface after one minute of RML prion exposure strongly suggests that conversion of PrP^{C} to PrP^{Sc} first occurs on the plasma membrane prior to endocytosis and intracellular trafficking. To test this hypothesis, pre-cooled PrP-224AlaMYC cells were incubated with RML prions at 4°C. This temperature shift effectively abolished endocytosis, as confirmed by the lack of transferrin uptake (Figure 5-16 A and B). Significantly, PrP^{Sc} accumulated only on the cell surface under these conditions (Figure 5-16 A, arrows). Orthogonal projections of confocal sections taken through these infected cells revealed the plasma membrane distribution of MYC-tagged PrP^{Sc} (Figure 5-16 B, arrows). These data clearly demonstrated that endocytosis is not necessary to produce misfolded PrP^{Sc}, and that a direct plasma membrane interaction between cellular PrP^{C} and exogenous prions is sufficient to generate *de novo* PrP^{Sc}. However, the efficiency of the conversion at 4°C was reduced, consistent with the data showed in section 5.3.2 (Figure 5-16 C).

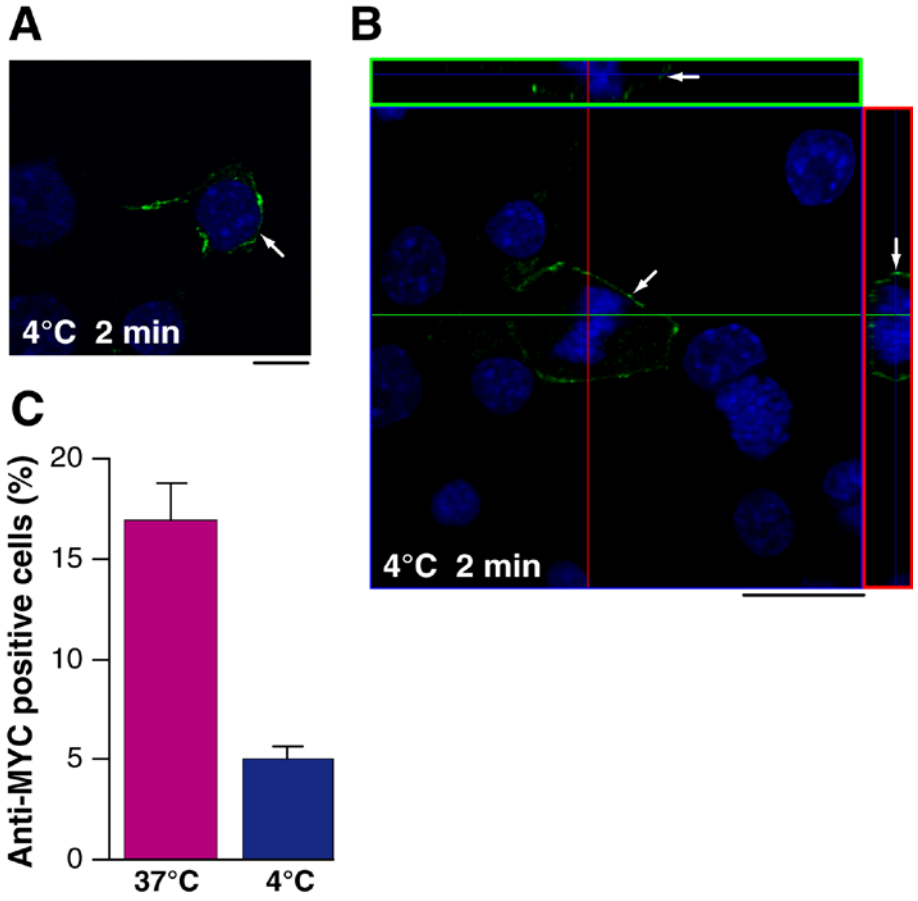

Figure 5-16 Conversion of PrP^{C} to PrP^{Sc} occurs initially on the cell surface

(A) Pre-cooled PrP-224AlaMYC cells were exposed to RML prions, and Texas red-labelled transferrin (red) was added for 2 minutes on ice. The cells were then fixed and formic acid extracted. Merged confocal images of cells stained with anti-MYC antibodies (green). MYC-tagged PrP^{Sc} was detected only at the plasma membrane (arrow). No transferrin has been endocytosed at this temperature. Nuclei were stained with DAPI (blue). Scale bar = 15 µm. **(B)** Pre-cooled PrP-224AlaMYC cells were exposed to RML prions for 2 minutes on ice then fixed and formic acid extracted. Orthogonal reconstructions of serial confocal slices are shown (red and green boxes) alongside one z-slice taken from near the middle of the cells (as indicated by the guide lines). The cells were fixed after 2 minutes and stained with anti-MYC antibodies (green). Formic acid-resistant PrP (PrP^{Sc}) is formed on the cell surface of one of the cells in the field (arrow), no intracellular PrP^{Sc} was detected. Nuclei were stained with DAPI (blue). Scale bar = 15 µm. **(C)** PrP-224AlaMYC cells were exposed to RML prions for 3 hours at 37°C or on ice then fixed and formic acid extracted. The percentage of anti-MYC positive (prion infected) cells observed at 37°C and 4°C was quantified. Intact lipid raft integrity on the cell surface requires for efficient prion conversion. Mean + SEM of three independent experiments Intact lipid raft integrity on the cell surface required for efficient prion conversion is shown (background levels found in uninfected cells for each condition has been subtracted from the mean).

Rapid prion conversion on the cell surface may point to a mechanism whereby PrP misfolding is a stochastic event catalysed by an interaction with PrP^{Sc} in a favourable environment. This could be provided by lipid rafts, specialised membrane microdomains known to be present in the plasma membrane and enriched in PrP^{C} (Madore *et al*., 1999; Vey *et al*., 1996). Therefore, the role of lipid rafts in prion protein conversion was tested using reagents that disrupt lipid raft integrity. Two reagents were used that affect lipid raft function by different mechanisms: filipin (Ying *et al*., 1992), which binds and sequesters plasma membrane cholesterol; and U18666A, which inhibits cholesterol transport to rafts (Cenedella, 2009). Both of these compounds abrogated the initial *de novo* prion conversion in our cellular system (Figure 5-17). This is consistent with a lipid raft-dependence of the prion conversion process as described previously (Marella *et al.*, 2002; Stengel *et al.*, 2006) and suggests that the initial conversion process is occurring within these domains on the plasma membrane

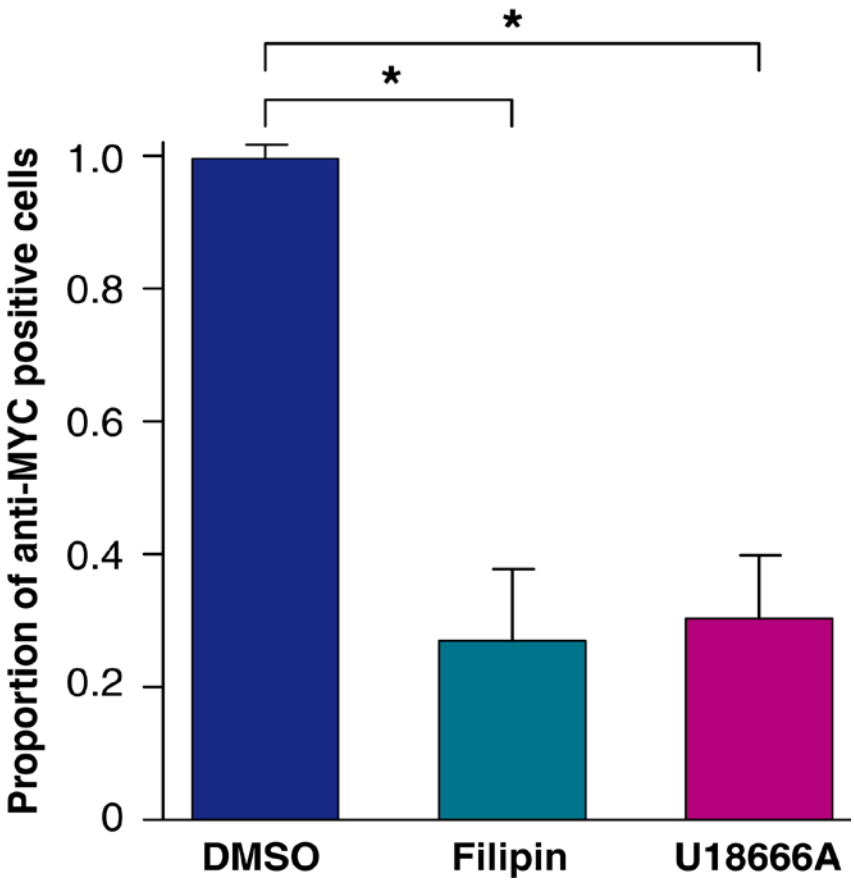

Figure 5-17 Intact lipid raft integrity on the cell surface required for efficient prion conversion

PrP-224AlaMYC cells were pre-treated with filipin or DMSO for 30 minutes or U18666A for 16 hours then exposed to RML prions for 3 hours in the continued presence of inhibitors or DMSO. Cells were then fixed and formic acid extracted prior to immunostaining with anti-MYC antibodies. The percentage of anti-MYC positive (RML prion infected) cells was quantified. Mean + SEM of three independent experiments are shown (background levels found in non-infected cells for each condition have been subtracted from the mean). * $P < 0.05$. Filipin and U18666A abrogated the initial *de novo* prion conversion in our cellular system indicating lipid raft integrity is required for prion infection**.**

5.4 Discussion

Conversion of PrP^{C} to PrP^{Sc} is the key cellular event in prion pathogenesis. Prion conversion is thought to occur at a site where the two protein forms meet and are able to physically interact (Prusiner, 1998a). To date, no specific intracellular compartment has been definitely identified as having sole responsibility for this event, as several compartments have been proposed using different cell systems (Caughey *et al*., 1991; McKinley *et al*., 1991b; Arnold *et al*., 1995; Barmada and Harris, 2005; Pimpinelli *et al*., 2005; (Godsave *et al*., 2008; Marijanovic *et al*., 2009). Based on analyses of the sub-cellular localisation of different PrP forms, the plasma membrane and endolysosomal compartments have been proposed as possible locations for the PrP conversion process (Section 1.6.2 and Section 5.1). There are contrasting data about PrP^{C} and PrP^{Sc} localisation (Shyng *et al*., 1993; Sunyach *et al*., 2003), and these inconsistencies are mostly likely related to the lack of antibodies specific to PrP^{Sc}, and the need for a protein denaturation step to hydrolyse PrP^{C} and reveal the PrP^{Sc} epitope. Moreover, study of the cellular site where PrP^{C} and PrP^{Sc} first meet for conversion to be catalysed has proven difficult as newly made PrP^{Sc} is immunologically indistinguishable from PrP^{Sc} species in the brain homogenate inocula. Therefore, previous works studying the cellular site of initial PrP conversion have relied on prolonged culture of cell lines that stably propagate prions to clear any inocula-derived PrP^{Sc}, which is known to persist in cell cultures for two weeks or more (Giri *et al*., 2006; Cronier *et al*., 2004), before the cell biology of newly formed PrP^{Sc} can be analysed (Bosque and Prusiner, 2000). This means that fundamental information such as where the initial site of PrP conversion occurs has not yet been elucidated. Impairment of PrP trafficking in the unique cell system in which epitope

tagged-PrP^{Sc} is produced, combined with effective protocols to remove PrP^{C}, have allowed examination of the initial site of PrP conversion, in this thesis work.

Several studies indicate that the conversion of PrP^{C} to PrP^{Sc} is a post-translational event that occurs after the protein reaches the cell surface (Caughey and Raymond, 1991; Borchelt *et al*., 1992; Taraboulos *et al*., 1992). Indeed, both the exposure of PrP^{C} to anti-PrP antibodies and the release of nascent PrP from the cell surface, either by PIPLC or hydrolysis with dispase and trypsin prevent the formation of PrP^{Sc} (Caughey and Raymond, 1991; Borchelt *et al*., 1992; Enari *et al*., 2001). Gilch *et al*., showed that down-regulation of PrP^{C} on the cell surface using Suramin, which induces intracellular re-routing of PrP from post-ER compartments to acidic vesicles, interferes with PrP^{Sc} propagation in cell culture and scrapie infected animals (Gilch *et al*., 2001). BFA has shown to inhibit PrP^{C} export to the plasma membrane by blocking its transport from ER to Golgi (Misumi *et al.*, 1986; Doms *et al.*, 1989); (Lippincott-Schwartz *et al*., 1989; Taraboulos *et al*., 1992). The data presented in this chapter demonstrated that treatment of PrP-224AlaMYC cells with BFA significantly reduced PrP^{Sc} formation and propagation suggesting that the ER-Golgi is insufficient for synthesis of PrP^{Sc}, and that PrP^{C} transport to the cell surface is essential for this process, consistent with previous findings (Taraboulos *et al*., 1992). Recent findings have shown that stimulating the retrograde transport and accumulation of PrP in the ER through over-expression of the constitutively active, small GTPase Rab6a, increases the production of PrP^{Sc} in infected cells (Beranger *et al*., 2002). This suggests the possibility that PrP^{Sc} undergoes retrograde transport to the Golgi apparatus and/or to the ER following its production. These findings might explain the diffuse PrP^{Sc} staining noted in RML prion-infected PrP-224AlaMYC cells treated

with BFA. PrP^{C} has a half-life of approximately three to five hours. Therefore, it is possible that in the cell system presented here BFA treatment was not long enough to completely deplete cellular PrP^{C} and the residual protein on the plasma membrane or in the endocytic compartments converted to PrP^{Sc}, and via retrograde transport PrP^{Sc} then reached the Golgi apparatus and the ER followed by many GPI-linked proteins (Muñiz and Riezman, 2000). Due to the BFA treatment, the Golgi stacks get dispersed and fuse with the ER. In addition, the trans-Golgi network (TGN) mixes with the early endosomal system after BFA treatment (Lippincott-Schwartz *et al.*, 1991; Wood *et al*., 1991), which may explain why the PrP^{Sc} staining looked diffuse.

Arnolds *et al.*, showed the presence of PrP^{Sc} in sub-cellular structures that contain the cation-independent mannose 6-phosphate receptor, ubiquitin-protein conjugates, beta-glucuronidase, and cathepsin B, and termed them late endosome-like organelles (Arnold *et al.*, 1995). PrP^{C} will enter such compartments for normal degradation and, therefore, it was suggested that these organelles may be the site of PrP^{C} conversion into infectious PrP^{Sc}. In contrast, the data presented in this chapter demonstrated that impairment of PrP trafficking beyond early endocytosis (by incubating the cells at 20°C or using nocodazole or bafilomycin) does not affect PrP conversion and prion propagation, arguing against the involvement of late endosomes/lysosomes in PrP^{Sc} production. This is in agreement with several lines of evidence that suggest the formation of PrP^{Sc} occurs prior to entry into lysosomes. First, lysosomotropic amines block the digestion of the NH_2-terminal ninety amino acids of PrP^{Sc}, but they do not interfere with the formation of PrP^{Sc} (Caughey *et al*., 1991; Taraboulos *et al*., 1991)**.** Second, lysosomotropic amines do not alter substantially the degradation of PrP^{C} (Taraboulos *et al*., 1991a)**,** suggesting that it might be degraded

before reaching lysosomes. Thirdly, kinetic studies indicate that PrP^{Sc} acquires protease resistance approximately one hour before exposure to lysosomal proteases and digestion of the NH_2 terminus (Taraboulos *et al*., 1991b). Moreover, Marijanovic *et al*., identified the ERC as the likely site of PrP conversion (Gousset *et al*., 2009). However, blocking the PrP trafficking to the ERC by incubating PrP-224AlaMYC cells at 4°C or 20°C, or treating them with nocodazole, bafilomycin or dynasore did not affect the conversion of PrP^{C} into PrP^{Sc}. These data rule out the absolute necessity for the ERC in PrP^{Sc} formation, and suggest that PrP conversion and prion propagation occurs at the plasma membrane and/or early in the endocytic pathways in agreement with previous findings (Section 1.6.2 and Section 5.1).

In neuronal cells, a major pathway for internalisation of prion protein appears is via clathrin-mediated endocytosis, a process that is dynamin-dependent (Sunyach *et al*., 2003; Sarnataro *et al*., 2009) (Section 1.6.1). Moreover, transfection of neuronal cell lines with a dominant negative mutant of dynamin I (K44A), which blocks fission of invaginated coated pits from the plasma membrane, inhibits PrP^{C} endocytosis suggesting that PrP^{C} is internalised via a dynamin-dependent (clathrin-mediated endocytosis) pathway (Magalhaes *et al*., 2002). However, inhibition of any dynamin-dependent processes in PrP-224AlaMYC cells using dynasore did not inhibit the internalisation, formation and propagation of PrP^{Sc}, implying that the internalisation of PrP^{Sc} is not dynamin-dependent in our cell system. This observation is supported by Wadia and colleagues showing that endocytic uptake of PrP in N2a cells occur by lipid raft-dependent macropincytosis, which does not require dynamin (Wadia *et al*., 2008). These data also propose that PrP^{C} and PrP^{Sc} might use different internalisation pathways.

Furthermore, MYC-tagged PrP^{Sc} accumulated in the PNC of PrP-224AlaMYC cells treated with dynasore, with no PrP^{Sc} localised on the cell surface. This suggests that although the internalisation of PrP^{Sc} is not dynamin-dependent, its recycling back to the cell surface is. These data also propose that PrP^{Sc} formation does not require cell-surface recycling, again in agreement with previous findings (Beranger *et al*., 2002).

Blocking of endocytosis by incubating PrP-224AlaMYC cells at 4°C clearly demonstrated that endocytosis is not necessary to produce misfolded PrP^{Sc}, and that a direct plasma membrane interaction between cellular PrP^{C} and exogenous prions is sufficient to generate *de novo* PrP^{Sc}. This concurs with previous findings proposing that the plasma membrane is a potential site of PrP conversion (Caughey and Raymond, 1991; Kanu *et al*., 2002; Veith *et al*., 2008), and is consistent with the observed PrP^{Sc} distribution reported in different cell and *in vivo* systems (Jeffrey *et al*., 2000; Caughey and Baron, 2006; Veith *et al*., 2008). Detailed spatial analysis of PrP-224AlaMYC cells shortly after RML prion exposure further confirmed that PrP^{Sc} forms on the plasma membrane. However, the efficiency of the PrP conversion at 4°C was reduced. This may reflect a slower reaction rate due to the lower temperature, as might be expected for a protein folding-driven phenomenon (Oliveberg *et al.*, 1995). Alternatively, it might reflect a reduced prion conversion rate in the absence of a contribution from internal components. This suggests also that the plasma membrane is the initial site of prion conversion and early endocytic compartments may continue or accelerate the PrP conversion process following the endocytosis of PrP^{Sc}. Therefore, the observation that prion infection was reduced at 4°C may be consistent with an important role for internal cellular compartments in PrP^{Sc} propagation.

Our data also suggest that PrP conversion and prion propagation is dependent on the presence of intact lipid rafts (Madore *et al*., 1999; Vey *et al*., 1996). Supporting this idea, co-factors found enriched in lipid rafts have been shown to stimulate synthetic prion conversion (Deleault NR *et al*., 2007; Taylor *et al*., 2009; Abid and Soto, 2006) and reagents that disrupt raft integrity abrogate PrP^{Sc} propagation in cells (Marella *et al*., 2002; Gousset *et al*., 2009). Recombinant trans-membrane forms of PrP^{C} that are not directed to rafts do not seed PrP^{Sc} formation in prion-infected N2a cells (Taraboulos *et al*., 1995; Kaneko *et al*., 1997b). Furthermore, lipid rafts have shown to be the key intermediates in the retrograde transport route. Preventing PrP conversion and prion propagation with filipin and U18666A reagents, which disrupt lipid rafts, further supported the possible involvement of the retrograde route in prion trafficking.

The unique cell system utilised here has allowed new insights into the dynamic nature of PrP^{Sc} trafficking in the cell. The ability to analyse the trafficking events immediately following exposure to exogenous prions has revealed that PrP^{Sc} initially forms at the cell surface and is then rapidly endocytosed via a dynamin-independent process and possibly travel through retrograde route to the Golgi-ER. Indeed, after one minute exposure to RML prions, many cells already contain intracellular PrP^{Sc}, often in a diffuse cellular distribution that possibly reflects a transition through an endosomal compartment. After four minutes exposure to prions, the distribution of PrP^{Sc} obtains a steady-state that is concentrated at the PNC and at the cell surface, as described previously (Kristiansen *et al*., 2005; Caughey *et al*., 1991; Arnold *et al*., 1995).

5.5 Summary

The work in this chapter revealed that intracellular re-routing of PrP prevents propagation of PrP^{Sc}. It suggests that the conversion of PrP^{C} to PrP^{Sc} is a post-translational event that occurs after the protein reaches the cell surface. It was shown that the late endosomes, lysosomes and ERC do not appear to be key sites of PrP conversion and prion propagation, whilst the plasma membrane and early endocytic compartments are involved in this key process. Most importantly, studying the early events of RML prion infection suggests that the plasma membrane is the initial site of prion conversion and that the cell surface is sufficient for the process. Finally, it was suggested that PrP^{Sc} may travel to the perinuclear region of the cell via retrograde transport system and intact lipid rafts are essential for this pathway and the production of PrP^{Sc}.

6 Conclusions and future plans

6.1 Thesis summary and conclusions

The work presented in this thesis aimed to investigate the earliest event in prion infection using a novel cell system. Specifically, it aimed to assess the timescale that PrP^{C} is converted to PrP^{Sc} following exposure to RML prions and identify the initial cellular site of PrP^{Sc} formation and propagation.

Work presented here reported on the generation of a unique cell system in which a novel MYC-tagged PrP^{C} is expressed in a neuroblastoma cell line where the endogenous PrP^{C} has been silenced using RNAi. This engineered PrP^{C} chimera (PrP-224AlaMYC) was shown to support prion replication resulting in the production, for the first time, of a true *bona fide*, infectious epitope-tagged PrP^{Sc} as evidenced by both *in vitro* and mouse bioassays. The capacity of PrP-224AlaMYC cells to produce epitope-tagged PrP^{Sc} combined with established methods to remove PrP^{C} and specifically visualise *de novo* PrP^{Sc} generated in the recipient cell (pre-treatment with formic acid and proteinase K), allowed the earliest events in cellular prion infection and PrP misfolding to be studied for the first time. The work has also enabled initial dissection of intracellular PrP^{Sc} trafficking pathways.

The data presented here showed that prion infection of cells is extremely rapid, occurring within one minute of prion exposure. It was also suggested that conversion of PrP^{C} to PrP^{Sc} is a post-translational event and that the plasma membrane is the initial site of prion conversion. Pharmacological interventions revealed that late endosomes, lysosomes and the endosomal recycling compartments do not appear to be primary sites of PrP conversion and prion propagation. Instead, it appears that *de novo*

PrP^{Sc} is first synthesised at the plasma membrane as early as one minute and is rapidly endocytosed via a dynamin-independent process and trafficked to internal compartments adjacent to the nucleus (*i.e.* PNC). Disruption of the Golgi apparatus and the ER altered the sub-cellular distribution of PrP^{Sc} preventing PNC build up. This suggests that following synthesis on the plasma membrane, PrP^{Sc} is endocytosed and undergoes retrograde transport through the trans-Golgi network, the Golgi apparatus and the ER in a similar manner to other GPI-linked proteins (Muñiz and Riezman, 2000). Consistent with this theory, disruption of lipid rafts by filipin and U18666A treatment prevented prion infection and PrP^{Sc} propagation. The critical link between PrP^{Sc} trafficking and prion-mediated neurotoxicity currently remains unclear. Further work will therefore investigate how PrP^{Sc} accesses the cytosol and subsequently interacts with the UPS.

6.2 Suggestions for future work

6.2.1 Understanding the pathways by which PrP^{Sc} accesses the cytosol

Several lines of evidence have suggested a role for ubiquitin-proteasome system (UPS) dysfunction in the pathogenesis of prion diseases (Kristiansen *et al*., 2005; Kristiansen *et al*., 2007). Kristiansen and colleagues demonstrated that mild proteasome inhibition in prion-infected neuronal cells results in the formation of large cytosolic perinuclear aggresomes containing PrP^{Sc}, heat shock chaperone 70 (Hsc70), ubiquitin, proteasome subunits, and vimentin. Aggresome formation was associated with activation of caspases 3 and 8 and subsequent apoptosis (Kristiansen *et al*., 2005). Two well-characterised UPS substrates (IκB and P27) were found to accumulate in the brains of prion-infected mice, supporting the hypothesis that prion diseases are

associated with UPS dysfunction (Kristiansen *et al*., 2005). A follow-up study has since demonstrated that disease-associated PrP specifically inhibits the proteolytic β subunits of the 26S proteasome via a direct, high affinity interaction (Kristiansen *et al*., 2007; Deriziotis *et al*., unpublished data). These studies suggest that direct inhibition of the proteasome by PrP^{Sc} is a key component in prion toxicity. In order to inhibit the proteasome directly, PrP^{Sc} must gain access to the cytosolic compartment, a process that is currently poorly understood. As a membrane protein, mature PrP^{C} would not normally be exposed to the cytosol. In combination with previous studies, the work presented in this thesis demonstrated that PrP^{Sc} is generated from PrP^{C} at the cell surface and/or shortly after internalization (Campana *et al*., 2005) (Chapter 5). As a result, PrP^{Sc} must traverse, either the plasma membrane itself, or one of the internal membranes, in order to access the cytosol.

Possible sites of PrP^{Sc} entry to the cytosol could be investigated using the unique PrP-224AlaMYC expressing neuroblastoma cell system. After internalisation PrP^{Sc} may undergo retrograde transport to the trans-Golgi network, the Golgi apparatus and the ER where PrP^{Sc} transfer to the cytosol could be facilitated by ER translocation machinery. This hypothesis is supported by studies suggesting that wild type and certain mutant forms of PrP misfolded in the ER are substrates for endoplasmic reticulum associated protein degradation (ERAD) (Zanusso *et al*., 1999; Yedidia *et al*., 2001). Due to the UPS inhibition observed in prion diseases, subsequent degradation of cytosolic misfolded PrP may be impaired, leading to accumulation in the cytosol (Ma and Lindquist, 2001; Yedidia *et al*., 2001). Alternatively, cytosolic build up of misfolded PrP species may result from inefficient translocation into the ER, resulting

in a proportion of the PrP molecules to not enter the ER at all (Ashok and Hegde, 2009).

Independent from ER, PrP^{Sc} may traffic to lysosomes and leak to the cytosol from lysosomal compartments. Several lines of evidence suggest trafficking of PrP^{Sc} to lysosomes: a) the N-terminal domain of PrP^{Sc} can be truncated by lysosomal proteases (Caughey *et al*., 1991); b) PrP^{Sc} accumulates rapidly in the cell following lysosomal protease inhibition (Marijanovic *et al.*, 2009); and c) the work presented in this thesis and several other studies have demonstrated the partial colocalisation of PrP^{Sc} with lysosomal markers (Caughey *et al*., 1991; McKinley *et al*., 1991b; Borchelt *et al*., 1992). Amyloid protofibrils have been shown to form pores in cell membranes leading to destabilisation (Lashuel *et al*., 2002). This provides a plausible mechanism for PrP^{Sc} release into the cytosol from lysosomes or autophagosomes. In support of this theory, PrP^{C} and PrP^{Sc} are both known to interact with lipids (Campana *et al*., 2005) and recombinant β-sheet rich PrP has been reported to disrupt membrane integrity (Sanghera and Pinheiro, 2002). It is therefore possible that PrP^{Sc} is transported through the lysosomal system and enters the cytosol via membrane destabilisation. Interestingly, lysosomal rupture has been identified as a possible source of spongiform vacuolar appearances in prion-infected neurons (Lowe *et al*., 1992).

The above trafficking pathways can be mapped using a panel of endomembrane regulating Rab proteins tagged with monomeric red fluorescent proteins (mRFP) (Deinhardt *et al*., 2006). Rab GTPases regulate many steps of membrane trafficking, including vesicle formation, vesicle movement along actin and tubulin networks, and membrane fusion (Martinez and Goud, 1998). Following transfection with wild type versions of these small GTPases, PrP-224AlaMYC cells could be prion infected and

colocalisation with PrP^{Sc} could be investigated by segmenting and counting punctate structures from confocal immunofluorescence images (Gniadek and Warren, 2007). In parallel, the effect of blocking the endocytic trafficking pathway at specific sites could be investigated by expressing dominant-negative versions of Rabs and RNAi knock down of key trafficking intermediates. This will result in the blockage of the endocytic trafficking pathway at specific sorting positions. In particular, the effect of loss of Rab 5 (early endosomes), Rab 4 and Rab 11 (recycling endosomes), Rab 7 (late endosomes), Rab 9 (late endosomes/trans-Golgi network), Rab 6a (trans-Golgi network/ER), Rab 6 (early endosomes/ trans-Golgi network) and clathrin heavy chain RNAi (CHC RNAi, clathrin dependent endocytosis) can be examined on PrP^{Sc} localisation and aggregate formation. After applying the trafficking manipulation on the cells, cytosolic accumulation of PrP^{Sc} could be monitored by colocalisation with specific cytosolic marker proteins (Hsc70 and the 20S proteosome (Kristiansen *et al*., 2005)) and proteosome activity assays (a surrogate assay of cytosolic PrP^{Sc}, (Dantuma *et al*., 2000; Berkers *et al*., 2005; Kisselev and Goldberg, 2005; Kristiansen *et al*., 2007)). Cytosolic PrP^{Sc} build up will indicate the role of the donor compartment immediately prior to the trafficking impairment in production of cytosolic PrP^{Sc}. This approach has already been used successfully to map intracellular trafficking pathways (Deinhardt *et al*., 2006a; Deinhardt *et al*., 2006b) and may enable us to identify the site(s) where PrP^{Sc} accesses the cytosol to inhibit the UPS and potentially mediate neurotoxicity.

6.2.2 A novel cell system to study the UPS activity

Chronically infected PK1 cells stably propagating prions show decreased proteasomal activity and are more sensitive to cell death after mild UPS inhibition than

non-infected cells (Kristiansen *et al*., 2005). This suggests that their UPS is impaired due to the presence of PrP^{Sc}. PrP-224AlaMYC cells present the unique opportunity to study the temporal relationship between the uptake of exogenous PrP^{Sc}, production of *de novo* PrP^{Sc} and inhibition of the UPS. The total and cytosolic PrP^{Sc} build up can be followed using anti-MYC antibodies. Infection of PrP-224AlaMYC cells with RML prions would allow levels of total and cytosolic PrP^{Sc} to be correlated with UPS activity in a detailed time-course. The proteasome activity in cell lysates could be assayed by using highly sensitive fluorogenic peptide substrates (Kristiansen *et al*., 2007). Furthermore, UPS activity in intact cells could be measured by adding cell permeable fluorescent β-subunit activity probes (Verdoes *et al*., 2006) or by assessing proteasome reporter substrate accumulation in cells stably transfected with Ub^{G76V}-GFP (Dantuma *et al.*, 2000; Kristiansen *et al*., 2007). The effect of mild proteasome inhibition could also be analysed as a mimetic of cell toxicity. The unique cell system presented in this thesis allows differentiation of individual cells that have internalised exogenous PrP^{Sc} but not synthesised *de novo* PrP^{Sc} (Figure 4-9). UPS activity can be assessed in these cells using fluorescent, cell-permeable activity-based probes such as Bodipy TMR-Ahx3L3VS (MV151), which specifically targets all active subunits of the proteasome and immunoproteasome in individual living cells, to determine if *de novo* PrP^{Sc} production is necessary to cause UPS inhibition (Verdoes *et al*., 2006). Prion infection of PrP-KD cells, which do not propagate prions (Section 3.3.1 and Figure 3-1 B), could also be used to determine whether *de novo* PrP^{Sc} production is necessary for UPS impairment. In this way the intracellular effects of prion exposure and *de novo* PrP^{Sc} synthesis could be dissociated.

6.2.3 A novel cell system to study prion cytotoxicity

Whilst *in vivo* studies of prion disease pathogenesis have repeatedly identified marked neuronal loss (Aguzzi *et al*., 2008), mouse neuroblastoma cells and their derivatives do not exhibit prion-induced cell death under normal *in vitro* conditions. The cells may be able to compensate by dividing before the PrP^{Sc} load reaches toxic levels or by metabolising misfolded PrP with greater efficiency. Creating a model of prion infection induced cell toxicity in post-mitotic neurons would therefore be useful. Differentiated mouse neuronal stem cells (NSC) are susceptible to prion infection and replicate many disease characteristics including prion-induced toxicity and ultimately cell death (Milhavet *et al*., 2006). However, NCS have limited use as models of early prion infection due to the difficulties in the distinction of *de novo* PrP^{Sc} from inocula-derived PrP which is known to persist in the cells for several weeks (Giri *et al*., 2006; Cronier *et al*., 2004). To overcome this limitation, NSC lines expressing MYC-tagged PrP construct (Figure 3-2) could be generated. Transduction of NSC derived from FVB $PrP^{-/-}$ mice with retroviral constructs encoding 224AlaMYC-tagged PrP would allow isolation of prion susceptible NSC lines expressing MYC-tagged PrP^{Sc}. To avoid problems with inocula clearance, previous NSC studies used semi-purified prions or a low dose of inocula (Milhavet *et al*., 2006; Cronier *et al*., 2004). Both approaches were associated with poor prion infection and propagation efficiency. The development of NSC lines expressing MYC-tagged PrP^{Sc} could avoid these limitations through the use of high dose inocula. NSC differentiation can be induced by growth factor withdrawal using established methods (Milhavet *et al*., 2006). This produces a mixed population of post-mitotic neuronal cells (neurons, astrocytes and glia) which can be manipulated towards different cell fates by trophic factor treatment, allowing cultures enriched in

neurons to be produced (Panchision *et al*., 1998). Studying prion-infected, differentiated NSC lines will allow comparison of the spatial and temporal features of prion infection already observed in the neuroblastoma cell model (Chapter 4 and Chapter 5) with those in differentiated neurons. It will also enable us to study prion trafficking in compartmentalised neurons using the methods outlined in this thesis.

Prion infected, differentiated NSC and immortalised human stem cells die earlier in culture than mock infected control cells (Milhavet *et al*., 2006). If PrP-224AlaMYC neural stem cell derivates recapitulate this characteristic, they could therefore provide a unique model to study prion induced cytotoxicity and cell death. PrP-224AlaMYC neural stem cells could be infected with prions and alterations in nuclear morphology, terminal deoxynucleotidyl transferase (TdT)-mediated dUTP nick end labelling (TUNEL), membrane permeability, lysosomal physiology and casapse activation could be analysed at serial time-points.

Manipulating proteasome activity in chronically infected PK1 cells is known to affect PrP^{Sc} levels (Kristiansen *et al*., 2005). Furthermore, a detailed *in vivo* study in Professor Tabrizi's lab has revealed that UPS impairment is a very early event in prion disease pathogenesis (unpublished data). These data therefore suggest that the UPS plays a crucial role in PrP^{Sc} metabolism. Differentiated mouse neuronal stem cells expressing PrP-224AlaMYC can provide a unique model to examine the temporal relationship between prion infection, dysfunction of the UPS and neurotoxicity. A detailed time-course study could be performed on PrP-224AlaMYC mouse neuronal stem cells to correlate PrP^{Sc} levels with UPS activity and cellular toxicity. A range of proteosome activators and inhibitors (Lee *et al.*, 2010; Verdoes *et al.*, 2006), are currently available and could be used to investigate the direct effects of UPS

modulation on PrP^{Sc} levels and cytotoxicity. For example, RML prion-infected, differentiated NSC can be treated with proteasome activators to examine if this treatment will extend the cell's lifespan and determine if this corresponds to increased PrP^{Sc} clearance.

The temporal relationship between UPS function and ER stress in prion disease could also be addressed using a NSC system. N2a neuroblastoma cells treated with PrP^{Sc} produce a fast and sustained increase in intracellular calcium levels (Hetz *et al*., 2003). Pre-treatment with thapsigargin that depletes ER calcium stores is known to reduce the increase in calcium observed with PrP^{Sc} (Hetz *et al*., 2003). This indicates that the ER is involved in PrP^{Sc} cytotoxicity, however, it remains unclear whether the role of the ER in prion disease pathogenesis is primary or secondary to the UPS dysfunction (Hetz *et al*., 2003; Hetz *et al*., 2007). UPS dysfunction that occurs in response to prion infection (Kristiansen *et al*., 2007), may result in the accumulation of misfolded proteins in the ER that were destined for degradation by ERAD, resulting in ER stress (Ciechanover and Brundin, 2003; Imai *et al*., 2001; Nishitoh *et al*., 2002). Recently, abortive translocation of nascent PrP in response to ER stress has been demonstrated (Rane *et al*., 2008). This results in the accumulation of cytosolic PrP which is known to be cytotoxic in both cell and *in vivo* systems (Ma *et al*., 2002; Rane *et al*., 2004; Rambold *et al*., 2008; Wang *et al*., 2009), representing another possible mechanism of prion-induced toxicity. Serial time-course studies in RML prion-infected, differentiated NSC would help to determine the relative contribution of ER stress and UPS dysfunction to neurotoxicity and thus assess to what extent UPS dysfunction can be considered a true pathogenic mechanism rather than an epiphenomenon of the disease process itself.

7 Appendices

Appendix I

Mammalian PrP protein schematic with putative FLAG and MYC tag insert sites

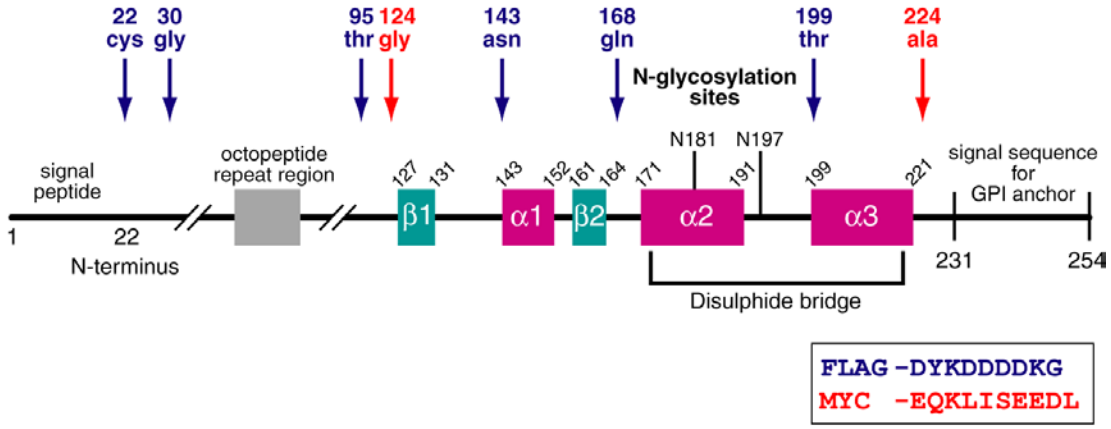

Appendix II

Mouse PrP amino acid sequence with highlighted FLAG and MYC tag insert sites

MANLGYWLLALFVTMWTDVGL**C**(DYKDDDDKG)KKRPKPG**G**(DYKDDDDKG)WNTGGSRYPGQGSPGGNRYPPQGGTWGQPHGGGWGQPHGGSWGQPHGGSWGQPHGGGWGQGGG**T**(DYKDDDDKG)HNQWNKPSKPKTNLKHVAGAAAAGAVVG**G**(EQKLISEEDL)LGGYMLGSAMSRPMIHFG**N**(DYKDDDDKG)DWEDRYYRENMYRYPNQVYYRPVD**Q**(DYKDDDDKG)YSNQNNFVHDCVNITIKQHTVTTTTKGENF**T**(DYKDDDDKG)ETDVKMMERVVEQMCVTQYQKESQ**A**(EQKLISEEDL)YYDGRRSSSTVLFSSPPVILLISFLIFLIVG

Blue = signal peptide

Red = GPI anchor signal sequence

Highlighted = positions for FLAG tag insert

Highlighted = positions for MYC tag insert

Appendix III

pLNCX2 retroviral vector map[1]

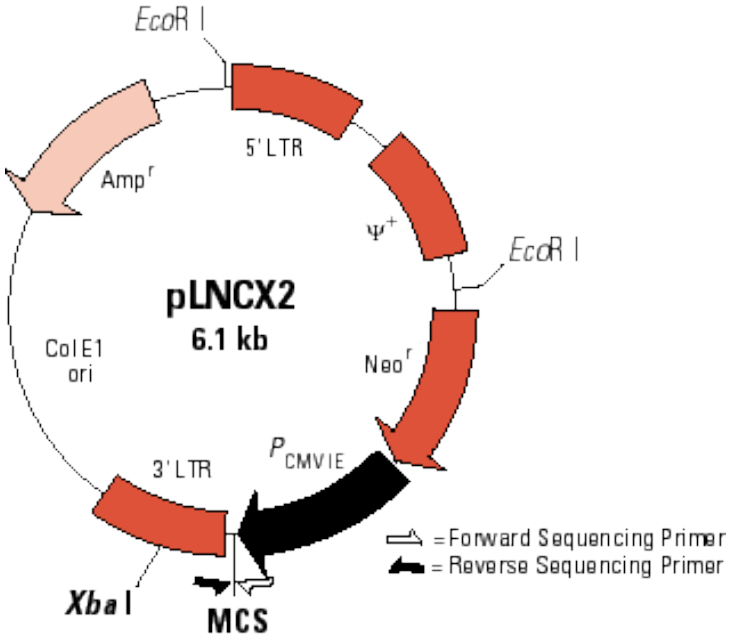

[1]From http://www.clontech.com/products/detail.asp?product_id=10523&tabno=2

Appendix IV

Primers for generation of FLAG and MYC-tagged PrP constructs

FLAG1 N-C

5’- GACTACAAAGACGATGACGATAAAGGCAAAAAGCGGCCAAAGCCTGG-3’

FLAG1 C-N

3’-CTGACTACAGCCGGAGACGCTGATGTTTCTGCTACTGCTATTTCCG-5’
5’-GCCTTTATCGTCATCGTCTTTGTAGTCGCAGAGGCCGACATCAGTC-3’

FLAG 2 N-C

5’- GACTACAAAGACGATGACGATAAAGGCTGGAACACCGGTGGAAGCC-3’

FLAG 2 C-N

3’-GCCGGTTTCGGACCTCCCCTGATGTTTCTGCTACTGCTATTTCCG-5’
5’-GCCTTTATCGTCATCGTCTTTGTAGTCCCCTCCAGGCTTTGGCCG-3’

FLAG3 N-C

5’-GACTACAAAGACGATGACGATAAAGGCCATAATCAGTGGAACAAGCCC-3’

FLAG 3 C-N

3’-CCGGTTCCTCCCCCATGGCTGATGTTTCTGCTACTGCTATTTCCG-5’
5’-GCCTTTATCGTCATCGTCTTTGTAGTCGGTACCCCCTCCTTGGCC-3’

FLAG 4 N-C

5’- GACTACAAAGACGATGACGATAAAGGCGACTGGGAGGACCGCTAC-3’

FLAG 4 C-N

3’-GGGTACTAGGTAAAACCGTTGCTGATGTTTCTGCTACTGCTATTTCCG-5’
5’-GCCTTTATCGTCATCGTCTTTGTAGTCGTTGCCAAAATGGATCATGGG-3’

FLAG 5 N-C

5’- GACTACAAAGACGATGACGATAAAGGCTACAGCAACCAGAACAACTTC-3’

FLAG 5 C-N

3’-GATGTCCGGTCACCTAGTCCTGATGTTTCTGCTACTGCTATTTCCG-5’
5’-GCCTTTATCGTCATCGTCTTTGTAGTCCTGATCCACTGGCCTGTAG-3’

FLAG 6 N-C

5’-GACTACAAAGACGATGACGATAAAGGCGAGACCGATGTGAAGATGATG-3’

FLAG 6 C-N

3’-GTTCCCCCTCTTGAAGTGGCTGATGTTTCTGCTACTGCTATTTCCG-5’
5’-GCCTTTATCGTCATCGTCTTTGTAGTCGGTGAAGTTCTCCCCCTTG-3’

MYC1 N-C

5’-GAACAGAAACTGATCTCTGAAGAAGACCTGCTTGGTGGCTACATGCTG-3’

MYC1 C-N

3’- CACGACACCACCCGCCACTTGTCTTTGACTAGAGACCTCTTCTGGAC-5’
5’- CAGGTCTTCTTCAGAGATCAGTTTCTGTTCGCCCCCCACTACTGCCC-3’

MYC2 N-C

5’-GAACAGAAACTGATCTCTGAAGAAGACCTGTATTACGACGGGAGAAGA-3’

MYC2 C-N

3’-TGTTTCTTAGAGTCCGACTTGTCTTTGACTAGAGACCTCTTCTGGAC-5’
5’-CAGGTCTTCTTCAGAGATCAGTTTCTGTTCGGCCTGGGACTCCTTCT-3’

FLAG sequence

5’-GACTACAAAGACGATGACGATAAAGGC-3’ 

3’-CTGATGTTTCTGCTACTGCTATTTCCG-5’ 

MYC sequence

5’-GAACAGAAACTGATCTCTGAAGAAGACCTG-3’ 

3’-CTTGTCTTTGACTAGAGACCTCTTCTGGAC-5’ 

mPrP Sequence 

5' primer (Clontech):

5'-AGCTCGTTTAGTGAACCGTCAGATC-3'

My version

5’-CGGAATTCCGTTTAGTGAACCGTCAGATC-3’

3' primer (Clontech):

5'-ACCTACAGGTGGGGTCTTTCATTCCC-3'

My version

5’-CCGCTCGAGTACAGGTGGGGTCTTTCATTC-3’

8 Reference list

Abazeed, M., Blanchette, E., Fuller, R. S. (2005). Cell-free transport from the trans-Golgi network to late endosome requires factors involved in formation and consumption of clathrin-coated vesicles. *J.Biol.Chem.* **280**, 4442-4450.

Abid, K., Soto, C. (2006). The intriguing prion disorders. *Cell Mol.Life Sci.* **63**, 2342-2351.

Aguzzi, A., Baumann, F., Bremer, J. (2008). The Prion's Elusive Reason for Being. *Annu Rev Neurosci* **31**, 439-477.

Aguzzi, A., Polymenidou, M. (2004). Mammalian prion biology. One century of evolving concepts. *Cell* **116**, 313-327.

Almer, G., Hainfellner, H. A., Jellinger, K., Kleinert, R., Bayer, G., Windl, O., Kretzschmar, H., Hill AF, Sidle, K. C., Collinge J, Budka, H. (1999). Fatal familial insomnia: a new Austrian family. *Brain* **122**, 5-16.

Alper, T., Cramp, W. A., Haig, D. A., Clarke, M. C. (1967). Does the agent of scrapie replicate without nucleic acid?. *Nature* **214**, 764-766.

Alper, T., Haig, D. A., Clarke, M. C. (1966). The exceptionally small size of the scrapie agent. *Biochem.Biophys.Res.Commun.* **22**, 278-284.

Alpers, M. P. (1987). Epidemiology and clinical aspects of kuru. *In* "Prions: Novel infectious Pathogens Causing Scrapie and Creutzfeldt-Jakob Disease" (S. B. Prusiner and M. P. McKinley, Eds.). *Academic Press*, San Diego. 451-465.

Arnold, J. E., Tipler, C., Laszlo, L., Hope, J., Landon, M., Mayer, R. J. (1995). The abnormal isoform of the prion protein accumulates in late-endosome-like organelles in scrapie-infected mouse brain. *J.Pathol.* **176**, 403-411.

Ashok, A., Hegde, R. S. (2009). Selective processing and metabolism of disease-causing mutant prion proteins. *PLoS Pathog.* **5**, e1000479.

Atarashi, R., Sim, V. L., Nishida, N., Caughey, B., Katamine, S. (2006). Prion strain-dependent differences in conversion of mutant prion proteins in cell culture. *J.Virol.* **80**, 7854-7862.

Aucouturier, P., Geissmann, F., Damotte, D., Saborio, G. P., Meeker, H. C., Kascsak, R., Carp, R. I., Wisniewski, T. (2001). Infected splenic dendritic cells are sufficient for prion transmission to the CNS in mouse scrapie. *J. Clin. Invest*. **108**, 703-708.

Barmada, S. J., Harris, D. A. (2005). Visualization of prion infection in transgenic mice expressing green fluorescent protein-tagged prion protein. *J Neurosci.* **25**, 5824-5832.

Baron, G. S., Wehrly, K., Dorward, D. W., Chesebro, B., Caughey, B. (2002). Conversion of raft associated prion protein to the protease-resistant state requires insertion of PrP-res (PrP(Sc)) into contiguous membranes. *EMBO Journal* **21**, 1031-1040.

Baron, T., Bencsik, A., Biacabe, A. G., Morignat, E., Bessen, R. A. (2007). Phenotypic similarity of transmissible mink encephalopathy in cattle and L-type bovine spongiform encephalopathy in a mouse model. *Emerg.Infect.Dis.* **13**, 1887-1894.

Basler, K., Oesch, B., Scott, M., Westaway, D., Walchli, M., Groth, D. F., McKinley, M. P., Prusiner, S. B., Weissmann, C. (1986). Scrapie and cellular PrP isoforms are encoded by the same chromosomal gene. *Cell* **46**, 417-428.

Baumann, F., Tolnay, M., Brabeck, C., Pahnke, J., Kloz, U., Niemann, H. H., Heikenwalder, M., Rulicke, T., Burkle, A., Aguzzi, A. (2007). Lethal recessive myelin toxicity of prion protein lacking its central domain. *EMBO J* **26**, 538-547.

Bayer, N., Schober, D., Prchila, E., Murphy, R. F., Blaas, D., Fuchs, R. (1998). Effect of bafilomycin A1 and nocodazole on endocytic transport in HeLa cells: Implications for viral uncoating and infection. *J.Virol*, **72**, 9645–9655.

Beghi, E., Gandolfo, C., Ferrarese, C., Rizzuto, N., Poli, G., Tonini, M. C., Vita, G., Leone, M., Logroscino, G., Granieri, E., Salemi, G., Savettieri, G., Frattola, L., Ru, G., Mancardi, G. L., Messina, C. (2004). Bovine spongiform encephalopathy and Creutzfeldt-Jakob disease: facts and uncertainties underlying the causal link between animal and human diseases. *Neurol Sci* **25**, 122-129.

Behrens, A., Aguzzi, A. (2002). Small is not beautiful: antagonizing functions for the prion protein PrP(C) and its homologue Dpl. *Trends in Neurosciences* **25**, 150-154.

Belay, E. D. (1999). Transmissible spongiform encephalopathies in humans. *Annual Review of Microbiology* **53**, 283-314.

Bell, J. E., Gentleman, S. M., Ironside, J. W., McCardle, L., Lantos, P. L., Doey, L., Lowe, J., Fergusson, J., Luthert, P., McQuaid, S., Allen, I. V. (1997). Prion protein

immunocytochemistry - UK five centre consensus report. *Neuropathol & Appl Neurobiol* **23**, 26-35.

Bell, J. E., Ironside, J. W. (1993). Neuropathology of spongiform encephalopathies in humans. *Br.Med.Bull.* **49**, 738-777.

Bendheim, P. E., Barry, R. A., DeArmond, S. J., Stites, D. P., Prusiner, S. B. (1984). Antibodies to a scrapie prion protein. *Nature* **310**, 418-421.

Beranger, F., Mange, A., Goud, B., Lehmann, S. (2002). Stimulation of PrP^{C} retrograde transport towards the endoplasmic reticulum increases accumulation of PrP^{Sc} in prion-infected cells. *J.Biol.Chem.* **277**, 38972-38977.

Bergstrom, A. L., Jensen, T. K., Heegaard, P. M., Cordes, H., Hansen, V. B., Laursen, H., Lind, P. (2006). Short-term Study of the uptake of PrP(Sc) by the Peyer's Patches in Hamsters after Oral Exposure to Scrapie. *J Comp Pathol.* **134**, 126-133.

Berkers, C. R., Verdoes, M., Lichtman, E., Fiebiger, E., Kessler, B. M., Anderson, K. C., Ploegh, H. L., Ovaa, H., Galardy, P. J. (2005). activity probe for *in vivo* profiling of the specificity of proteasome inhibitor bortezomib: *Nat. Methods*. **2**, 357-362.

Bessen, R. A., Marsh, R. F. (1992). Biochemical and physical properties of the prion protein from two strains of the transmissible mink encephalopathy agent. *J.Virol.* **66**, 2096-2101.

Bessen, R. A., Marsh, R. F. (1994). Distinct PrP properties suggest the molecular basis of strain variation in transmissible mink encephalopathy. *J Virol* **68**, 7859-7868.

Billette de Villemeur, T., Fournier, J.G., Robain, O., Escaig-Haye, F., Brown, P. (1995). Electronmicroscopic detection of prion-protein-positive fibres in brain from iatrogenic Creutzfeldt-Jakob disease. *Lancet* **345**, 861-862.

Blighta,G. D., Morgana, E. H. (1987) Transferrin and ferritin endocytosis and recycling in guinea-pig reticulocytes. *Biochimica et Biophysica Acta (BBA) - Molecular Cell Research*. **929**, 18-24.

Bolton, D. C., Bendheim, P. E. (1988). A modified host protein model of scrapie. *Ciba.Found.Symp.* **135**, 164-181.

Bolton, D. C., McKinley, M. P., Prusiner, S. B. (1982). Identification of a protein that purifies with the scrapie prion. *Science* **218**, 1309-1311.

Borchelt, D. R., Koliatsos, V. E., Guarnieri, M., Pardo, C. A., Sisodia, S. S., Price, D. L. (1994). Rapid anterograde axonal transport of the cellular prion glycoprotein in the peripheral and central nervous systems. *J.Biol.Chem.* **269**, 14711-14714.

Borchelt, D. R., Rogers, M., Stahl, N., Telling, G., Prusiner, S. B. (1993). Release of the cellular prion protein from cultured cells after loss of its glycoinositol phospholipid anchor. *Glycobiology.* **3**, 319-329.

Borchelt, D. R., Taraboulos, A., Prusiner, S. B. (1992). Evidence for synthesis of scrapie prion proteins in the endocytic pathway. *J Biol.Chem.* **267**, 16188-16199.

Bosque, P. J., Prusiner, S. B. (2000). Cultured cell sublines highly susceptible to prion infection. *Journal of Virology* **74**, 4377-4386.

Botto, L., Masserini, M., Cassetti, A., Palestini, P. (2004). Immunoseparation of Prion protein-enriched domains from other detergent-resistant membrane fractions, isolated from neuronal cells. *FEBS Lett.* **557**, 143-147.

Brandner S, Raeber, A., Sailer, A., Blattler, T., Fischer, M., Weissmann, C., Aguzzi, A. (1996). Normal host prion protein (PrP^{C}) is required for scrapie spread within the central nervous system. *Proc Natl Acad Sci USA* **93**, 13148-13151.

Brown, D. R. (2001). Copper and prion disease. *Brain Research Bulletin* **55**, 165-173.

Brown, D. R., Herms, J., Kretzschmar, H. A. (1994). Mouse cortical cells lacking cellular PrP survive in culture with a neurotoxic PrP fragment. *Neuroreport* **5**, 2057-2060.

Brown, D. R., Schmidt, B., Kretzschmar, H. A. (1996). Role of microglia and host prion protein in neurotoxicity of a prion protein fragment. *Nature* **380**, 345-347.

Brown, P., Bradley, R. (1998). 1755 and all that: a historical primer of transmissible spongiform encephalopathy. *BMJ.* **317**, 1688-1692.

Brown, P., Cathala, F., Raubertas, R. F., Gajdusek, D. C., Castaigne, P. (1987). The epidemiology of Creutzfeldt-Jakob disease: conclusion of a 15-year investigation in France and review of the world literature. *Neurology* **37**, 895-904.

Brown, P., Liberski, P. P., Wolff, A., Gajdusek, D. C. (1990). Resistance of scrapie infectivity to steam autoclaving after formaldehyde fixation and limited survival after ashing at 360 degrees C: practical and theoretical implications. *J Infect.Dis.* **161**, 467-472.

Brown, P., Preece M, Brandel, J. P., Sato, T., McShane, L., Zerr, I., Fletcher, A., Will, R. G., Pocchiari, M., Cashman, N. R., D'Aignaux, J. H., Cervenáková, L., Fradkin, J., Schonberger, L. B., Collins, S. J. (2000). Iatrogenic Creutzfeldt-Jakob disease at the millennium. *Neurology* **55**, 1075-1081.

Brown, P., Preece, M. A., Will, R. G. (1992). "Friendly fire" in medicine: hormones, homografts, and Creutzfeldt-Jakob disease. *Lancet* **340**, 24-27.

Brownell, B., Oppenheimer, D. (1965). An ataxic form of presenile polioencephalopathy (Creutzfeldt-Jakob disease): J Neurol Neurosurg Psychiatry **28**, 350-361.

Browning, S. R., Mason, G. L., Seward, T., Green, M., Eliason, G. A., Mathiason, C., Miller, M. W., Williams, E. S., Hoover, E., Telling, G. C. (2004). Transmission of Prions from Mule Deer and Elk with Chronic Wasting Disease to Transgenic Mice Expressing Cervid PrP. *J Virol* **78**, 13345-13350.

Bruce, M., Chree, A., McConnell, I., Foster, J., Pearson, G., Fraser, H. (1994). Transmission of bovine spongiform encephalopathy and scrapie to mice: Strain variation and the species barrier. *Philosophical Transactions of the Royal Society of London.B:Biological Sciences* **343**, 405-411.

Bruce, M. E., Will, R. G., Ironside, J. W., McConnell, I., Drummond, D., Suttie, A., McCardle, L., Chree, A., Hope, J., Birkett, C., Cousens, S., Fraser, H., Bostock, C. J. (1997). Transmissions to mice indicate that 'new variant' CJD is caused by the BSE agent. *Nature* **389**, 498-501.

Budka, H. (2003). Neuropathology of prion diseases. *Br.Med Bull.* **66**, 121-130.

Budka, H., Aguzzi, A., Brown, P., Brucher, J. M., Bugiani, O., Gullotta, F., Haltia, M., Hauw, J. J., Ironside, J. W., Jellinger, K., Kretzschmar, H. A., Lantos, P. L., Masullo, C., Schlote, W., Tateishi, J., Weller, R. O. (1995). Neuropathological diagnostic criteria for Creutzfeldt-Jakob disease (CJD) and other human spongiform encephalopathies (Prion diseases). *Brain Pathol.* **5**, 459-466.

Budka, H., Hainfellner, J. A., Almer, G., Brucke, T., Windl, O., Kretzschmar, H. A., Hill, A. F, Collinge, J. (1997). A new Austrian family with Fatal Familial Insomnia: brain pathology without detectable PrP^{res}. Brain Pathology **7**, 1267.

Bueler, H., Aguzzi, A., Sailer, A., Greiner, R. A., Autenried, P., Aguet, M., and Weissmann, C. (1993). Mice devoid of PrP are resistant to scrapie. *Cell* **73**, 1339-1347.

Bueler, H., Fischer, M., Lang, Y., Bluethmann, H., Lipp, H.-P., DeArmond, S. J., Prusiner, S. B., Aguet, M., Weissmann, C. (1992). Normal development and behaviour of mice lacking the neuronal cell-surface PrP protein. *Nature* **356**, 577-582.

Butler, D. A., Scott, M. R., Bockman, J. M., Borchelt, D. R.,Taraboulos, A., Hsiao, K. K., Kingsbury, D. T., Prusiner, S. B. (1988). Scrapie-infected murine neuroblastoma cells produce protease- resistant prion proteins. *J Virol*. **62**, 1558-1564.

Campana, V., Sarnataro, D., Zurzolo, C. (2005). The highways and byways of prion protein trafficking. *Trends Cell Biol* **15**, 102-111.

Cao, H., Weller, S., Orth, J. D., Chen, J., Huang, B., Chen, J. L., Stamnes, M., McNiven, M. A. (2005). Actin and Arf1-dependent recruitment of a cortactin-dynamin complex to the Golgi regulates post-Golgi transport: *Nat. Cell Biol*. **7**, 483-492.

Caramelli, M., Ru, G., Acutis, P., Forloni, G. (2006). Prion diseases : current understanding of epidemiology and pathogenesis, and therapeutic advances. *CNS Drugs* **20**, 15-28.

Caspi, S., Halimi, M., Yanai, A., Sasson, S. B., Taraboulos, A., Gabizon, R. (1998). The anti-prion activity of Congo red. Putative mechanism. *J Biol Chem.* **273**, 3484-3489.

Caughey, B. (2001). Interactions between prion protein isoforms: the kiss of death? *Trends in Biochemical Sciences* **26**, 235-242.

Caughey, B. (2003). Prion protein conversions: insight into mechanisms, TSE transmission barriers and strains. *Br.Med.Bull.* **66**, 109-120.

Caughey, B., Baron, G. S. (2006). Prions and their partners in crime. *Nature* **443**, 803-810.

Caughey, B., Chesebro, B. (1997). Prion protein and the transmissible spongiform encephalopathies. *Trends Cell Biol.* **7**, 56-62.

Caughey, B., Kocisko, D. A., Raymond, G. J., Lansbury-PT, J. (1995). Aggregates of scrapie-associated prion protein induce the cell-free conversion of protease-sensitive prion protein to the protease-resistant state. *Current Biology* **2**, 807-817.

Caughey, B., Neary, K., Buller, R., Ernst, D., Perry, L. L., Chesebro, B., Race, R. E. (1990). Normal and scrapie-associated forms of prion protein differ in their sensitivities to phospholipase and proteases in intact neuroblastoma cells. *J Virol.* **64**, 1093-1101.

Caughey, B., Race, R. E. (1992). Potent inhibition of scrapie-associated PrP accumulation by Congo red. *J Neurochem.* **59**, 768-771.

Caughey, B., Race, R. E., Chesebro, B. (1988). Detection of prion protein mRNA in normal and scrapie-infected tissues and cell lines. *J Gen.Virol.* **69**, 711-716.

Caughey, B., Raymond, G. J. (1991). The scrapie-associated form of PrP is made from a cell surface precursor that is both protease- and phospholipase-sensitive. *J Biol.Chem.* **266 No 27**, 18217-18223.

Caughey, B., Raymond, G. J., Ernst, D., Race, R. E. (1991). N-terminal truncation of the scrapie-associated form of PrP by lysosomal protease(s): implications regarding the site of conversion of PrP to the protease-resistant state. *J Virol.* **65 No 12**, 6597-6603.

Caughey, W. S., Raymond, L. D., Horiuchi, M., Caughey, B. (1998). Inhibition of protease-resistant prion protein formation by porphyrins and phthalocyanines. *Proc Natl Acad Sci USA* **95**, 12117-12122.

Cenedella, R. J. (2009). Cholesterol Synthesis Inhibitor U18666A and the Role of Sterol Metabolism and Trafficking in Numerous Pathophysiological Processes. *Lipids*. **44**, 477-487.

Chakrabarti, O., Hegde, R. S. (2009). Functional depletion of mahogunin by cytosolically exposed prion protein contributes to neurodegeneration. *Cell* **137**, 1136-1147.

Chandler, R. L. (1961). Encephalopathy in mice produced by inoculation with scrapie brain material. *Lancet* **1**, 1378-1379.

Chesebro, B., Trifilo, M., Race, R., Meade-White, K., Teng, C., LaCasse, R., Raymond, L., Favara, C., Baron, G., Priola, S., Caughey, B., Masliah, E., Oldstone, M. (2005). Anchorless prion protein results in infectious amyloid disease without clinical scrapie. *Science* **308**, 1435-1439.

Chiarini, L. B., Freitas, A. R., Zanata, S. M., Brentani, R. R., Martins, V. R., Linden, R. (2002). Cellular prion protein transduces neuroprotective signals. *EMBO Journal* **21**, 3317-3326.

Cho, H. J. (1976). Is the scrapie agent a virus? *Nature* **262**, 411-412.

Ciechanover, A., Brundin, P. (2003). The ubiquitin proteasome system in neurodegenerative diseases. Sometimes the chicken, sometimes the egg. *Neuron* **40**, 427-446.

Cohen, F. E., Pan, K. M., Huang, Z., Baldwin, M., Fletterick, R. J., and Prusiner, S. B. (1994). Structural clues to prion replication. *Science* **264**, 530-531.

Coimbra, E. R., Rezek, K., Escorsi-Rosset, S., Landemberger, M. C., Castro, R. M., Valadao, M. N., Guarnieri, R., Velasco, T. R., Terra-Bustamante, V. C., Bianchin, M. M., Wichert-Ana, L., Alexandre, V., Jr., Brentani, R. R., Martins, V. R., Sakamoto, A. C., Walz, R. (2006). Cognitive performance of patients with mesial temporal lobe epilepsy is not associated with human prion protein gene variant allele at codons 129 and 171. *Epilepsy Behav.* **8**, 635-642.

Collinge, J. (1996). Prion Diseases. *In* "Oxford Textbook of Medicine" (D. J. Weatherall, J. G. G. Ledingham, and D. A. Warrell, Eds.), Vol. 3, pp. 3977-3981. Oxford University Press, Oxford. 3977-3981.

Collinge, J. (1997). Human prion diseases and bovine spongiform encephalopathy (BSE). *Hum Mol Genetics* **6**, 1699-1705.

Collinge J, Palmer, M. S. (1997). "Prion Diseases." Oxford University Press, Oxford.

Collinge, J., Prusiner, S. B. (1992). Terminology of Prion Disease. *In* "Prion Diseases of Humans and Animals" (S. B. Prusiner, Collinge J, J. Powell, and B. Anderton, Eds.), pp. 5-12. Ellis Horwood, London. 5-12.

Collinge, J., Whittington, M. A., Sidle, K. C. L., Smith, C. J., Palmer, M. S., Clarke A, and Jefferys, J. G. R. (1994). Prion protein is necessary for normal synaptic function. *Nature* **370**, 295-297.

Collinge, J., Palmer, M. S., Dryden, A. J. (1991a). Genetic predisposition to iatrogenic Creutzfeldt-Jakob disease. *Lancet* **337**, 1441-1442.

Collinge, J. (1999). Variant Creutzfeldt-Jakob disease. *Lancet* **354**, 317-323.

Collinge, J. (2001). Prion diseases of humans and animals: their causes and molecular basis. *Annual Review of Neuroscience* **24**, 519-550.

Collinge, J., Brown, J., Hardy, J., Mullan, M., Rossor, M. N., Baker, H., Crow, T. J., Lofthouse, R., Poulter, M., Ridley, R., Owen, F., Bennett, C., Dunn, G., Harding, A. E., Quinn, N., Doshi, B., Roberts, G. W., Honavar, M., Janota, I., Lantos, P. L. (1992). Inherited prion disease with 144 base pair gene insertion: II: Clinical and pathological features. *Brain* **115**, 687-710.

Collinge, J., Palmer, M. S., Dryden, A. J. (1991b). Genetic predisposition to iatrogenic Creutzfeldt-Jakob disease. *Lancet* **337**, 1441-1442.

Collinge, J., Palmer, M. S., Sidle, K. C. L., Hill, A. F., Gowland, I., Meads, J., Asante, E. A., Bradley, R., Doey, L. J., Lantos, P. L. (1995). Unaltered susceptibility to BSE in transgenic mice expressing human prion protein. *Nature* **378**, 779-783.

Collinge, J., Sidle, K. C., Meads, J., Ironside, J., Hill, A. F. (1996). Molecular analysis of prion strain variation and the aetiology of 'new variant' CJD. *Nature* **383**, 685-690.

Collinge, J., Whitfield, J., McKintosh, E., Beck, J., Mead, S., Thomas, D. J., Alpers, M. P. (2006). Kuru in the 21st century--an acquired human prion disease with very long incubation periods. *Lancet* **367**, 2068-2074.

Collins, S. J., Sanchez-Juan, P., Masters, C. L., Klug, G. M., van Duijn, C., Poleggi, A., Pocchiari, M., Almonti, S., Cuadrado-Corrales, N., Pedro-Cuesta, J., Budka, H., Gelpi, E., Glatzel, M., Tolnay, M., Hewer, E., Zerr, I., Heinemann, U., Kretszchmar, H. A., Jansen, G. H., Olsen, E., Mitrova, E., Alperovitch, A., Brandel, J. P., Mackenzie, J., Murray, K., Will, R. G. (2006). Determinants of diagnostic investigation sensitivities across the clinical spectrum of sporadic Creutzfeldt-Jakob disease. *Brain* **129**, 2278-2287.

Come, J. H., Lansbury, P. T., J. (1994). Predisposition of prion protein homozygotes to Creutzfeldt- Jakob disease can be explained by a nucleation-dependent polymerization mechanism. *Journal of the American Chemical Society* **116**, 4109-4110.

Cousens, S. N., Vynnycky, E., Zeidler, M., Will, R. G., Smith, P. G. (1997). Predicting the CJD epidemic in humans. *Nature* 16, 197-198.

Cronier, S., Laude, H., Peyrin, J. M. (2004). Prions can infect primary cultured neurons and astrocytes and promote neuronal cell death. *Proceedings of the National Academy of Sciences of the United States of America* **101**, 12271-12276.

Cuillé, J., Chelle, P. L. (1936). La maladie dite tremblante du mouton est-elle inocuable? *Compte rendu de l'Academie des Sciences* **203**, 1552-1554.

Cuillé, J., Chelle, P. L. (1939). Experimental transmission of trembling to the goat. *CR Seances Acad Sci* **208**, 1058-1160.

Dahlmann, B. (2007). Role of proteasomes in disease. *BMC Biochem* **22**, 1471-2091.

Damke, H., Baba, T., Warnock, D. E., Schmid, S. L. (1994). Induction of mutant dynamin specifically blocks endocytic coated vesicle formation. *J. Cell Biol* **127**, 915-934.

Dantuma, N. P., Lindsten, K., Glas, R., Jellne, M., Masucci, M. G. (2000). Short-lived green fluorescent proteins for quantifying ubiquitin/proteasome-dependent proteolysis in living cells. *Nat. Biotechnol* **18**, 538-543.

Daude, N., Marella, M., Chabry, J. (2003). Specific inhibition of pathological prion protein accumulation by small interfering RNAs. *J Cell Sci* **116**, 2775-2779.

Deinhardt, K., Salinas, S., Verastegui, C., Watson, R., Worth, D., Hanrahan, S., Bucci, C, Schiavo, G. (2006a). Rab5 and Rab7 control endocytic sorting along the axonal retrograde transport pathway. *Neuron* **52**, 293-305.

Deinhardt, K., Berninghausen, O., Willison, H. J., Hopkins, C. R., Schiavo, G. (2006b). Tetanus toxin is internalized by a sequential clathrin-dependent mechanism initiated within lipid microdomains and independent of epsin1. *J Cell Biol* **174**, 459–471.

Deleault NR, Harris BT, Rees JR, Supattapone, S. (2007). Formation of native prions from minimal components in vitro. *Proc Natl Acad Sci U S A* **104**, 9741-9746.

Deli, M. A., Sakaguchi, S., Nakaoke, R., Abrahám, C. S., Takahata, H., Kopacek, J., Shigematsu, K., Katamine, S., Niwa, M. (2000). PrP fragment 106-126 is toxic to cerebral endothelial cells expressing PrP^{C}. *Neuroreport* **11**, 3931-3936.

Diedrich, J. F., Bendheim, P. E., Kim, Y. S., Carp, R. I., Haase, A. T. (1991). Scrapie-associated prion protein accumulates in astrocytes during scrapie infection. *Proc.Natl.Acad.Sci.U.S.A.* **88**, 375-379.

Doh-ura, K., Iwaki, T., Caughey, B. (2000). Lysosomotropic agents and cysteine protease inhibitors inhibit scrapie-associated prion protein accumulation. *J Virol* **74**, 4894-4897.

Doms, R. W., Russ, G., Yewdell, J.W. (1989). Brefeldin A redistributes resident and itinerant Golgi proteins to the endoplasmic reticulum. *J. Cell Biol* **109**, 61-72.

Dron, M., Dandoy-Dron, F., Salamat, M. K., and Laude, H. (2009). Proteasome inhibitors promote the sequestration of PrPSc into aggresomes within the cytosol of prion-infected CAD neuronal cells. *J Gen Virol*. **90**, 2050-2060.

Enari, M., Flechsig, E., Weissmann, C. (2001). Scrapie prion protein accumulation by scrapie-infected neuroblastoma cells abrogated by exposure to a prion protein antibody. *Proceedings of the National Academy of Sciences of the United States of America* **98**, 9295-9299.

Endo, T., Groth, D., Prusiner, S. B., Kobata, A. (1989). Diversity of oligosaccharide structures linked to asparagines of the scrapie prion protein. *Biochemistry* **28**, 8380-8388.

Farquhar, C. F., Dickinson, A. G. (1986). Prolongation of scrapie incubation period by an injection of dextran sulphate 500 within the month before or after infection. *J Gen.Virol.* **67**, 463-473.

Fevrier, B., Vilette, D., Archer, F., Loew, D., Faigle, W., Vidal, M., Laude, H., Raposo, G. (2004). Cells release prions in association with exosomes. *Proc.Natl.Acad Sci USA* **101**, 9683-9688.

Fischer, M., Rulicke, T., Raeber, A., Sailer, A., Moser, M., Oesch, B., Brandner S, Aguzzi, A., Weissmann, C. (1996). Prion protein (PrP) with amino-proximal deletions restoring susceptibility of PrP knockout mice to scrapie. *EMBO Journal* **15**, 1255-1264.

Flechsig, E., Hegyi, I., Enari, M., Schwarz, P., Collinge, J., Weissmann, C. (2001). Transmission of scrapie by steel-surface-bound prions. *Molecular Medicine* **7**, 679-684.

Flechsig, E., Shmerling, D., Hegyi, I., Raeber, A. J., Fischer, M., Cozzio, A., von Mering, C., Aguzzi, A., Weissmann, C. (2000). Prion protein devoid of the octapeptide repeat region restores susceptibility to scrapie in PrP knockout mice. *Neuron* **27**, 399-408.

Forloni, G., Angeretti, N., Chiesa, R., Monzani, E., Salmona, M., Bugiani, O., Tagliavini, F. (1993). Neurotoxicity of a prion protein fragment. *Nature* **362**, 543-546.

Fournier, J.-G., Escaig-Haye, F., Grigoriev, V. (2000). Ultrastructural localization of prion proteins: Physiological and pathological implications. *Microsc Res Tech* **50**, 76-88.

Gabriel, J. M., Oesch, B., Kretzschmar, H., Scott, M., Prusiner, S. B. (1992). Molecular cloning of a candidate chicken prion protein. *Science.* **89**, 9097-9101.

Gajdusek, D. C. (1977). Unconventional viruses and the origin and disappearance of kuru. *Science* **197**, 943-960.

Gajdusek, D. C., Gibbs, C. J. J., Alpers MP (1966). Experimental transmission of a kuru-like syndrome to chimpanzees. *Nature* **209**, 794-796.

Galvan, C., Camoletto, P. G., Dotti, C. G., Aguzzi, A., Dolores, L. M. (2005). Proper axonal distribution of PrP(C) depends on cholesterol-sphingomyelin-enriched membrane domains and is developmentally regulated in hippocampal neurons. *Mol Cell Neurosci.*

Gambetti, P., Kong, Q., Zou, W., Parchi, P., Chen, S. G. (2003). Sporadic and familial CJD: classification and characterisation. *Br.Med Bull.* **66**, 213-239.

Gambetti, P., Parchi, P., Petersen, R. B., Chen, S. G., Lugaresi, E. (1995). Fatal familial insomnia and familial Creutzfeldt-Jakob disease: Clinical, pathological and molecular features. *Brain Pathol.* **5**, 43-51.

Gasset, M., Baldwin, M. A., Fletterick, R. J., Prusiner, S. B. (1993). Perturbation of the secondary structure of the scrapie prion protein under conditions that alter infectivity. *Proc.Natl.Acad.Sci.U.S A.* **90**, 1-5.

Gauczynski, S., Peyrin, J. M., Haïk, S., Leucht, C., Hundt, C., Rieger, R., Krasemann, S., Deslys, J. P., Dormont, D., Lasmézas, C. I., Weiss, S. (2001). The 37-kDa/67-kDa laminin receptor acts as the cell-surface receptor for the cellular prion protein. *EMBO Journal* **20**, 5863-5875.

Geissen, M., Mella, H., Saalmuller, A., Eiden, M., Proft, J., Pfaff, E., Schatzl, H. M., Groschup, M. H. (2009). Inhibition of prion amplification by expression of dominant inhibitory mutants - a systematic insertion mutagenesis study. *Infect Disord Drug Targets* **9**, 40-47.

Ghani, A. C., Donnelly, C. A., Ferguson, N. M., Anderson, R. M. (2002). The transmission dynamics of BSE and vCJD. *C.R.Acad.Sci.III* **325**, 37-47.

Ghani, A. C., Ferguson, N. M., Donnelly, C. A., Hagenaars, T. J., Anderson, R. M. (1999). Epidemiological determinants of the pattern and magnitude of the vCJD epidemic in Great Britain. *Proc R Soc Lond B* **265**, 2443-2452.

Ghosh, R. N., Gelman, D. L., Maxfield, F. R. (1994). Quantification of low density lipoprotein and transferrin endocytic sorting HEp2 cells using confocal microscopy. *J. Cell Sci.* **107**, 2177-2189.

Gibbs, C. J. Jr., Gajdusek, D. C., Asher, D. M., Alpers MP, Beck, E., Daniel, P. M., Matthews, W. B. (1968). Creutzfeldt-Jakob Disease (Spongiform Encephalopathy): Transmission to the Chimpanzee. *Science* **161**, 388-389.

Gilch, S., Kehler, C., Schatzl, H. M. (2007). Peptide Aptamers Expressed in the Secretory Pathway Interfere with Cellular PrP(Sc) Formation. *J Mol Biol*. **371**, 362-373.

Gilch, S., Krammer, C., Schatzl, H. M. (2008). Targeting prion proteins in neurodegenerative disease. *Expert Opin Biol Ther*. **8**, 923-940.

Gilch, S., Schatzl, H. M. (2003). Promising developments bringing prion diseases closer to therapy and prophylaxis. *Trends Mol.Med.* **9**, 367-369.

Gilch, S., Winklhofer, K. F., Groschup, M. H., Nunziante, M., Lucassen, R., Spielhaupter, C., Muranyi, W., Riesner, D., Tatzelt, J., and Schätzl, H. M. (2001). Intracellular re-routing of prion protein prevents propagation of PrP^{Sc} and delays onset of prion disease. *EMBO Journal* **20**, 3957-3966.

Gilch, S., Wopfner, F., Renner-Muller, I., Kremmer, E., Bauer, C., Wolf, E., Brem, G., Groschup, M. H., and Schatzl, H. M. (2003). Polyclonal anti-PrP auto-antibodies induced with dimeric PrP interfere efficiently with PrPSc propagation in prion-infected cells. *J.Biol.Chem.* **278**, 18524-18531.

Giri, R. K., Young, R., Pitstick, R., DeArmond, S. J., Prusiner, S. B., Carlson, G. A. (2006). Prion infection of mouse neurospheres. *Proc Natl Acad Sci U S A*. **103**, 3875-3880.

Gniadek, T. J., Warren, G. (2007). WatershedCounting3D: A New Method for Segmenting and Counting Punctate Structures from Confocal Image Data. *Traffick* **8**, 339-346.

Godsave, S. F., Wille, H., Kujala, P., Latawiec, D., DeArmond, S. J., Serban, A., Prusiner, S. B., Peters, P. J. (2008). Cryo-Immunogold Electron Microscopy for Prions: Toward Identification of a Conversion Site. *J Neurosci* **28**, 12489-12499.

Goldberg, A. L. (2003). Protein degradation and protection against misfolded or damaged proteins. *Nature* **426**, 895–899.

Goldenthal, K.L., Pastan, I., Willingham, M. C. (1984). Initial steps in receptor-mediated endocytosis. The influence of temperature on the shape and distribution of plasma membrane clathrin-coated pits in cultured mammalian cells. *Exp Cell Res* **152**, 558-564.

Goldfarb, L. G., Brown, P., Haltia, M., Ghiso, J., Frangione, B., Gajdusek, D. C. (1993). Synthetic peptides corresponding to different mutated regions of the amyloid

gene in familial Creutzfeldt-Jakob disease show enhanced in vitro formation of morphologically different amyloid fibrils. *Proc.Natl.Acad.Sci.U.S A.* **90**, 4451-4454.

Golding, M. C., Long, C. R., Carmell, M. A., Hannon, G. J., Westhusin, M. E. (2006). Suppression of prion protein in livestock by RNA interference. *Proc Natl Acad Sci U S A.* **103**, 5285-5290.

Goldmann, W., Hunter, N., Foster, J. D., Salbaum, J. M., Beyreuther, K., and Hope, J. (1990). Two alleles of a neural protein gene linked to scrapie in sheep. *Proc.Natl.Acad.Sci.U.S.A.* **87**, 2476-2480.

Goldmann, W., Hunter, N., Martin, T., Dawson, M., Hope, J. (1991). Different forms of the bovine PrP gene have five or six copies of a short, G-C-rich element within the protein-coding exon. *Journal of General Virology* **72**, 201-204.

Gordon, W. S. (1946). Advances in veterinary research. Louping-ill, tick-borne fever and scrapie. *Veterinary Record* **58**, 516-520.

Gossert, A. D., Bonjour, S., Lysek, D. A., Fiorito, F., and Wuthrich, K. (2005). Prion protein NMR structures of elk and of mouse/elk hybrids. *Proc.Natl.Acad Sci U.S.A* **102**, 646-650.

Gousset, K., Schiff, E., Langevin, C., Marijanovic, Z., Caputo, A., Browman, D. T., Chenouard, N., de Chaumont, F., Martino, A., Enninga, J., Olivo-Marin, J. C., Mannel, D., and Zurzolo, C. (2009). Prions hijack tunnelling nanotubes for intercellular spread. *Nat Cell Biol*.

Graner, E., Mercadante, A. F., Zanata, S. M., Forlenza, O. V., Cabral, A. L. B., Veiga, S. S., Juliano, M. A., Roesler, R., Walz, R., Minetti, A., Izquierdo, I., Martins, V. R., Brentani, R. R. (2000). Cellular prion protein binds laminin and mediates neuritogenesis. *Molecular Brain Research* **76**, 85-92.

Greil, C. S., Vorberg, I. M., Ward, A. E., Meade-White, K. D., Harris, D. A., Priola, S. A. (2008). Acute cellular uptake of abnormal prion protein is cell type and scrapie-strain independent. *Virology*. **379**, 284-293.

Griffith, J. S. (1967). Self Replication and scrapie. *Nature* **215**, 1043-1044.

Grigoriev, V., Escaig-Haye, F., Streichenberger, N., Kopp, N., Langeveld, J., Brown, P., Fournier, J. G. (1999). Submicroscopic immunodetection of PrP in the brain of a patient with a new-variant of Creutzfeldt-Jakob disease. *Neuroscience Letters* **264**, 57-60.

Gruenberg, J., Howell, k. E. (1989). Membrane traffic in endocytosis: insights from cell-free assays. *Annu. Rev. Cell Biol.* **5**, 453–481.

Gruenberg, J., Maxfield, F. R. (1995) Membrane transport in the endocytic pathway. *Curr opin cell biol* **7**, 552–563.

Hainfellner, J. A., Brantner-Inthaler, S., Cervenáková, L., Brown, P., Kitamoto, T., Tateishi, J., Diringer, H., Liberski, P. P., Regele, H., Feucht, R., Mayr, N., Wessely, P., Summer, K., Seitelberger, F., Budka, H. (1995). The original Gerstmann-Straussler-Scheinker family of Austria: Divergent clinicopathological phenotypes but constant PrP genotype. *Brain Pathol.* **5**, 201-211.

Hainfellner, J. A., Jellinger, K., Diringer, H., Guentchev, M., Kleinert, R., Pilz, P., Maier, H., Budka, H. (1996). Creutzfeldt-Jakob disease in Austria. *Journal of Neurology, Neurosurgery and Psychiatry* **61**, 139-142.

Haraguchi, T., Fisher, S., Olofsson, S., Endo, T., Groth, D., Tarentino, A., Borchelt, D. R., Teplow, D., Hood, L. E., Burlingame, A. L., Lycke, E., Kobata, A., Prusiner, S. B. (1989). Asparagine-linked glycosylation of the Scrapie and cellular prion proteins. *Arch Biochem.Biophys.* **274**, 1-13.

Harper, J. D., Lansbury, P. T. (1997). Models of amyloid seeding in Alzheimer's disease and scrapie: mechanistic truths and physiological consequences of the time-dependent solubility of amyloid proteins. *Annu. Rev. Biochem* **66**, 385-407.

Harris, D. A. (1999). Cellular biology of prion diseases. *Clinical Microbiology Reviews* **12**, 429-444.

Harris, D. A. (2003). Trafficking, turnover and membrane topology of PrP. *Br.Med.Bull.* **66**, 71-85.

Harris, D. A., Huber, M. T., Van Dijken, P., Shyng, S. L., Chait, B. T., and Wang, R. (1993a). Processing of a cellular prion protein: identification of N- and C-terminal cleavage sites. *Biochemistry* **32**, 1009-1016.

Harris, D. A., Lele, P., Snider, W. D. (1993b). Localization of the mRNA for a chicken prion protein by in situ hybridization. *Proc.Natl.Acad.Sci.U.S A.* **90**, 4309-4313.

Harris, D. A., True, H. L. (2006). New insights into prion structure and toxicity. *Neuron* **50**, 353-357.

Hay, B., Barry, R. A., Lieberburg, I., Prusiner, S. B., Lingappa, V. R. (1987). Biogenesis and transmembrane orientation of the cellular isoform of the scrapie prion protein. *Mol.Cell Biol.* **7**, 914-920.

Heath, C. A., Barker, R. A., Esmonde, T. F., Harvey, P., Roberts, R., Trend, P., Head, M. W., Smith, C., Bell, J. E., Ironside, J. W., Will, R. G., Knight, R. S. (2006). Dura mater-associated Creutzfeldt-Jakob disease: experience from surveillance in the UK. *J Neurol.Neurosurg.Psychiatry*. **77**, 880-882.

Hegde, R. S., Mastrianni, J. A., Scott, M. R., DeFea, K. A., Tremblay, P., Torchia, M., DeArmond, S. J., Prusiner, S. B., Lingappa, V. R. (1998). A transmembrane from of the prion protein in neurodegenerative disease. *Science* **279**, 827-834.

Hegde, R. S., Tremblay, P., Groth, D., DeArmond, S., Prusiner, S. B., Lingappa, V. R. (1999). Transmissible and genetic prion diseases share a common pathway of neurodegeneration. *Nature* **402**, 822-826.

Hegde, R. S., Voigt, S., Lingappa, V. R. (1998). Regulation of protein topology by trans-acting factors at the endoplasmic reticulum. *Molecular Cell* **2**, 85-91.

Heidenhain, A. (1929). Klinische und anatomische Untersuchungen über eine eigenartige Erkrankung des Zentralnervensystems im Praesenium. *Z ges Neurol Psychiatr* **118**, 49-114.

Heppner, F. L., Musahl, C., Arrighi, I., Klein, M. A., Rülicke, T., Oesch, B., Zinkernagel, R. M., Kalinke, U., Aguzzi, A. (2001). Prevention of scrapie pathogenesis by transgenic expression of anti-prion protein antibodies. *Science* **294**, 178-182.

Herms, J., Tings, T., Gall, S., Madlung, A., Giese, A., Siebert, H., Schürmann, P., Windl, O., Brose, N., Kretzschmar, H. (1999). Evidence of presynaptic location and function of the prion protein. *Journal of Neuroscience* **19**, 8866-8875.

Hetz, C., Castilla, J., Soto, C. (2007). Perturbation of endoplasmic reticulum homeostasis facilitates prion replication. *J Biol.Chem.* **282**, 12725-12733.

Hetz, C., Russelakis-Carneiro, M., Maundrell, K., Castilla, J., Soto, C. (2003). Caspase-12 and endoplasmic reticulum stress mediate neurotoxicity of pathological prion protein. *EMBO J* **22**, 5435-5445.

Hetz, C. A., Soto, C. (2006). Stressing Out the ER: A Role of the Unfolded Protein Response in Prion-Related Disorders. *Curr.Mol Med* **6**, 37-43.

Hewitt, P. E., Llewelyn, C. A., Mackenzie, J., Will, R. G. (2006). Creutzfeldt-Jakob disease and blood transfusion: results of the UK Transfusion Medicine Epidemiological Review study. *Vox Sanguinis* **91**, 221-230.

Hill, A. F., Butterworth, R. J., Joiner S, Jackson GS, Rossor, M. N., Thomas, D. J., Frosh, A., Tolley, N., Bell, J. E., Spencer, M., King, A., Al-Sarraj, S., Ironside, J. W., Lantos, P. L., Collinge, J. (1999). Investigation of variant Creutzfeldt-Jakob disease and other human prion diseases with tonsil biopsy samples. *Lancet* **353**, 183-189.

Hill, A. F., Collinge, J. (2003). Subclinical prion infection. *Trends Microbiology* **11**, 578-584.

Hill, A. F., Joiner S, Beck J, Campbell, T. A., Dickinson, A., Poulter, M., Wadsworth J. D., Collinge, J. (2006). Distinct glycoform ratios of protease resistant prion protein associated with *PRNP* point mutations. *Brain* **129**, 676-685.

Hill, A. F., Joiner S, Linehan J, Desbruslais, M., Lantos, P. L., Collinge, J. (2000). Species barrier independent prion replication in apparently resistant species. *Proc Natl Acad Sci USA* **97**, 10248-10253.

Hill, A. F, Joiner S, Wadsworth, J. D, Sidle, K. C., Bell, J. E., Budka, H., Ironside, J. W., Collinge, J. (2003). Molecular classification of sporadic Creutzfeldt-Jakob disease. *Brain* **126**, 1333-1346.

Hill, A. F., Zeidler, M., Ironside, J., Collinge, J. (1997). Diagnosis of new variant Creutzfeldt-Jakob disease by tonsil biopsy. *Lancet.* **349**, 99-100.

Hill, A. F., Desbruslais, M., Joiner, S., Sidle, K. C., Gowland, I., Collinge, J., Doey, L. J., Lantos, P. (1997). The same prion strain causes vCJD and BSE. *Nature* **389**, 448-50, 526.

Hill, E., Van Der Kaay, J., Downes, C.P., Smythe, E. (2001). The role of dynamin and its binding partners in coated pit invagination and scission. *J. Cell Biol*., **152**, 309-323.

Hilmert, H., Diringer, H. (1984). A rapid and efficient method to enrich SAF-protein from scrapie brains of hamsters. *Biosci.Rep.* **4**, 165-170.

Hölscher, C., Delius, H., Bürkle, A. (1998). Overexpression of nonconvertible PrP^{c}Delta114-121 in scrapie-infected mouse neuroblastoma cells leads to *trans*-dominant inhibition of wild-type PrP^{Sc} accumulation. *J.Virol.* **72**, 1153-1159.

Hope, J., Morton, L. J., Farquhar, C. F., Multhaup, G., Beyreuther, K., and Kimberlin, R. H. (1986). The major polypeptide of scrapie-associated fibrils (SAF) has the same

size, charge distribution and N-terminal protein sequence as predicted for the normal brain protein (PrP). *EMBO J* **5**, 2591-2597.

Horiuchi, M., Caughey, B. (1999). Specific binding of normal prion protein to the scrapie form via a localized domain initiates its conversion to the protease-resistant state. *EMBO Journal* **18**, 3193-3203.

Horiuchi, M., Priola, S. A., Chabry, J., Caughey, B. (2000). Interactions between heterologous forms of prion protein: Binding, inhibition of conversion, and species barriers. *Proc. Natl. Acad. Sci. U. S. A.* **97**, 5836-5841.

Hornemann, S., Korth, C., Oesch, B., Riek, R., Wider, G., Wüthrich, K., Glockshuber, R. (1997). Recombinant full-length murine prion protein, mPrP(23–231): purification and spectroscopic characterization. *FEBS Lett* **413**, 277-281.

Hosszu, L. L. P., Baxter, N. J., Jackson G. S., Power, A., Clarke A, Waltho, J. P., Craven, C. J., Collinge. J. (1999). Structural mobility of the human prion protein probed by backbone hydrogen exchange. *Nature Structural Biology* **6**, 740-743.

Hsiao, K., Baker, H. F., Crow, T. J., Poulter, M., Owen, F., Terwilliger, J. D., Westaway, D., Ott, J., Prusiner, S. B. (1989). Linkage of a prion protein missense variant to Gerstmann- Straussler syndrome. *Nature* **338**, 342-345.

Hsiao, K. K., Cass, C., Schellenberg, G. D., Bird, T. D., Devine-Gage, E., Wisniewski, H., Prusiner, S. B. (1991). A prion protein variant in a family with the telencephalic form of Gerstmann-Straussler-Scheinker syndrome. *Neurology* **41**, 681-684.

Hundt, C., Peyrin, J. M., Haïk, S., Gauczynski, S., Leucht, C., Rieger, R., Riley, M. L., Deslys, J. P., Dormont, D., Lasmézas, C. I., and Weiss, S. (2001). Identification of interaction domains of the prion protein with its 37-kDa/67-kDa laminin receptor. *EMBO Journal* **20**, 5876-5886.

Imai, Y., Soda, M., Inoue, H., Hattori, N., Mizuno, Y., Takahashi, R. (2001). An unfolded putative transmembrane polypeptide, which can lead to endoplasmic reticulum stress, is a substrate of Parkin. *Cell* **105**, 891-902.

Ingrosso, L., Ladogana, A., Pocchiari, M. (1995). Congo red prolongs the incubation period in scrapie-infected hamsters. *J.Virol.* **69**, 506-508.

Ironside, J. W., McCardle, L., Hayward, P. A., and Bell, J. E. (1993). Ubiquitin immunocytochemistry in human spongiform encephalopathies. *Neuropathology and Applied Neurobiology* **19**, 134-140.

Ivanova, L., Barmada, S., Kummer, T., Harris, D. A. (2001). Mutant prion proteins are partially retained in the endoplasmic reticulum. *Journal of Biological Chemistry* **276**, 42409-42421.

Jackson, G. S., Murray, I., Hosszu, L. L. P., Gibbs, N., Waltho, J. P., Clarke A, Collinge, J. (2001). Location and properties of metal-binding sites on the human prion protein. *Proceedings of the National Academy of Sciences of the United States of America* **98**, 8531-8535.

Jarrett, J. T., Lansbury, P. T. J. (1993). Seeding "one-dimensional crystallization" of amyloid: a pathogenic mechanism in Alzheimer's disease and scrapie? *Cell* **73**, 1055-1058.

Jeffrey, M., Gonzalez, L. (2004). Pathology and pathogenesis of bovine spongiform encephalopathy and scrapie. *Curr.Top.Microbiol.Immunol.* **284**, 65-97.

Jeffrey, M., Goodsir, C. M., Bruce, M. E., McBride, P. A., Scott, J. R. (1994). Infection-specific prion protein (PrP) accumulates on neuronal plasmalemma in scrapie-infected mice. *Ann.NY Acad.Sci.* **724**, 327-330.

Jeffrey, M., Goodsir, C. M., Bruce, M. E., McBride, P. A., Scott, J. R., Halliday, W. G. (1992). Infection specific prion protein (PrP) accumulates on neuronal plasmalemma in scrapie infected mice. *Neurosci Lets* **147**, 106-109.

Jeffrey, M., McGovern, G., Goodsir, C. M., Brown, K. L., Bruce, M. E. (2000). Sites of prion protein accumulation in scrapie-infected mouse spleen revealed by immuno-electron microscopy. *Journal of Pathology* **191**, 323-332.

Jen, A., Parkyn, C. J., Mootoosamy, R. C., Ford, M. J., Warley, A., Liu, Q., Bu, G., Baskakov, I. V., Moestrup, S., McGuinness, L., Emptage, N., Morris, R. J. (2010). Neuronal low-density lipoprotein receptor-related protein 1 binds and endocytoses prion fibrils via receptor cluster 4. *J Cell Sci* **123**, 246-255.

Kaneko, K., Vey, M., Scott, M., Pilkuhn, S., Cohen, F. E., Prusiner, S. B. (1997). COOH-terminal sequence of the cellular prion protein directs subcellular trafficking and controls conversion into the scrapie isoform. *Proc.Natl.Acad Sci U.S.A* **94**, 2333-2338.

Kaneko, K., Zulianello, L., Scott, M., Cooper, C. M., Wallace, A. C., James, T. L., Cohen, F. E., Prusiner, S. B. (1997). Evidence for protein X binding to a discontinuous epitope on the cellular prion protein during scrapie prion propagation. *Proceedings of the National Academy of Sciences of the United States of America* **94**, 10069-10074.

Kang, S. W., Rane, N. S., Kim, S. J., Garrison, J. L., Taunton, J., Hegde, R. S. (2006). Substrate-Specific Translocational Attenuation during ER Stress Defines a Pre-Emptive Quality Control Pathway. *Cell* **127**, 999-1013.

Kanu, N., Imokawa, Y., Drechsel, D. N., Williamson, R. A., Birkett, C. R., Bostock, C. J., Brockes, J. P. (2002). Transfer of scrapie prion infectivity by cell contact in culture

246. *Current Biology* **12**, 523-530.

Kascsak, R. J., Rubenstein, R., Merz, P. A., Tonna DeMasi, M., Fersko, R., Carp, R. I., Wisniewski, H. M., Diringer, H. (1987). Mouse polyclonal and monoclonal antibody to scrapie-associated fibril proteins. *J Virol.* **61**, 3688-3693.

Kaski, D., Mead, S., Hyare, H., Cooper, S., Jampana, R., Overell, J., Knight, R., Collinge, J., Rudge, P. (2009). Variant CJD in an individual heterozygous for PRNP codon 129. *Lancet* **374**, 2128.

Kimberlin, R. H., Marsh, R. F. (1975). Comparison of scrapie and transmissible mink encephalopathy in hamsters. I. Biochemical studies of brain during development of disease. *J Infect.Dis.* **131**, 97-103.

Kimberlin, R. H., Walker, C. A. (1979). Pathogenesis of scrapie: agent multiplication in brain at the first and second passage of hamster scrapie in mice. *J Gen Virol* **42**, 107-117.

Kirkwood, J. K., Cunningham, A. A. (1994). Epidemiological observations on spongiform encephalopathies in captive wild animals in the British Isles. *Vet.Rec.* **135**, 296-303.

Kisselev, A. F., Goldberg, A. L. (2005). Monitoring activity and inhibitionof 26S proteasomes with fluorogenic peptide substrates. *Methods Enzymol* **398**, 364-378.

Kitamoto, T., Tateishi, J. (1988). Immunohistochemical confirmation of Creutzfeldt-Jakob disease with a long clinical course with amyloid plaque core antibodies. *Am.J Pathol.* **131**, 435-443.

Klohn, P., Stoltze, L., Flechsig, E., Enari, M., Weissmann, C. (2003). A quantitative, highly sensitive cell-based infectivity assay for mouse scrapie prions. *Proc.Natl.Acad. Sci U.S.A* **100**, 11666-11671.

Kocisko, D. A., Come, J. H., Priola, S. A., Chesebro, B., Raymond, G. J., Lansbury, P. T., Caughey, B. (1994). Cell-free formation of protease-resistant prion protein. *Nature* **370**, 471-474.

Korth, C., May, B. C., Cohen, F. E., Prusiner, S. B. (2001). Acridine and phenothiazine derivatives as pharmacotherapeutics for prion disease. *Proc Natl Acad Sci U.S.A* **98**, 9836-9841.

Kovacs, G. G., Trabattoni, G., Hainfellner, J. A., Ironside, J. W., Knight, R. S., Budka, H. (2002b). Mutations of the prion protein gene phenotypic spectrum. *J Neurol* **249**, 1567-1582.

Kovacs, G. G., Trabattoni, G., Hainfellner, J. A., Ironside, J. W., Knight, R. S., Budka, H. (2002a). Mutations of the prion protein gene phenotypic spectrum. *J.Neurol.* **249**, 1567-1582.

Kretzschmar, H. A., Neumann, M., Riethmuller, G., Prusiner, S. B. (1992). Molecular cloning of a mink prion protein gene. *J Gen.Virol.* **73**, 2757-2761.

Kretzschmar, H. A., Prusiner, S. B., Stowring, L. E., DeArmond, S. J. (1986a). Scrapie prion proteins are synthesized in neurons. *Am.J Pathol.* **122**, 1-5.

Kretzschmar, H. A., Stowring, L. E., Westaway, D., Stubblebine, W. H., Prusiner, S. B., DeArmond, S. J. (1986b). Molecular cloning of a human prion protein cDNA. *DNA* **5**, 315-324.

Kristiansen, M., Deriziotis, P., Dimcheff, D. E., Jackson, G. S, Ovaa, H., Naumann, H., Clarke A, van Leeuwen, F. W., Menendez-Benito, V., Dantuma, N. P., Portis, J. L., Collinge J, Tabrizi S. J., (2007). Disease-Associated Prion Protein Oligomers Inhibit the 26S Proteasome. *Molecular Cell* **26**, 175-188.

Kristiansen, M., Messenger, M. J., Klohn, P., Brandner S, Wadsworth JD, Collinge J, Tabrizi S. J. (2005). Disease-related prion protein forms aggresomes in neuronal cells leading to caspase-activation and apoptosis. *Journal of Biological Chemistry* **280**, 38851-38861.

Kubler, E., Oesch, B., Raeber, A. J. (2003). Diagnosis of prion diseases. *Br.Med.Bull.* **66**, 267-279.

Ladogana, A., Casaccia, P., Ingrosso, L., Cibati, M., Salvatore, M., Xi, Y., Masullo, C., Pocchiari, M. (1992). Sulphate polyanions prolong the incubation period of scrapie- infected hamsters. *Journal of General Virology* **73**, 661-665.

Lamb, B. T., Sisodia, S. S., Lawler, A. M., Slunt, H. H., Kitt, C. A., Kearns, W. G., Pearson, P. L., Price, D. L., Gearhart, J. D. (1993). Introduction and expression of the 400 kilobase amyloid precursor protein gene in transgenic mice. *Nat.Genet.* **5**, 22-30.

Lantos, P. L., McGill, I. S., Janota, I., Doey, L. J., Collinge, J., Bruce, M. T., Whatley, S. A., Anderton, B. H., Clinton, J., Roberts, G. W., Rossor, M. N. (1992). Prion protein immunocytochemistry helps to establish the true incidence of prion diseases. *Neurosci.Lett.* **147**, 67-71.

Lashuel, H. A., Hartley, D., Petre, B., Walz, T., Lansbury, P. T. (2002). Neurodegenerative diseases, amyloid pores from pathogenic mutations. *Nature* **418**, 291.

Lasmézas, C. I., Deslys, J. P., Robain, O., Jaegly, A., Beringue, V., Peyrin, J. M., Fournier, J. G., Hauw, J. J., Rossier, J., Dormont, D. (1997). Transmission of the BSE agent to mice in the absence of detectable abnormal prion protein. *Science* **275**, 402-405.

Laurent, M. (1998). Bistability and the species barrier in prion diseases: stepping across the threshold or not. *Biophysical Chemistry* **72**, 211-222.

Lee, H. S., Brown, P., Cervenáková, L., Garruto, R. M., Alpers MP, Gajdusek, D. C., Goldfarb, L. G. (2001a). Increased susceptibility to Kuru of carriers of the *PRNP* 129 methionine/methionine genotype. *Journal of Infectious Diseases* **183**, 192-196.

Lee, K. S., Linden, R., Prado, M. A., Brentani, R. R., Martins, V. R. (2003). Towards cellular receptors for prions. *Rev.Med.Virol.* **13**, 399-408.

Lee, K. S., Magalhaes, A. C., Zanata, S. M., Brentani, R. R., Martins, V. R., and Prado, M. A. M. (2001b). Internalization of mammalian fluorescent cellular prion protein and N-terminal deletion mutants in living cells. *Journal of Neurochemistry* **79**, 79-87.

Lee, B. H., Lee, M. J., Park, S., Oh, D., C., Elsasser, S., Chen, P. C., Gartner, C., Dimova, N., Steven, L. H., Gygi, P., Wilson, S. M., King, R. W., Finley, D. (2010). Enhancement of proteasome activity by a small-molecule inhibitor of USP14. *Nature* **467**, 179-184.

Legname, G., Nguyen, H. O., Baskakov, I. V., Cohen, F. E., DeArmond, S. J., Prusiner, S. B. (2005). Strain-specified characteristics of mouse synthetic prions. *Proc.Natl.Acad Sci U.S.A.* **102**, 2168-2173.

Lehmann, S., Harris, D. A. (1997). Blockade of glycosylation promotes acquisition of scrapie- like properties by the prion protein in cultured cells. *J.Biol.Chem.* **272**, 21479-21487.

Lewis, P. A., Properzi F, Prodromidou, K., Clarke, A., Collinge, J., Jackson, G.S. (2006). Removal of the glycosylphosphatidylinositol anchor from PrP(Sc) by cathepsin D does not reduce prion infectivity. *Biochemical Journal* **395**, 443-448.

Li, A., Barmada, S. J., Roth, K. A., Harris, D. A. (2007). N-terminally deleted forms of the prion protein activate both Bax-dependent and Bax-independent neurotoxic pathways. *J Neurosci* **27**, 852-859.

Li, A., Christensen, H. M., Stewart, L. R., Roth, K. A., Chiesa, R., Harris, D. A. (2007). Neonatal lethality in transgenic mice expressing prion protein with a deletion of residues 105-125. *EMBO J* **26**, 548-558.

Li, A., Harris, D. A. (2005). Mammalian prion protein suppresses Bax-induced cell death in yeast. *J Biol chem*. **280**, 17430-17434.

Liao, Y. C., Lebo, R. V., Clawson, G. A., Smuckler, E. A. (1986). Human prion protein cDNA: molecular cloning, chromosomal mapping, and biological implications. *Science* **233**, 364-367.

Liao, Y. C., Tokes, Z., Lim, E., Lackey, A., Woo, C. H., Button, J. D., Clawson, G. A. (1987). Cloning of rat "prion-related protein" cDNA. *Lab.Invest.* **57**, 370-374.

Lippincott-Schwartz, J., Yuan, L., Tipper, C., Amherdt, M., Orci, L., Klausner, R. D. (1991). Brefeldin A's effects on endosomes, lysosomes, and the TGN suggest a general mechanism for regulating organelle structure and membrane traffic. *Cell* **67**, 601-616.

Llewelyn, C. A., Hewitt, P. E., Knight, R. S., Amar, K., Cousens, S., Mackenzie, J., Will, R. G. (2004). Possible transmission of variant Creutzfeldt-Jakob disease by blood transfusion. *Lancet* **363**, 417-421.

Lloyd, S., Onwuazor, O. N., Beck, J., Mallinson, G., Farrall, M., Targonski, P., Collinge, J., Fisher, E. (2001). Identification of multiple quantitative trait loci linked to prion disease incubation period in mice. *Proceedings of the National Academy of Sciences of the United States of America* **98**, 6279-6283.

Lloyd, S., Uphill, J. B., Targonski, P. V., Fisher, E, Collinge, J. (2002). Identification of genetic loci affecting mouse-adapted bovine spongiform encephalopathy incubation time in mice. *Neurogenetics* **4**, 77-81.

Locht, C., Chesebro, B., Race, R., Keith, J. M. (1986). Molecular cloning and complete sequence of prion protein cDNA from mouse brain infected with the scrapie agent. *Proc.Natl.Acad.Sci.U.S A.* **83**, 6372-6376.

Lopez, C. D., Yost, C. S., Prusiner, S. B., Myers, R. M., Lingappa, V. R. (1990). Unusual topogenic sequence directs prion protein biogenesis. *Science* **248**, 226-229.

Lowe, J., Errington, E. R., Lennox, G., Pike, I., Spendlove, I., Landon, M., Mayer, R. J. (1992). Ballooned neurons in several neurodegenerative diseases and stroke contain alpha-B crystallin. *Neuropathol & Appl Neurobiol* **18**, 341-350.

Ma, J., Lindquist, S. (2002). Conversion of PrP to a Self-Perpetuating PrP^{Sc}-like Conformation in the Cytosol. *Science*. **298**, 1785-1788.

Ma, J., Wollmann, R., Lindquist, S. (2002). Neurotoxicity and neurodegeneration when PrP accumulates in the cytosol. *Science*. 298, 1781-1785

Ma, J. Y., Lindquist, S. (2001). Wild-type PrP and a mutant associated with prion disease are subject to retrograde transport and proteasome degradation. *Proceedings of the National Academy of Sciences of the United States of America* **98**, 14955-14960.

Macia, E, Ehrlich, M., Massol, R., Boucrot, E., Brunner, C., Kirchhausen, T. (2006). Dynasore, a cell-permeable inhibitor of dynamin. *Dev Cell* **10**, 839-850.

Madore, N., Smith, K. L., Graham, C. H., Jen, A., Brady, K., Hall, S., Morris, R. (1999). Functionally different GPI proteins are organized in different domains on the neuronal surface. *EMBO* **18**, 6917-6926.

Magalhaes, A. C., Baron, G. S., Lee, K. S., Steele-Mortimer, O., Dorward, D., Prado, M. A., Caughey, B. (2005). Uptake and neuritic transport of scrapie prion protein coincident with infection of neuronal cells. *J Neurosci.* **25**, 5207-5216.

Magalhaes, A. C., Silva, J. A., Lee, K. S., Martins, V. R., Prado, V. F., Ferguson, S. S., Gomez, M. V., Brentani, R. R., Prado, M. A. (2002). Endocytic intermediates involved with the intracellular trafficking of a fluorescent cellular prion protein. *J.Biol.Chem.* **277**, 33311-33318.

Mahal, S. P., Demczyk, C. A., Smith, E. W., Klohn, P. C., Weissmann, C. (2008). Assaying prions in cell culture: the standard scrapie cell assay (SSCA) and the scrapie cell assay in end point format (SCEPA). *Methods Mol Biol* **459**, 49-68.

Mallucci, G., Collinge, J., (2005). Rational targeting for prion therapeutics. *Nature Reviews Neuroscience* **6**, 23-34.

Mallucci, G., Dickinson, A., Linehan J, Klohn, P., Brandner, S., Collinge, J. (2003). Depleting neuronal PrP in prion infection prevents disease and reverses spongiosis. *Science* **302**, 871-874.

Mallucci, G., Ratté, S., Asante, E., Linehan, J., Gowland, I., Jefferys, J. G. R., Collinge, J. (2002). Post-natal knockout of prion protein alters hippocampal CA1 properties, but does not result in neurodegeneration. *EMBO Journal* **21**, 202-210.

Mange, A., Crozet, C., Lehmann, S., Beranger, F. (2004). Scrapie-like prion protein is translocated to the nuclei of infected cells independently of proteasome inhibition and interacts with chromatin. *J Cell Sci* **117**, 2411-2416.

Mangé, A., Nishida, N., Milhavet, O., McMahon, H. E. M., Casanova, D., Lehmann, S. (2000). Amphotericin B inhibits the generation of the scrapie isoform of the prion protein in infected cultures. *J Virol* **74**, 3135-3140.

Manson, J. C., Clarke, A., Hooper, M. L., Aitchison, L., McConnell, I., Hope, J. (1994). 129/Ola mice carrying a null mutation in PrP that abolishes mRNA production are developmentally normal. *Mol.Neurobiol.* **8**, 121-127.

Manuelidis, L., Fritch, W., Xi, Y. (1997). Evolution of a strain of CJD that induces BSE-like plaques. *Science* **227**, 94-98.

Marella, M., Gaggioli, C., Batoz, M., Deckert, M., Tartare-Deckert, S., Chabry, J. (2004). Pathological prion protein exposure switches on neuronal MAP-kinase pathway resulting in microglia recruitment. *J Biol chem*. **280**, 1529-1534.

Marella, M., Lehmann, S., Grassi, J., and Chabry, J. (2002). Filipin prevents pathological prion protein accumulation by reducing endocytosis and inducing cellular PrP release. *J.Biol.Chem.* **227**, 25457-25464.

Marijanovic, Z., Caputo, A., Campana, V., Zurzolo, C. (2009). Identification of an intracellular site of prion conversion. *PLoS Pathog* **5**, e1000426.

Marsh, R. F. (1992). Transmissible Mink Encephalopathy. *In* "Prion Diseases of Humans and Animals" (S. B. Prusiner, Collinge J, J. Powell, and B. Anderton, Eds.), Ellis Horwood, London. 497-508.

Marsh, R. F., Bessen, R. A., Lehmann, S., Hartsough, G. R. (1991). Epidemiological and experimental studies on a new incident of transmissible mink encephalopathy. *J Gen.Virol.* **72**, 589-594.

Martinez, O., Goud, B. (1998). Rab proteins. *Biochim Biophys Acta* **14**, 101-112.

Masters, C. L., Gajdusek, D. C., Gibbs, C. J. J. (1981). Creutzfeldt-Jakob disease virus isolations from the Gerstmann- Straussler syndrome with an analysis of the various

forms of amyloid plaque deposition in the virus-induced spongiform encephalopathies. *Brain* **104**, 559-588.

Mathiason, C. K., Powers, J. G., Dahmes, S. J., Osborn, D. A., Miller, K. V., Warren, R. J., Mason, G. L., Hays, S. A., Hayes-Klug, J., Seelig, D. M., Wild, M. A., Wolfe, L. L., Spraker, T. R., Miller, M. W., Sigurdson, C. J., Telling, G. C., Hoover, E. A. (2006). Infectious prions in the saliva and blood of deer with chronic wasting disease. *Science* **314**, 133-136.

Maxfield, F. R., McGraw, T. E. (2004). Endocytic recycling. *Nat. Rev. Mol. Cell Bio.* **5**, 121–132.

Mayor, S., Pagano, R. E. (2007). Pathways of clathrin-independent endocytosis. *Nat. Rev. Mol. Cell Bio.* **8**, 603–612.

McKinley, M. P., Meyer, R. K., Kenaga, L., Rahbar, F., Cotter, R., Serban, A., Prusiner, S. B. (1991). Scrapie Prion Rod Formation Invitro Requires Both Detergent Extraction and Limited Proteolysis. *Journal of Virology* **65**, 1340-1351.

McKinley, M. P., Meyer, R. K., Kenaga, L., Rahbar, F., Cotter, R., Serban, A., Prusiner, S. B. (1991a). Scrapie prion rod formation *in vitro* requires both detergent extraction and limited proteolysis. *J. Virol*. **65**, 1340-1351.

McKinley, M. P., Taraboulos, A., Kenaga, L., Serban, D., Stieber, A., DeArmond, S. J., Prusiner, S. B., Gonatas, N. (1991b). Ultrastructural localization of scrapie prion proteins in cytoplasmic vesicles of infected cultured cells. *Laboratory Investigation* **65**, 622-630.

Mead, S., Poulter, M., Beck, J., Webb, T., Campbell, T., Linehan, J., Desbruslais, M., Joiner, S., Wadsworth, J. D., King, A., Lantos, P., Collinge, J. (2006). Inherited prion disease with six octapeptide repeat insertional mutation--molecular analysis of phenotypic heterogeneity. *Brain* **129**, 2297-2317.

Mead, S., Mahal, S. P, Beck, J., Campbell, T., Farrall, M., Fisher, E., Collinge, J. (2001). Sporadic - but not variant - Creutzfeldt-Jakob disease is associated with polymorphisms upstream of *PRNP* Exon 1. *American Journal of Human Genetics* **69**, 1225-1235.

Mead, S., Stumpf, M. P., Whitfield, J., Beck, J., Poulter, M., Campbell, T., Uphill, J., Goldstein, D., Alpers, M. P., Fisher, E., Collinge, J. (2003). Balancing selection at the prion protein gene consistent with prehistoric kuru-like epidemics. *Science* **300**, 640-643.

Mead, S. (2006b). Prion disease genetics. *Eur J Hum Genet* **14**, 273-281.

Mead, S. (2006a). Prion disease genetics. *European Journal of Human Genetics* **14**, 273-281.

Mead, S., Poulter, M., Uphill, J., Beck, J., Whitfield, J., Webb, T. E., Campbell, T., Adamson, G., Deriziotis, P., Tabrizi, S. J., Hummerich, H., Verzilli, C., Alpers, M. P., Whittaker, J. C., and Collinge, J. (2009). Genetic risk factors for variant Creutzfeldt-Jakob disease: a genome-wide association study. *Lancet Neurol* **8**, 57-66.

Medori, R., Tritschler, H. J., LeBlanc, A. C., Villare, F., Manetto, V., Montagna, P., Cortelli, P., Avoni, P., Mochi, M., Lugaresi, E., Autilio-Gambetti, L., Gambetti, P. (1992). Fatal Familial Insomnia, a prion disease with a mutation in codon 178 of the prion protein gene: study of two kindreds. *In* "Prion Diseases of Humans and Animals" (S. B. Prusiner, Collinge J, J. Powell, and B. Anderton, Eds.). Ellis Horwood, London. 180-187.

Milhavet, O., Casanova, D., Chevallier, N., McKay, R. D., Lehmann, S. (2006). Neural stem cell model for prion propagation. *Stem Cells*. **24**, 2284-2291.

Miller, M. W., Williams, E. S. (2003). Prion disease: horizontal prion transmission in mule deer. *Nature* **425**, 35-36.

Mironov, A., J., Latawiec, D., Wille, H., Bouzamondo-Bernstein, E., Legname, G., Williamson, R. A., Burton, D., DeArmond, S. J., Prusiner, S. B., Peters, P. J. (2003). Cytosolic prion protein in neurons. *J Neurosci.* **23**, 7183-7193.

Misumi,Y., Miki, K., Takatsuki, A., Tamura, G., Ikehara, Y. (1986). Novel blockade by brefeldin A of intracellular transport of secretory roteins in cultured rat hepatocytes. *J. Biol. Chem.* **261**, 11398-11403.

Montagna, P., Gambetti, P., Cortelli, P., Lugaresi, E. (2003). Familial and sporadic fatal insomnia. *Lancet Neurol.* **2**, 167-176.

Moore, R. A., Vorberg, I., Priola, S. A. (2005). Species barriers in prion diseases--brief review. *Arch Virol Suppl* 187-202.

Morris, R. J., Parkyn, C. J., Jen, A. (2006). Traffic of prion protein between different compartments on the neuronal surface, and the propagation of prion disease. *FEBS Lett.* **580**, 5565-5571.

Moser, M., Colello, R. J., Pott, U., Oesch, B. (1995). Developmental expression of the prion protein gene in glial cells. *Neuron* **14**, 509-517.

Muñiz, M, Riezman, H. (2000). Intracellular transport of GPI-anchored proteins. *EMBO. J.* **19**, 10-15.

Muramoto, T., DeArmond, S., Scott, M., Telling, G. C., Cohen, F. E., Prusiner, S. B. (1997). Heritable disorder reseming neuronal storage disease in mice expressing prion protein with deletion of an alpha-helix. *Nature Med.* **3**, 750-755.

Muramoto, T., Scott, M., Cohen, F. E., Prusiner, S. B. (1996). Recombinant scrapie-like prion protein of 106 amino acids is soluble. *Proceedings of the National Academy of Sciences of the United States of America* **93**, 15457-15462.

Nabi, I. R., Le, P. U. (2003). Caveolae/raft-dependent endocytosis: *J. Cell Biol*. **161**, 673-677.

Naslavsky, N., Stein, R., Yanai, A., Friedlander, G., Taraboulos, A. (1997). Characterization of detergent-insoluble complexes containing the cellular prion protein and its scrapie isoform. *J.Biol.Chem.* **272**, 6324-6331.

Nishitoh, H., Matsuzawa, A., Tobiume, K., Saegusa, K., Takeda, K., Inoue, K., Hori, S., Kakizuka, A., Ichijo, H. (2002). ASK1 is essential for endoplasmic reticulum stress-induced neuronal cell death triggered by expanded polyglutamine repeats. *Genes Dev* **16**, 1345-1355.

Norstrom, E. M., Mastrianni, J. A. (2005). The AGAAAAGA palindrome in PrP is required to generate a productive PrPSc-PrPC complex that leads to prion propagation. *J Biol chem*. **280**, 27236-27243.

Oesch, B., Westaway, D., Walchli, M., McKinley, M. P., Kent, S. B. H., Aebersold, R., Barry, R. A., Tempst, P., Teplow, D. B., Hood, L. E., Prusiner, S. B., Weissmann, C. (1985). A Cellular Gene Encodes Scrapie Prp 27-30 Protein. *Cell* **40**, 735-746.

Oliveberg, M., Tan, Y. J., Fersht, A. R. (1995). Negative activation enthalpies in the kinetics of protein folding. *Proc Natl. Acad Sci USA*. **92**, 8926-8929.

Owen, J. P., Maddison, B. C., Whitelam, G. C., Gough, K. C. (2007). Use of thermolysin in the diagnosis of prion diseases. *Mol Biotechnol.* **35**, 161-170.

Pagano, A., Crottet, P., Prescianotto-Baschong, C., Spiess, M. (2004). *In vitro* formation of recycling vesicles from endosomes requires adaptor protein 1/clathrin and is regulated by Rab4 and the connector rabaptin-5. *Mol Biol Cell* **15**, 4990–5000.

Palmer, M. S., Dryden, A. J., Hughes, J. T., Collinge, J. (1991). Homozygous prion protein genotype predisposes to sporadic Creutzfeldt-Jakob disease. *Nature* **352**, 340-342.

Pan, K. M., Baldwin, M. A., Nguyen, J., Gasset, M., Serban, A., Groth, D., Mehlhorn, I., Huang, Z., Fletterick, R. J., Cohen, F. E., Prusiner, S. B. (1993). Conversion of -helices into -sheets features in the formation of the scrapie prion proteins. *Proc Natl Acad Sci USA* **90**, 10962-10966.

Pan, T., Wong, B. S., Liu, T., Li, R., Petersen, R. B., Sy, M. S. (2002). Cell surface prion protein interacts with glycosaminoglycans. *Journal of Biochemistry* **368**, 81-90.

Panchision, D. M., Hazel, T. H., McKay, R. D. (1998). Plasticity and stem cells in the vertebrate nervous system. *Curr. Opin. Cell Biol*. **10**, 727-733.

Parchi, P., Castellani, R., Capellari, S., Ghetti, B., Young, K., Chen, S. G., Farlow, M., Dickson, D. W., Sims, A. A. F., Trojanowski, J. Q., Petersen, R. B., Gambetti, P. (1996). Molecular Basis of Phenotypic Variability in Sporadic Creutzfeldt-Jakob Disease. *Annals of Neurology* **39**, 669-680.

Parchi, P., Giese, A., Capellari, S., Brown, P., Schulz-Schaeffer, W., Windl, O., Zerr, I., Budka, H., Kopp, N., Piccardo, P., Poser, S., Rojiani, A., Streichenberger, N., Julien, J., Vital, C., Ghetti, B., Gambetti, P., Kretzschmar, H. (1999). Classification of sporadic Creutzfeldt-Jakob Disease based on molecular and phenotypic analysis of 300 subjects. *Annals of Neurology* **46**, 224-233.

Park, T. S., Kleinman, G. M., Richardson, E. P. (1980). Creutzfeldt-Jakob disease with extensive degeneration of white matter. *Acta Neuropathol (Berl)* **52**, 239-242.

Parkin, E. T., Watt, N. T., Hussain, I., Eckman, E. A., Eckman, C. B., Manson, J. C., Baybutt, H. N., Turner, A. J., Hooper, N. M. (2007). Cellular prion protein regulates {beta}-secretase cleavage of the Alzheimer's amyloid precursor protein. *Proc Natl Acad Sci U S A.* **104**, 11062-11067.

Parkyn, C. J., Vermeulen, E. G., Mootoosamy, R. C., Sunyach, C., Jacobsen, C., Oxvig, C., Moestrup, S., Liu, Q., Bu, G., Jen, A., and Morris, R. J. (2008). LRP1 controls biosynthetic and endocytic trafficking of neuronal prion protein. *J Cell Sci*. **121**, 773-783.

Pattison, I. H. (1965). Experiments with scrapie with special reference to the nature of the agent and the pathology of the disease. *In* "Slow, Latent and Temperate Virus Infections, NINDB Monograph 2" (C. J. Gajdusek, C. J. Gibbs, and Alpers MP, Eds.), pp. 249-257. US Government Printing, Washington DC. 249-257.

Pauly, P. C., Harris, D. A. (1998). Copper stimulates endocytosis of the prion protein. *Journal of Biological Chemistry* **273**, 33107-33110.

Peden, A. H., Head, M. W., Ritchie, D. L., Bell, J. E., Ironside, J. W. (2004). Preclinical vCJD after blood transfusion in a PRNP codon 129 heterozygous patient. *Lancet* **364**, 527-529.

Peretz, D., Williamson, R. A., Matsunaga, Y., Serban, H., Pinilla, C., Bastidas, R. B., Rozenshteyn, R., James, T. L., Houghten, R. A., Cohen, F. E., Prusiner, S. B., Burton, D. R. (1997). A conformational transition at the N terminus of the prion protein features in formation of the scrapie isoform. *J Mol Biol* **273**, 614-622.

Pergami, P., Jaffe, H., Safar, J. (1996). Semipreparative chromatographic method to purify the normal cellular isoform of the prion protein in nondenatured form. *Anal.Biochem.* **236**, 63-73.

Perrier, V., Kaneko, K., Safar, J., Vergara, J., Tremblay, P., DeArmond, S. J., Cohen, F. E., Prusiner, S. B., Wallace, A. C. (2002). Dominant-negative inhibition of prion replication in transgenic mice. *Proc.Natl.Acad.Sci.U.S.A* **99**, 13079-13084.

Peters, P. J., Mironov, A., Jr., Peretz, D., Van Donselaar, E., Leclerc, E., Erpel, S., DeArmond, S. J., Burton, D. R., Williamson, R. A., Vey, M., Prusiner, S. B. (2003). Trafficking of prion proteins through a caveolae-mediated endosomal pathway. *J Cell Biol.* **162**, 703-717.

Pfeifer, A., Eigenbrod, S., Al Khadra, S., Hofmann, A., Mitteregger, G., Moser, M., Bertsch, U., Kretzschmar, H. (2006). Lentivector-mediated RNAi efficiently suppresses prion protein and prolongs survival of scrapie-infected mice. *J Clin.Invest* **116**, 3204-3210.

Pimpinelli, F., Lehmann, S., Maridonneau-Parini, I. (2005). The scrapie prion protein is present in flotillin-1-positive vesicles in central- but not peripheral-derived neuronal cell lines. *Eur J Neurosci.* **21**, 2063-2072.

Porter, D. D., Porter, H. G., Cox, N. A. (1973). Failure to demonstrate a humoral immune response to scrapie infection in mice. *J Immunol.* **111**, 1407-1410.

Prado, M. A., Alves-Silva, J., Magalhaes, A. C., Prado, V. F., Linden, R., Martins, V. R., Brentani, R. R. (2004). PrPc on the road: trafficking of the cellular prion protein. *J Neurochem.* **88**, 769-781.

Premzl, M., Sangiorgio, L., Strumbo, B., Marshall Graves, J. A., Simonic, T., Gready, J. E. (2003). Shadoo, a new protein highly conserved from fish to mammals and with similarity to prion protein. *Gene* **314**, 89-102.

Priola, S., Chabry, J., Chan, K. (2001). Efficient conversion of normal prion protein (PrP) by abnormal hamster PrP is determined by homology at amino acid residue 155. *Journal of Virology* **75**, 4673-4680.

Priola, S. A., Caughey, B., Race, R. E., Chesebro, B. (1994). Heterologous PrP molecules interfere with accumulation of protease-resistant PrP in scrapie-infected murine neuroblastoma cells. *J.Virol.* **68**, 4873-4878.

Priola, S. A., Caughey, B., Wehrly, K., Chesebro, B. (1995). A 60-kDa prion protein (PrP) with properties of both the normal and scrapie-associated forms of PrP. *J.Biol.Chem.* **270**, 3299-3305.

Priola, S. A., Chesebro, B. (1995). A single hamster PrP amino acid blocks conversion to protease- resistant PrP in scrapie-infected mouse neuroblastoma cells. *J.Virol.* **69**, 7754-7758.

Prusiner, S. B. (1982). Novel proteinaceous infectious particles cause scrapie. *Science* **216**, 136-144.

Prusiner, S. B. (1998a). Prions. *Proc Natl Acad Sci U S A* **95**, 13363-13383.

Prusiner, S. B., Gajdusek, D. C., Alpers M. P., (1982). Kuru with incubation periods exceeding two decades. *Ann Neurol* **12**, 1-9.

Prusiner, S. B., Groth, D., Serban, A., Koehler, R., Foster, D., Torchia, M., Burton, D., Yang, S. L., DeArmond, S. J. (1993). Ablation of the prion protein (PrP) gene in mice prevents scrapie and facilitates production of anti-PrP antibodies. *Proc Natl Acad Sci USA* **90**, 10608-10612.

Prusiner, S. B., Groth, D. F., Bolton, D. C., Kent, S. B., Hood, L. E. (1984). Purification and structural studies of a major scrapie prion protein. *Cell* **38**, 127-134.

Prusiner, S. B., McKinley, M. P., Bowman, K., Bolton, D. C., Bendheim, P. E., Groth, D. F., Glenner, G. G. (1983). Scrapie prions aggregate to form amyloid-like birefringent rods. *Cell* **35**, 349-358.

Prusiner, S. B., Scott, M., Foster, D., Pan, K. M., Groth, D., Mirenda, C., Torchia, M., Yang, S. L., Serban, D., Carlson, G. A., Raeber, A. J. (1990). Transgenetic studies

implicate interactions between homologous PrP isoforms in scrapie prion replication. *Cell* **63**, 673-686.

Prusiner, S. B., Torchia, M., Westaway, D. (1991). Molecular biology and genetics of prions--implications for sheep scrapie, "mad cows" and the BSE epidemic. Historical background. *Cornell.Vet.* **81**, 85-101.

Puckett, C., Concannon, P., Casey, C., Hood, L. (1991). Genomic Structure of the Human Prion Protein Gene. *Am.J Hum.Genet.* **49**, 320-329.

Race, R. E., Fadness, L. H., Chesebro, B. (1987). Characterization of scrapie infection in mouse neuroblastoma cells. *J Gen.Virol.* **68**, 1391-1399.

Raeber, A. J., Borchelt, D. R., Scott, M., Prusiner, S. B. (1992). Attempts to convert the cellular prion protein into the scrapie isoform in cell-free systems. *J Virol.* **66 (10)**, 6155-6163.

Rambold, A. S., Muller, V., Ron, U., Ben Tal, N., Winklhofer, K. F., Tatzelt, J. (2008). Stress-protective signalling of prion protein is corrupted by scrapie prions. *EMBO J.* **27**, 1974-1984.

Rane, N. S., Kang, S. W., Chakrabarti, O., Feigenbaum, L., Hegde, R. S. (2008). Reduced translocation of nascent prion protein during ER stress contributes to neurodegeneration. *Dev Cell* **15**, 359-370.

Rane, N. S., Yonkovich, J. L., Hegde, R. S. (2004). Protection from cytosolic prion protein toxicity by modulation of protein translocation. *EMBO J.*, **23**, 4550-4559.

Reynolds, A., Leake, D., Boese, Q., Scaringe, S., Marshall, W. S., and Khvorova, A. (2004). Rational siRNA design for RNA interference. *Nat Biotechnol.* **22**, 326-330.

Richardson, E. P. J., Masters, C. L. (1995). The nosology of Creutzfeldt-Jakob disease and conditions related to the accumulation of PrP^{CJD} in the nervous system. *Brain Pathol.* **5**, 33-41.

Rieger, R., Edenhofer, F., Lasmézas, C. I., Weiss, S. (1997). The human 37-kDa laminin receptor precursor interacts with the prion protein in eukaryotic cells. *Nature Medicine* **3**, 1383-1388.

Riek, R., Hornemann, S., Wider, G., Glockshuber, R., Wüthrich, K. (1997). NMR characterization of the full-length recombinant murine prion protein, mPrP(23-231). *FEBS Lett*, **413**, 282-288.

Riek, R., Wider, G., Billeter, M., Hornemann, S., Glockshuber, R., Wuthrich, K. (1998). Prion protein NMR structure and familial human spongiform encephalopathies. *Proc Natl Acad Sci U.S.A.* **95**, 11667-11672.

Riesner, D. (2003). Biochemistry and structure of PrP(C) and PrP(Sc). *Br.Med.Bull.* **66**, 21-33.

Rivera-Milla, E., Stuermer, C. A., Malaga-Trillo, E. (2003). An evolutionary basis for scrapie disease: identification of a fish prion mRNA. *Trends Genet.* **19**, 72-75.

Robakis, N. K., Devine Gage, E. A., Jenkins, E. C., Kascsak, R. J., Brown, W. T., Krawczun, M. S., Silverman, W. P. (1986). Localization of a human gene homologous to the PrP gene on the p arm of chromosome 20 and detection of PrP-related antigens in normal human brain. *Biochem.Biophys.Res.Commun.* **140**, 758-765.

Roucou, X., LeBlanc, A. C. (2005). Cellular prion protein neuroprotective function: implications in prion diseases. *J Mol.Med* **83**, 3-11.

Rubenstein, R., Carp, R. I., Callahan, S. M. (1984). *In vitro* replication of scrapie agent in a neuronal model: infection of PC12 cells. *J Gen.Virol.* **65**, 2191-2198.

Rudd, P. M., Endo, T., Colominas, C., Groth, D., Wheeler, S. F., Harvey, D. J., Wormald, M. R., Serban, H., Prusiner, S. B., Kobata, A., Dwek, R. A. (1999). Glycosylation differences between the normal and pathogenic prion protein isoforms. *Proceedings of the National Academy of Sciences of the United States of America* **96**, 13044-13049.

Rudd, P. M., Wormald, M. R., Wing, D. R., Prusiner, S. B., Dwek, R. A. (2001). Prion glycoprotein: Structure, dynamics, and roles for the sugars. *Biochemistry* **40**, 3759-3766.

Rutishauser, D., Mertz, K. D., Moos, R., Brunner, E., Rulicke, T., Calella, A. M., Aguzzi, A. (2009). The comprehensive native interactome of a fully functional tagged prion protein. *PLoS ONE* **4**, e4446.

Ryder, S. J., Wells, G. A. H., Bradshaw, J. M., Pearson, G. R. (2001). Inconsistent detection of PrP in extraneural tissues of cats with feline spongiform encephalopathy. *Veterinary Record* **148**, 437-441.

Saborio, G. P., Permanne, B., Soto, C. (2001). Sensitive detection of pathological prion protein by cyclic amplification of protein misfolding. *Nature* **411**, 810-813.

Safar, J., Wille, H., Itri, V., Groth, D., Serban, H., Torchia, M., Cohen, F. E., Prusiner, S. B. (1998). Eight prion strains PrP^{Sc} molecules with different conformations. *Nature Medicine* **4**, 1157-1165.

Safar, J. G., Geschwind, M. D., Deering, C., Didorenko, S., Sattavat, M., Sanchez, H., Serban, A., Vey, M., Baron, H., Giles, K., Miller, B. L., DeArmond, S. J., Prusiner, S. B. (2005). Diagnosis of human prion disease. *Proc Natl Acad Sci U S A* **102**, 3501-3506.

Sanghera, N., Pinheiro, T. J. T. (2002). Binding of prion protein to lipid membranes and implications for prion conversion. *Journal of Molecular Biology* **315**, 1241-1256.

Sarnataro, D., Paladino, S., Campana, V., Grassi, J., Nitsch, L., Zurzolo, C. (2002). PrP^{C} Is Sorted to the Basolateral Membrane of Epithelial Cells Independently of its Association with Rafts. *Traffic.* **3**, 810-821.

Sarnataro, D., Campana, V., Paladino, S., Stornaiuolo, M., Nitsch, L., Zurzolo, C. (2004). PrP(C) association with lipid rafts in the early secretory pathway stabilizes its cellular conformation. *Mol. Biol. Cell*, **15**, 4031-4042.

Schatzl, H. M. (2003). Present-Day Knowledge of BSE and Creutzfeldt-Jakob Disease. *Gesundheitswesen* **65 Suppl 1**, 13-19.

Schätzl, H. M., Da Costa, M., Taylor, L., Cohen, F. E., Prusiner, S. B. (1995). Prion protein gene variation among primates. *J.Mol.Biol.* **245**, 362-374.

Schatzl, H. M., Laszlo, L., Holtzman, D. M., Tatzelt, J., DeArmond, S. J., Weiner, R. I., Mobley, W. C., Prusiner, S. B. (1997). A hypothalamic neuronal cell line persistently infected with scrapie prions exhibits apoptosis. *J Virol* **71**, 8821-8831.

Scott, M., Foster, D., Mirenda, C., Serban, D., Coufal, F., Wälchli, M., Torchia, M., Groth, D., Carlson, G., DeArmond, S. J., Westaway, D., Prusiner, S. B. (1989). Transgenic mice expressing hamster prion protein produce species- specific scrapie infectivity and amyloid plaques. *Cell* **59**, 847-857.

Scott, M., Groth, D., Foster, D., Torchia, M., Yang, S. L., DeArmond, S. J., Prusiner, S. B. (1993). Propagation of prions with artificial properties in transgenic mice expressing chimeric PrP genes. *Cell* **73**, 979-988.

Scott, M. R., Groth, D., Tatzelt, J., Torchia, M., Tremblay, P., DeArmond, S. J., Prusiner, S. B. (1997). Propagation of prion strains through specific conformers of the prion protein. *J.Virol.* **71**, 9032-9044.

Scott, M. R., Kohler, R., Foster, D., Prusiner, S. B. (1992). Chimeric prion protein expression in cultured cells and transgenic mice. *Protein Science* **1**, 986-997.

Serio, T. R., Cashikar, A. G., Kowal, A. S., Sawicki, G. J., Moslehi, J. J., Serpell, L., Arnsdorf, M. F., Lindquist, S. L. (2000). Nucleated conformational conversion and the replication of conformational information by a prion determinant. *Science* **289**, 1317-1321.

Shmerling, D., Hegyi, I., Fischer, M., Blättler, T., Brandner S, Götz, J., Rülicke, T., Flechsig, E., Cozzio, A., von Mering, C., Hangartner, C., Aguzzi, A., Weissmann, C. (1998). Expression of amino-terminally truncated PrP in the mouse leading to ataxia and specific cerebellar lesions. *Cell* **93**, 203-214.

Shyng, S. L., Huber, M. T., Harris, D. A. (1993). A prion protein cycles between the cell surface and an endocytic compartment in cultured neuroblastoma cells. *J Biol.Chem.* **268**, 15922-15928.

Shyng, S. L., Heuser, J. E., Harris, D. A. (1994). A glycolipid-anchored prion protein is endocytosed via clathrin-coated pits. *J. Cell Biol*. **125**, 1239-1250.

Sigurdsson, E. M., Brown, D. R., Daniels, M., Kascsak, R. J., Kascsak, R., Carp, R., Meeker, H. C., Frangione, B., Wisniewski, T. (2002). Immunization delays the onset of prion disease in mice. *Am.J.Pathol.* **161**, 13-17.

Smith, P. G., Bradley, R. (2003). Bovine spongiform encephalopathy (BSE) and its epidemiology. *Br.Med.Bull.* **66**, 185-198.

Solassol, J., Crozet, C., Perrier, V., Leclaire, J., Beranger, F., Caminade, A. M., Meunier, B., Dormont, D., Majoral, J. P., Lehmann, S. (2004). Cationic phosphorus-containing dendrimers reduce prion replication both in cell culture and in mice infected with scrapie. *J Gen.Virol*. **85**, 1791-1799.

Solforosi, L., Criado, J. R., McGavern, D. B., Wirz, S., Sanchez-Alavez, M., Sugama, S., DeGiorgio, L. A., Volpe, B. T., Wiseman, E., Abalos, G., Masliah, E., Gilden, D., Oldstone, M. B., Conti, B., Williamson, R. A. (2004). Cross-linking cellular prion protein triggers neuronal apoptosis in vivo. *Science* **303**, 1514-1516.

Somerville, R. A., Ritchie, L. A. (1990). Differential glycosylation of the protein (PrP) forming scrapie- associated fibrils. *J Gen.Virol.* **71**, 833-839.

Soto, C. (2008). Endoplasmic reticulum stress, PrP trafficking, and neurodegeneration. *Dev Cell* **15**, 339-341.

Soto, C., Estrada, L., Castilla, J. (2006). Amyloids, prions and the inherent infectious nature of misfolded protein aggregates. *Trends Biochem.Sci*. **31**, 150-155.

Soto, C., Kascsack, R. J., Saborío, G. P., Aucouturier, P., Wisniewski, T., Prelli, F., Kascsak, R., Mendez, E., Harris, D. A., Ironside, J., Tagliavini, F., Carp, R. I., Frangione, B. (2000). Reversion of prion protein conformational changes by synthetic beta-sheet breaker peptides. *Lancet* **355**, 192-197.

Sparkes, R. S., Simon, M., Cohn, V. H., Fournier, R. E., Lem, J., Klisak, I., Heinzmann, C., Blatt, C., Lucero, M., Mohandas, T., Raeber, A. J. (1986). Assignment of the human and mouse prion protein genes to homologous chromosomes. *Proc.Natl.Acad.Sci.U.S.A.* **83**, 7358-7362.

Spraker, T. R., Miller, M. W., Williams, E. S., Getzy, D. M., Adrian, W. J., Schoonveld, G. G., Spowart, R. A., O'Rourke, K. I., Miller, J. M., Merz, P. A. (1997). Spongiform encephalopathy in free-ranging mule deer (*Odocoileus hemionus*), white-tailed deer (*Odocoileus virginianus*) and Rocky Mountain elk (*Cervus elaphus nelsoni*) in northcentral Colorado. *Journal of Wildlife Diseases* **33**, 1-6.

Spencer, M. D., Knight, R. S., Will, R. G. (2002). First hundred cases of variant Creutzfeldt-Jakob disease: retrospective case note review of early psychiatric and neurological features. *British Medical Journal* **324**, 1479-1482.

Stahl, N., Baldwin, M. A., Teplow, D. B., Hood, L., Gibson, B. W., Burlingame, A. L., Prusiner, S. B. (1993). Structural Studies of the scrapie prion protein using mass spectrometry and amino acid sequencing. *Biochemistry* **32**, 1991-2002.

Stahl, N., Borchelt, D. R., Hsiao, K., Prusiner, S. B. (1987). Scrapie prion protein contains a phosphatidylinositol glycolipid. *Cell* **51**, 229-240.

Steele, A. D., Emsley, J. G., Ozdinler, P. H., Lindquist, S., Macklis, J. D. (2006). Prion protein (PrPc) positively regulates neural precursor proliferation during developmental and adult mammalian neurogenesis. *Proc Natl Acad Sci U S A.* **103**, 3416-3421.

Stengel, A., Bach, C., Vorberg, I., Frank, O., Gilch, S., Lutzny, G., Seifarth, W., Erfle, V., Maas, E., Schatzl, H., Leib-Mosch, C., Greenwood, A. D. (2006). Prion infection influences murine endogenous retrovirus expression in neuronal cells. *Biochem Biophys Res Commun*. **343**, 825-831.

Stephenson, D. A., Chiotti, K., Ebeling, C., Groth, D., DeArmond, S. J., Prusiner, S. B., Carlson, G. A. (2000). Quantitative trait loci affecting prion incubation time in mice. *Genomics* **69**, 47-53.

Stewart, R. S., Piccardo, P., Ghetti, B., Harris, D. A. (2005). Neurodegenerative illness in transgenic mice expressing a transmembrane form of the prion protein. *J Neurosci.* **25**, 3469-3477.

Strumbo, B., Ronchi, S., Bolis, L. C., Simonic, T. (2001). Molecular cloning of the cDNA coding for *Xenopus laevis* prion protein. *FEBS Letters* **508**, 170-174.

Sunyach, C., Jen, A., Deng, J., Fitzgerald, K. T., Frobert, Y., Grassi, J., McCaffrey, M. W., Morris, R. (2003). The mechanism of internalization of glycosylphosphatidylinositol-anchored prion protein. *EMBO J* **22**, 3591-3601.

Supattapone, S., Bosque, P., Muramoto, T., Wille, H., Aagaard, C., Peretz, D., Nguyen, H. O. B., Heinrich, C., Torchia, M., Safar, J., Cohen, F. E., DeArmond, S. J., Prusiner, S. B., Scott, M. (1999). Prion protein of 106 residues creates an artificial transmission barrier for prion replication in transgenic mice. *Cell* **96**, 869-878.

Suzuki, T., Kurokawa, T., Hashimoto, H., Sugiyama, M. (2002). cDNA sequence and tissue expression of Fugu rubripes prion protein-like: a candidate for the teleost orthologue of tetrapod PrPs. *Biochem.Biophys.Res.Commun.* **294**, 912-917.

Tagliavini, F., Prelli, F., Verga, L., Giaccone, G., Sarma, R., Gorevic, P., Ghetti, B., Passerini, F., Ghibaudi, E., Forloni, G., Salmona, M., Bugiani, O., Frangione, B. (1993). Synthetic peptides homologous to prion protein residues 106-147 form amyloid-like fibrils in vitro. *Proc.Natl.Acad.Sci.U.S A.* **90**, 9678-9682.

Taraboulos, A., Borchelt, D., McKinley, M. P., Raeber, A., Serban, D., Prusiner, S. B. (1991). Prion diseases in humans and animals. *Plenum Press*, **134**, 305-306.

Tarahoulos,A, A Raeher, D Borchelt, M P McKinley, S B Prusiner, 1991, FASEB J., v. 5, p. A1177.

Taraboulos, A., Raeber, A., Borchelt, D. R., Serban, D., Prusiner, S. B. (1992). Synthesis and trafficking of prion proteins in cultured cells. *Molecular Biology of the Cell* **3**, 851-863.

Taraboulos, A., Rogers, M., Borchelt, D. R., McKinley, M. P., Scott, M., Serban, D., Prusiner, S. B. (1990a). Acquisition of protease resistance by prion proteins in scrapie-infected cells does not require asparagine-linked glycosylation. *Proceedings of the National Academy of Sciences of the United States of America* **87**, 8262-8266.

Taraboulos, A., Scott, M., Semenov, A., Avraham, D., Laszlo, L., Prusiner, S. B. (1995). Cholesterol depletion and modification of COOH-terminal targeting sequence

of the prion protein inhibit formation of the scrapie isoform. *Journal of Cell Biology* **129**, 121-132.

Taraboulos, A., Scott, M., Semenov, A., Avrahami, D., Prusiner, S. B. (1994). Biosynthesis of the prion proteins in scrapie-infected cells in culture. *Braz.J Med Biol Res* **27**, 303-307.

Taraboulos, A., Serban, D., Prusiner, S. B. (1990b). Scrapie prion proteins accumulate in the cytoplasm of persistently infected cultured cells. *Cell Biol.* **110**, 2117-2132.

Taylor, D. R., Hooper, N. M. (2007). Role of lipid rafts in the processing of the pathogenic prion and Alzheimer's amyloid-beta proteins. *Semin Cell Dev Biol*. **18**, 638-648.

Taylor, D. R., Watt, N. T., Perera, W. S., Hooper, N. M. (2005). Assigning functions to distinct regions of the N-terminus of the prion protein that are involved in its copper-stimulated, clathrin-dependent endocytosis. *J Cell Sci* **118**, 5141-5153.

Taylor, D. R., Whitehouse, I. J., and Hooper, N. M. (2009). Glypican-1 mediates both prion protein lipid raft association and disease isoform formation. *PLoS Pathog.* **5**, e1000666.

Telling, G. C., Haga, T., Torchia, M., Tremblay, P., DeArmond, S. J., Prusiner, S. B. (1996). Interactions between wild-type and mutant prion proteins modulate neurodegeneration transgenic mice. *Genes Dev.* **10**, 1736-1750.

Telling, G. C., Parchi, P., DeArmond, S. J., Cortelli, P., Montagna, P., Gabizon, R., Mastrianni, J., Lugaresi, E., Gambetti, P., Prusiner, S. B. (1996). Evidence for the conformation of the pathologic isoform of the prion protein enciphering and propagating prion diversity. *Science* **274**, 2079-2082.

Telling, G. C., Scott, M., Hsiao, K. K., Foster, D., Yang, S.-L., Torchia, M., Sidle, K. C. L., Collinge J, DeArmond, S. J., Prusiner, S. B. (1994). Transmission of Creutzfeldt-Jakob disease from humans to transgenic mice expressing chimeric human-mouse prion protein. *Proc Natl Acad Sci USA* **91**, 9936-9940.

Telling, G. C., Scott, M., Mastrianni, J., Gabizon, R., Torchia, M., Cohen, F. E., DeArmond, S. J., Prusiner, S. B. (1995). Prion propagation in mice expressing human and chimeric PrP transgenes implicates the interaction of cellular PrP with another protein. *Cell* **83**, 79-90.

Telling, G. C., Tremblay, P., Torchia, M., Dearmond, S. J., Cohen, F. E., Prusiner, S. B. (1997). N-terminally tagged prion protein supports prion propagation in transgenic mice. *Protein Sci* **6**, 825-833.

Thackray, A. M., Hopkins, L., Klein, M. A., Bujdoso, R. (2007). Mouse-adapted ovine scrapie prion strains are characterized by different conformers of PrPSc. *J Virol.* **81**, 12119-12127.

Tobler, I., Gaus, S. E., Deboer, T., Achermann, P., Fischer, M., Rulicke, T., Moser, M., Oesch, B., McBride, P. A., Manson, J. C. (1996). Altered circadian activity rhythms and sleep in mice devoid of prion protein. *Nature* **380**, 639-642.

Turk, E., Teplow, D. B., Hood, L. E., Prusiner, S. B. (1988). Purification and properties of the cellular and scrapie hamster prion proteins. *Eur.J Biochem.* **176**, 21-30.

Van Dam, E. M., Stoorvogel, W. (2002). Dynamin-dependent transferrin receptor recycling by endosome-derived clathrin-coated vesicles. *Mol Biol Cell* **13**, 169-182.

Veith, N. M., Plattner, H., Stuermer, C. A., Schulz-Schaeffer, W. J., Burkle, A. (2008). Immunolocalisation of PrP(Sc) in scrapie-infected N2a mouse neuroblastoma cells by light and electron microscopy. *Eur J Cell Biol*. **88**, 45-63.

Verdoes, M., Florea, B. I., Menendez-Benito, V., Maynard, C. J., Witte, M. D., Van Der Linden, W. A., Van Den Nieuwendijk, A. M. C., Hofmann, H. C., Berkers, R., Van Leeuwen, F. W. B., Groothuis, T. A., Leeuwenburgh, M. A., Ovaa, H., Neefjes, J. J., Filippov, D. V., Van Der Marel, G. A., Dantuma, N. P., Overkleeft, H.S. (2006). A fluorescent broad-spectrum proteasome inhibitor for labeling proteasomes *in vitro* and *in vivo*. *Chem & Biol* **13**, 1217-1226.

Vey, M., Pilkuhn, S., Wille, H., Nixon, R., DeArmond, S. J., Smart, E. J., Anderson, R. G. W., Taraboulos, A., Prusiner, S. B. (1996). Subcellular colocalization of the cellular and scrapie prion proteins in caveolae-like membranous domains. *Proceedings of the National Academy of Sciences of the United States of America* **93**, 14945-14949.

Vollmert, C., Windl, O., Xiang, W., Rosenberger, A., Zerr, I., Wichmann, H. E., Bickeboller, H., Illig, T., Kretzschmar, H. A. (2006). Significant association of a M129V independent polymorphism in the 5' UTR of the PRNP gene with sporadic Creutzfeldt-Jakob disease in a large German case-control study. *J Med Genet.* **43**, e53.

Vorberg, I., Raines, A., Priola, S. A. (2004a). Acute formation of protease-resistant prion protein does not always lead to persistent scrapie infection in vitro. *J Biol.Chem.* **279**, 29218-29225.

Vorberg, I., Raines, A., Priola, S. A. (2004b). Acute formation of protease-resistant prion protein does not always lead to persistent scrapie infection in vitro. *Journal of Biological Chemistry* **279**, 29218-29225.

Wadia, S. J., Schaller, M., Williamson, R. A., Dowdy, S. F. (2008). Pathologic prion protein infects cells by lipid-raft dependent macropinocytosis. *PLoS ONE* **3**, e3314.

Wadsworth, J. D., Hill, A. F., Beck, J., Collinge, J. (2003). Molecular and clinical classification of human prion disease. *British Medical Bulletin* **66**, 241-254.

Wadsworth, J. D., Joiner, S., Linehan, J., Cooper, S., Powell, C., Mallinson, G., Buckell, J., Gowland, I., Asante, E. A., Budka, H., Brandner, S., Collinge, J. (2006). Phenotypic heterogeneity in inherited prion disease (P102L) is associated with differential propagation of protease-resistant wild-type and mutant prion protein. *Brain* **129**, 1557-1569.

Wadsworth, J. D., Joiner, S., Linehan, J. M., Asante, E. A., Brandner, S., Collinge, J. (2008). The origin of the prion agent of kuru: molecular and biological strain typing. *Philos Trans R Soc Lond B Biol Sci* **363**, 3747-3753.

Wang, S., Herndon, M. E., Ranganathan, S., Godyna, S., Lawler, J., Argraves, W. S., Liau, G. (2004). Internalization but not binding of thrombospondin-1 to low density lipoprotein receptor-related protein-1 requires heparan sulfate proteoglycans. *J. Cell Biochem*. **91**, 766-776.

Wang, X., Bowers, S. L., Wang, F., Pu, X. A., Nelson, R. J., Ma, J. (2009). Cytoplasmic Prion Protein Induces Forebrain Neurotoxicity. *Biochim Biophys Acta*. **1792**, 555-563.

Warner, R. G., Hundt, C., Weiss, S., Turnbull, J. E. (2002). Identification of the heparan sulfate binding sites in the cellular prion protein. *J.Biol.Chem.* **277**, 18421-18430.

Watt, N. T., Hooper, N. M. (2003). The prion protein and neuronal zinc homeostasis. *Trends Biochem.Sci* **28**, 406-410.

Weissmann, C. (1994). Molecular biology of prion diseases. *Trends Cell Biol.* **4**, 10-14.

Weissmann, C., Aguzzi, A. (1997). Bovine spongiform encephalopathy and early onset variant Creutzfeldt-Jakob disease. *Curr Opin Neurobiol.* **7**, 695-700.

Wells, G. A. H., Scott, A. C., Johnson, C. T., Gunning, R. F., Hancock, R. D., Jeffrey, M., Dawson, M., Bradley, R. (1987). A novel progressive spongiform encephalopathy in cattle. *Vet.Rec.* **31**, 419-420.

Westaway, D., Cooper, C., Turner, S., Da Costa, M., Carlson, G. A., Prusiner, S. B. (1994). Structure and polymorphism of the mouse prion protein gene. *Proceedings of the National Academy of Sciences of the United States of America* **91**, 6418-6422.

Westaway, D., Prusiner, S. B. (1986). Conservation of the cellular gene encoding the scrapie prion protein. *Nucleic.Acids.Res.* **14**, 2035-2044.

Wilesmith, J. W., Wells, G. A. (1991). Bovine spongiform encephalopathy. *Curr.Top.Microbiol Immunol.* **172**, 21-38.

Wilesmith, J. W., Wells, G. A., Cranwell, M. P., Ryan, J. B. (1988). Bovine spongiform encephalopathy: epidemiological studies. *Vet.Rec.* **123**, 638-644.

Will, R. G., Ironside, J. W., Zeidler, M., Cousens, S. N., Estibeiro, K., Alperovitch, A., Poser, S., Pocchiari, M., Hofman, A., Smith, P. G. (1996). A new variant of Creutzfeldt-Jakob disease in the UK. *Lancet* **347**, 921-925.

Wille, H., Michelitsch, M. D., Guenebaut, V., Supattapone, S., Serban, A., Cohen, F. E., Agard, D. A., Prusiner, S. B. (2002). Structural studies of the scrapie prion protein by electron crystallography. *Proc.Natl.Acad.Sci.U.S.A* **99**, 3563-3568.

Williams, E. S., Young, S. (1980). Chronic wasting disease of captive mule deer: a spongiform encephalopathy. *J Wildl.Dis.* **16**, 89-98.

Windl, O., Dempster, M., Estibeiro, J. P., Lathe, R., De Silva, R., Esmonde, T., Will, R., Springbett, A., Campbell, T. A., Sidle, K. C. L., Palmer, M. S., Collinge, J. (1996). Genetic basis of Creutzfeldt-Jakob disease in the United Kingom: a systematic analysis of predisposing mutations and allelic variation in the *PRNP* gene. *Human Genetics* **98**, 259-264.

Windl, O., Dempster, M., Estibeiro, P., and Lathe, R. (1995). A candidate marsupial *PrP* gene reveals two domains conserved in mammalian PrP proteins. *Gene* **159**, 181-186.

Wopfner, F., Weidenhöfer, G., Schneider, R., Von Brunn, A., Gilch, S., Schwarz, T. F., Werner, T., Schätzl, M. (1999). Analysis of 27 mammalian and 9 avian PrP^{Sc} reveals high conservation of flexible regions of the prion protein. *Journal of Molecular Biology* **289**, 1163-1178.

Wroe, S. J., Pal S, Siddique, D., Hyare, H., Macfarlane, R., Joiner S, Linehan J, Brandner S, Wadsworth JD, Hewitt, P., Collinge, J. (2006). Clinical presentation and pre-mortem diagnosis of variant Creutzfeldt-Jakob disease associated with blood transfusion: a case report. *Lancet* **368**, 2061-2067.

Yedidia, Y., Horonchik, L., Tzaban, S., Yanai, A., Taraboulos, A. (2001). Proteasomes and ubiquitin are involved in the turnover of the wild-type prion protein. *EMBO Journal* **20**, 5383-5391.

Ying, Y. S., Anderson, R. G., Rothberg, K. G. (1992). Each caveola contains multiple glycosyl-phosphatidylinositol- anchored membrane proteins. *Cold Spring Harb.Symp.Quant.Biol* **57**, 593-604.

Yuan, F. F., Biffin, S., Brazier, M. W., Suarez, M., Cappai, R., Hill, A. F., Collins, S. J., Sullivan, J. S., Middleton, D., Multhaup, G., Geczy, A. F., Masters, C. L. (2005). Detection of prion epitopes on PrP and PrP of transmissible spongiform encephalopathies using specific monoclonal antibodies to PrP. *Immunol Cell Biol* **83**, 632-637.

Zanusso, G., Petersen, R. B., Jin, T. C., Jing, Y., Kanoush, R., Ferrari, S., Gambetti, P., Singh, N. (1999). Proteasomal degradation and N-terminal protease resistance of the codon 145 mutant prion protein. *Journal of Biological Chemistry* **274**, 23396-23404.

Zerr, I., Giese, A., Windl, O., Kropp, S., Schulz-Schaeffer, W., Riedemann, C., Skworc, K., Bodemer, M., Kretzschmar, H. A., Poser, S. (1998). Phenotypic variability in fatal familial insomnia (D178N-129M) genotype. *Neurology* **51**, 1398-1405.

Zhang, C. C., Steele, A. D., Lindquist, S., Lodish, H. F. (2006). Prion protein is expressed on long-term repopulating hematopoietic stem cells and is important for their self-renewal. *Proc Natl Acad Sci U S A* **103**, 2184-2189.

Zuber, C., Mitteregger, G., Schuhmann, N., Rey, C., Knackmuss, S., Rupprecht, W., Reusch, U., Pace, C., Little, M., Kretzschmar, H. A., Hallek, M., Buning, H., Weiss, S. (2008). Delivery of single-chain antibodies (scFvs) directed against the 37/67 kDa laminin receptor into mice via recombinant adeno-associated viral vectors for prion disease gene therapy. *J Gen Virol* **89**, 2055-2061.

Zulianello, L., Kaneko, K., Scott, M., Erpel, S., Han, D., Cohen, F. E., Prusiner, S. B. (2000). Dominant-negative inhibition of prion formation diminished by deletion mutagenesis of the prion protein. *Journal of Virology* **74**, 4351-4360.